Stream channel adjustment in upland swamps, Barrington Tops, New South Wales, Australia

Author:
Nanson, Rachel

Publication Date:
2006

DOI:
https://doi.org/10.26190/unsworks/18952

Stream channel adjustment in upland swamps, Barrington Tops, New South Wales, Australia

Rachel A. Nanson

2005

A thesis submitted in fulfilment of the requirements for the degree of Doctor of Philosophy

School of Physical, Environmental and Mathematical Sciences

(Geography)

University of New South Wales

@ the Australian Defence Force Academy

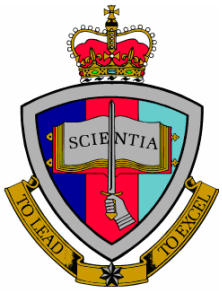

Abstract

The study of stable, channelled, upland swamps is relatively new and the processes by which they attain and maintain stability are of particular interest. Channels can adjust three elements of their morphology: cross-section, bedform and planform. This thesis examines unusual extremes in the adjustment of these elements in several swamp channels at Barrington Tops, New South Wales.

In these channels, high bank strength is afforded by dense vegetation that has enabled the channels to achieve unusually low width/depth ratios. The resultant at-a-station hydraulic geometry is such that width barely increases with flow stage, depth increases moderately and velocity increases markedly; the channels have particularly high hydraulic efficiencies. Shear stress calculations suggest that bankfull flows are more than capable of transporting the scant sediment with which they are supplied. This economic use of energy means that, to maintain equilibrium, the excess must be consumed by the remaining elements; bedform and planform.

Bedform magnitude (steepness) is strongly linked to flow resistance and there are large variations in the scale of bedforms between the channels studied here. In the smaller but more sinuous Polblue Creek, power is moderate and bed features display moderate steepness values. In contrast, the larger but less sinuous Barrington River and Edwards Creek channels have higher stream powers and their armoured bedforms have developed with much greater steepness. The considerable turbulence associated with these larger features are unable to destabilise the highly resistant channel banks but are sufficient to generate energy losses that reduce grain shear-stresses and prevent bed erosion.

Polblue Creek, Barrington River and Edwards Creek have each developed sinuous planforms, with some examples of very tight bends. The reduction in the energy slope associated with planform development and the substantial turbulence that these tight bends generate combine with bedform development to counter the exceptional hydraulic efficiency of the channel cross-sections. The development of extreme bedform and planform morphologies have enabled system stability, despite high shear stresses and limited energy expenditure on sediment transport. This research suggests that bed armouring, high bank strengths and the development of highly sinuous planforms are integral to the maintenance of channel equilibrium, as has been demonstrated by channelled-swamp stability over the last ~1ka.

Originality Statement

I hereby declare that this submission is my own work and to the best of my knowledge it contains no materials previously published or written by another person, or substantial proportions of material which have been accepted for the award of any other degree or diploma at UNSW or any other educational institution, except where due acknowledgement is made in the thesis. Any contribution made to the research by others, with whom I have worked at UNSW or elsewhere, is explicitly acknowledged in the thesis. I also declare that the intellectual content of this thesis is the product of my own work, except to the extent that assistance from others in the project's design and conception or in style, presentation and linguistic expression is acknowledged.

Rachel Nanson

Acknowledgements

Funding for this thesis was provided from several sources: a University College Postgraduate Scholarship through the UNSW@ADFA, a UNSW Faculty Research Grant, ANSTO, a UNSW@ADFA Overseas Travel Grant, a UNSW@ADFA Completion Scholarship and the School of Physical, Environmental and Mathematical Sciences, formerly the School of Geography and Oceanography (UNSW@ADFA).

I would like to thank my supervisors, Professor Roger McLean and Dr Geoff Pickup, for useful discussions, help and encouragement throughout this project. Your reviews and comments on my thesis content, approach and interpretation have greatly improved both my thesis and my research technique.

My additional advisors, Professor Geoff Hope and Professor Gerald Nanson, have excelled as encouragers, educators and mentors. You have both made my research experience all the more enjoyable and rewarding and for that, I am sincerely grateful.

Regarding my field assistants, I can only wonder at your tolerance of trying field conditions and my sometimes manic approach to data collection. In order of their *time-served*, I would like to thank: Daniel Rickleman, Dr Tim Cohen, Tim Robinson, James Boyle, Paul Grevenitz, Taki Kawakami, Benjo Keaney, Glen Bann, Dr John Jansen, Professor Gerald Nanson, Peter Palmer, Dr Jon East, Lloyd Hedges, Dr Geoff Pickup, Assoc. Professor Jacky Croke and Simon Mockler. I would also like to apologise for the misbehaviour of the Barrington weather – but the show must go on!

Specialist field devices were made available for my use by DIPNR (OTT counters), the University of Wollongong (OTT devices), Braddon Dive Shop (discounted dry-suit hire) and ANU (a push corer). The Victoria Hotel (Moonan Flat) provided discounted accommodation and a friendly welcome each night, and the NSW NPWS provided me with the use of a hut over two field seasons. Professor Geoff Hope provided access to, and consumables in, the ANU Department of Archaeology and Natural History. Thankyou all for your generous support.

The preparation of field equipment and specialist devices were greatly facilitated by Peter Palmer (general equipment) and Dr Graham Symonds, Ray Lawton and Paul van der Male (ADV's). Computer analyses of data were supported by Dr Graham Symonds, Dr Andrew Kiss and Dr Jianxin Wei (Matlab), Dr Wendy Anderson (Minitab) and Dr Dave Paull and Simon Mockler (ArcGIS) and Ali Arezi provided continual computer assistance. Your help was invaluable and so generously provided. Thankyou.

Penny Turner and Julie Kesby helped to source a great number of reference articles and solved many a formatting problem. Thankyou both for saving my sanity.

Informal discussions of research methods and approaches, and other entertaining topics, were facilitated by friends, colleagues and advisors. In particular, I would like to thank and acknowledge the support and inspiration provided by Dr Do Seong Byun, Dr Jia Shu Shen, Dr Jon Olley, Tim Pietsch, Tim Cohen, Chris Thompson, Dr Kathryn Amos, Dr Hua Huang, Professor Colin Thorne and Dr David Knighton.

Finally, the unerring support of my family has helped me to get to where I have come. Thankyou Glen, Mum, Dad, Jeremy and Gran. Your encouragement has been limitless and I love you all the more for it.

Table of contents

List of Figures

List of Tables

Abbreviations and Symbols

ADV	Acoustic Doppler Velocimeter
AMS	Accelerator Mass Spectrometry
b	width exponent
Q_{bf}	bankfull discharge
BP	Before Present
c	depth coefficient
d	depth (*in context*)
d	diameter (*in context*)
D_{50}	median grain size
D_{90}	particle size of which 90% of sediment sample is smaller
f	depth exponent
f	Darcy-Weisbach's friction coefficient
Fr	Froude number
g	acceleration due to gravity
h	height of bed feature
ka	thousands of years
l	length of bed feature
LAP	Least Action Principal
m	velocity exponent (*in context*)
m	metre (*in context*)
M	Schumm's bank material silt/clay ratio
MFE	Maximum Flow Efficiency
MVF	Maximum Velocity Filament
n	Manning's n
P	channel sinuosity index
p	Darcy-Weisbach's *f* exponent
Q	discharge (m^3/s)
Q_s	bedload sediment discharge
R	hydraulic radius
r_c	radius of curvature
s	slope
SNR	Signal to Noise Ratio
T	Threshold
TKE	Turbulent Kinetic Energy
U_R	reference velocity
v	velocity
w	width
W	Watts
y	Manning's n exponent
Z	height

Δ	change
ζ	optimum width/depth ratio
θ_c	dimensionless critical shear stress
ρ	water density
ρ_s	sediment density
Ω	total stream power (W/m)
ω	specific stream power (W/m^2)
%SF	wall shear as a percentage of total
τ	shear stress (N/m^2)

Chapter 1 Introduction and study area

1.1 Introduction

Streams that flow through wetlands are usually very sinuous and are bound by vertical, organic and/or peat banks. Their beds are comprised of sand and gravel, peat or basement material (bed-rock) and they tend to exhibit slot-like cross-sections. Some research has focused on the cross-sectional and planform geometry of such organic streams (Jurmu and Andrle, 1997; Jurmu, 2002), however, little if any research has examined their geometry-flow interactions.

This thesis examines the morphology of several streams that flow through two upland wetlands on the Barrington Tops plateau, New South Wales. These streams are remarkably narrow and deep and as such, they offer the opportunity to study channel adjustments under conditions that have rarely been examined. While nearly all the world's streams have relatively large width/depth ratios, this study offers an opportunity to examine flow conditions when this element is remarkably low. The capacity for wetland streams to self-adjust, and their subsequent stability, are assessed with investigations of five characteristics: their evolution and Quaternary history; bedform morphology; planform morphology; the development of secondary currents; an assessment of their "graded" or equilibrium condition.

This chapter provides the geomorphic context within which this research is based and then it identifies the specific research questions and objectives that have guided the project. It then describes those aspects of the study area that are related to the objectives of the thesis.

1.1.1 Channelled swamps: their definition, morphology and significance

1.1.1.1 Swamp and floodplain classification

The term *swamp* is used to describe wetlands, mires and marshes (Gore, 1983) and previous palynological studies of the Barrington Tops have also described them as swamps, mires *and* wetlands (Dodson et al., 1986; Dodson and Myers, 1986; Dodson, 1987). The pH values for water in the swamp channels at Barrington Tops range from ~6.0 to 6.9 and

thereby define them as eutrophic (minerotrophic) fens (Mitsch and Gosselink, 1986). In contrast to bogs, which predominantly obtain their minerals from rainfall (Mitsch and Gosselink, 1986), fen minerals are supplied from surrounding soils. While a 'quagmire' of terminology exists that might describe the Barrington environments (e.g. Gore, 1983; Mitsch and Gosselink, 1986), this thesis deals largely with stream channels and therefore more specific terminology is not required. For the sake of simplicity, they will be referred to as swamps, consistent with the names that were given to each system by early Europeans (e.g. Polblue Swamp, Edwards Swamp).

It is worth noting that while these features are truly swamps, near the stream channels they also experience inundation and minor sedimentation similar to floodplains. Furthermore, the relationship of the swamps to the streams closely mimics that of floodplains; they receive overbank flows and the frequency and longitudinal consistency with which bankfull flows were observed suggests their function, if not their sedimentology, mimics that of alluvial floodplains. Nanson and Croke (1992) provided a floodplain classification system based on sedimentology and energy (stream power). While the sedimentology of the Barrington Tops channelled swamp systems is largely organic, their most appropriate alluvial classification is the Class C Low-Energy Cohesive Floodplains, with specific stream powers less than 10 W/m^2. The swamp surfaces will therefore also be referred to as *floodplains* where appropriate.

1.1.1.2 Channel classification

The swamp channels examined here at Barrington Tops are continuous, perennial and apparently stable. Their continuity marks them as very different from the sand choked, discontinuous channels of the Woronora Plateau (NSW) dells, described by Young (1983; 1986a; 1986b). They also do not exhibit obvious or significant bank or bed erosion and are thus distinct from erosive groughs (Ingram, 1983). Ingram (1983) has described the process by which swamp drainage channels become increasingly constricted by vegetation growth and how they can be translated upward and outward over broad valley margins as the swamps grow in these same directions. While wetland outflows are common features of upland environments, specific reference to their hydraulic and geometric characteristics and relationships are rare (e.g. Jurmu and Andrle, 1997; Jurmu, 2002).

The channels in this study flow through swamps which may loosely be defined as *riparian wetlands* (Mitsch and Gosselink, 1986). However, in contrast to the Barrington examples the surfaces of riparian wetlands are generally inundated for extended periods. The existence of well-defined channels at Barrington Tops appears to reduce the duration of swamp inundation to relatively infrequent events.

The Barrington Tops swamp channels are not adequately covered by existing fluvial classification systems. For example, the "River Styles" framework, developed in Australia for channel classification (Brierley et al., 2002; Brierley and Fryirs, 2005) is an open-ended and generic approach to the classification and management of *alluvial* and *bedrock* streams but *organic* channels do not lend themselves to such classification. The River Styles technique is also a means by which rare and unusual geomorphic features, worthy of preservation, can be identified (Brierley et al., 2002; Brierley and Fryirs, 2005) and such would appear to be the status of swamp channels.

A more prescriptive approach to river classification by Rosgen (1994) has described similar alluvial channels within his classification of seven major stream types (Type A to Type G). He described narrow and deep, sinuous, well vegetated channels that occur on low gradients in broad valleys and meadows and classified them as Type E channels. They exhibit a high to very-high sensitivity to disturbance, low to moderate sediment supply, moderate to high bank erosion potential and a very strong influence from vegetation in controlling channel morphology. These characteristics generally describe the Barrington swamp channels. However, unlike the Barrington swamp channels, Type E channels are *not* organic channels. Montgomery and Buffington (1997) classified channels based on their bed morphology and the Barrington swamp channels conform loosely to their *Pool-Riffle Channels,* but neither these, nor Rogsen's Type E channels, can adequately describe the unique morphological or hydraulic characteristics of the Barrington Tops channels.

The conditions in which these swamp channels occur lies somewhere between alluvial and organic. Their very morphology is a balance between fluvial erosive forces, flow resistance elements and boundary strength supplied by vegetation (Zimmerman et al., 1967), with a minor amount of sediment transport and alluvial deposition. Their morphology and

development are so unique as to prompt the suggestion by Ingram (1983, pp. 131) that swamp channels are:

> *"…biologically driven, constrictive types of channel formation* [which have] *no exact counterpart in other ecosystems."*

This thesis does not specifically aim to classify these channels, as such an attempt would provide little insight into their behaviour until matched by a thorough account of channel longevity, geometry and flow hydraulics in a variety of swamp settings. Research so far has examined only swamp-channel morphology. Jurmu and Andrle (1997) and Jurmu (2002) have described the morphology of several *wetland streams* in the United States and found that they are different from conventional alluvial channels in several ways. They have: unusually tight bends, which lack point bars; lengthy straight reaches between bends; narrow and deep cross-sections; and unusually wide bend apices. Jurmu (2002) concluded that, owing to these anomalous morphological characteristics, the relationships between swamp-channel morphology and fluvial processes require further investigation, a very suitable justification for this thesis.

Thus far, the longevity of swamp channels remains largely unknown; are these transient, erosive features or have they achieved some level of stability within the swamp landscape? In Connecticut (USA) Jurmu and Andrle (1997) found that one such swamp channel had existed and maintained position since at least the 1930's. Young (1983; 1986a; 1986b) described the episodic flushing of dells on the Woronora Plateau (NSW) following fire and storm events during the Late Pleistocene and Holocene, but these are (currently) discontinuous channels, choked with sand. Records of *channelled* swamp development and behaviour over the longer-term have therefore not yet been determined. This is one of the objectives of this study.

This thesis directly links swamp channel-flow hydraulics and channel morphology and examines the nature of this relationship using established analytical techniques. Despite their organic settings, swamp-channel processes *can* be investigated using the conventional techniques developed for alluvial channels, as the channels demonstrate variations in cross-

sectional form along their length, planform adjustment through meander cut-offs and concave bank erosion, and the development of bedforms, in much the same manner as do alluvial channels. As the morphology of a channel directly infers the adjustment processes that have formed it (Rosgen, 1994), hydraulic geometry, bed and plan morphology analyses will establish the ability of such channels to self-adjust and will reveal their geometry-flow interactions.

1.1.2 Research questions, objectives and hypotheses

Several questions emerge from these considerations of swamp-channel evolution, morphology and contemporary fluvial behaviour:

- How geomorphically persistent and hydraulically stable are these channelled swamps?
- What are the main morphologic and hydraulic characteristics of these swamp channels?
- What are the flow characteristics, and in particular the secondary currents, in such unusually narrow and often sinuous channels?
- Have such channels adjusted to maintain stability and if so, how?

From these questions emerge the primary objectives of this thesis, which are to:

1. Assess the evolution and stability of the channel corridors within the swamps,
2. Describe interactions between channel geometry and flow in these narrow and deep, sediment-deficient channels,
3. Describe bed adjustments in such narrow, sediment-deficient channels,
4. Describe the planform adjustments and bend-flow characteristics in systems with such narrow and deep, tightly curving bends.

1.2 Study area

1.2.1 Location and environment

The channels and swamps of the Barrington Tops are unusual for Australia in that they are situated on an upland plateau ~1500m above sea level. The plateau is situated approximately 200km north of Sydney and 100km directly north of Newcastle, between the townships of Scone (to the west) and Gloucester (to the east) (Figure 1.1), and incorporates both the Barrington Tops National Park (National Parks and Wildlife Service) and the Barrington Tops Reserve (New South Wales State Forests). The rugged landscape supports several endangered and vulnerable species including the broad-toothed rat (*Mastacomys fuscus*), Hastings River mouse (*Pseudomys oralis*) and the brush-tailed rock-wallaby (*Petrogale penicillata*). The plateau also supports the most southern extent of Australia's Antarctic beech (*Nothofagus moorei*), an ancient and primitive rainforest tree, and in 1986 was included on the *Central Eastern Rainforest Reserves of Australia* World Heritage listing.

The plateau extends over an area of approximately 1000km^2. Zoete (2000) stated that mean annual precipitation, in the form of rain, fog and snowfalls, reaches 2000mm in areas over 700m a.s.l. and Tweedie (1963) described a rainfall gradient across the Tops that declines to 1000mm in the northwest. The western slopes rise ~1000m in less than 8km, from the township of Moonan to the edge of the undulating surface of the plateau at ~1400m (Figure 1.1). Mount Barrington (1556m) and Brumlo Top (1586m) represent the highest peaks (Figure 1.1). As a result of its high altitude and steep terrain the region is subject to radical weather fluctuations and daily temperatures vary more than those in the valleys below. At 1300m a.s.l., average July temperatures range from -2.3 to 8.8°C and January temperatures from 9.1 to 22.8°C (Tweedie, 1963). Areas above 1100m a.s.l. experience up to five snowfalls each year, generally up to ~0.2m deep (Zoete, 2000). *Montane Peatlands and Swamps* have formed in the broad, flat hollows (Dodson, 1987) of this sub-alpine environment (Figure 1.1) and are listed as *Threatened Ecological Communities* by the Department of Environment and Conservation (NSW). Many of the Barrington swamps

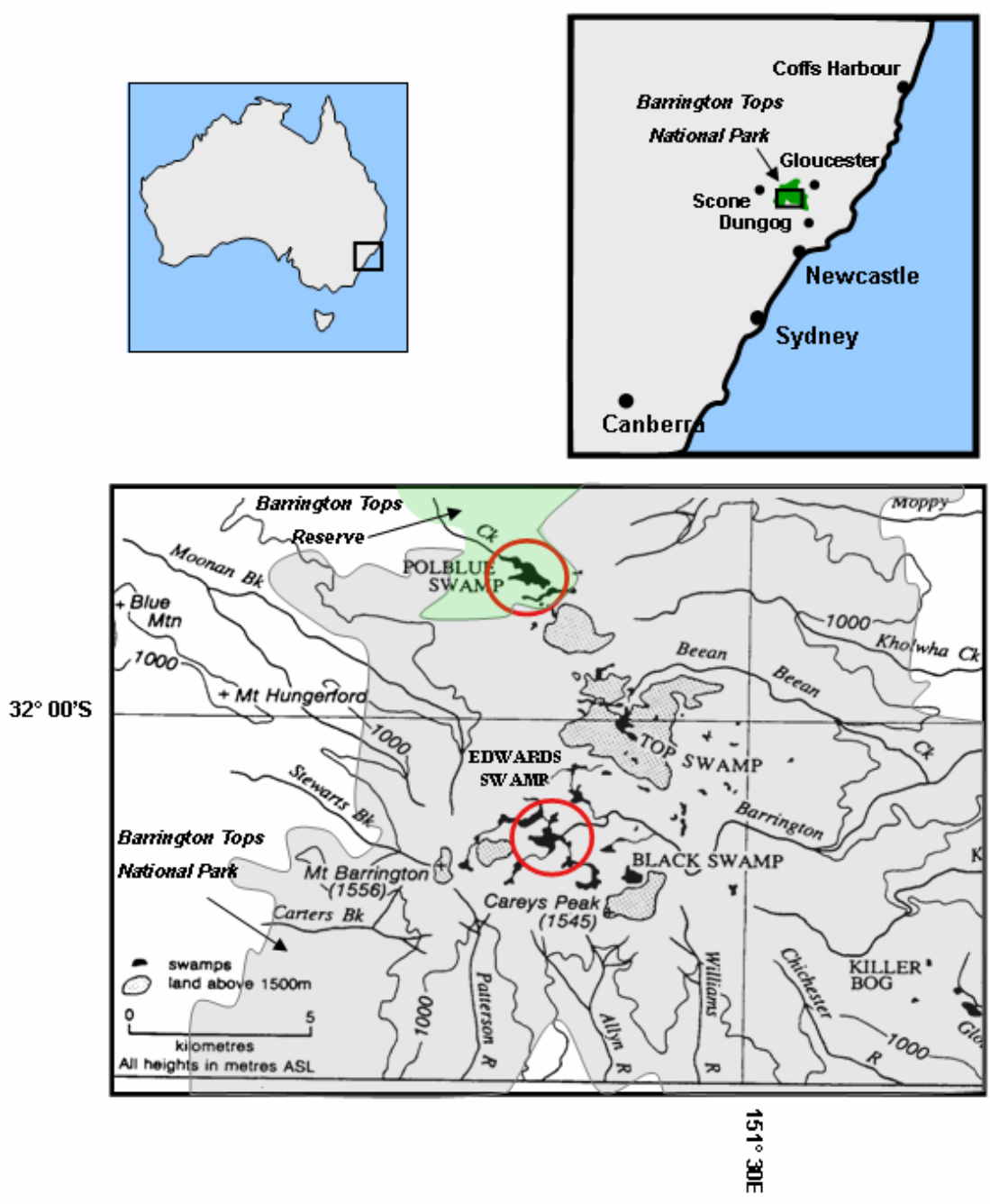

Figure 1.1 Location of the study area. Red circles indicate location of Polblue (top) and Edwards (bottom) swamps. Bottom map is modified from Dodson (1987).

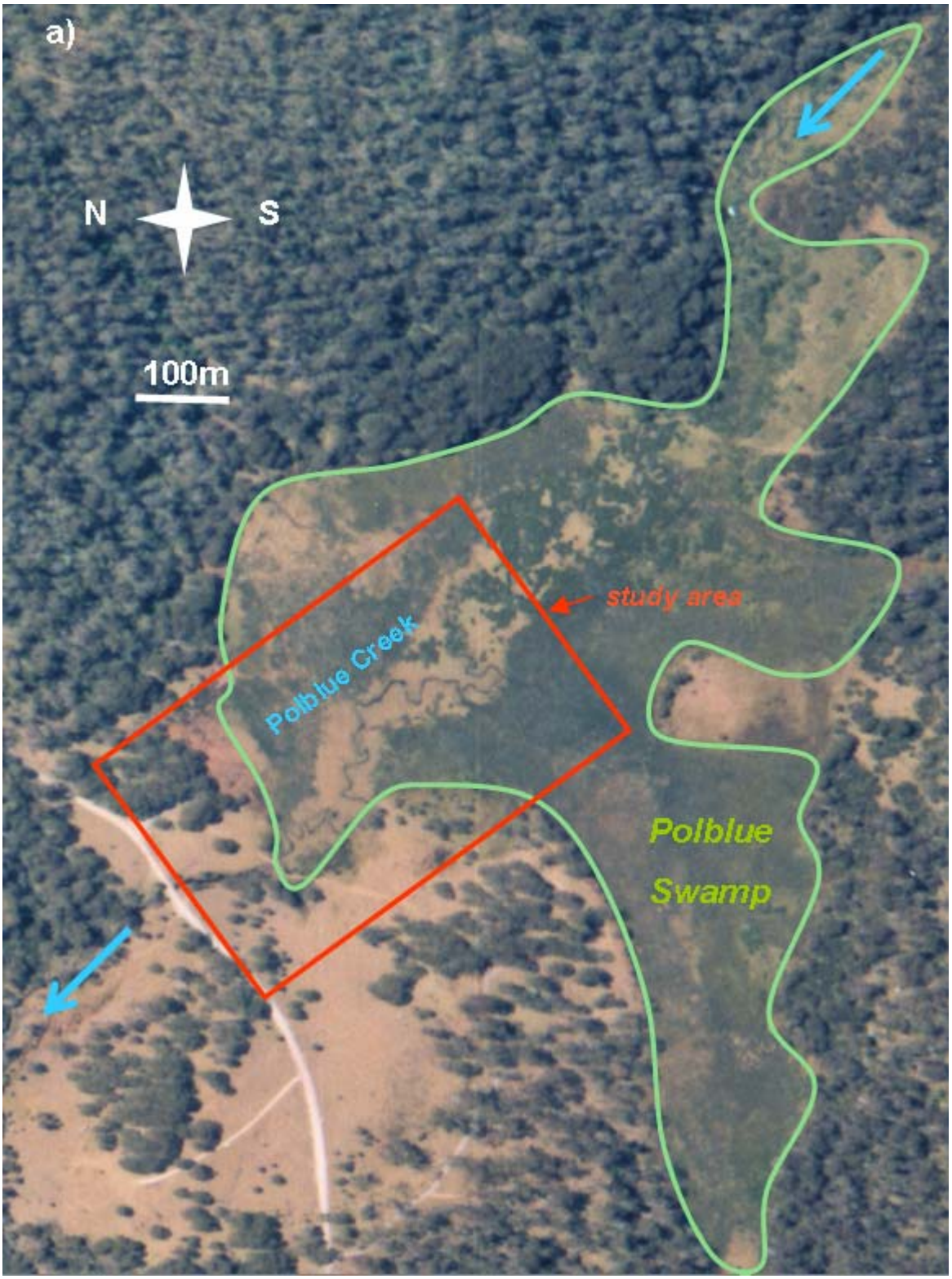
a)
N
S
100m
study area
Polblue Creek
Polblue
Swamp

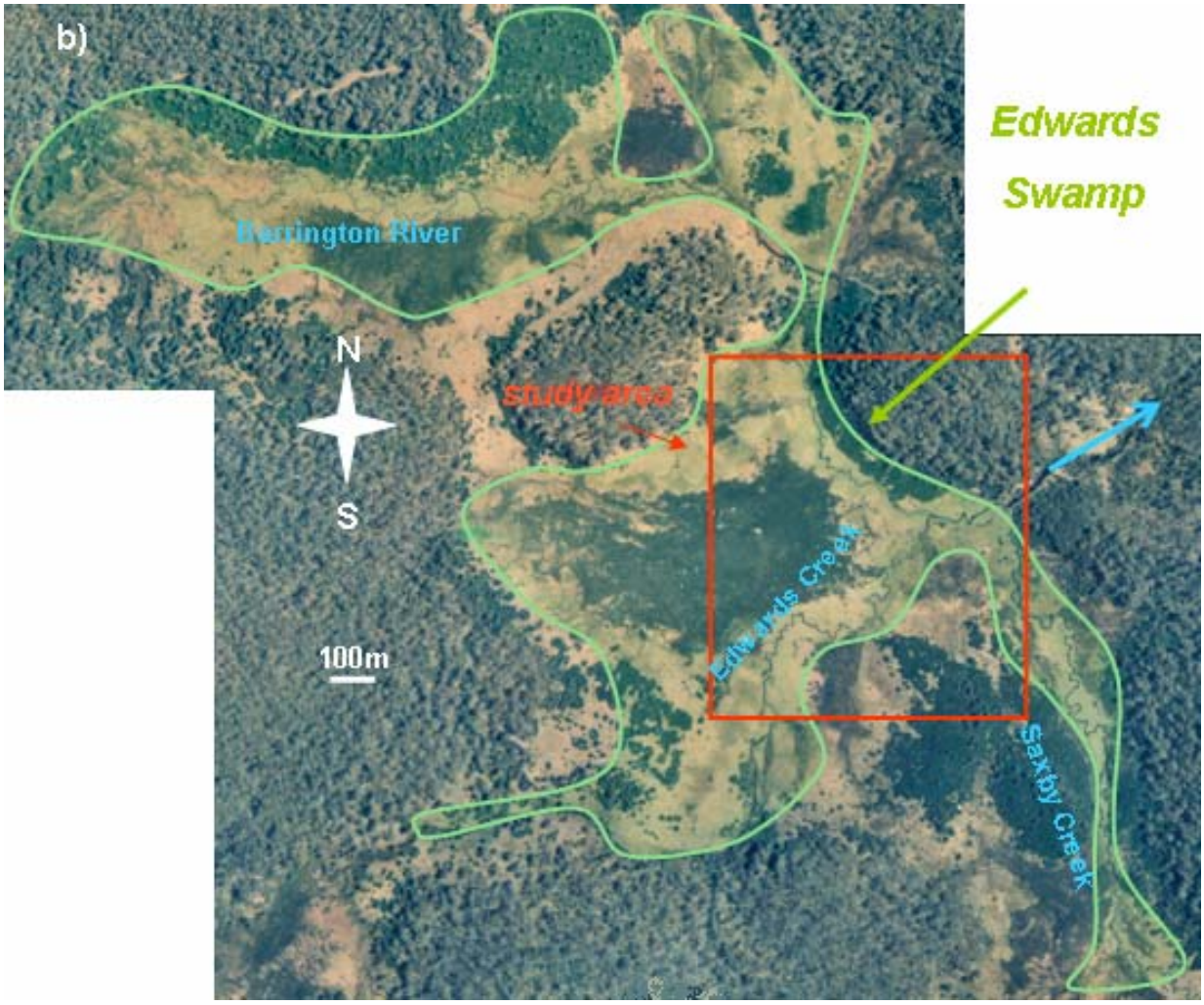

Figure 1.2 (a) Polblue and (b) Edwards Swamps, showing each of their major channels and the study areas that are examined in this thesis. The channels flow approximately centrally through each swamp. Note the difference in scale between the two maps.

have developed meandering channels and this thesis specifically examines three such channels in the Polblue (1480-1500m a.s.l.) and Edwards (1400-1420m a.s.l.) Swamps. These are Polblue Creek, Barrington River and Edwards Creek (Figure 1.2). Each of these channels drain sub-catchments approximating 4km^2, and Edwards Swamp is collectively supplied by 8km^2 of catchment as it is situated at the confluence of both Edwards Creek and the Barrington River. Both Polblue and Edwards swamps cover areas of approximately 0.5km^2. However, elongated arms of Edwards Swamp extend further up both tributaries of that swamp. The vegetation of the swamps are either *Sphagnum* hummock-hollow communities or Cyperaceae-Restionaceae sedgelands, surrounded by *Poa sieberana* and

Epacris paludosa in better-drained locales (Dodson et al., 1986; Dodson and Myers, 1986). The beds of the channels are sparsely vegetated with several ribbon-weed species, but these were not collected for taxonomic identification so are not defined more specifically.

1.2.2 Land use history

In addition to droughts and natural fires, swamp environments have long been subject to direct (e.g. draining) and indirect (e.g. fires) land use pressures (Mitsch and Gosselink, 1986). The draining of many swamps and valley fills post-European settlement in Australia is well documented (e.g. Eyles, 1977b; Fryirs and Brierley, 1998) and tempts the suggestion that the swamp channels of the Barrington Tops may be anthropogenically induced. A synthesis of the land use history of the Barrington Tops region provides a perspective from which to view their contemporary condition and from which to assess the contribution of human disturbance to their formation.

The use of the Barrington Tops plateau by Aboriginal people during summer months was first documented by European settlers in the late 1800's (Randell et al., 2003) and their previous use of the area is evidenced by stone artefacts, scarred trees and the inclusion of Barrington Tops locations in Aboriginal dreaming stories (National Parks and Wildlife Service, 2005). While the scale of Aboriginal impacts on the area is unclear, mosaic burning and hunting were likely to have been practiced at some level. However, Dodson et al. (1994) suggested that, at Burraga Swamp located ~6km south of the Barrington Tops plateau, these activities probably had little impact. On the other hand, more significant modifications and threats to the environment have resulted from European occupation of the area, starting in the Nineteenth Century. Randell et al. (2003) reviewed newspaper reports, journal publications, unpublished reports and various other written and oral data and produced a comprehensive anthropogenic history of the region. European farming and colonisation of the lowland areas around the Barrington Tops was established by the 1830's, but use of the Tops itself was limited to sheep droving across the plateau. By 1850 most suitable grazing land in the surrounding regions had become fully-occupied and squatters increasingly utilised the Tops for summer grazing to extend their farming

capacity. However, the high altitude and inaccessibility of the Tops protected it from year-round occupation and grazing.

Lower altitude areas surrounding Barrington Tops were logged for cedar until ~1835, when economically viable timbers were exhausted and the "cedar getters" were forced onto the steeper slopes approaching the plateau itself. Gold mining had commenced by this time in the surrounding lowlands, but did not extend onto the plateau. Ruby mining, however, caused the reworking of the Gloucester Tops swamps, but the Barrington Tops swamps escaped the same fate.

In 1892, 480ha near Polblue Swamp was dedicated as a camping area for stockmen to facilitate summer grazing practices and presumably the swamp itself became subject to increasing grazing pressures. Land purchases near both Polblue and Edwards Swamps in 1905 were followed by the construction of various huts around the plateau and the increasing popularity of the Tops for both recreational bushwalkers and graziers led to their more regular seasonal occupation. Stockyards around, and fences on, the swamps are evidence of their past use (Figure 1.3), and photographs of a cricket match held in 1924 on a flat-topped terrace near Edwards Swamp are testament to the accessibility and use of the area at this time.

A proposal to dam Edwards Swamp for the purpose of developing a recreational lake and adjacent resort was made in 1923 and in 1924 a further proposal was made to construct a snow-skiing resort. While access problems dogged and subsequently defeated these proposals, Edwards Swamp was in 1949 again under threat of damming when a plan to construct a hydro-electric power station was proposed. By this time, the "conservation movement" and economic good-sense prevented such a development. It was not until 1960 that logging of the forests on the plateau facilitated the construction of formal roadways, resulting in the opening of the Tops to all-weather road traffic. In 1978 there were 10 000 visitors recorded over the Easter holidays alone; pressures on the swamp environments from pedestrians, fishing and swimming were rising. Today, the widespread ownership of four wheel drive vehicles by the general public has greatly added to recreational use of the region, well away from the main public roadways.

Figure 1.3 The remains of fence posts at Edwards Swamp are evidence of previous grazing in the region. Flow is away from the reader, towards the hill in the background. Photo by Wynne Eldridge, 2002.

Early scientific research in the late 1930's determined that, despite light summer grazing and nearby logging activities, no important changes in the region's flora had occurred. Later researchers agreed with this conclusion and, primarily as a consequence of the region's inaccessibility and subsequent relative protection from European activities, it was deemed worthy of conservation. In 1969 much of the plateau and its steep foothills were declared the Barrington Tops National Park, which was later extended in 1984, 1997 and 1999 to its current extent of 75 000ha (National Parks and Wildlife Service, 2005). Annual grazing leases ceased in the 1960's. Current threats to Barrington Tops National Park include invasions of scotch broom, increased four-wheel drive access (and the subsequent spread of exotic weeds and erosion), the spread of *Phytophthora cinnamomi* (a root-rotting mould that effects many native plants, including Eucalyptus, Epacris, Tasmannia and Westringia species), feral animal predation and damage from brumbies (wild horses), foxes, wild dogs, cats, pigs, goats and rabbits, and the stocking of plateau streams with exotic trout (since the mid 1920's (Randell et al., 2003)). Many of these threats are

currently being addressed by the NSW National Parks and Wildlife Service. The channelled, or otherwise, state of the swamps were not described in historical reviews of the region and their development requires more detailed investigation. This is pursued in Chapter 2.

1.2.3 Regional geology

The geology of the Barrington Tops region has played a significant role in determining swamp development. The region is situated within the New England Fold Belt, a sequence of marine and freshwater sediments that were deposited during the Palaeozoic (Roberts et al., 1991). Uplift, folding and faulting of this sequence occurred during the Late Permian, at which time granodiorite was also intruded. A period of relative tectonic stability and landscape denudation followed (Sutherland and Graham, 2003), during which the granodiorite became exposed at the surface (Figure 1.4b).

Volcanism commenced in the region around 69 Ma as eastern Australia migrated over asthenospheric (lower crustal) plumes (hot spots) (Sutherland and Fanning, 2001). Basalt flows were deposited over both the granodiorite and the Carboniferous beds (Figure 1.4b). A large shield volcano had formed by about 50 Ma (Pain, 1983) (Figure 1.4a), and many of the pre-existing valleys were filled with basalt (Sutherland and Graham, 2003). A number of extrusive centres have been inferred (Sutherland and Graham, 2003) and are indicated in Figure 1.4. While most basalt flows were deposited between 55 and 51 Ma, further flows occurred up until 18 Ma with final volcanic activity around 5Ma at the south-eastern end of the plateau (Sutherland and Fanning, 2001).

The erosion-resistant capping of the upper Cenozoic basalt flows have dictated most of the major topographic features of the modern landscape (Galloway, 1963; Pain, 1983) and basalt capping covers much of the plateau. Some of these flows are exposed in road-cuttings on the Barrington Tops Forest Road. Figure 1.5 illustrates one such flow at the western edge of the plateau, beneath which is a krasnozem palaeosol that developed over a previous (lower) basalt flow. The deposit displays distinct columnar jointing, typical of much of the exposed basalt in this region.

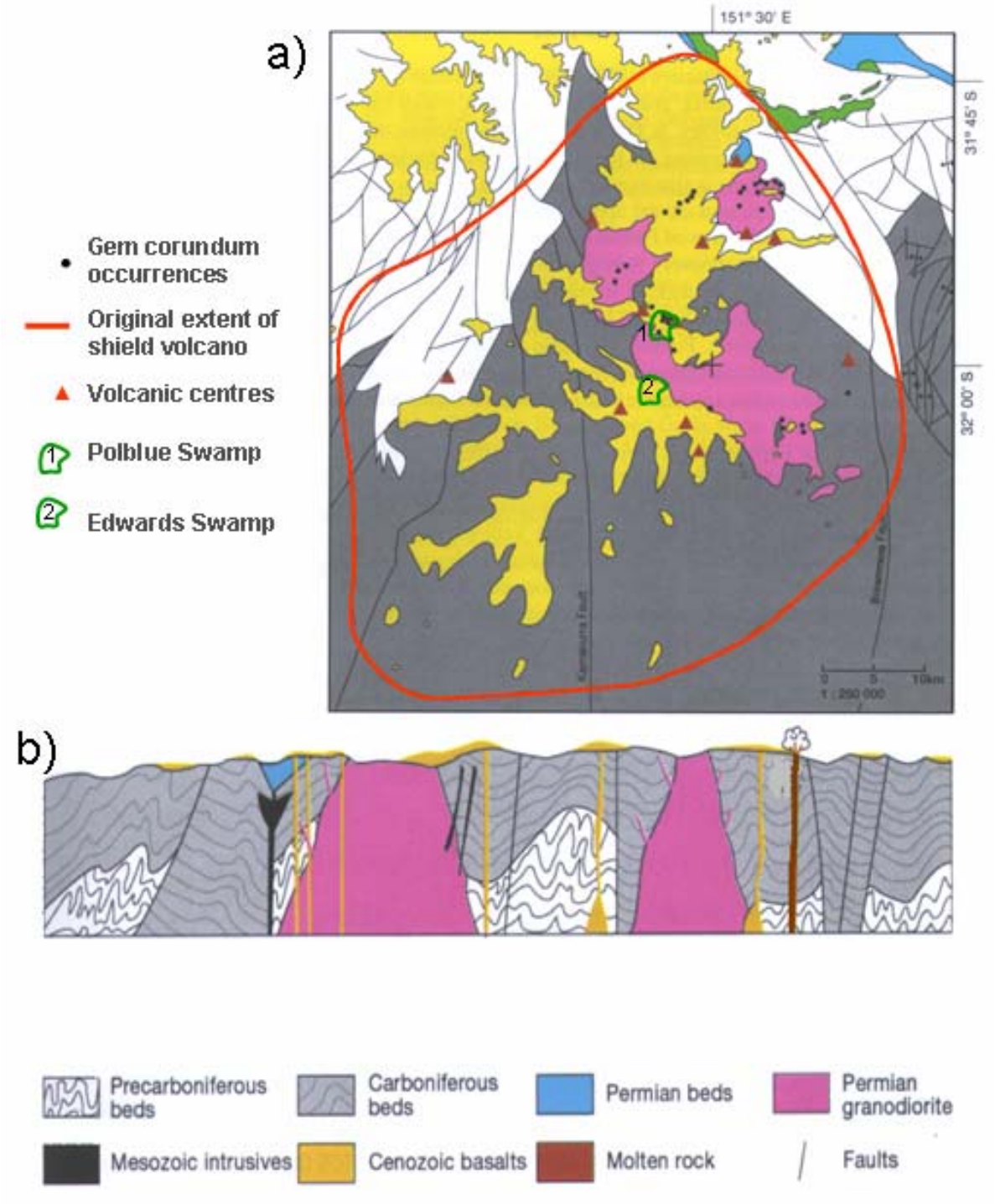

Figure 1.4 Geology of the Barrington Tops region (a) generalised plan view and (b) generalised transect through the Barrington Plateau. Both diagrams are modified from Sutherland and Graham (2003).

Figure 1.5 A basalt flow, with columnar jointing, overlying a krasnozem palaeosol. The visible portion of the post at bottom left is approximately 0.5m in height. Other flows lie beneath these exposures.

The Barrington Tops swamps have primarily developed over basalt lithology and often lie adjacent to outcrops of granodiorite (Offenberg, 1967; Roberts et al., 1991). The eastern extent of Edwards Swamp is bounded by granodiorite and accumulations of boulders from this rock-type have combined with basalt cobbles to constrict the valley outlet. In Polblue Swamp, the valley is also partially confined at its downstream end by basalt cobbles (Figure 1.6). Basalt terraces surround both swamps and several terraces, presumably resulting from incision through each overlying flow, are evident at Edwards Swamp. The highest of these is marked in Figure 1.7 and can be traced between discontinuous outcrops around the swamp margin.

Each of the swamp channels flow over basalt cobbles. These are either *in-situ* or were redeposited via periglacial processes during Quaternary glacial maximums.

Figure 1.6 A basalt terrace, ~100m downstream of Polblue Swamp, lies in the background and the foreground illustrates a lower surface, underlain by basalt cobbles, that has been stripped of vegetative cover by water overtopping the bank of a tight channel bend. Flow would have been from left to right.

Figure 1.7 Basalt flows appear as terraces around Edwards Swamp and their surfaces can be traced from valley side to valley side, dissected by the channelled swamp. The white dashed line indicates basalt terrace surfaces of approximately equal elevation. Note that the photo was taken standing on one such surface and note also the channel (Barrington River) in the foreground, and its confluence with Edwards Creek at the left of the photo, marked by a black arrow. Flow is from right to left.

1.2.4 Swamp-channel hydrology

Field observations indicated that precipitation falling over the swamp surfaces was quickly transferred to the channels, consistent with observations from other channelled swamp environments (Ingram, 1983). The interaction between the swamp water-table and channel flow appears to be very rapid, more so than in other less saturated alluvial settings. In extreme examples of channelled swamps, discharge can *decrease* downstream as flow is lost to the surrounding swamp, such as in the wetlands of the Okavango Delta (Tooth and McCarthy, 2004). The Barrington swamps discharge does not *decrease* downstream, but slightly increases. However, swamp-floodplain water tables and channel water levels are presumably similarly closely linked.

Andeera Water Level Recorders were deployed in each swamp during two three-week field trips, the first during November/December 2003 (early summer) and the second during May/June 2004 (early winter). Field observations showed that the most significant water level rises were directly linked to rainfall events, the steep rising limbs of the hydrographs confirming this observation (Figure 1.8). However, a major difference between the hydrographs for Edwards and Polblue Swamp channels is the steeper falling limb of the Polblue hydrograph in summer, suggesting that its smaller catchment area produces flashier flows. On the other hand, Edwards Swamp (at the location of the water level recorder) is supplied by two major catchments, and runoff from both moderates the falling limb of its flow hydrograph. Antecedent precipitation significantly affects channel and swamp hydrographs (Mitsch and Gosselink, 1986). However, as detailed rainfall data were not recorded for this study, more interpretation is not possible.

Figure 1.8 illustrates small daily fluctuations in flow stage in both the summer and winter records for both swamp channels, but the pattern in the winter record is more subdued. In a statistical sense, these fluctuations are comprised of trend (larger-scale fluctuations) and seasonal (smaller-scale fluctuations) components. When the trend cycle (that component of the hydrograph directly related to large rainfall events and slowly falling flow-stage) of the summer water level recordings is removed from selected sub-datasets (see Figure 1.8, circled in red) using an *additive* decomposition (see Appendix 1), a dominant seasonal-

cycle of diurnal fluctuations is exhibited by both swamps. This is illustrated in Figure 1.9 and a more detailed description of the data analysis technique that identified these patterns is provided in Appendix 1.

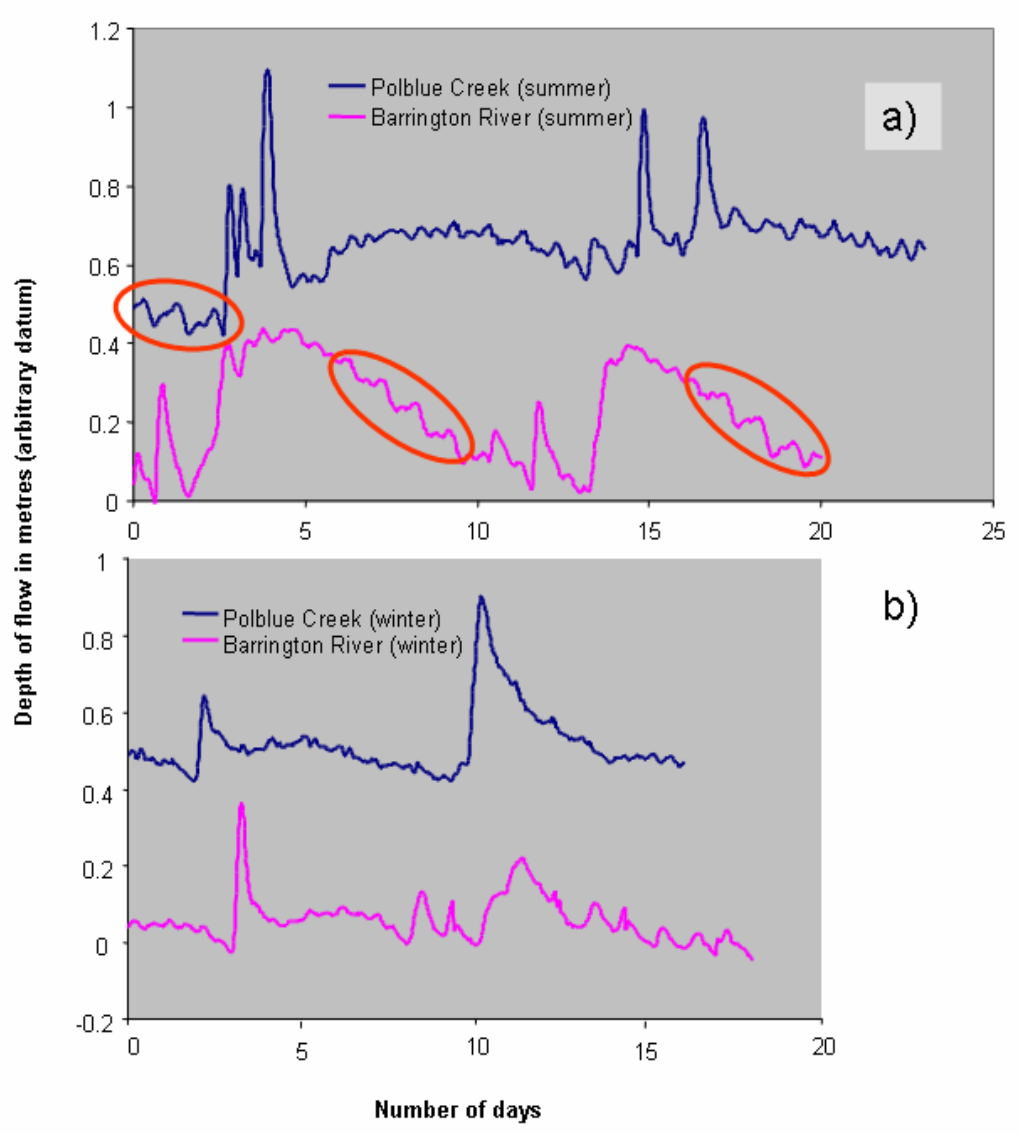

Figure 1.8 Flow hydrographs for Polblue Creek and the Barrington River over (a) one summer (2003) and (b) one winter (2004) field season. Circled records are those used to determine daily (seasonal) stage fluctuations.

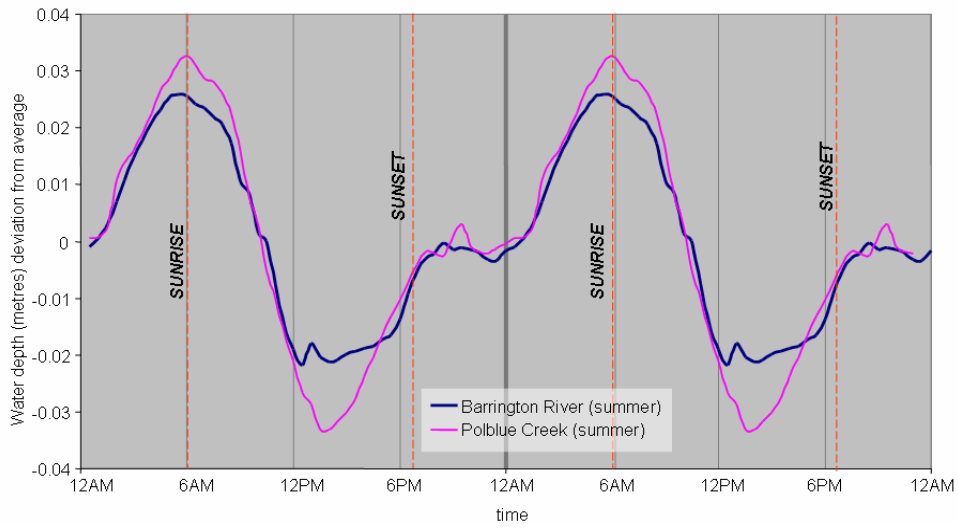

Figure 1.9 Average seasonal (daily detrended) flow stage variations in Polblue Creek and the Barrington River for selected days during summer. A full description of the analysis techniques applied to water level data to determine the average daily patterns (seasonality) of fluctuation during summer is provided in Appendix 1.

Channel flow stages fluctuate through 0.06m and 0.05m seasonal (statistical) cycles in Polblue Creek and the Barrington River, respectively (Figure 1.9). In both channels, flow reached its maximum stage at approximately 6am, immediately prior to sunrise, from which time it dropped until ~2pm, levelled off and then rose again until ~10pm. From then until midnight, the pattern plateaued, then rose again until 6am.

Daylight and/or temperature has a clear impact on summer flow fluctuations in the Barrington swamp channels, consistent with the (statistically) seasonal variations described by Todd (1964). Day-time losses in channel flow may well be related to the drawing of water into the swamps by plants during daylight hours, when evapotranspiration is at a maximum (Todd, 1964; Mitsch and Gosselink, 1986). Measures of the fluctuations in water tables have been used to directly calculate the amount of water lost to evapotranspiration (Todd, 1964; Ward, 1967; Mitsch and Gosselink, 1986), an estimation that is most accurate in environments where plant roots are very close to the water table (Todd, 1964), such as in swamps. As the plants need for water reduces during night-time hours, particularly between the hours of midnight and 4am (Todd, 1964) (or 6am in the Barrington swamps) the pressure gradient is reversed toward the channel, thereby increasing flow-stage. The result

is the moderated release of water from the swamps and steadier base-flow supply to lowland reaches.

Moderated flow releases resulting from swamp-channel interactions have important implications for low flow release rates in both the swamps and the lower reaches (Mitsch and Gosselink, 1986), with consequences for channel ecology (Ingram, 1983; Hope, 2003), particularly during the summer months. Investigations by A. Wade (pers. comm., in Hope, 2003) revealed that after six months of drought, Snowy Flat Bog (near Canberra) was still releasing 2.1 mega litres (ML) of water / day (or ~0.02 cumecs). In comparison, the Barrington River and Polblue Creek each discharge 62.2 and 28.5 ML / day during bankfull flow, and approximately 3.5 and 2.6 ML/day during base flow, respectively. Clearly, they too provide a significant quantity of water to their downstream reaches during both high and low flows, the latter flow presumably regulated by moderated releases from the swamp floodplain, with important ecological implications.

When swamp vegetation is significantly altered or destroyed, local and downstream hydrology can be greatly altered (Mitsch and Gosselink, 1986). This can follow swamp channelisation, which occurs consequent to catalysts for incision, that may include: fire followed by large storms (e.g. Woronora Plateau dells (Young, 1986b)), or the retreat of nick-points and subsequent *peat bursts* (Hope, 2003), caused by the collapse of super-saturated peat. The expected response of a swamp to such events is that, as the water table is lowered, existing vegetation dies and fluctuations within the swamp water table increase. Swamp vegetation is then replaced by more terrestrial species and the cycle of swamp development might recommence (Young, 1986b). In contrast, the Barrington Tops channelled swamps illustrate healthy swamp vegetation and an intimate exchange between the channels and swamp-floodplain hydrology. If the channel water levels were not balanced with the swamp water-table, then it is expected that the swamp vegetation would die. That the hydrological balance between the swamps and the channels is so satisfactory to both swamp vegetation *and* bankfull flow frequency implies the stability of both features. Furthermore, this balance indicates the importance of channel morphology in determining swamp height. Channel morphology determines flow stage height, which, in

turn, determines the height of the swamp water table. The swamp water table height controls swamp growth, in a manner that closely imitates the link between more conventional alluvial channels and their adjacent floodplain growth by overbank sedimentation. The evolution of both the swamps and the channels is examined in Chapter 2, before channel dimensions are more closely considered in Chapter 3.

1.3 Thesis approach

While channelled swamp stability was implied by the channel-swamp hydrological conditions described above, a more detailed account of their morphological adjustments toward an apparently stable end-point are required. It is widely accepted that self-forming alluvial streams are adjusted towards what are broadly termed "equilibrium conditions". G.K Gilbert recognised this in his summary work (1914) but Mackin (1948) enunciated the concept clearly in his classic paper, focusing primarily on the river's ability to adjust channel slope, and describing such adjusted rivers as "graded". His definition was subsequently expanded by Leopold and Bull (1979, pp.195), to read:

> *"A graded stream is one in which, over a period of years, slope, velocity, roughness, pattern and channel morphology delicately and mutually adjust to provide the power and the efficiency necessary to transport the load supplied from the drainage basin without aggradation or degradation of the channels. The threshold of critical power is passed and the stream is not graded when the volume of load supplied is insufficient or is too large to be transported, and the channel bed aggrades or degrades"*

They considered the inclusion of velocity, roughness, channel pattern and cross-sectional morphology, in addition to slope, to be consistent with Mackin's original considerations (1948, pp. 484).

The evolution of a channel towards a stable endpoint, therefore, involves the adjustment of all four morphological elements: slope, planform, bedform, and cross-section (Figure 1.10). Slope and the vertical component of bedforms are measured on the vertical plane parallel to

the flow, the channel cross-section is measured on the vertical plane perpendicular to the flow and planform is measured on the horizontal plane, so that all four are best considered separate elements of a channel's morphology on three interconnected planes. These elements respond to variations in water and sediment supply. Subsequent to Mackin's (1948) work, the importance of adjustments in each plane were investigated in various early works: slope (e.g. Mackin, 1948; Leopold and Bull, 1979); planform (e.g. Leopold et al., 1960; Bettess and White, 1983); bedforms (e.g. Simons and Richardson, 1966; Langbein and Leopold, 1968) and cross-section (e.g. Leopold and Maddock, 1953). The interconnectedness of each plane leads to a multi-focused approach, from which has come a more comprehensive understanding of each plane of adjustment and a thorough basis with which to examine a channel's adjustment to supplied sediment and water, and to imposed constraints.

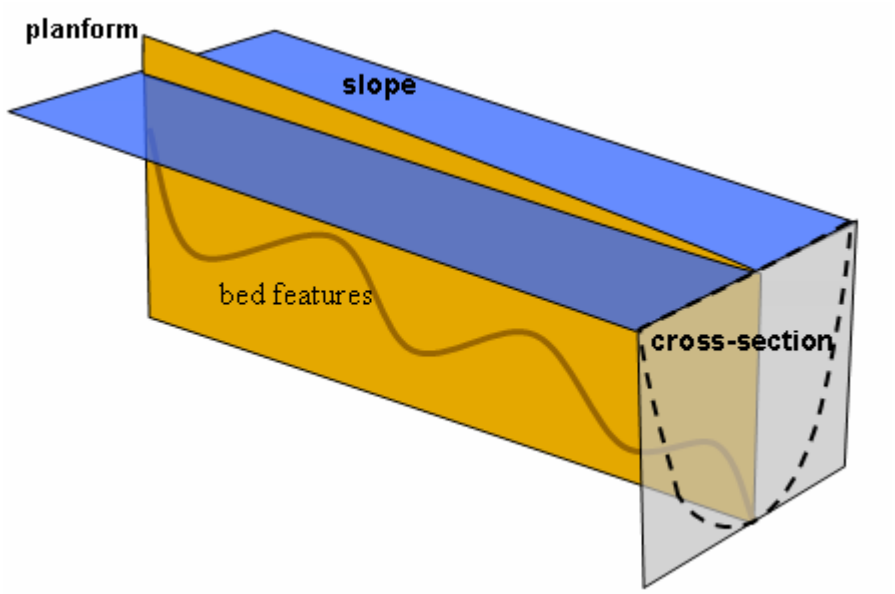

Figure 1.10 Morphological elements and planes of channel adjustment, modified from Knighton (1998).

The streams flowing through Polblue and Edwards/Barrington swamps' provide an opportunity for examining some rarely observed extremes in the adjustment of flow resistance to cross-sectional efficiency through these planes. By definition, extremes lie beyond the normal range and, therefore, they provide insights into which variables control

particular channel characteristics and how this is accomplished. This thesis documents the morphology of these unusual streams and examines the adjustments that combine to produce such morphologies.

Channel adjustments might best be viewed in the context of the force of the flow and resistance to that force. Flow force is represented by shear stress, but can be more simply considered using flow velocity (m/s) of which it is partly a function. Flow resistance can be divided into three main types: skin, internal distortion and spill (Leopold et al., 1960). *Skin resistance* is provided by contact between the flow and the channel boundary, and channels can best adjust this element by the modification of cross-sectional form. This changes the ratio between the volume of flow and the area of resisting boundary, a relationship that can be expressed in terms of the hydraulic radius (R), the ratio of cross-sectional area / wetted perimeter. *Internal distortion resistance* results from the shearing between parcels of water within the flow; such flow distortion usually results from bank and bed irregularities, bedforms and channel curvature. *Spill resistance* occurs in critical flow, or in discrete sections of sub-critical flow (Leopold et al., 1960), and is caused by abrupt changes in flow velocity resulting, for example, from abrupt channel expansion or flow changes from supercritical to subcritical. While present in many flows, spill resistance is very hard to quantify. It also comprises far less of the total flow resistance than the other two elements, especially in the slowly flowing channels that characterise Barrington Tops, and is therefore is not pursued herein.

Considerations of flow resistance adjustments in the Barrington swamp channels are based on the four morphological elements in Figure 1.10: 1. slope, 2. planform 3. bedform and 4. cross-section. Adjustments in these streams are systematically examined using each of these morphological elements, which also provide the two main types of flow resistance; skin and internal distortion. The thesis is primarily structured around these planes of adjustment.

1.4 Thesis outline

This thesis is divided into seven chapters. The five substantial chapters are conceptually linked in Figure 1.11, which illustrates the context of temporal and spatial scale comparisons between the chapters that address these varying scales. Because of these scale differences, the subject matter of each chapter is quite specific and necessitates reviews of the relevant literature early in each chapter.

Chapter 2 provides the temporal context for the channelled swamps. It reviews and builds on previous studies and adds new data on riparian stratigraphy and pollen and radiometric analyses. These results allow the construction of an evolutionary model and indicate that the channels have been present for ~1000 years and provide a temporal perspective with which to view the remainder of the thesis results (Figure 1.11).

The next three chapters are principally concerned with channel adjustment that takes place in all three planes, illustrated in Figure 1.10, each of which is dealt with in a separate chapter.

Chapter 3 quantitatively examines the interaction between channel geometry and flow hydraulics. It considers the interactions between channel shape, boundary characteristics, bed material and bed morphology, and variations in flow velocity, resistance and shear stress. The chapter primarily identifies the hydraulic efficiency of the swamp-channel cross-sections and determines system constraints.

The role that bedforms play in moderating channel flows is examined in Chapter 4. The capacity of the channels to adjust their resistance to flow by bedform development and inferred sediment supply are provided by this chapter. In some channel reaches, bedforms with unique morphologies are identified which contribute considerable flow resistance.

Chapter 5 examines the adjustment of planform as a means by which the swamp channels reduce slope and expend surplus energy. The adjustments of cross-sectional geometry and bedforms are then related to water-surface long profiles as a means of determining if these channels have achieved graded or equilibrium conditions.

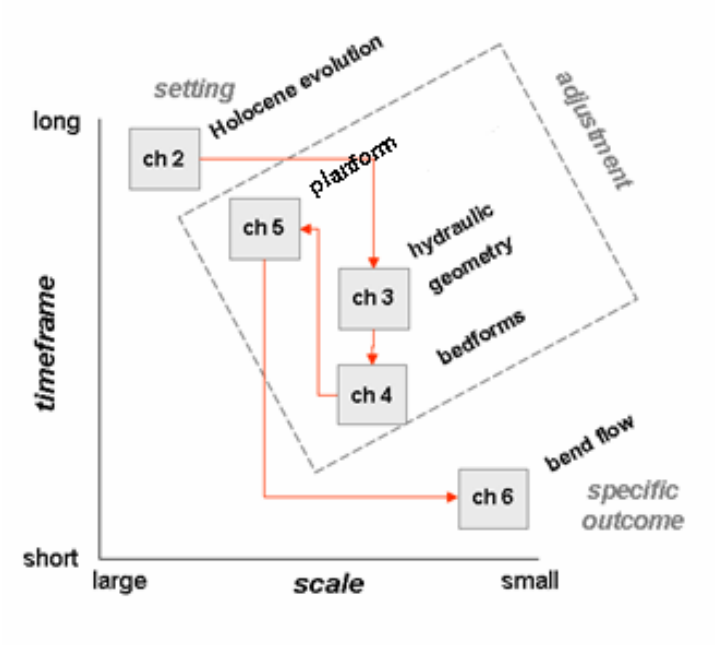

Figure 1.11 This schematic illustrates the temporal and spatial scales that are addressed in each chapter. The thesis moves from a long time-frame, swamp scale approach (Chapter 2) to a short-term, detailed investigation of bend flow (Chapter 6), via considerations of three specific modes of channel adjustment.

In order to account for the channel planform and cross-sectional morphology, and especially to account for the unusually tight bends, peculiarities in bend flow resulting from extremes in channel adjustment are examined in Chapter 6. Bend flow structures resulting from the unique cross-sectional, longitudinal and planform geometries of the swamp channels are described in this chapter. The development and maintenance of peculiar morphological features, largely specific to swamp-streams, are also described.

The results of this investigation are integrated and synthesised in Chapter 7, and the findings are reviewed in terms of the specific objectives identified earlier in this chapter. Chapter 7 concludes with the key outcomes of the thesis and suggests future research tasks.

Chapter 2 The development of the Barrington swamp channels

2.1 Introduction

Narrow, deep and sinuous swamp channels represent extremes in both the morphology and hydraulics of natural streams. However, their unusual geometry and consequent flow behaviour raises an important question. Are the channels transient features, arising as a result of predominantly non-equilibrium fluvial processes and over a short period of time, or are they more stable features in the swamp landscape, having evolved over a longer time? This chapter attempts to answer this question by reconstructing the conditions that have led to swamp-channel development using both new and existing stratigraphic, pollen and radiocarbon dating data. The purpose is to develop an evolutionary model for Edwards Swamp (containing both Edwards Creek and the Barrington River) and Polblue Swamp, and to determine the longevity and hence the stability of the channels in these systems.

2.2 Quaternary climate and swamp development

Swamps provide detailed accounts of their own vegetative and climatic history through palynological and sedimentological deposits (Hope, 2003). Radiocarbon dating of the deposits in Barrington region swamps by various authors (Dodson et al., 1986; Dodson and Myers, 1986; Dodson et al., 1994; Sweller and Martin, 2001) allow for detailed interpretations of the Late Quaternary history of these environments. However, these investigations have not incorporated the histories of the swamp channels and associated alluvium, yet on the Woronora Plateau near Wollongong (NSW), other studies have provided important information on interpretation of climate from geomorphic analyses of similar swamps (Young, 1983, 1986a, 1986b).

A synthesis of previously reported Barrington swamp Quaternary data is provided below, followed by the presentation of new alluvial stratigraphic data based on the present research.

2.2.1 Regional conditions during the Late Pleistocene

Burraga Swamp has the longest known sedimentological and palynological record of any swamp in the region. It is located on an isolated ridge, 6km south of the Barrington Tops plateau and at an altitude of 895m. The swamp has no channel drainage and has developed in an enclosed basin, which presumably formed as a result of an ancient landslip (Sweller and Martin, 2001), and has captured a possibly uninterrupted sedimentological and vegetative record of local climate change over the last 40ka.

Sweller and Martin (2001) suggest that clay sediments at the base of Burraga Swamp indicate a period of high lake levels (low energy) and low sediment input rates, indicative of a fairly dry, yet stable, hill slope environment from 40-30ka BP. The introduction of interbedded sandy material and clay deposits further up the sequence indicates an increase in energy associated with greater slope instability from a lack of vegetative cover resulting from a drying climate and low fluctuating lake levels, until 21ka BP. From 21ka BP to 17ka BP, rapid deposition of coarser material resulted from increased slope instability caused by an even drier climate, sparser vegetation and likely periglacial activity. This period culminated in maximum sedimentation rates at ~17ka BP, when conditions were at their driest and when periglacial activity peaked in south-eastern Australia (Barrows et al., 2004). However, fluctuations in sediments, from gravels and sands to silts and clays, may indicate substantial variations in slope stability and vegetative cover, even during this period. A change to finer sediments and wetter conditions occurred by 15ka BP, whereby the slopes became increasingly stable with vegetation and sediment grain size and rates of accumulation reduced. *Dicksonia* spp. pollen, a wet rainforest fern, appeared in the swamp stratigraphy around 15ka BP, indicating wetter conditions in the surrounding hills and *Nothofagus moorei*, a tree which requires even wetter conditions (>1500mm/annum), appeared around 9ka BP, then reached current levels of abundance by 6ka BP. Wetter conditions peaked around 6.5ka BP, peat began to develop and cool-temperate rainforest has since been a feature of the region (Sweller and Martin, 2001).

2.2.2 Regional conditions during the Holocene

More specific Holocene sedimentological, vegetative and climatic interpretations of the Barrington Tops have been produced using data from the Holocene swamps on the plateau. These swamps range in altitude from 1170m to 1500m, considerably higher than Burraga Swamp. Data sourced from nine swamps on the Barrington Tops and Gloucester Tops plateaus by Dodson and Myers (1986), Dodson (1987), Dodson et al. (1986) and Dodson et al. (1994) indicate that sediment deposition in these swamps started around 11ka BP. Figure 2.1 illustrates a summary log of their data. Clay sediments at the base of swamp profiles (beneath peat deposits) indicate accumulation under forested and stable conditions, whereby slowly accumulating sediments were trapped on valley floors by denser vegetation and less intense snow or snow melts (Dodson, 1987) than in the preceding period, or alternatively under open water conditions (Dodson et al., 1986). Hope (2003) found that peat swamp development in southern NSW was widespread by 10ka BP. Clay deposition gave way to peat development in some swamps at the south-eastern end of the plateau around 8.6ka BP (Dodson, 1987). This was followed by peat development in more centrally located swamps at ~5.4ka BP (even later at higher altitudes in this area - 3.3ka BP), and at about 2.5ka BP to 2.0ka BP in the north-west of the plateau, illustrating a gradient in the timing of increased rainfall across the plateau, from the south-east toward the north-west (Figure 2.1). Dodson's (1987) data are consistent with other regional data (Bowler et al., 1976; Cohen and Nanson, in prep) which suggest a Holocene peak in effective precipitation between 8-5ka BP and an associated "gap" in regional lowland-catchment fluvial-deposit basal ages spanning this same period and caused by larger river flows (Cohen and Nanson, in prep). Around this time the swamps, including Burraga (Sweller and Martin, 2001), began to accumulate peat and cool-temperate rainforests in the region reached their maximum extent (Dodson et al., 1986).

From 5.0-1.6ka BP, pollen evidence suggests a drying and cooling of the Barrington Tops region, as surrounding rainforests retreated and sediment accumulation in the swamps accelerated (Dodson et al., 1986; Dodson, 1987). Renewed rainforest expansion in

sheltered locations began 1-1.5 ka BP and in some areas as late as 500-200 years ago, likely indicating slight increases in effective precipitation (Dodson et al., 1986).

The development of channels through these swamps may have occurred either: (i) concurrently with swamp development, such as the varied open-channels described by Ingram (1983) in swamp environments, or (ii) later, following incisional events. The temporal gradient in rainfall change across the Tops during the Holocene suggests care should be taken in the application of regional climate models as broad catalysts for channel development; local factors may have more effect on the timing of this occurrence (e.g. Young, 1983, 1986a, 1986b; Proser [sic], 1987). Recent findings by Eriksson et al. (2002) in the Naas Valley, near Canberra, indicate two incisions of Holocene valley fill deposits around 1500-1200BP and 700BP, which they suggest were likely encouraged by decreased rainfall across the region during this period, but which were probably *initiated* by more catchment scale influences such as fire. Fryirs and Brierley (1998) likewise documented two incisional episodes in which Holocene valley fills were also partially excavated by narrow, deep channel development in Wolumla Creek, NSW; one prior to 840BP and another since European settlement. This latter episode is commonly acknowledged as a period of enhanced gullying across large regions of NSW (Eyles, 1977a, 1977b) and attributed to the transition from Aboriginal to European land management practices. Stanley and De Deckker (2002) suggested that the period 5.5ka BP to present has been one of instability, during which rainfall has fluctuated dramatically. Recent valley fill incisions may be a response to these conditions, combined with more localised catalysts such as fire *and* land management practices (Prosser et al., 1994) which are probably responsible for the asynchronous timing of the incision of these valley fills.

2.2.3 Mechanisms of swamp channel development

While mineralogical (sediment rich) valley fills differ significantly from organic (sediment deficient) swamp environments (Fryirs and Brierley, 1998), the timing of and triggers for channel or gully development are probably very similar. Bedrock controls at the outlet of the Barrington swamp channels have safeguarded these systems from the retreat of nick-

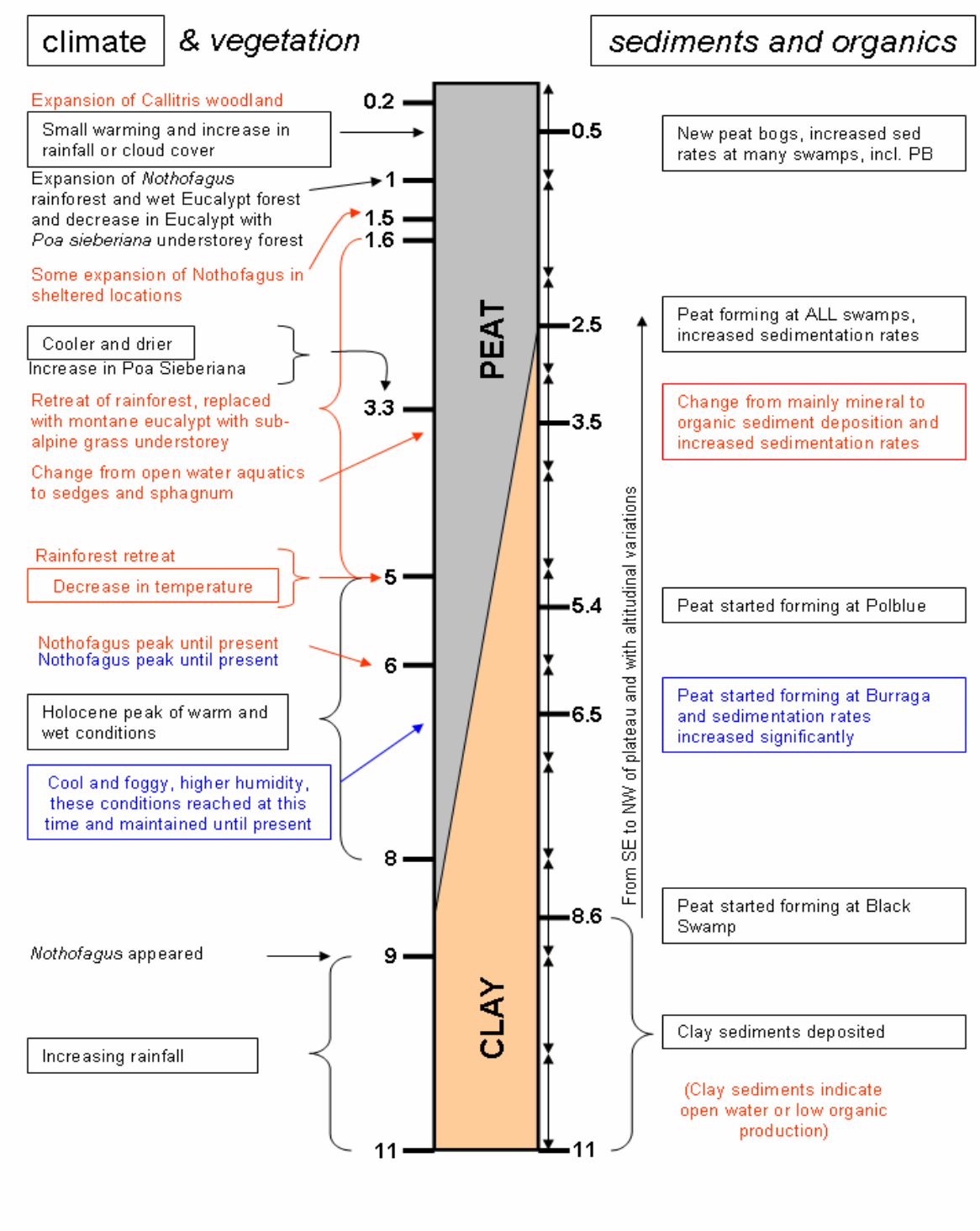

Figure 2.1 Summary and synthesis of Holocene climatic and vegetative history of the Barrington Tops. Data sources: text in red from Dodson et al. (1986), text in black from Dodson (1987) and text in blue from Sweller and Martin (2001). Ages are in ka BP and arrows on the right of the core indicate 1ka intervals.

points. Triggers for incisional channel development are, therefore, either locally specific (e.g. fire) or climatic in nature. The asynchronous timing of swamp incisions on the Woronora Plateau suggests that regional climatic shifts are not always the catalysts for swamp incision (Young, 1983, 1986a, 1986b). Despite the extensive palynological and sedimentological account of Holocene climatic conditions provided by the Barrington swamp deposits, the timing and nature of channel development within these same swamps has not been examined. As channel incision in swamps is often a catastrophic process (Southern, 1982; Hope, 2003), the apparent equilibrium condition of channels in the Barrington Tops swamps encourages further investigation to determine whether the channels formed with the swamp, or whether they became stabilised following an incisional event.

2.3 Stratigraphic techniques

2.3.1 Stratigraphic logging

A total of 61 auger holes and 18 pits were logged across 10 transects which were each passed through meander bend apices (Figure 3.3). Most transects were on the floodplain adjacent to the channels. However, one long transect of ~120m at Polblue Swamp (Auger Transect 2) was surveyed to illustrate that swamp's topography.

Sediment sampling techniques included the use of soil head (bucket) augers, D-samplers and pit excavations (Figure 2.2). Depths were estimated to be accurate to ±0.1m, owing to both compaction during augering and uneven swamp surfaces confounding accurate surface height estimations. Six transects were produced for Edwards Swamp and four for Polblue Swamp (Figure 2.3).

2.4 Stratigraphic logging results

All of the floodplain profiles in both swamp systems consisted of basal sapric peat (smooth), overlain by hemic (blocky) peat (McDonald et al., 1990), with the top of every profile comprised of at least 0.1m of fibric (poorly decomposed organics) peat and roots.

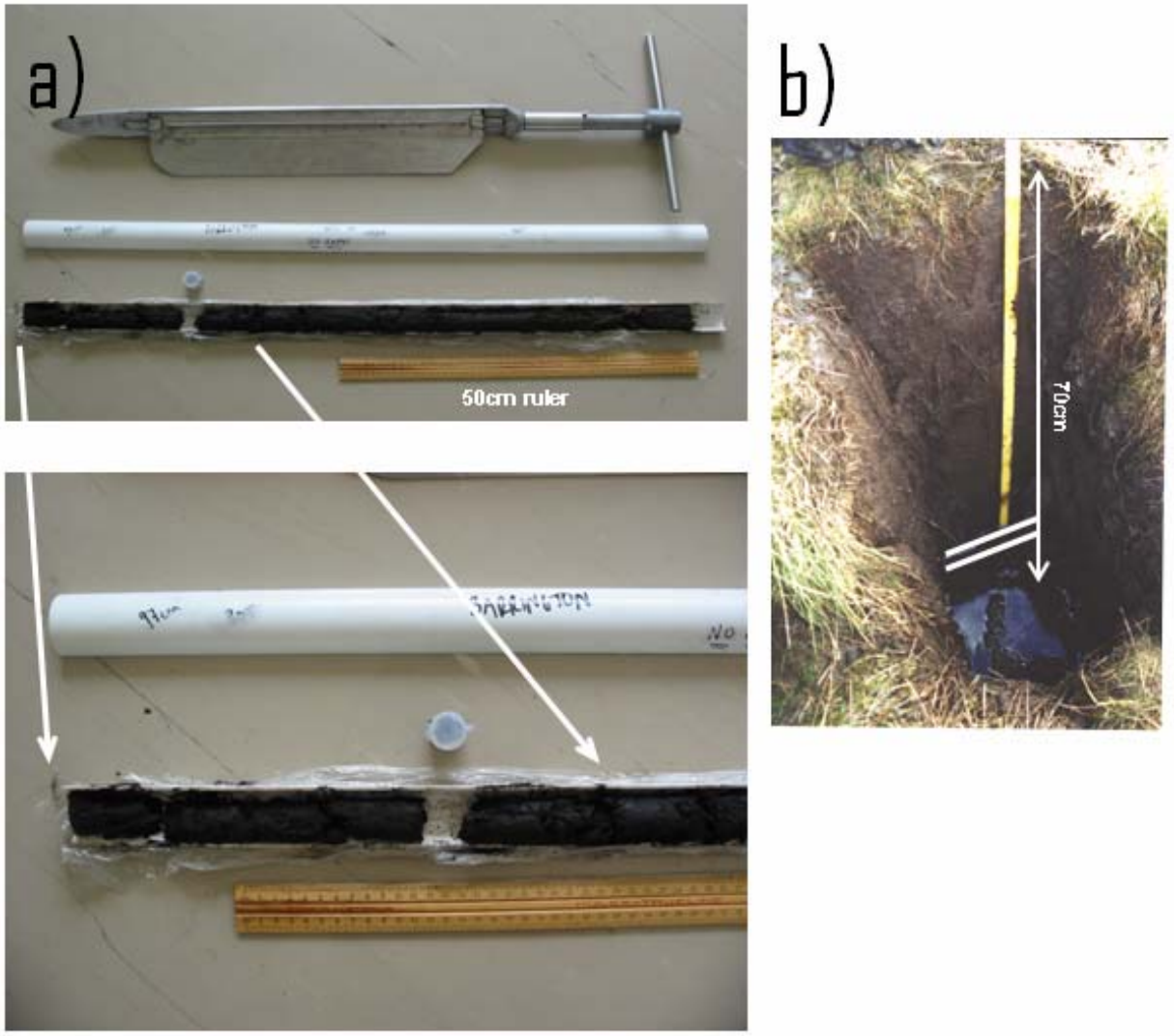

Figure 2.2 a. D-auger and b. pit stratigraphic logging and sampling techniques. Note the small vial marking the position of the AMS sample (a) and a layer sampled for standard radiometric dating, (horizontal white lines) (b), above the water table.

These sequences overlaid predominantly basal clays, in Polblue Swamp, and cobbles, in Edwards Swamp (Figure 2.3).

Many pits showed piping (up to 0.1m diameter pipes) near the low-water level water-table. Disturbed mud contaminated the water, but cleared via pipes which washed turbid water away. Turbid water was sometimes observed entering the channel, downstream of the dug pits, as obvious point-source entry flow. Some flows also pass through the peat material itself (seepage) and through underlying gravel and sand deposits *and* pipe flow (Ingram,

1983), however, the focal topics of this thesis are not significantly effected by these flow volumes and they are not considered further.

Variations in the swampy floodplain surface sometimes coincided with stratigraphic variations. Two dominant swamp surfaces were identified; the general surface of each swamp is referred to as the *upper floodplain* and the lowermost unit adjacent to the channels is referred to as the *inset floodplain.* In some cases there is an intermediate surface referred to as the *middle floodplain.*

Examples of *upper floodplain* logs illustrated either very little (Polblue Swamp) or little to no (Edwards Swamp) sand and gravel at the base of the peat profiles, immediately above basal clay or cobbles. *Inset floodplain* profiles, however, were more variable in their sedimentology, but all presented some degree of basal silt, sand and gravel interbedded or upward fining sequences, grading into peat nearer the swamp surfaces. *Inset floodplains* are thus consistent with fluvially derived deposits.

More complex stratigraphy was recorded in Polblue Auger Transect 1 and Barrington Auger Transect 5. Outer bank floodplain deposits in both transects were comprised of fining upward peat or interbedded silt, sand and gravel, respectively. These deposits appear to be fluvially derived and their position on the swamp indicates deposition via the inward migration of tight channel bends; such accumulations can be called *concave bank benches* (Nanson and Page, 1983).

All transects illustrated floodplain surfaces sloping away from the channel, resulting in large areas of saturated *back-swamp*. Such features were particularly apparent in Polblue Auger Transect 2, in which paired levees isolated the alluvial region from the remainder of the swamp on both sides of the channel. However, a fining upward sequence that may represent a previous channel position was evidenced in the fourth profile from the left bank in this transect.

The stratigraphic sequences differ primarily by the *upper floodplain* having developed classic peat profiles and the *inset floodplain* consisting of similar peat profiles, which are

underlain by interbedded or fining upward silt-gravel sediments suggestive of successive fluvial origins.

2.4.1 Radiocarbon dating

Traditional radiocarbon dating utilises the *standard radiometric* dating technique, which indirectly measures the radioactive emissions of relatively large samples. However, peat samples are prone to contamination by younger carbon through root penetration and the percolation of hemic and fulvic acids through the profile. The least mobile of all carbon matter in peat is the pollen fraction (Vandergoes and Prior, 2003). This component, however, comprises a very small portion of the total sample and requires the application of the *Accelerator Mass Spectrometry (AMS)* radiocarbon dating technique, which directly measures the number of ^{14}C atoms and therefore requires a smaller sample. The *AMS* technique is more expensive than the *standard radiometric* technique and a combination of both techniques was therefore applied to this research.

D-samplers were used to collect eight samples for *AMS* radiocarbon dating by the Australian Nuclear Science & Technology Organisation (ANSTO). Discs of peat 1.5cm thick were extracted in the laboratory from solid cores (Figure 2.2a). Sample pre-treatment prior to measurement was approximately consistent with the technique described by Vandergoes and Prior (2003). At the Department of Archaeology and Natural History preparation laboratory of the Australian National University (ANU), peat samples were sieved through 180μm mesh, then heat treated with HCL and NaOH and centrifuged to isolate the pollen fraction. Pollen analyses were also conducted on the AMS samples to determine the dominant vegetative species at their time of development and to search for possible contaminants.

Four samples were obtained from the walls of pits dug into the swamp surface (Figure 2.2b) for *standard radiometric* dating at the Waikato Radiocarbon Dating Laboratory. They were separated into fine and coarse fractions by wet sieving through a 2mm mesh, and then chemically treated with HCl and NaOH to remove most contaminants prior to measurement.

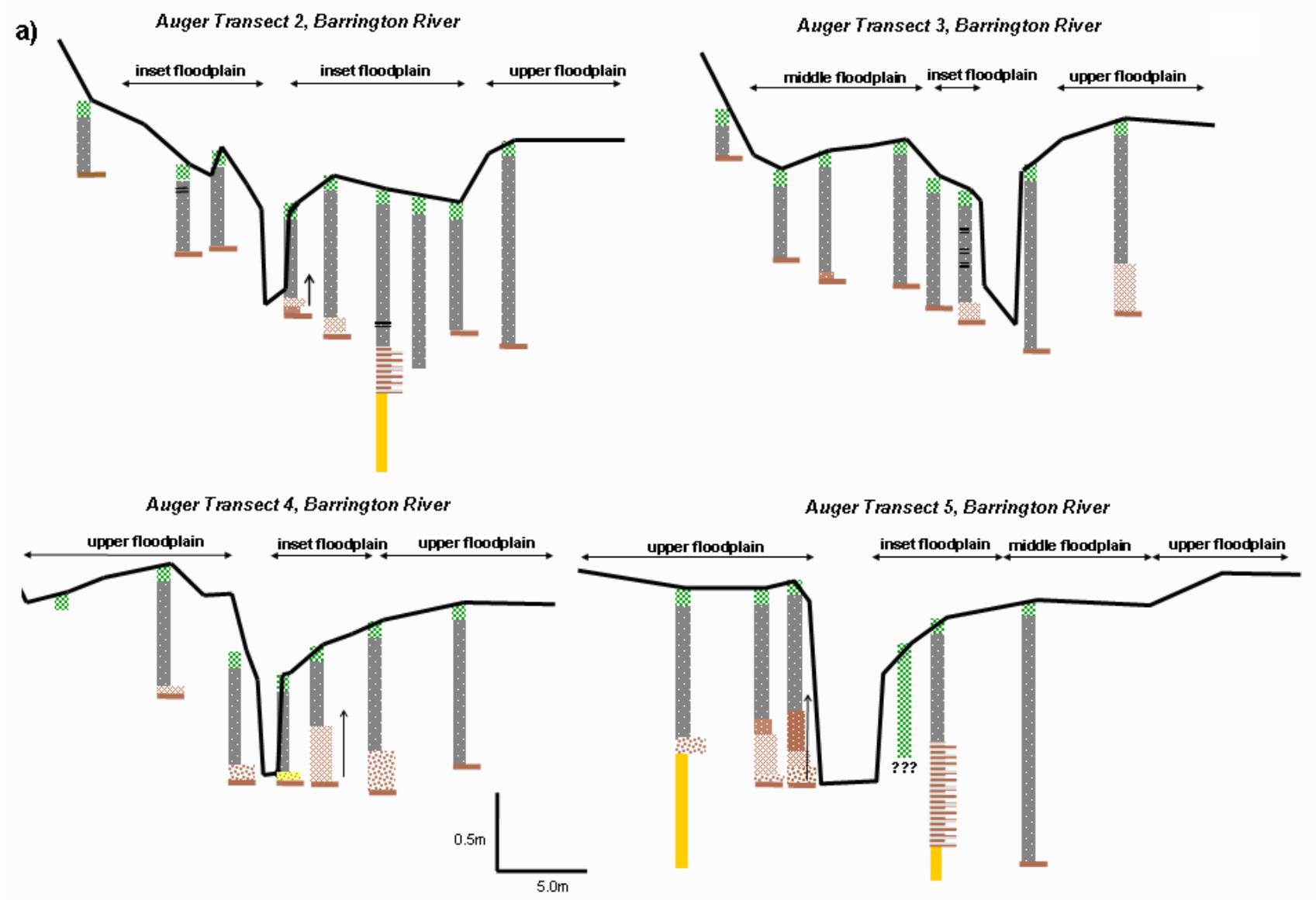
a)
Auger Transect 2, Barrington River
inset floodplain
inset floodplain
upper floodplain
Auger Transect 3, Barrington River
middle floodplain
inset floodplain
upper floodplain
Auger Transect 4, Barrington River
upper floodplain
inset floodplain
upper floodplain
0.5m
5.0m
Auger Transect 5, Barrington River
upper floodplain
inset floodplain
middle floodplain
upper floodplain
???

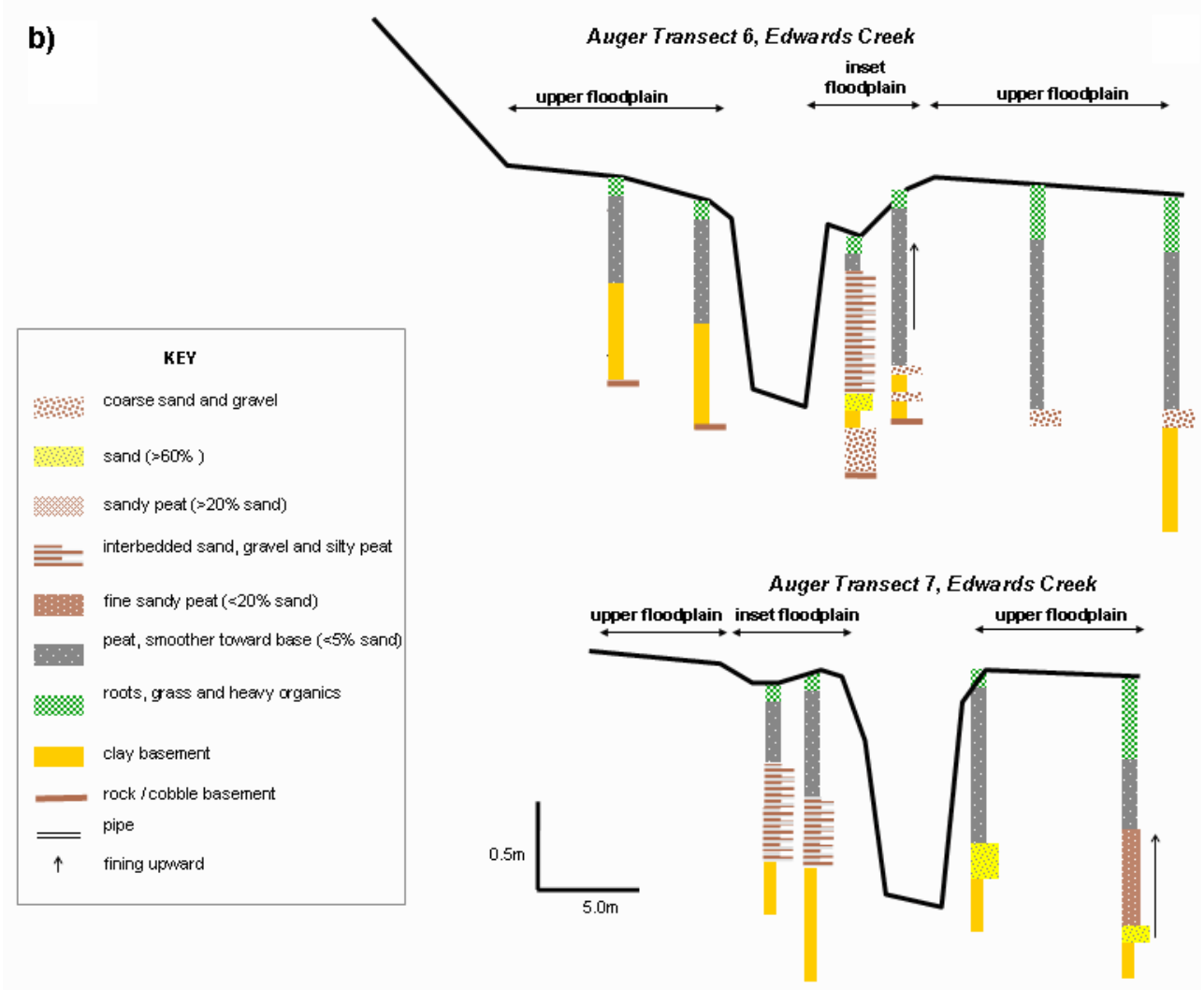

Figure 2.3 Auger transects (a) Barrington River within Edwards Swamp, (b) Edwards Creek within Edwards Swamp and (c) Polblue Creek within Polblue Swamp.

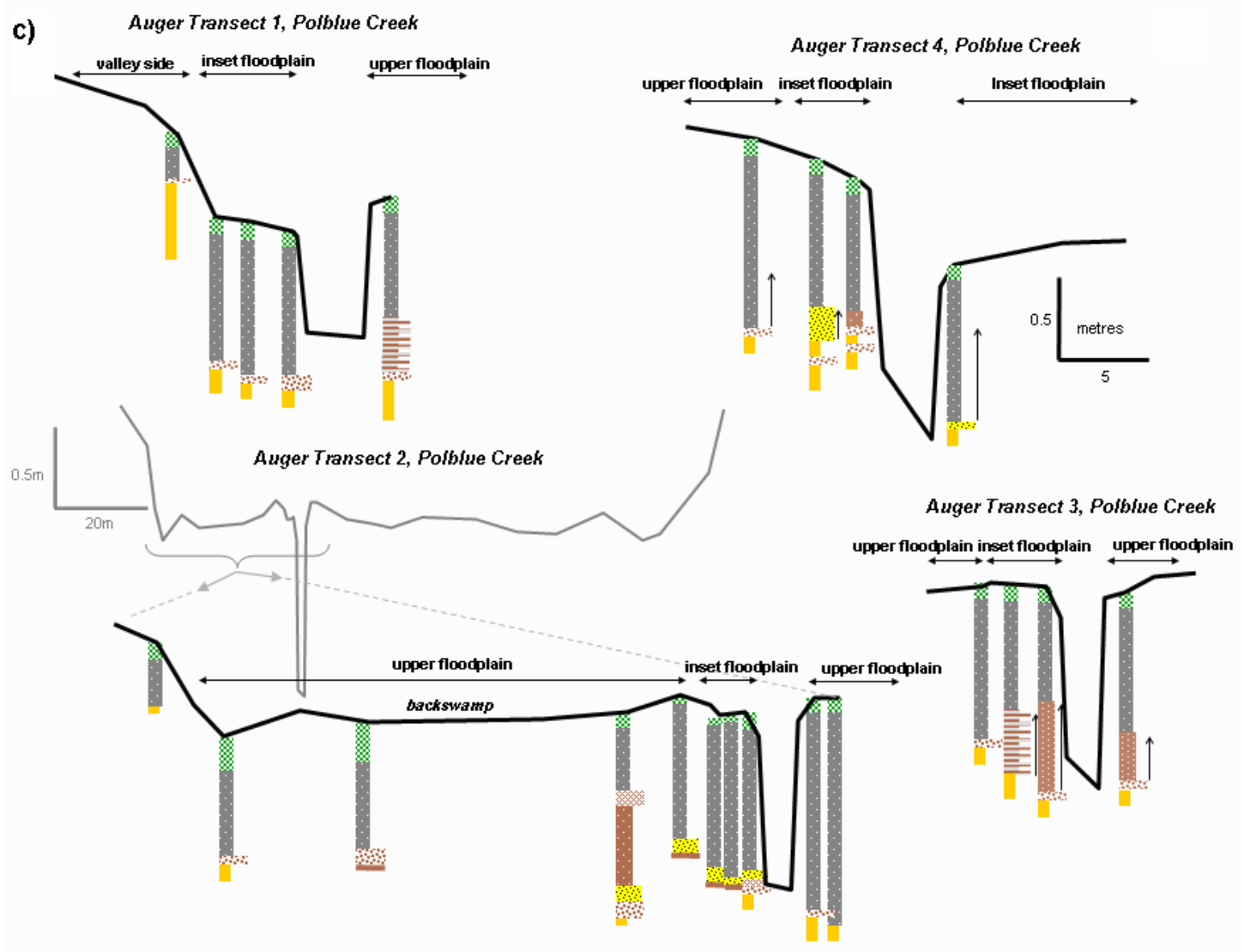
c)
Auger Transect 1, Polblue Creek
valley side
inset floodplain
upper floodplain
Auger Transect 4, Polblue Creek
upper floodplain
inset floodplain
Inset floodplain
0.5
metres
5
0.5m
20m
Auger Transect 2, Polblue Creek
Auger Transect 3, Polblue Creek
upper floodplain
inset floodplain
upper floodplain
backswamp
upper floodplain
inset floodplain
upper floodplain

Samples determined using standard radiometric dating were collected from the cleaned walls of shallow pits and their retrieval was restricted to a constant layer <0.1m in height (Goudie, 1990), with sampling extending as a recess into the pit wall (Figure 2.2b). Four samples from the Barrington River Transect 2 in Edwards Swamp were collected.

2.5 Radiocarbon dating, pollen analyses and stratigraphic interpretation

Radiocarbon dating was used to interpret the chronology of the two major swamp units in each swamp along each major watercourse; the *upper floodplain* (or general swamp unit) and the *inset floodplain*. These are illustrated in Figure 2.4.

Twelve radiocarbon dates were obtained for eleven stratigraphic units across three transects (Table 2.1). Two dates from samples taken in the same stratigraphic horizon in the same log were used to compare results from the standard radiometric and AMS dating techniques; these paired dates were statistically inseparable (770±50BP and 770±61BP, respectively) and thus supported the direct comparison of results obtained by the two techniques. Standard radiometric dates are illustrated within the dated transects in Figure 2.4. Relative amounts of wet forest, dry forest, shrubs, herbs and aquatic pollen species for each of the AMS dated samples are illustrated in Figure 2.5 and provide a guide to the prevailing regional conditions during swamp development.

Full pollen analysis results, on which the summary Figure 2.5 is based, are provided in Appendix 2.

The Barrington Auger Transect 2 was the most extensively dated transect and the following sequence is interpreted from this example. The *upper floodplain* unit commenced forming within 20m of the present channel by approximately 3600 BP. The *inset floodplain* unit in Barrington River transect yielded two basal dates: 800±60 BP and 770±61 (AMS) or 770±50 BP (standard radiometric), indicating that this unit commenced forming at a time when *Nothofagus moorei* rainforests were again expanding and conditions were becoming wetter across the region (Dodson, 1987). A near-surface (and near channel) sample of this same profile yielded a date of 659±61 BP. Evidently, the development of this unit was rapid and has slowed significantly since ~660 BP (Figure 2.6). Additional samples from the

inset floodplain at the outer bank provided dates of 697±43 BP near the base of the profile, to 533±49 BP nearer the surface. These are not statistically different from the inside of the bend and illustrate rapid vertical accretion during the development of this alluvial reach (Figure 2.6).

Table 2.1 Radiocarbon dates, both AMS and standard radiometric techniques. All dates are expressed as *conventional* ages, by which years BP relate to the year AD 1950 and the *Libby half-life* of 5568 years was applied. Shaded dates represent the same unit, dated using both techniques.

Dating laboratory code	Sample ID	Depth (from surface) (m)	Date	Error (1 S.D.)
Australian Nuclear Science and Technology Organisation (ANSTO) - AMS				
OZH937	BAR 2-H5-1	0.75	770	50
OZH938	BAR 2-H6.5-1	1.09	800	60
OZH939	BAR 2-H8.5-1	1.22	3580	50
OZH940	EDW 6-H3-1	0.90	1220	40
OZH941	EDW 6-H4.5-1	1.06	950	40
OZH942	PBL 2-H1.5-1	0.88	1010	40
OZH943	PBL 2-H4.5-1	0.81	650	50
OZH944	PBL 2-H7.5-1	0.80	970	40
The University of Waikato Radiocarbon Dating Laboratory – Standard radiometric				
Wk-15443	Jun AT 2H3 10-15	0.13	533	49
Wk-15444	Jun AT 2H3 55	0.55	697	43
Wk-15445	Jun AT2 H5 20-25	0.23	659	61
Wk-15446	Jun AT2 H5 80	0.80	770	61

This transect therefore illustrates peat development from at least ~3600BP, at which time pollen results illustrate more abundant *true* aquatics (Restionaceae spp.) and fewer sedges (Cyperaceae spp.) (Figure 2.5), indicative of wetter conditions, followed by *inset floodplain* growth from 800BP. Rapid vertical accretion of the *inset floodplain* continued until approximately 660BP, during which time the pollen record illustrates the persistence of wet conditions, but with fewer *true* aquatic plants (Restionaceae spp.) than at the base of the *upper floodplain*, and with more abundant species of tussock grasses (Poacaeae spp.) (Figure 2.5).

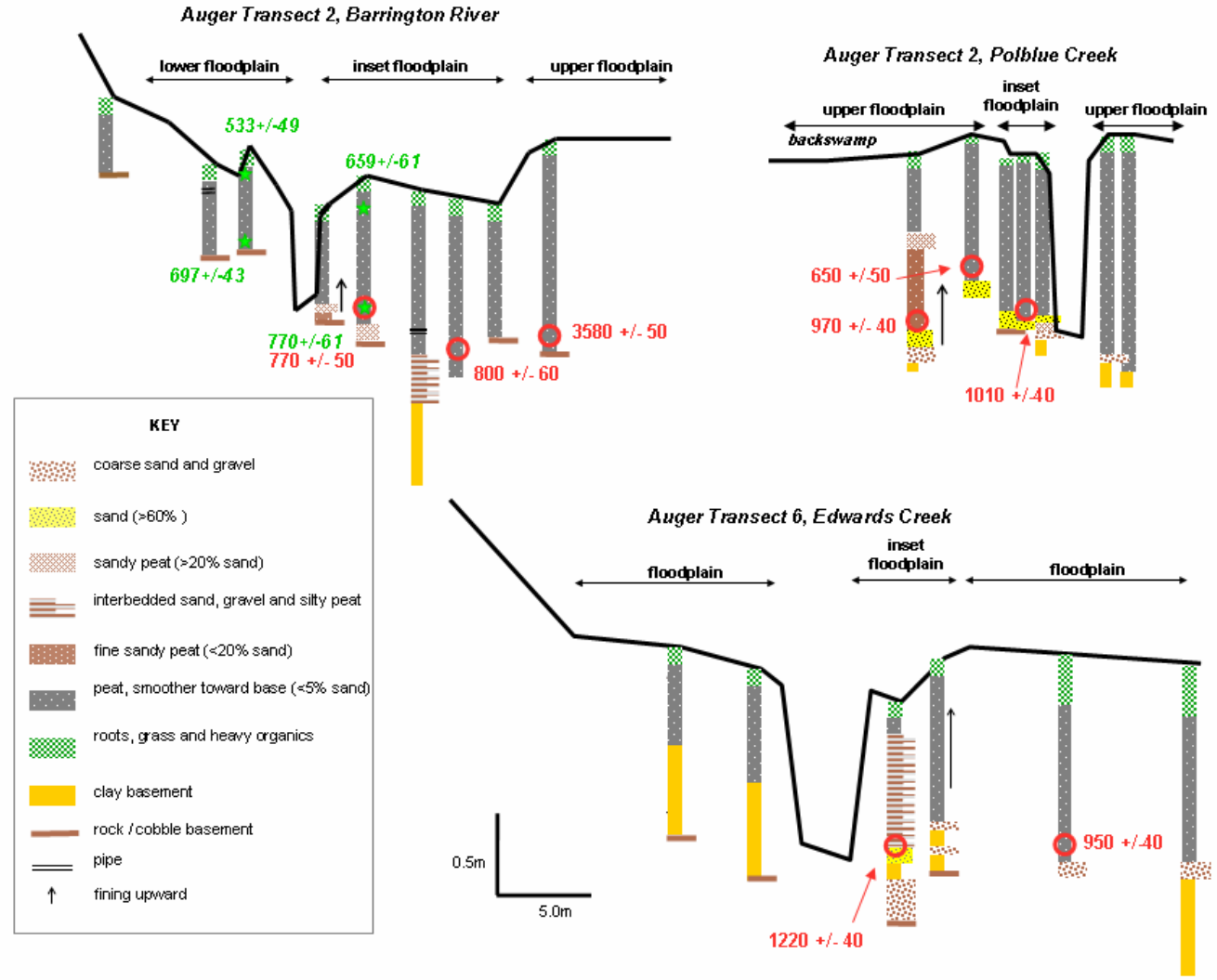

Figure 2.4 Morphostratigraphy and chronology of transects traversing the two major channels of Edwards Swamp (Edwards Creek and Barrington River) and of Polblue Swamp. Red circles represent AMS dated samples and green stars represent standard radiometric dated samples.

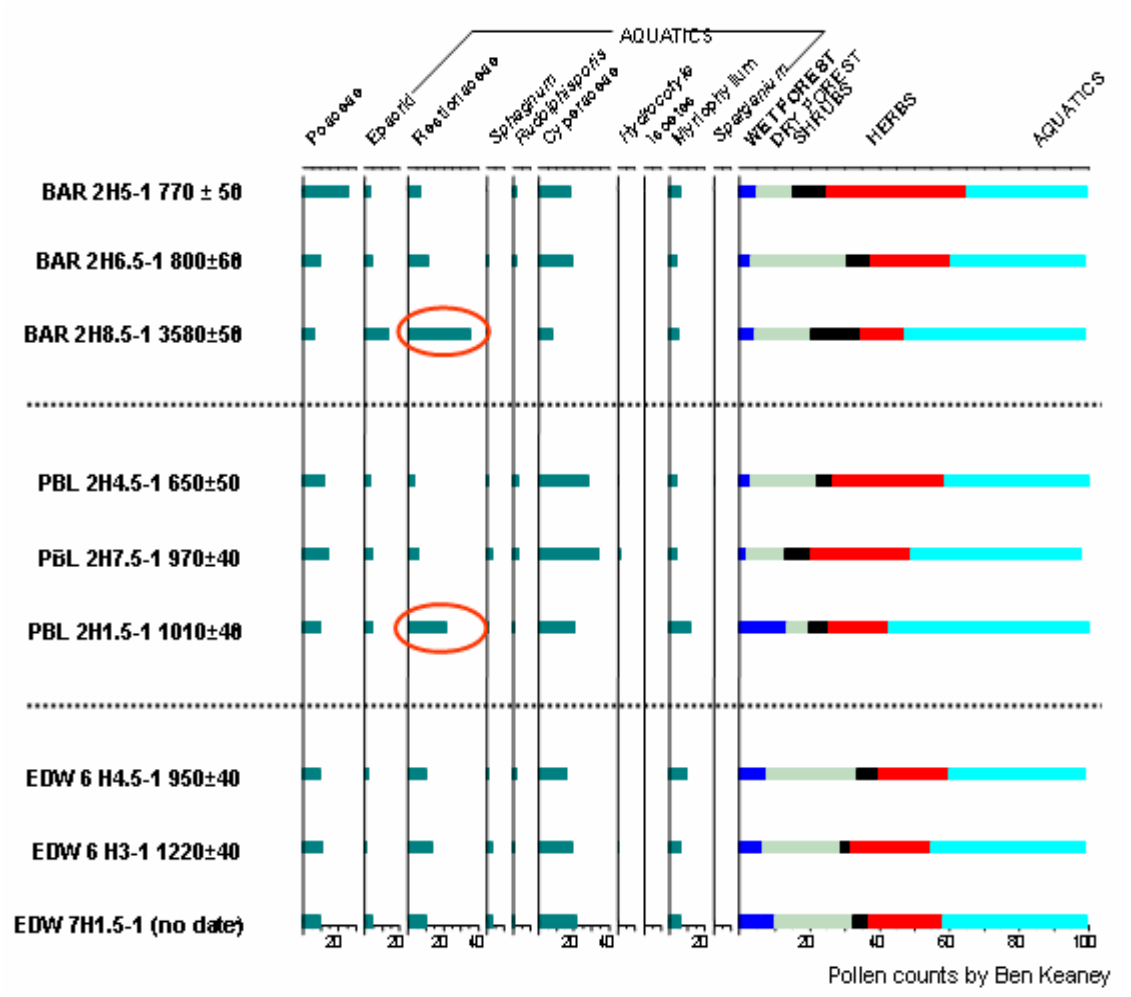

Figure 2.5 Pollen summary diagram for all AMS dated samples and sample EDW 7H1.5-1. Circled counts highlight particularly high levels of *Restionaceae*, a genus that is indicative of saturated (and therefore likely unchannelled or back-swamp) conditions.

Dodson (1987) identified increased accumulation rates within several swamps across the Tops during the last few centuries, however the results presented here suggest that rapid peat growth was also occurring at about 800 to 500 BP on the *inset floodplain* (Figure 2.4 and Figure 2.6). Since this time, slow accumulation of peat deposits have persisted within this unit, indicated by the proximity of ~500-600 year samples near the units surface (Figure 2.6). It is proposed that this change in rate may be the result of within-swamp hydrological controls rather than overall climate change. In other words, the *inset floodplain* surface grew vertically until reaching the approximate height of the *upper*

floodplain and then slowed as the surface reached the elevation of the broader swamp surface and became inundated less frequently. Thus far, the incised swamp model is favoured over the co-evolution of the swamp and the channel owing to two key results: the higher proportion of saturated pollen species in the older (*upper*) floodplain and the rapid growth of the younger (*inset*) floodplain to just below the older floodplain elevation. This means that growth rates for swamps are not necessarily just climatically controlled and emphasises the points made by Young (1983; 1986a; 1986b); the geomorphic history of a swamp must be understood as hydrological conditions (e.g. channel development) may influence swamp vegetation and hence pollen preservation and the interpretation of climatic records.

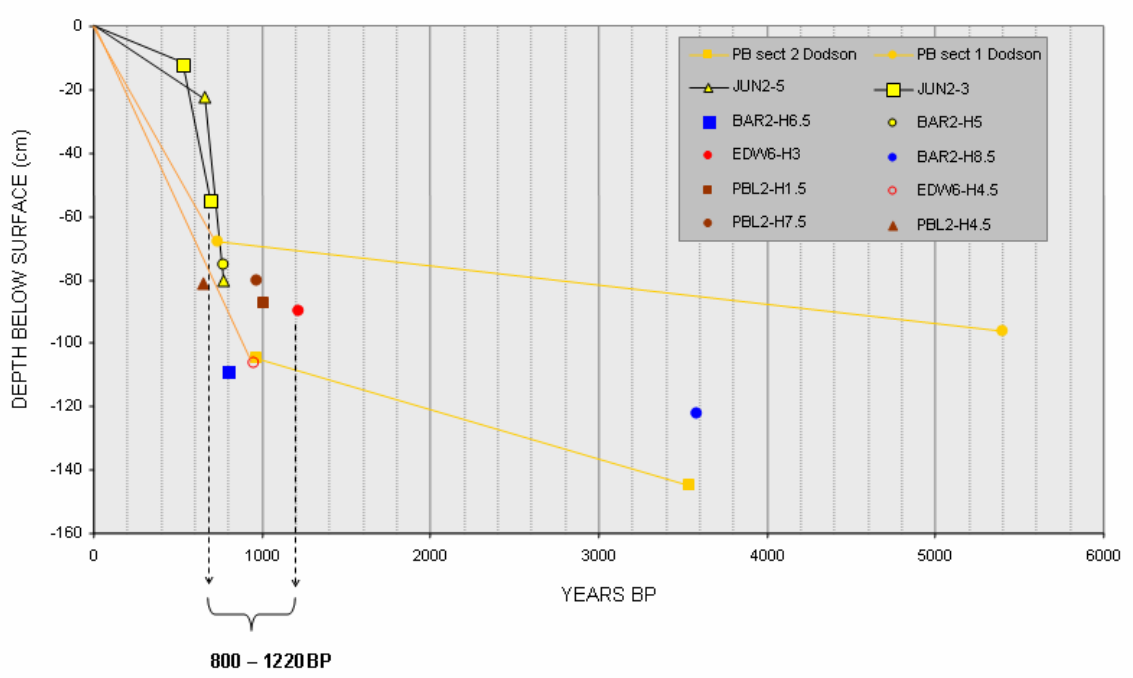

Figure 2.6 Combined data from Dodson (1987) and new results (presented in this thesis), illustrating slow growth rates of the swamps prior to 800-1220BP and then more rapid growth in auger holes JUN2-5 and JUN2-3. The basal dates of inset floodplain features cluster around 800-1220BP and represent a period of inset floodplain growth, probably following swamp incision.

The second dated transect, Edwards Auger Transect 6, is located 250m upstream of the confluence of Edwards Creek and the Barrington River, and shows a somewhat different result to that of Barrington Auger Transect 2. Despite the topographic inference of differing units, radiocarbon dates support a vertical accretion model for a unit spanning the entire

transect; the basal sample near the channel beneath the *inset floodplain* produced a date of 1220±40 years BP, an era associated with the onset of increased effective precipitation across the region (Dodson, 1987), and the nearby date of 950±40 BP beneath the upper floodplain most likely reflects a simple upward growth of the same *inset floodplain* unit. As this transect also dissects the Edwards Swamp, it is expected that basal deposits in the *upper floodplain* further from the channel would yield older dates, similar to that at Barrington Auger Transect 2 (~3600BP). All pollen analyses of the Edwards Auger transect 6 samples also illustrated very similar vegetation structure to the *inset floodplain* of the Barrington Auger Transect 2 samples. It is thus proposed that this transect also illustrates a period of swamp incision dating back to approximately 1220BP, since which time the swamp has rebuilt this *inset floodplain* and developed the channel. Since the formation of the inset unit, the channel has likely been confined to a location *near* its current position, with interbedded silt, sand and gravel deposits on the inner bank *inset floodplains* probably indicating early point bar deposits. The timing of the onset of *inset floodplain* development in Edwards Creek is similar to the 800BP date for the same unit in the Barrington River transect. Wetter, or fluctuating (Stanley and De Deckker, 2002), conditions from around 1ka BP (Dodson, 1987) may be responsible for the timing of the growth of these inset units.

The third and last dated transect, Polblue Creek Auger Transect 2, is similar to Edwards Auger Transect 2 in that topographic variations in swamp height do not correspond to different basal ages. A basal date of 1010±40 BP near the channel beneath the *inset floodplain* is statistically no different to a slightly deeper sample taken further from the channel of 970±40 BP beneath the *upper floodplain*. Beneath a levee-like surface between these two dates, but at a shallower depth, another date of 650±50 BP was obtained. As Dodson (1987) found that Polblue swamp commenced peat development around 5.4ka BP, it is proposed here that the dated sediments presented herein illustrate an incisional episode ~1ka BP, since which time the *alluvial* swamp reach has redeveloped via vertical accretion and vegetation growth. Persistence in swamp species, indicated by the pollen analyses, within these three samples support this argument; moderate levels of *true* aquatics, such as Restionaceae, and prolific sedges (Cyperaceae) indicate wet, yet unsaturated, conditions, supportive of channelled conditions (Figure 2.5). Slightly higher levels of Restionaceae

associated with the ~970BP sample probably indicate its back-swamp (and hence more saturated) position, rather than radical changes in vegetation or swamp hydrology.

While the swamp incision model is favoured by the rapid growth rate of the Barrington Auger Transect 2 *inset floodplain*, and by the change from saturated to only wet pollen species in this same transect, there remains the possibility that the channels were existent in these swamps during their growth, consistent with the "open channels" described in other swamps (Ingram, 1983). The following section therefore details both models.

2.5.1 A model of channelled swamp development

A five phase model of swamp evolution, based on both the results presented here, and on other detailed dated chronologies in the region (Dodson et al., 1986; Dodson, 1987; Dodson et al., 1994; Sweller and Martin, 2001), is illustrated in Figure 2.7 and described below.

Phase 1

Basalt cobbles were probably deposited on the valley floor as a result of periglacial activity during the last glacial maximum (LGM). Such activity was widespread in south-eastern Australia's upland regions from 16 000BP to 23 000BP (Barrows et al., 2004), and extended to altitudes as low as 600m in some areas (Galloway, 1965).

Phase 2

Clay sediments, probably washed from the valley sides, were deposited over the bedrock valley floors, and amongst the periglacially deposited cobbles, prior to 11 000BP in most of the swamps in the study region. This was a response to an increase in vegetative cover and associated valley-side stability brought about by warmer and wetter conditions following the LGM (Dodson et al., 1986; Dodson, 1987; Dodson et al., 1994; Sweller and Martin, 2001).

Phase 3

The onset of peat formation in Edwards Swamp occurred at least prior to ~3600BP and data presented by Dodson et al. (1986) indicates that Polblue Swamp initiated peat formation around 5400BP. Pollen evidence from Edwards Swamp suggests that conditions were

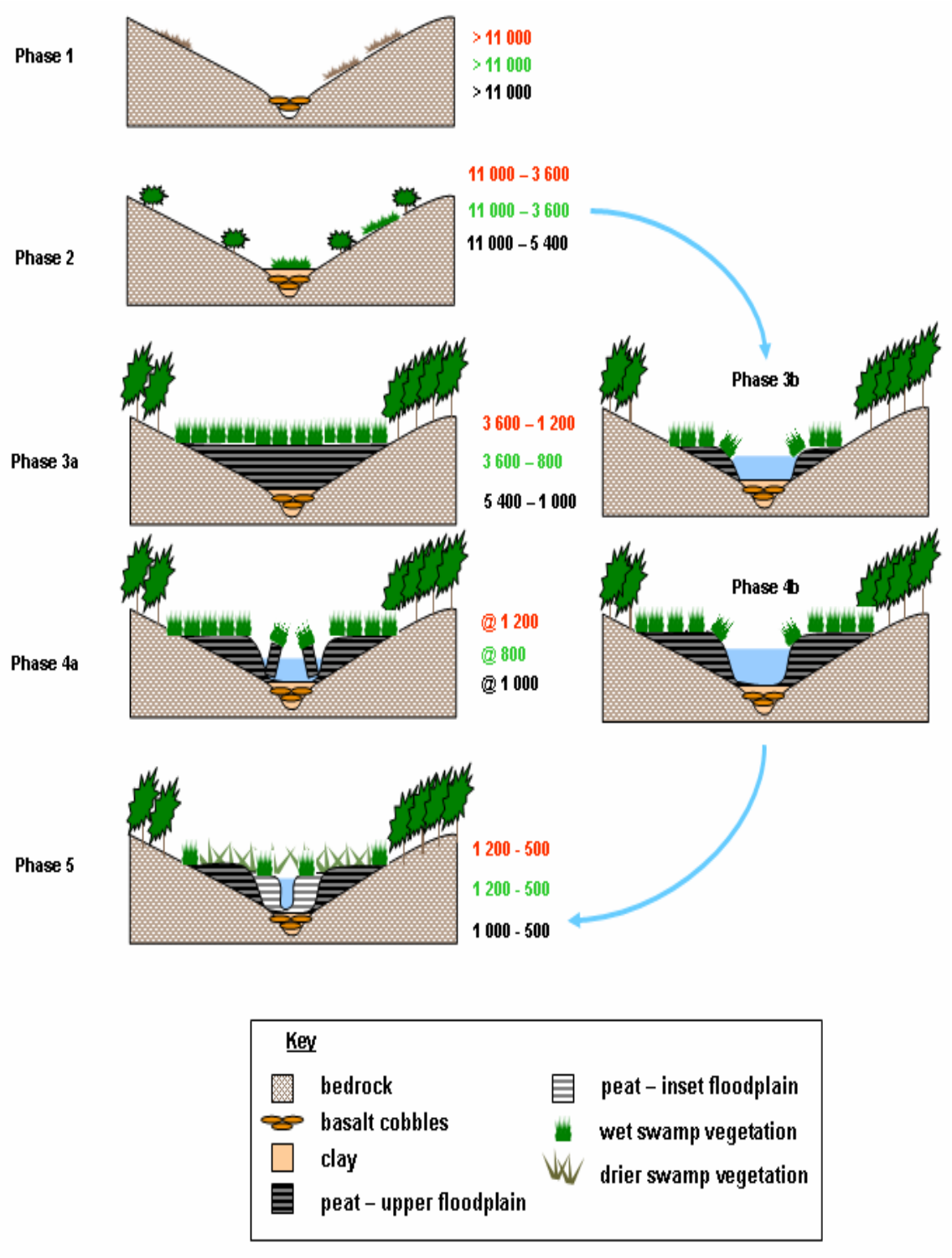

Figure 2.7 Phases in Edwards and Polblue swamp evolution, based on new and existing (Dodson 1987) data. Phases are described in the text and ages are provided for Edwards Creek in red, Barrington River in green and Polblue Creek in black.

saturated and that the water table was fairly constant. There are two possible explanations for the conditions of Phase 3. Based on pollen data, the favoured model (Phase 3a) is that the swamps were essentially unchannelled at this time. The second model (Phase 3b) considers that a relatively large channel may have existed in each swamp, similar to the "open channels" described in other swamp environments (e.g. Ingram, 1983; Hope et al., 2005) during their peat development.

Phase 4

If swamp incision commenced along what are now the Barrington River, Edwards Creek and Polblue Creek prior to ~800, ~1220 and ~1010 BP, respectively, then their timing broadly conforms to the onset of higher effective precipitation in the region ~1000BP (Dodson, 1987). Clustered basal ages around this era from all *inset floodplain* samples support this regional trend (Figure 2.6). It is likely that more open vegetation cover, inherited from previously drier conditions, responded to increasing rainfall by producing flashier flow conditions conducive to incision of the swamps (Phase 4a). These conditions are much like those proposed by Stanley and De Deckker (2002) for the latter Holocene in southern NSW. Furthermore, drier conditions prior to 1ka BP may also have made swamps more susceptible to burning by either lightening strike or Aboriginal land use (e.g. Hughes and Sullivan, 1981; Hope, 2003), which when combined, essentially primed these systems for incision by concentrated runoff from larger storms or wetter conditions.

Alternatively, the swamps may have gradually accreted beside relatively large channels. However, Phases 3 and 4 (a) are favoured as pollen evidence suggests less saturated conditions within the *inset floodplain* than in the *upper floodplain* in the Barrington Transect. Furthermore, rapid vertical growth of the Barrington *inset floodplain* supports the idea of a disturbed swamp quickly reattaining stability by the vertical growth of an *inset floodplain*. However, the reliance of the 3 and 4 (a) phases on a single basal pollen sample illustrating more saturated conditions, and on data from the same transect suggesting rapid vertical growth of the *inset floodplain* unit, cannot adequately disprove Phases 3 and 4 (b).

Phase 5

Channel development likely occurred concurrently with the growth of the *inset floodplain*. Plant species from the base of the inset units are adapted to fluctuating water levels. Observed bankfull flows occur on a regular basis to equally fill the modern channels along their lengths. Such a close relationship between the surface elevation of the *inset floodplain* and channel hydrology implies that the two elements have developed concurrently, similar to the development of leveed channels in the Kutai swamps of Kalimantan that are described by Hope et al. (2005). The Barrington swamp data also indicate rapid *inset floodplain* accumulation from ~1ka BP to 500 BP and the persistence of channels since then.

2.6 Swamp channels as fluvial systems?

Basal dates from the *inset floodplains* provide no evidence for any substantial lateral migration of these channels. Lateral stability, caused by high bank strength and relatively low stream powers, has been reported in other swamp channels (Garofalo, 1980; Jurmu and Andrle, 1997; Jurmu, 2002), however, similarities in the morphology of swamp and alluvial channels indicate that self-adjusting fluvial mechanisms *must* operate in the channels. Contemporary observations indicate undercutting of the outer channel banks in bends and the deposition of small amounts of coarse sand and gravel at the inner banks as point bars. Periods of prolonged low-flow, observed during the course of this study, encouraged vegetative growth on point bars and subsequent redeposition of coarser materials on these features during higher flows. It is likely that very slow channel migration and cross-sectional adjustment may be occurring along some reaches, particularly in tight bends, despite a lack of supportive radiocarbon evidence in the selected transects. The dated transects were located in fairly open bends and these may have undergone less dramatic planform adjustment than the tighter bends.

Outer bank fining upward sequences were also observed in some (undated) swamp transects and are indicative of concave-bank bench development in very tight bends. Such deposits form as bends migrate back through their convex banks (*inset floodplains* or effectively point bars) and build up materials in the slack-water created by separation zones

attached to the concave bank (Nanson and Page, 1983). This phenomenon will be examined more thoroughly in a later chapter (Chapter 6), but at present supports the notion that these channels *are* capable of some migration and hence planform and cross-sectional adjustment.

A comprehensive analysis of swamp channel morphology in three streams in the United States was provided by Jurmu and Andrle (1997) and Jurmu (2002) in which they illustrated unusual, but clearly fluvial, channel morphologies. Despite the lateral stability of the Barrington swamp channels, they are also clearly fluvial in their morphology and hence in their behaviour, and have persisted in the swamp landscape for at least the last ~800 years. They will be examined throughout the remainder of this thesis using conventional techniques applied to channels that are capable of self-adjustment. While the work of Jurmu and Andrle (1997) and Jurmu (2002) has focused primarily on the morphology of swamp streams, little data has yet been provided on the hydraulics of flow in such channels. This thesis will now examine the interaction between the channel geometry and flow of the streams that have formed in the Barrington Tops swamps.

Chapter 3 Hydraulic geometry

3.1 Introduction

Freshwater swamp streams represent conditions well beyond the normal range of hydraulic geometry studies. Their extremes provide useful insights into the variables and processes that control particular channel characteristics.

The Barrington swamp streams transport very little bedload and have exceptionally resistant banks. This chapter describes the theory of hydraulic geometry approach. It then applies the concept to both channel cross-sections (at-a-station) and to channel reaches (downstream), to enable the identification of the controls on these channels and their adjustment to these controls.

While the general morphology of freshwater swamp streams has received increasing attention (Garofalo, 1980; Jurmu and Andrle, 1997; 2002; Smith and Perez-Arlucea, 2004), a lack of data exists for their hydraulic geometry. Some data are available from tidal salt marshes (e.g. Myrick and Leopold, 1963; Ashley and Zeff, 1988; Zeff, 1988, 1999), however, despite similarities between freshwater and estuarine swamp channel geometries, the controls on these systems are obviously very different, particularly with respect to the directions of flow and role of riparian vegetation.

Perhaps the most visually striking features of the Barrington swamp channels are their clear water, which frequently flows at close to bankfull, and their very low width/depth ratios, generally between 1.2 and 4. The clear water allows easy observation of the vertical, vegetated and overhung banks and the roots that bind the bank material together (Figure 3.1). An immediate assumption may be that their channel geometry is primarily due to remarkably high bank strength and that channel morphology is primarily the result of botanical, rather than fluvial, processes. Upon more detailed inspection it becomes apparent that while bank vegetation remains relatively constant, the geometry of the channels varies along their length, and that a more comprehensive examination of controls other than vegetation is warranted.

In this chapter the at-a-station and downstream hydraulic geometry are first defined and their literature reviewed. Both sets of relationships are then described for the Barrington Tops swamp channels before they are interpreted and compared with results from other environments. The unusual results obtained in this study are then examined in the context of controls on the system, the ultimate objective being to document the hydraulic geometry of these channels and to determine what controls their hydraulic and morphological characteristics.

Figure 3.1 Aerial view of clear water flowing through a narrow and deep section of channel with vegetation overhanging the vertical banks. Water is approximately 1m deep and 1m wide, and is flowing from the top to the bottom of the page.

3.2 Hydraulic geometry literature review

Equilibrium channels that are not eroding or filling with sediment have been referred to as 'regime' channels, a term coined by Lindley (1919). Regime equations were developed by Anglo-Indian engineers in the late 19th and early 20th centuries to design stable irrigation canals (Lacey, 1930; Blench, 1952). The relations require that a condition of steady-state equilibrium must exist over the short term, as a channel will adjust its solid boundary to accommodate imposed conditions and will maintain this shape over at least the short time

scale (Knighton, 1998). However, regime relationships were not intended for application to natural channels. Instead, the hydraulic geometry approach was pioneered by Leopold and Maddock (1953) as a technique for examining the cross sectional morphology and flow characteristics of natural channels.

Channel geometry is the measured cross sectional shape of the channel. When this shape is related to channel discharge it is termed the hydraulic geometry. Hydraulic geometry can be measured at a single channel cross-section (station) as the discharge changes during a flood, or can be measured through a series of stations (usually in the downstream direction) at a defined discharge condition. The former is termed *at-a-station* hydraulic geometry and the latter *downstream* hydraulic geometry (Leopold and Maddock, 1953). Discharge (Q), an independent variable, is the product of the dependent variables of width (w), depth (d) and velocity (v), and this relationship is described by the continuity equation:

$$Q = w\ d\ v$$

Because exponential bivariate relationships can be defined between discharge and width, depth and velocity:

$$w = a\,Q^{b}$$

$$d = c\,Q^{f}$$

$$v = k\,Q^{m}$$

and as

$$Q^{1} = aQ^{b}\ cQ^{f}\ kQ^{m}$$

therefore

$$b + f + m = 1$$

and

$$a\ c\ k = 1$$

As width, depth and velocity determine channel discharge, a change in any of these three variables will result in a compensatory adjustment of the other two, reflected in variations

in coefficient and/or exponent values. At-a-station hydraulic geometry is the relationship between channel width, depth and velocity with increasing discharge for any given cross-section, from low flow to bankfull. Downstream hydraulic geometry is the relationship between discharge and changing width, depth and velocity values measured at a selected discharge condition that increases through a series of stations within or between catchments or flumes of varying scales. As such, and in contrast to at-a-station hydraulic geometry, so called downstream channel form is commonly related to bankfull discharge, for this is what is believed to be the dominant channel-forming discharge (Leopold and Maddock, 1953; Wolman and Miller, 1960). Interestingly, and despite the name, such a series of stations need not necessarily consist of locations *downstream* of each other, but the locations are plotted in relation to increasing bankfull discharge which usually does increase along most streams. The following section will outline the relevant applications of each of these two approaches to hydraulic geometry.

3.2.1 At-a-station hydraulic geometry

3.2.1.1 Addressing problems with the approach

The relevance of at-a-station hydraulic geometry has been questioned for several reasons. It is important to address these issues, prior to more detailed considerations of the approach. The first issue is its focus on what have been termed *residual phase flows*; those flows of insufficient force to deform the channel boundary or to move sediment (Ferguson, 1994). The threshold of sediment motion is often associated with *bankfull* flow (Emmett and Wolman, 2001) which is also deemed to be the channel forming discharge. As cross-sectional geometry is inherited from active phase flow (those flows capable of deforming the boundary and/or sediment motion) (Ferguson, 1994), the examination of residual phase flows by at-a-station hydraulic geometry has been considered of little consequence. However, Andrews (1984) collated sediment transport data from several streams and illustrated that not all rivers are threshold channels which transport their bedload only at flows approximating bankfull; some gravel bed channels achieve active phase flow at stages well below bankfull. Critical shear stress (that required for the transport of bedload) varies with the channel width-depth ratio and Carling (1983) found that narrow streams

have higher critical shear values than do wide and shallow streams. This suggests that active phase flow may be initiated at varying stages in different shaped channels.

Importantly, the various controls which combine to form channel cross-sectional geometry and reach-scale channel adjustment during active channel forming flows are well illustrated by at-a-station hydraulic geometry. In equilibrium channel systems in which a given cross-section has evolved to imposed conditions (Mackin, 1948), at-a-station hydraulic geometry can be used to indicate dominant controls and to infer hydraulic processes (e.g. changes in resistance to flow with increasing discharge). The at-a-station hydraulic geometries are, therefore, useful for examining changes in the hydraulic efficiency of each cross section as discharge increases towards the bankfull condition, commonly accepted in most cases as the formative discharge.

It has also been considered a potential problem that at-a-station hydraulic geometries change through time with meander migration and bar development (Ferguson, 1986). However, positioning cross-sections at meander inflection points minimises this problem. Chapter 2 determined that the Barrington swamp channels are laterally stable and cross-sections and flows measured over the course of this project are almost certainly representative of their longer-term adjusted form.

A final concern is that hydraulic geometry relationships lack any physical justification for their being logarithmic, and any such assumption (i.e. use of the exponents) lacks a physical justification (e.g. Richards, 1973). But despite a lack of such justification, the relationships between discharge and width, depth and velocity at-a-station are commonly logarithmic, or nearly so, and they do reveal important information on the relative contributions to channel cross-sectional adjustment being made by each of the flow variables as discharge changes. In this study their usefulness for this purpose is confirmed as they co-vary with very high r^2 values.

3.2.1.2 Common at-a-station hydraulic geometry and causes of variation

Minimum variance theory proposes that natural river systems operate to minimise the temporal or spatial variation of their dependent variables- i.e. width, depth, velocity, slope,

flow resistance, shear stress and sediment transport (Langbein, 1964). The theory maintains that once an equilibrium condition has been reached, a system will minimise any imposed disturbance or stress by restoring or maintaining conditions close to the previous condition. This theory was used by Langbein (1964) to provide theoretical b (width), f (depth) and m (velocity) exponent values of 0.23, 0.42 and 0.35 these values supported the empirically derived values of Leopold and Maddock (1953); 0.26, 0.4 and 0.34. However, subsequent studies (e.g. Park, 1977; Rhodes, 1977) have collated the results of numerous other studies and have found a wide range of values, albeit centred in a histogram plot around these values (Rhodes, 1977). This suggests some consistency in at-a-station hydraulic geometry but with variations in the controls, both within and between catchments.

Ferguson (1986) suggested the rational division of controls on at-a-station hydraulic geometry into two groups; those which determine channel geometry, and hence width and depth relations, and those which determine the hydraulic and frictional characteristics on the flow, reflected directly by the velocity exponent. He proposed that channel geometry is largely a remnant of the previous competent flow, influenced by bank strength, and that flow resistance and sediment transport dynamics largely determine the velocity exponent.

But channel cross-sectional geometry also reflects the dominant sediment calibre transported by the channel (Leopold and Maddock, 1953). Wide and shallow channels tend to carry bedload more effectively (Wilcock, 1971; Pickup, 1976; Bettess and White, 1983) as shear across the bed is maximally distributed, whereas narrower and deeper channels have an enhanced suspended load transporting ability, provided by rapid increases in the velocity of the flow with increasing discharge (Leopold and Maddock, 1953). Sediment quantity is also reflected by the channel cross-sectional shape through the adjustment of channel planform. Braided channels form in response to high sediment supply over steep gradients, whereas meandering channels tend to form under lower sediment supply conditions and over lower slopes (Schumm and Khan, 1972; Bettess and White, 1983; Schumm, 1985). Braided and meandering channels have higher at-a-station width exponents than straight channel sections and lower velocity exponents, owing primarily to the resistance elements present in meandering and braided channel types and the steeper

channel banks of straight channels (Knighton, 1975). A complicated relationship exists between sediment calibre and quantity and channel morphology, manifest in channel planform and at-a-station hydraulic geometry, which are in turn influenced by other variables, including bank strength.

Ferguson (1986) also proposed the representation of channel hydraulic and frictional characteristics by at-a-station hydraulic geometry. The quantity of sediment load, and its calibre, also determine channel cross-sectional shape through the development of channel bed topography (Keller and Melhorn, 1978; Montgomery and Buffington, 1997). In turn, bed topography exerts a major influence on flow velocity through the provision of resistance (Simons and Richardson, 1966; Richards, 1973). The type of bed features that develop are a direct response to the quantity of sediment supplied and its calibre. Finer sediment tends to form ripples and dunes, whereas coarser sediment forms bars, riffles and steps (Montgomery and Buffington, 1997). Each type of bedform reduces channel velocity through the provision of form flow-resistance and the action of sediment transport itself provides further flow resistance as grains collide, an element termed *bedload transport resistance* (Gao and Abrahams, 2004). The provision of flow resistance necessarily causes a compensatory adjustment in width and depth with changing discharge; the more significant (measured by steepness; height/length) the bedform in proportion to flow and channel geometry, the larger its contribution to flow resistance (Smith and McLean, 1977). Channel geometry also varies through pool-riffle sequences (Knighton, 1975). Pools are narrower than riffles in cross-section (Richards, 1976) and with increasing stage, velocity tends to increase in pools more rapidly than it does over riffles (Keller, 1971), thereby causing local scale variation in at-a-station hydraulic geometry.

Local variations in bank strength, sediment supply and calibre, channel planform and bedforms usually preclude the development of useful regional average values (Park, 1977), or even averages for individual river reaches (Knighton, 1975). But an approach closely aligned with Ferguson's considerations of flow resistance and sediment (transport) dynamics is that of Rhodes (1977). Rhodes divided a ternary graph of the exponents b, f and m into ten channel groupings or types based on five channel process and geometry

conditions: the rate of change with increasing discharge in width/depth ratio, sediment transport competence, Froude number, velocity and roughness. These divisions can provide insight into channel geometry, hydraulics and some channel controls such as bank strength, characteristics that can be directly implied by the specific location of a plotted station on Rhodes graph. These divisions will be outlined and discussed in Section 3.5.1 to aid in the interpretation of controls on at-a-station hydraulic geometry in the Barrington swamp streams.

3.2.1.3 Sediment supply, bank strength and optimal channel geometry

Eaton et al. (2004) have recently described how channels adjust their morphology to maximise their resistance to flow in an effort to balance the supplied sediment load and water, and thereby attain equilibrium. They also describe how these adjustments may be constrained by the channel's bank strength and its ability to adjust slope. As bank strength constrains cross-sectional adjustment, a compromise is reached between the optimum channel cross-section for sediment transport and bank strength. Huang and Nanson (2000) applied the principal of least action (LAP), to demonstrate that optimum flow conditions are reached when the cross-sectional shape of a channel achieves the maximum sediment transporting capacity (MSTC) per unit available stream power. They called this condition maximum flow efficiency (MFE). Huang et al. (2002) and Huang et al. (2004) demonstrated that minimum potential energy, which can be more specifically expressed as the principal of minimum (total) energy (PME), in addition to MFE, is a second condition that must be met for optimal flow. In other words, MFE and PME describe the condition of a cross-section in which the transport of sediment and water are balanced. Excess, or insufficient, flow in proportion to sediment load will result in the need for an adjustment of the system towards stability, or equilibrium, and hence towards MFE. For example, a straight channel with little bedload may have energy in excess to that which will maintain stability. This excess can be consumed by the onset of meandering. Alternatively, a channel with excess sediment, in comparison to flow and hence energy, may braid to maximise its boundary shear and thereby increase its ability to transport sediment, thus attaining stability and MFE. So MFE is represented by a large range of channel geometries, dependent on the relative amount and calibre of sediment and water. Research by Huang and colleagues has

collectively demonstrated that the optimum width/depth ratio for minimum boundary friction *in the absence of bedload,* and hence MFE, is 2 for equilibrium flow regime (Huang and Nanson, 2000; Huang et al., 2002; Huang et al., 2004). They stated:

> *"Only when Q_s=0 is the most efficient alluvial channel geometry exactly the same as the best hydraulic section defined in frictional flow without transporting sediment, for both occur at ζ_m=2."*

where Q_s is the sediment discharge and ζ_m is defined as the optimum width/depth ratio (Huang et al., 2004, pp.6). This geometry is rarely attained in natural channels, primarily because of insufficient bank strength, but also as nearly all channels carry bedload. A width/depth ratio of 2 is ideal for the most efficient flow of sediment free water, with wider and shallow channels operating to most effectively transport bedload (Pickup, 1976).

High bank strength provided by fine, cohesive sediment (Schumm, 1960; Knighton, 1975; Millar and Quick, 1993) or vegetation (Zimmerman et al., 1967; Abernethy and Rutherfurd, 1998, 2000, 2001) can allow for steep channel banks and low width exponents. Depth and velocity increase with increasing discharge while width remains almost constant. Bank strength is clearly an important consideration in at-a-station hydraulic geometry analyses and a key objective of this study is to see how other variables respond when bank strengths are exceptionally high and when sediment supply is exceptionally low. This study is, therefore, able to assess the theoretical condition of natural channels almost completely lacking bedload and exhibiting very high bank strength: i.e. when ζ_m=2 (Huang et al., 2004).

3.2.2 Downstream hydraulic geometry

The use of an appropriate discharge is critical for the development of downstream hydraulic geometry relationships as the selected discharge is intended to represent the effective (sediment transporting and boundary deforming) flow (Wolman and Miller, 1960; Goodwin, 2004). However, channel forming discharge can be difficult to define and may occur with variable frequency along a length of channel (Pickup and Warner, 1976). Richards (1982) outlined two approaches for investigating downstream hydraulic geometry,

which differ in the discharge values that are used. The first examines discharges of a given flow frequency. A complication arises using this technique as the discharge flow frequency that is selected may not be competent at all cross-sections, or may be capable of transporting bedload but incapable of eroding the channel banks (Pickup and Warner, 1976). Therefore the fundamental supposition of the approach, that discharge is the primary control on channel cross-sectional shape, may be undermined because the selected discharge frequency may not be formative at all cross-sections (Grayson et al., 1996).

Richards (1982) second approach uses bankfull discharge which is either measured directly or estimated using either the Manning or Darcy-Weisbach flow resistance equations. This is essentially the approach originally adopted by Leopold and Maddock (1953) and referred to by them as downstream hydraulic geometry. Andrews (1984) found that sub-bankfull flows are sometimes able to transport sediment, but a recent paper by Emmett and Wolman (2001) has shown that a wide range of gravel bed rivers transport most of their bedload only at discharges in the vicinity of bankfull. Despite some variability (e.g. Knighton, 1998; Goodwin, 2004) many alluvial channels have been shown to have consistent bankfull flow frequencies of about once every 1-2 years (Wolman and Miller, 1960). This would be a remarkable coincidence if it were not because something close to bankfull flow is the formative discharge. As stated earlier in this chapter, downstream hydraulic geometry implies that stations are located within a single catchment with increasing downstream catchment area supplying a downstream increase in discharge. In fact, the process of stitching together datasets from various catchments to extend the discharge range of the investigation was undertaken in the original bankfull hydraulic geometry study (Leopold and Maddock, 1953) and has been adopted consistently since (e.g. Andrews, 1984; Ferguson, 1986; Hey and Thorne, 1986). Some large catchments show a decrease in discharge in the downstream direction (Leopold and Maddock, 1953; Knighton and Nanson, 1994; Kemp, 2005) while still satisfying the underlying approach to hydraulic geometry. Because the preferred flow used in many studies has been bankfull discharge, owing to its intended formative nature (Wolman and Miller, 1960; Emmett and Wolman, 2001), and because the term ‘downstream hydraulic geometry’ is imprecise and confusing, the term ‘bankfull hydraulic geometry’ is used here.

3.2.2.1 Common bankfull hydraulic geometry and controls

Empirically derived values of 0.5, 0.4 and 0.1 as the exponents for b, f and m have been replicated many times (Richards, 1982) for bankfull hydraulic geometry since initial publication of them by Leopold and Maddock (1953), and they compare reasonably well with those used in regime equations (Blench, 1952). In addition the application of minimum variance theory produced values of 0.5, 0.38 and 0.13 (Langbein, 1964), once again closely approximating the empirical results of Leopold and Maddock (1953). This regularity in bankfull hydraulic geometry can primarily be ascribed to two common controlling conditions: decreasing slope and sediment size in a downstream direction, usually associated with increasing bankfull discharge. The concavity of longitudinal stream profiles directly underlies downstream reductions in channel slope (Mackin, 1948). Sediment size tends to decrease with increasing bankfull discharge, primarily as a result of hydraulic sorting (Hoey and Bluck, 1999; Rice, 1999), with probably less than 10% of downstream fining caused by abrasion (Bradley et al., 1972). This results in a downstream reduction in flow resistance caused by individual grains, but an increase in form resistance provided by bedforms (Leopold and Maddock, 1953). Slight decreases in suspended sediment concentrations, and overall increases in width/depth ratio caused by limitations in depth adjustment due to a finite floodplain height and limitations of channel bank strength, combine with changes in form and grain roughness to result in slight decreases in flow resistance with increasing bankfull discharge. The combined effect of slightly decreased roughness and a decline in slope dictate only slight increases in velocity with increasing bankfull discharge, in other words with low m exponent values in most cases (Leopold and Maddock, 1953). The constraint of depth adjustment caused by bank height and strength combines with the low velocity exponent to predetermine that in most cases width adjusts more rapidly than depth (Church, 1992), resulting in the oft-quoted relation $b > f > m$ (e.g. Rhodes, 1987).

3.2.2.2 Causes of bankfull hydraulic geometry variation

Despite the frequency of the values 0.5, 0.4 and 0.1, generalised trends in bankfull hydraulic geometry often mask considerable scatter caused by local controls. As discussed in the previous section on at-a-station hydraulic geometry, channel pattern (e.g. Knighton,

1975), bank strength (e.g. Schumm, 1960) and bedforms (e.g. Simons and Richardson, 1966) can produce considerable and abrupt variations in channel cross sectional shape and flow hydraulics, and hence cause scatter in the bankfull hydraulic geometry exponents.

For example, while fining of channel sediments can result in increasing bank strength (Schumm, 1960) and variations in channel roughness resulting from bedform development (Simons and Richardson, 1966) in a downstream direction, so too does vegetation influence both bank strength and channel roughness (e.g. Zimmerman et al., 1967; Abernethy and Rutherfurd, 2001; Brooks and Brierley, 2002). While general downstream fining and trends in roughness components are common to most channels, localised variations in other parameters, such as vegetation, can play significant, and perhaps relatively unsystematic, roles in these relations (Hickin, 1984).

Because of a wide range of interacting variables, *determinant* bankfull hydraulic geometry analyses have required a multivariate approach. Three physical relations adjust to define flow geometry: flow continuity, flow resistance and sediment transport. Common to the equations that describe these variables are the independent variables of discharge and sediment load, the semi-independent variables of resistance and sediment size, and the dependent variables of width, depth, slope, velocity and channel pattern. There are more unknown (dependent) than known (independent) variables in these three equations (Bettess and White, 1987). Various techniques have been employed to enable the development of a fourth equation to produce definitive (determinant) hydraulic geometry equations, and hence the prediction of channel morphology, using extremal hypotheses and empirically derived relations.

The extremal hypothesis approach.

Extremal hypotheses maximise or minimise (optimise) particular flow conditions, thereby offering a theoretical basis for the finite solution of continuity, sediment transport and flow resistance equations. This requires a premise or hypothesis stating that the flow adopts a preordained condition, for example that the flow adjusts its conditions to maximise sediment transport for given flow conditions, or to maximise flow resistance. Such an optimising assumption is termed an extremal hypothesis (Bettess and White, 1987). Many

extremal hypotheses have been proposed with varying degrees of "success", and equivalence has been shown between a number of them (e.g. Huang and Nanson, 2000). "Success" is measured on the basis of the extent to which the theoretical model accurately predicts channel relationships obtained from actual field data. The development or use of predictive equations is not the focus of this thesis. In the relatively small scale streams of the Barrington swamps, the application of existing models would be difficult owing to the localised controls that may override bankfull hydraulic geometry trends. For these reasons, extremal hypothesis models considering bankfull hydraulic geometry are not discussed further in any detail. However, the development of the LAP and MFE theory by Huang and colleagues utilised bankfull relations, but its application to this thesis lies in its relevance to at-a-station hydraulic geometry relations in this chapter, and in assessing in later chapters the roles played by bedform and planform resistance in countering the effect of such hydraulically efficient channels.

Empirical approach.

Widely applicable models of bankfull hydraulic geometry, based on empirically derived relations, have been sought (e.g. Hey and Thorne, 1986; Huang and Warner, 1995). However, while general trends in the controls on bankfull hydraulic geometry are identified using these approaches, scatter in these relations determines that large variations in the catchment-specific applicability of these equations is not always appropriate.

Osterkamp (1979) has shown how the use of invariant power functions (b, f and m) can reduce scatter and significantly improve the understanding of local controls on bankfull hydraulic geometry through the examination of hydraulic geometry coefficients (a, c and k), a technique strongly advocated by Andrews (1984). Invariant power functions can provide a means for comparison between studies with clearly different coefficients and which would otherwise appear as scatter in a single regression if multiple exponents were allowed (Andrews, 1984; Ferguson, 1986). This is the simplest means by which multivariate controls on bankfull hydraulic geometry can be examined. The approach was first used by Osterkamp (1979) to determine variations in the coefficients in channels varying in bank sediment composition and hence strength, and then by Hey and Thorne (1986) to assess differences in the influence of vegetation type on channel width and more

recently by Huang and Nanson (1998), who were able to distinguish between bed and bank vegetation and bank strength categories using this type of analysis.

However, equations resulting from these techniques may also have limited application in small-catchment channels owing to threshold vegetation-channel interactions. For example in the Sleepers River, North America, Zimmerman et al. (1967) documented that there was no downstream increase in channel width until catchment areas exceeded five square miles (~13 km^2). From this they concluded that small streams are subject to "exaggerated" bank vegetation influence through the provision of either high bank strength or increased roughness imposed on the flow. The idea that vegetation growth and large woody debris dominates the controls on channel morphology and thwarts clear relationships between defined discharge and channel form has also been proposed by Brooks and Brierley (2002) in the Thurra River catchment, Victoria, Australia. The well vegetated banks of the Barrington swamp channels might produce similar channel response.

3.3 Hydraulic geometry methods

3.3.1 Field methods

Six hydraulic geometry stations were established on the Barrington River, two on Edwards Creek and 12 on Polblue Creek, totalling 20 stations. The locations for these stations were chosen at inflection points between bends, following Leopold and Maddock (1953) and Leopold and Wolman (1957), where the channels were relatively symmetrical and/or representative of that channel reach. The end points of each cross-section were established back from the bank top at essentially equal elevations and marked using wooden stakes (Figure 3.2). A 5m aluminium plank with 0.1m marked increments on its upstream side was placed between these points. For the duration of the project, the plank was re-placed at the same datum for the various discharges, and the cross-section dimensions were re-checked before flow measurements were repeated. These stations are indicated in Figure 3.3.

Flow measurements were made using an OTT C2 current meter and the number of revolutions over a 30 second period were recorded (Australian Standard 3778.3.1, 1990), with vertical spacings approximately 0.1-0.3m apart, depending on channel width. The

maximum number of data points for each cross-section were obtained which would also allow for measurements at all stations within that stream for a given flow event. These were determined to be at 0.6 of the depth of flow if total depth of flow was < 0.5m and at 0.4 and 0.6 of the flow depth (subsequently averaged) if > 0.5m. The number of verticals varied from 3 to 6 across the stream, depending on channel width, resulting in up to 10 points in any cross-section. Similar to the outcome of the one or two point method employed by Myrick and Leopold (1963), the constraints imposed by the practicalities of data collection were consistent with requirements for accuracy. This was demonstrated with an initially higher sampling density that gave very similar results to those obtained from the less dense array chosen as the design for the remainder of the study.

Figure 3.2 Deployment of the OTT meter from an aluminium plank extended over the channel. Flow from left to right.

3.3.2 Selection of an appropriate discharge for downstream hydraulic geometry

There is potential difficulty in defining channel banks in wetlands due to their permeability (Jurmu and Andrle, 1997; Tooth and McCarthy, 2004). Fortunately, the Barrington swamp

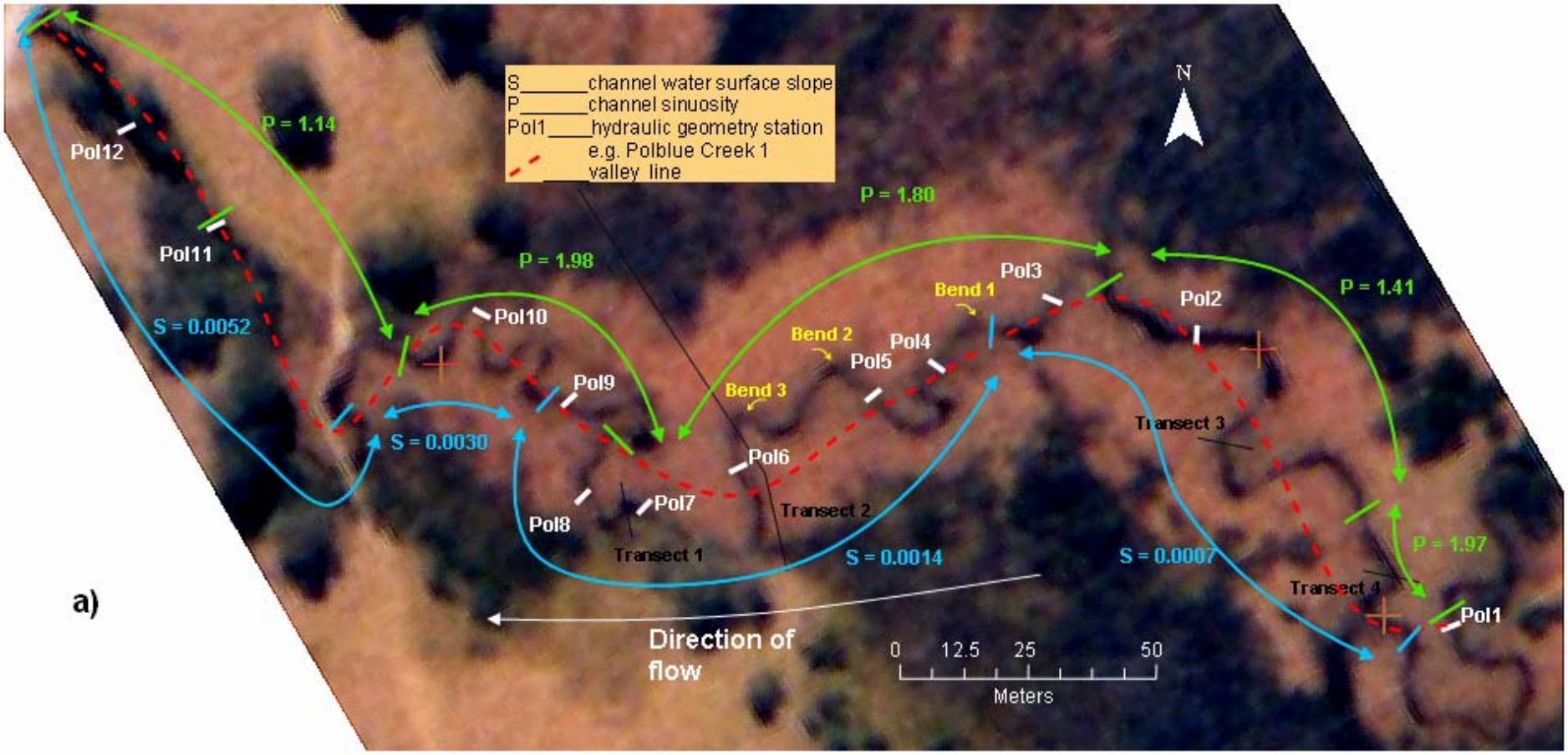

Figure 3.3 Aerial view of the Barrington swamp channels showing hydraulic geometry stations, breaks in channel water surface slope (S), divisions of channel sinuosity (P), auger transects (black lines) and bends examined in detail for a) Polblue Creek and b) Barrington River and Edwards Creek (over page).

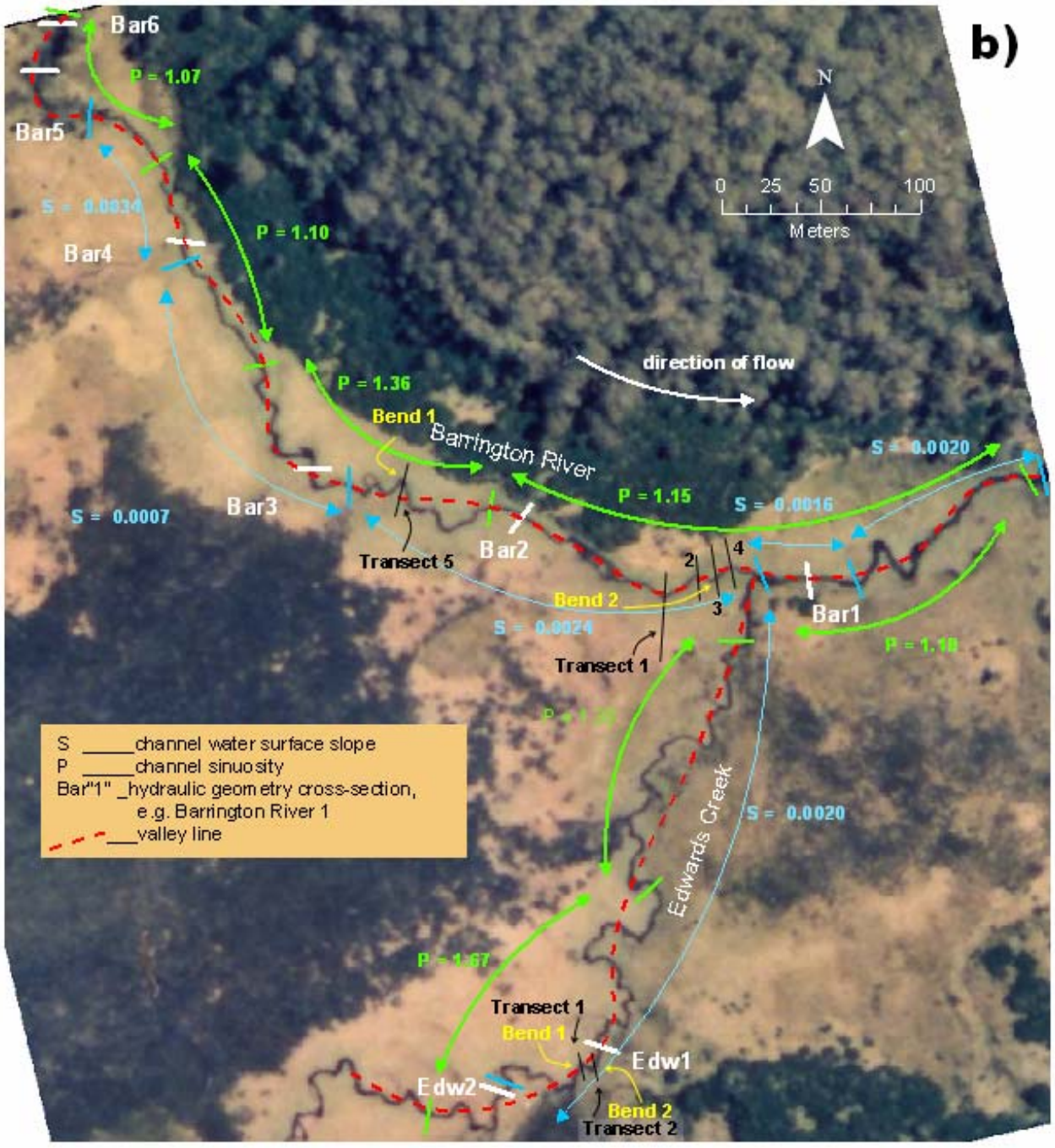
b)
Bar6
P = 1.07
Bar5
S = 0.0034
Bar4
P = 1.10
P = 1.36
Bend 1
Barrington River
direction of flow
S = 0.0020
P = 1.15
S = 0.0016
S = 0.0007
Bar3
Bar2
Transect 5
2
4
3
Bend 2
S = 0.0024
Transect 1
Bar1
P = 1.18
N
0 25 50 100
Meters
S _____channel water surface slope
P _____channel sinuosity
Bar"1" _hydraulic geometry cross-section,
e.g. Barrington River 1
___valley line
Edwards Creek
S = 0.0020
P = 1.67
Transect 1
Bend 1
Edw1
Edw2
Bend 2
Transect 2

channel banks are comprised of firm peat and are well defined, enabling bankfull flow to be readily determined by observing channel flow during several high flow events. Following the methodology of several authors (Myrick and Leopold, 1963; Hey and Thorne, 1975; Hey and Thorne, 1986) the bankfull stage height was assessed visually as the major break in slope between the vertical channel banks and the swamp surface. In the majority of cases, bankfull flow showed a remarkably consistent frequency along the Barrington channels, most cross-sections being equally full during high flow events.

3.3.3 Data processing methods

Cross-section dimensional and velocity data were used to calculate the average width, depth, velocity and channel cross-sectional area for every flow in each cross-section. The exponents b, f, m, y and p, representing the rates of change in width, depth, velocity, Manning's n ($n=vR^{2/3}s^{1/2}$) and Darcy-Weisbach's f ($f=8gRs/v^2$), respectively, were calculated from these results. This data was also used to calculate bankfull Froude number, total stream power (Ω), specific stream power (ω), bankfull n and f and the bankfull du Boys shear stress (τ).

A total of six flows were measured through all stations, including flows from very low base flow to bankfull. Of these, it was occasionally necessary to discard some flow data due to anomalous patterns in discharge variations downstream, resulting from either counter / operator error or rapidly rising / falling flow stages.

3.4 Hydraulic geometry results

3.4.1 At-a-station hydraulic geometry

The at-a-station hydraulic geometry log-log plots for width, depth, velocity, Manning's n and Darcy Weisbach's f for each of the 20 stations are presented in Figure 3.4. The exponents and r^2 for all power function regressions fitted to each of these bivariate plots are summarised in Table 3.2 and the station cross-sections are presented in Figure 3.5. It is clear from the high r^2 values for depth and velocity presented in Table 3.2, that discharge is indeed logarithmically related to width, depth, velocity, n and f in these channels, thereby

validating the use of the hydraulic geometry approach for investigating controls on these particular channel systems. Hydraulic geometry exponents for the study streams for width (b), depth (f) and velocity (m) averaged 0.05, 0.35 and 0.60, respectively. These results indicate that with increasing discharge rapid responses in velocity are accompanied by moderate rises in depth and almost no response in width.

3.4.2 Bankfull hydraulic geometry

Absolute variation in bankfull discharge between the smallest and largest capacity channels at bankfull was only 0.52 m^3/s, however, this constituted a 2.5 fold increase in discharge from approximately 0.20 m^3/s upstream at Polblue Creek hydraulic geometry Station 1 (P1), to approximately 0.30 m^3/s at P12, and from approximately 0.28 m^3/s at Barrington River hydraulic geometry Station 6 (B6) (upstream) to approximately 0.72 m^3/s at B1 (Table 3.2). Both Edwards Creek hydraulic geometry stations (E1 and E2) lay within these discharge values. If a continuum is then assumed between the two swamps, bankfull flow from 0.20 to 0.72 m^3/s through 20 cross-sections is a sufficient dataset for the analysis of bankfull hydraulic geometry (e.g. 23, 16 and 30 stations for: Leopold and Maddock (1953); Tabata and Hickin (2003); Huang and Nanson (1997), respectively).

Table 3.1 Bankfull hydraulic geometry exponents and coefficients

		width			**depth**			**velocity**		
	# sites	b	a	r^2	f	c	r^2	m	k	r^2
overall	19	0.53	0.14	0.14	-0.15	0.01	0.01	0.62	0.20	0.20
Polblue	11	-0.20	0.02	0.02	-0.33	0.04	0.04	1.53	0.58	0.58
Barrington & Edwards	8	0.21	0.08	0.08	0.38	0.07	0.07	0.41	0.10	0.10

Bankfull hydraulic geometry derived for the study reaches from Edwards Creek, Barrington River and Polblue Creek are summarised in Table 3.1 and illustrated in Figure 3.6 and provide average width, depth and velocity exponent values (b, f, and m) of 0.53, -0.15 and 0.62 for their combined data. These exponents were obtained from relationships with poor

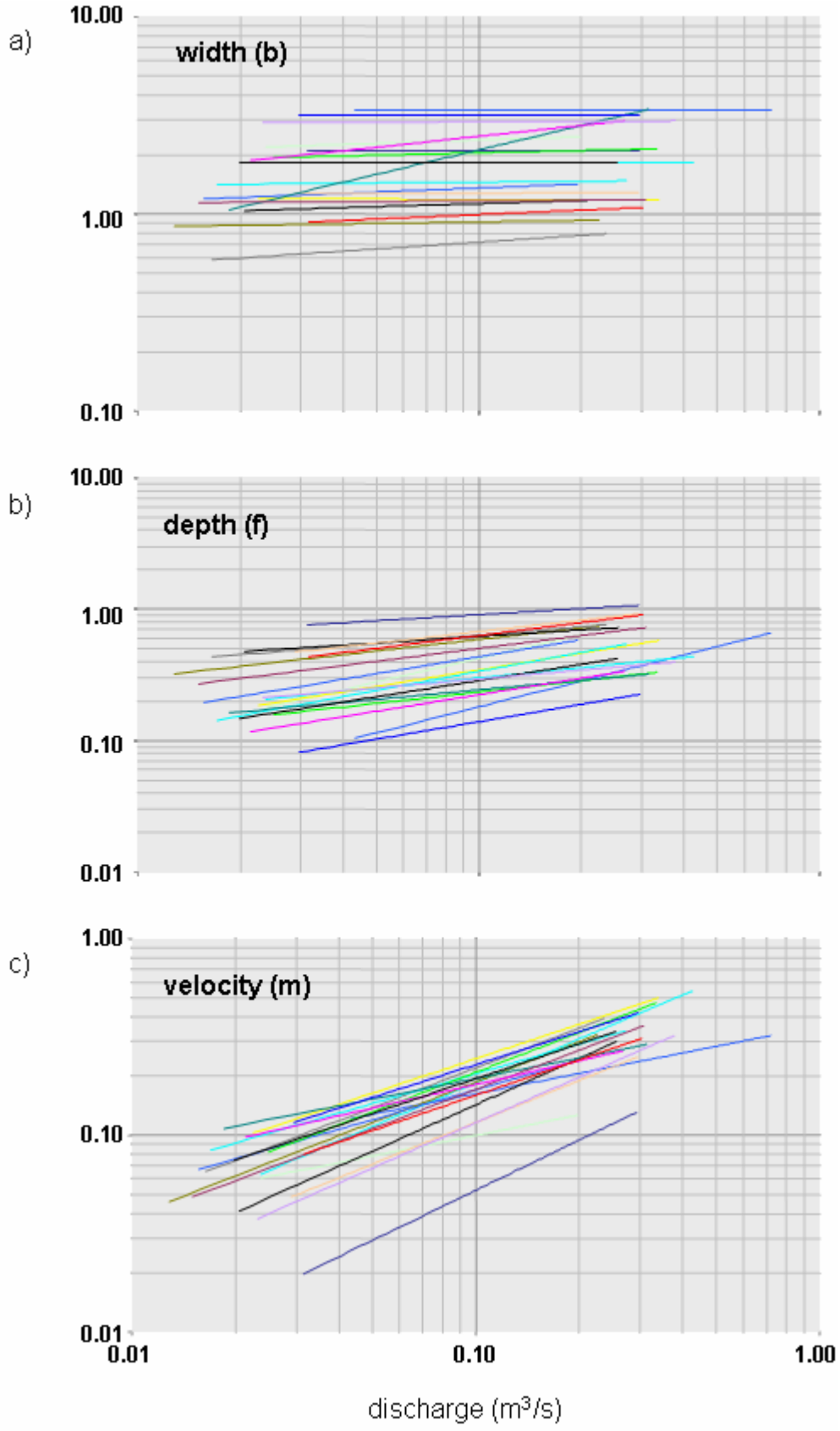
a)
10.00
width (b)
1.00
0.10
b)
10.00
depth (f)
1.00
0.10
0.01
c)
1.00
velocity (m)
0.10
0.01
0.01
0.10
1.00
discharge (m³/s)

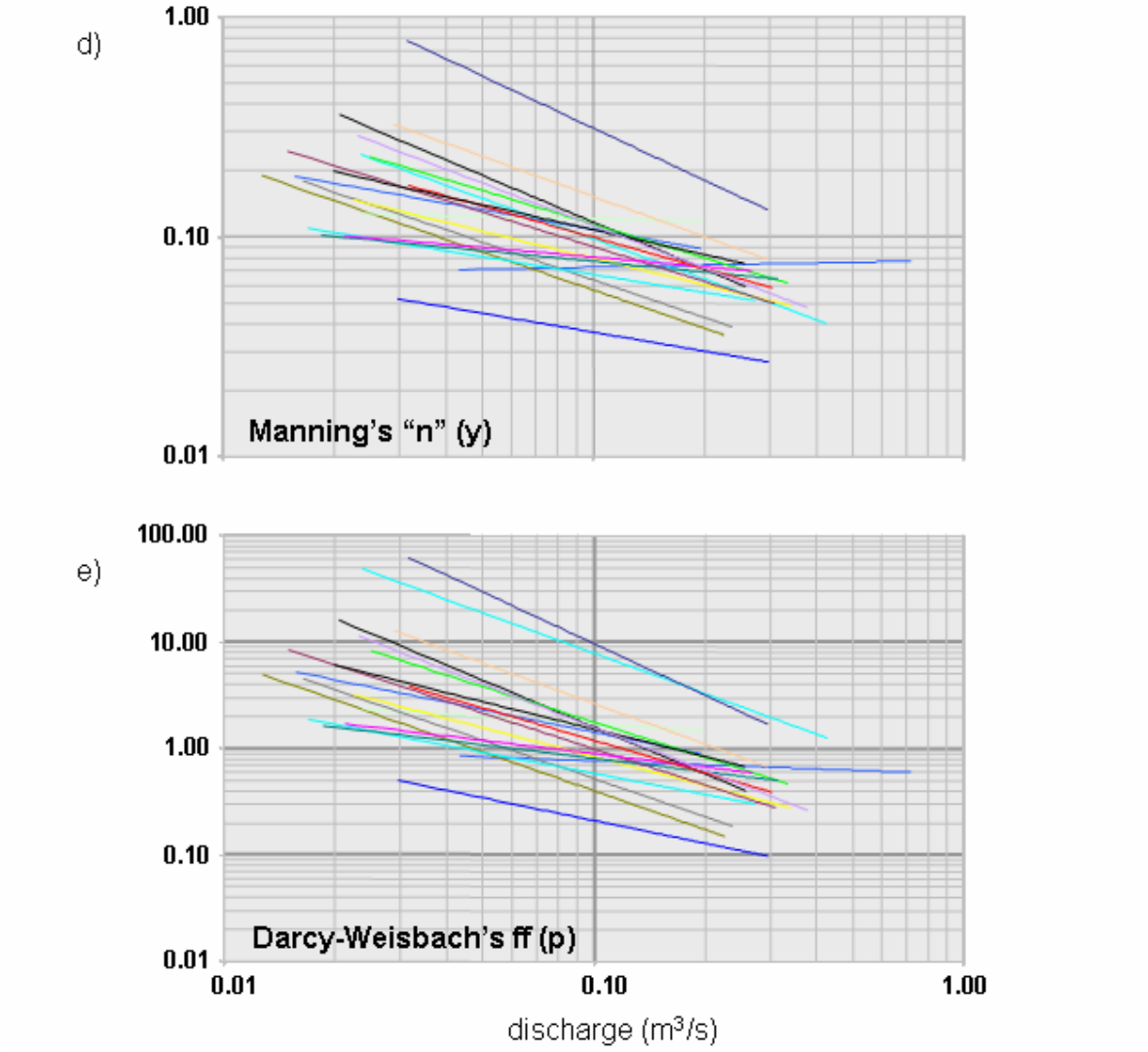

Figure 3.4 At-a-station hydraulic geometry relations for (a) width, (b) depth, (c) velocity, (d) Manning's n and (e) Darcy-Weisbach's ff, for all stations on Polblue Creek, Barrington River and Edwards Creek.

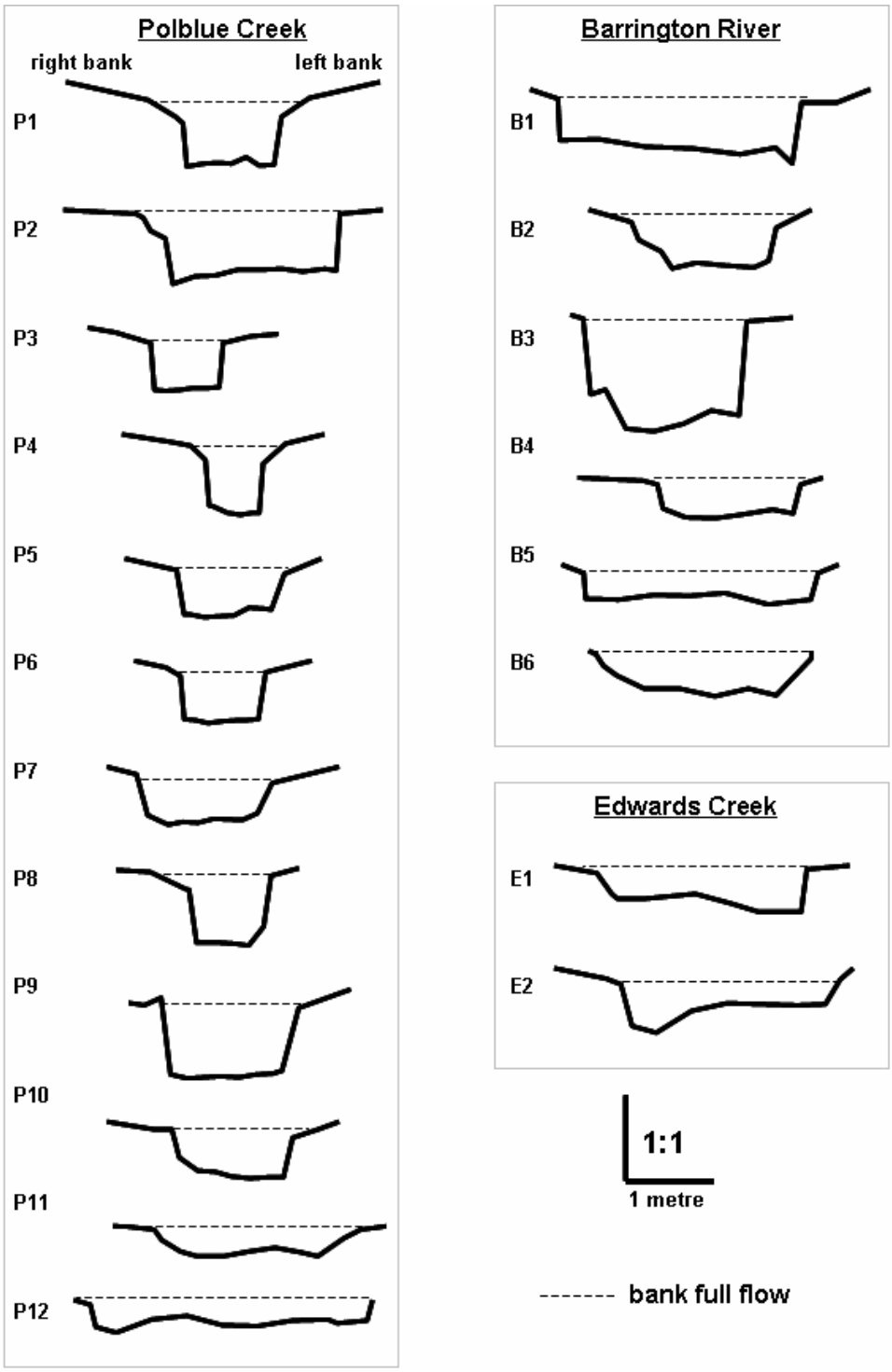

Figure 3.5 Hydraulic geometry station cross-sections. Flow is toward the reader, out of the page.

Table 3.2 At-a-station hydraulic geometry coefficients and exponents

		width			depth			velocity			a.c.k	b + f + m	Manning's "n"			Darcy-Weisbach's "f"		
site	# flows	b	a	r^2	f	c	r^2	m	k	r^2			y	t	r^2	p		r^2
P1	5	0.07	1.59	0.6	0.43	1.17	0.97	0.5	0.54	0.95	1	1	-0.3	0.05	0.8	-0.7	0.28	0.86
P2	6	0.06	2.7	0.64	0.6	1.67	0.94	0.35	0.22	0.8	0.99	1.01	-0.03	0.11	0.02	-0.22	1.02	0.19
P3	6	0.02	0.96	0.28	0.29	1.16	0.97	0.68	0.9	0.99	1	0.99	-0.58	0.01	0.97	-1.21	0.02	0.97
P4	6	0.12	0.94	0.3	0.21	1.03	0.96	0.67	1.03	0.94	1	1	-0.57	0.02	0.84	-1.19	0.03	0.87
P5	5	0.01	1.19	0.08	0.33	1.06	0.72	0.67	0.79	0.94	1	1.01	-0.53	0.03	0.83	-1.13	0.07	0.86
P6	5	0.05	1.27	0.54	0.16	0.91	0.69	0.78	0.87	0.98	1.01	0.99	-0.71	0.02	0.96	-1.46	0.05	0.96
P7	5	0.01	1.5	0.46	0.48	1.02	0.98	0.5	0.65	0.98	0.99	0.99	-0.27	0.04	0.9	-0.66	0.13	0.94
P8	6	0.08	1.18	0.48	0.32	1.33	0.96	0.6	0.63	0.99	0.99	1	-0.47	0.03	0.98	-1.01	0.12	0.99
P9	6	0	1.29	0.02	0.29	1.31	0.94	0.71	0.59	0.98	1	1	-0.61	0.04	0.96	-1.27	0.14	0.97
P10	6	-0.01	1.17	0.03	0.42	0.91	0.86	0.58	0.94	0.91	1	0.99	-0.41	0.03	0.72	-0.9	0.1	0.79
P11	6	0.04	2.23	0.26	0.29	0.45	0.8	0.67	0.99	0.92	0.99	1	-0.51	0.04	0.76	-1.11	0.14	0.81
B1	4	0	3.4	0	0.65	0.82	1	0.35	0.36	1	1	1	0.03	0.08	0.82	-0.12	0.57	0.96
B2	5	0	1.8	0	0.26	0.55	0.95	0.74	1.02	0.99	1.01	1	-0.61	0.02	0.98	-1.26	0.43	0.88
B3	5	0	2.1	0	0.15	1.29	0.75	0.85	0.37	0.99	1	1	-0.79	0.05	0.98	-1.61	0.24	0.98
B4	5	0	1.8	0	0.41	0.74	0.99	0.59	0.75	0.99	0.99	1	-0.38	0.05	0.97	-0.86	0.21	0.98
B5	5	0	3.15	0	0.44	0.38	0.97	0.56	0.83	0.98	1	1	-0.29	0.02	0.83	-0.71	0.04	0.9
B6	5	0.01	2.99	0.04	0.22	0.49	0.77	0.77	0.68	0.99	1	1	-0.65	0.03	0.95	-1.35	0.07	0.96
E1	4	0.18	3.77	0.89	0.42	0.58	0.79	0.4	0.45	0.89	0.98	1	-0.15	0.06	0.3	-0.42	0.34	0.51
E2	4	0.41	5.47	0.78	0.24	0.42	0.43	0.35	0.43	0.9	0.99	1	-0.16	0.05	0.33	-0.42	0.31	0.51
av.		0.06	2.13		0.35	0.91		0.6	0.69				-0.42			-0.93		

Table 3.3 Geometry, hydraulic and environmental characteristics for each hydraulic geometry station at bankfull flow

site	Q_{bf}	w:d	Fr	Ω (W)	w	ω (W/m^2)	n	ff	τ (N/m^2)	depth alluvium	average depth	valley width	Sv	Sws	P	Schumm M
P1	0.19	2.39	0.08	3.82	1.5	2.55	0.11	1.25	6.69	1.35	0.63	300	0.0026	0.0020	2.28	75.42
P2	0.2	3.79	0.05	1.36	2.6	0.53	0.13	1.81	3.02	1.3	0.67	280	0.0016	0.0007	1.49	49.3
P3	0.23	1.28	0.1	1.55	1	1.55	0.04	0.2	2.09	1.25	0.78	250	0.0016	0.0007	1.46	134.71
P4	0.24	1.39	0.12	3.25	1	3.25	0.05	0.3	4.04	1.38	0.72	215	0.0016	0.0014	1.64	124.35
P5	0.31	1.68	0.14	4.24	1.2	3.53	0.05	0.28	4.47	1.18	0.71	200	0.0021	0.0014	1.64	104.56
P6	0.26	1.5	0.09	3.51	1.3	2.81	0.08	0.65	4.9	1.23	0.83	105	0.0040	0.0014	1.82	116.09
P7	0.27	2.62	0.15	3.74	1.5	2.58	0.05	0.3	4.31	1.1	0.55	95	0.0040	0.0014	1.92	69.44
P8	0.3	1.2	0.1	4.16	1.1	3.78	0.06	0.42	4.72	1.15	0.92	90	0.0040	0.0014	1.92	143.33
P9	0.3	1.33	0.07	4.05	1.3	3.12	0.09	0.8	5.36	1.15	0.98	85	0.0040	0.0014	2.28	130.21
P10	0.34	1.86	0.17	9.96	1.2	8.3	0.06	0.38	9.13	0.73	0.64	65	0.0040	0.0030	2.04	95.03
P11	0.33	6.75	0.26	17.03	2.2	7.74	0.06	0.47	12.81	0.23	0.33	10	0.0073	0.0052	1.18	28.87
B1	0.72	5.14	0.13	11.28	3.4	3.32	0.08	0.58	7.46	0.85	0.66	30	0.0011	0.0016	1.15	37.12
B2	0.43	3.83	0.23	10.03	1.8	5.57	0.04	0.23	7.26	0.7	0.47	400	0.0031	0.0024	1.15	48.76
B3	0.29	1.76	0.03	1.97	2.1	0.94	0.16	2.34	3.83	1.5	1.19	400	0.0009	0.0007	1.36	100.23
B4	0.26	4.02	0.15	8.52	1.8	4.73	0.08	0.79	9.96	0.58	0.45	400	0.0036	0.0034	1.1	46.62
B5	0.3	13.71	0.27	44.72	3.2	14.2	0.03	0.1	2.16	0.48	0.23	40	0.0154	0.0154	1.07	14.97
B6	0.28	9.14	0.15	41.74	3.1	13.69	0.05	0.32	2.95	0.35	0.33	40	0.0154	0.0154	1.07	21.81
E1	0.27	6.51	0.12	5.25	2.7	1.94	0.09	0.87	6.22	1.43	0.41	400	0.0040	0.0020	1.67	29.83
E2	0.31	7.09	0.13	6.17	2.9	2.11	0.08	0.74	6.31	0.85	0.41	400	0.0040	0.0020	1.67	27.59
			PB av	5.15		3.61									Av:	73.59
			Bar av	16.21		5.81										

r^2 values of only 0.14, 0.01 and 0.20, respectively; it appears that width, depth and velocity are only weakly related to increasing discharge downstream.

If data are considered in the same order but separately for each swamp, the resulting exponents are 0.21, 0.38 and 0.41 for the Edwards / Barrington swamp system and -0.2, -0.33 and 1.53 for the Polblue system. The r^2 values for these are 0.08, 0.07 and 0.10 in the former system, and 0.02, 0.04 and 0.58 in the latter. The only notable improvement in these relationships with discharge is that for the velocity in Polblue Creek. It is clear that these variables are mostly very weakly related to discharge in the Barrington swamp streams, even within individual swamps.

3.5 Hydraulic geometry discussion

3.5.1 At-a-station hydraulic geometry discussion

The Barrington swamp channels accommodate increasing discharge by increasing their depth and velocity, while width remains essentially constant. Indeed, in some cases with undermined banks, but not recorded here, width may actually decline with increasing discharge. A physical constraint on channel geometry determines these results. These channels are typically slot-like in cross-section; they have near-vertical banks and fairly flat beds (Figure 3.5), little observed bedload and almost perfect bisymmetry. Because width is severely constrained, with increasing discharge, depth and velocity accommodate the required change.

On Edwards Creek, Stations 1 and 2 are asymmetrical and both experience higher rates of width adjustment than most of the swamp channel stations and consequently their rates of increase in velocity are more moderate. To determine the cause of Barrington swamp channels unusual hydraulic response to increasing discharge, it is useful to compare the values obtained here with results from a variety of other environments, using both average and individual station values.

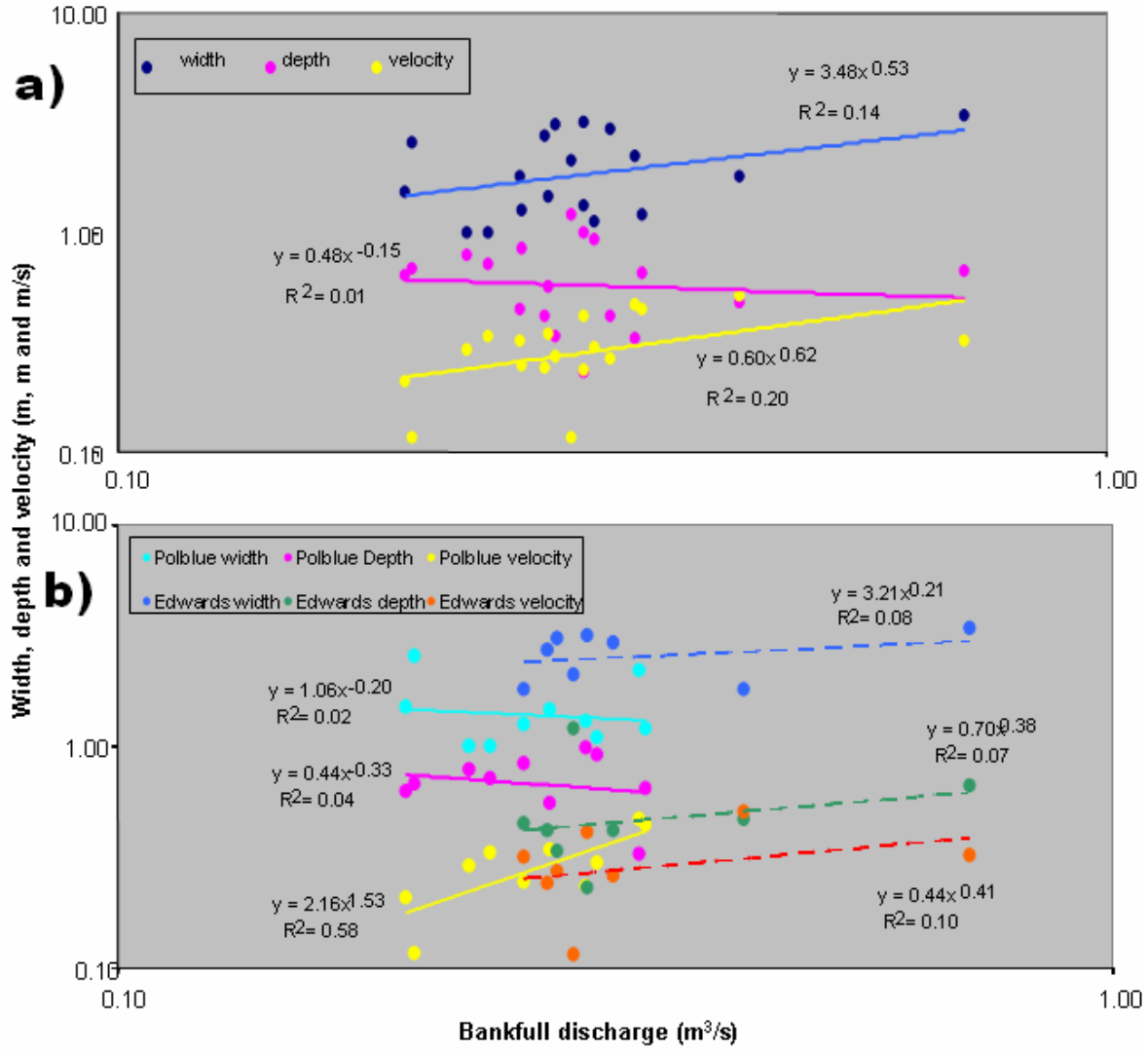

Figure 3.6 Bankfull hydraulic geometry relations for (a) all station data combined and (b) Polblue Creek separated from the combined Edwards Creek - Barrington River data.

3.5.1.1 Regional influences.

Using a ternary plot of the b, f and m exponents, Park (1977) attempted to delineate at-a-station hydraulic geometry exponents on the basis of climatic zones. His findings showed large variations in the exponents within regional climatic zones and caused him to conclude that localised conditions largely control hydraulic geometry. Figure 3.7 illustrates that the Barrington Tops swamp channels plot mostly within Park's regional division of tropical or humid-temperate channels, however the latter zone, while consistent with the Barrington Tops study area, is much more extensive (Park, 1977). The Barrington swamp channels

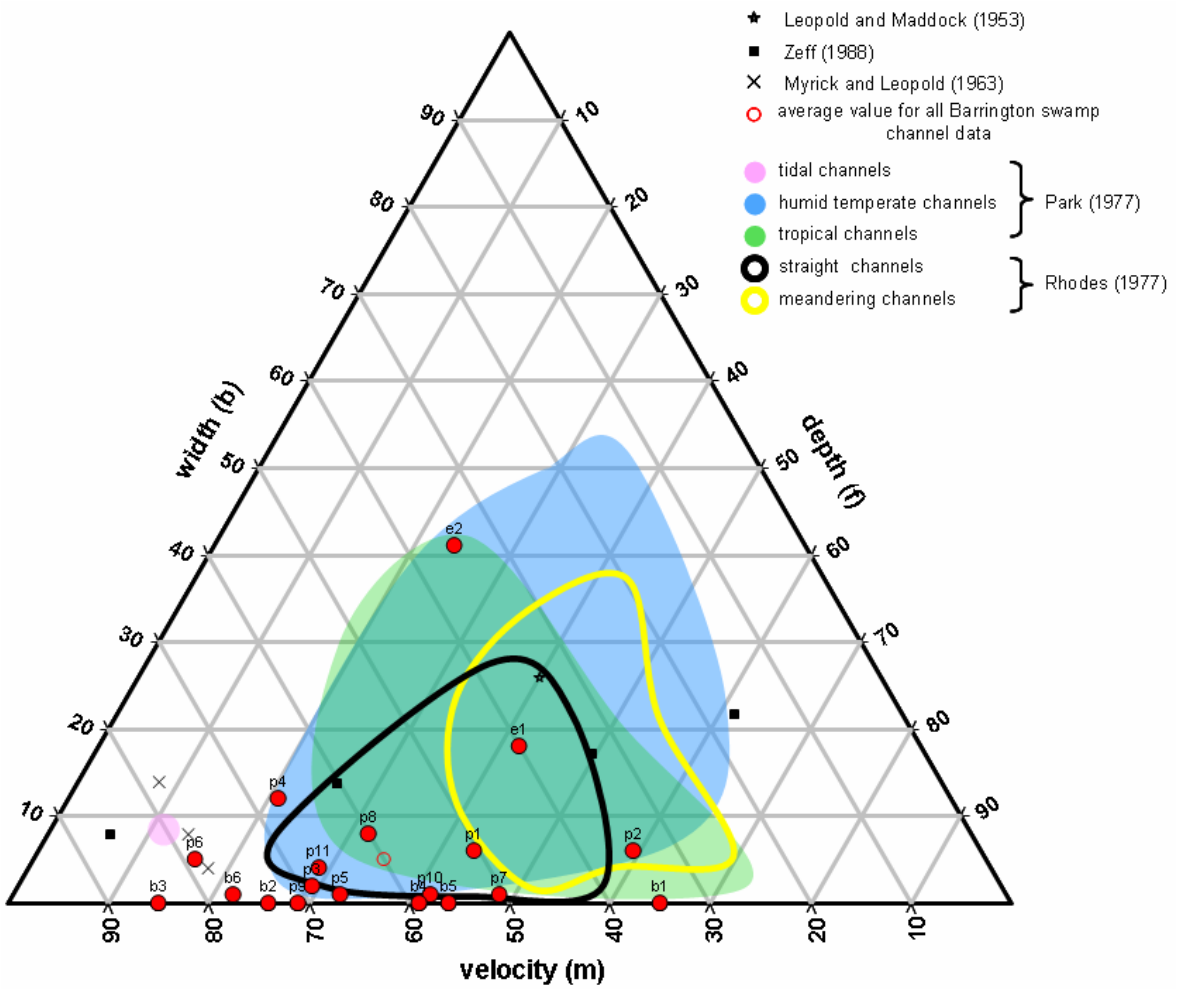

Figure 3.7 Ternary graph of at-a-station hydraulic geometry exponents from the Barrington Tops swamp channel stations (red dots) and the average values (open red dot), in comparison with planform and climate zone regions of the plot.

also plot close to the zone of tidal estuaries defined by (Myrick and Leopold, 1963, p.1). They obtained average values for the exponents b, f and m of 0.09, 0.08 and 0.78, respectively, for the flood tide through a set of six cross-sections in a small tidal estuary, representing what they describe as:

"one of the extremes in the continuum of river channels"

However, the results of subsequent investigations into estuarine channels have found that some display similar hydraulic geometry to the upland channels presented here (Myrick and Leopold, 1963; Zeff, 1988, 1999) and that some do not (Zeff, 1988) (Figure 3.7).

3.5.1.2 Channel morphology and hydraulic influences

The Barrington dataset plot primarily in the region of Rhodes (1977) channel Type 2 which exhibits the following conditions with increasing discharge: b<f, m>f, m>f/2, m>0.5 and m/f > 2/3. Stations E1, E2, P2 and B1 plot as channel Types 6, 3, 8 and 8, respectively. Rhodes (1977) provided a summary table of channel type characteristics, which is reproduced in Table 3.4. The variations within the Barrington swamp stream dataset clearly imply variations in their morphology and hydraulic behaviour, despite the data having been collected from a single channel type and within a very small geographical area. The cause of these variations must lie in locally variable controls on the channels which are best examined through the implications for each of the divisions in Rhodes (1977) diagram (Figure 3.8).

Table 3.4 Characteristics of each of the Barrington swamp channel stations, implied by Rhodes (1977) ternary plot

Channel type	Width/depth ratio	Competence	Froude number	Velocity-area ratio	Slope – roughness ratio
2	Decreases	Increases	Increases	Increases	Increases
3	Increases	Increases	Increases	Decreases	Increases
6	Decreases	Increases	Increases	Decreases	Increases
8	Decreases	Increases	Increases	Decreases	Decreases

(i) b < f (Δ width < Δ depth) on the Rhodes diagram

This condition defines three general characteristics: 1. with increasing discharge, channel width increases more slowly than depth (i.e. more rectangular rather than trapezoidal channels); 2. The strength of the banks is greater than that of the bed; 3. The suspended load exceeds the bedload (Leopold and Maddock, 1953) (or there is very little sediment load of any kind). In the Barrington swamp channels, b is much less than f; in-fact it is often less than one third of f (Figure 3.8), implying that these characteristics are present in the extreme.

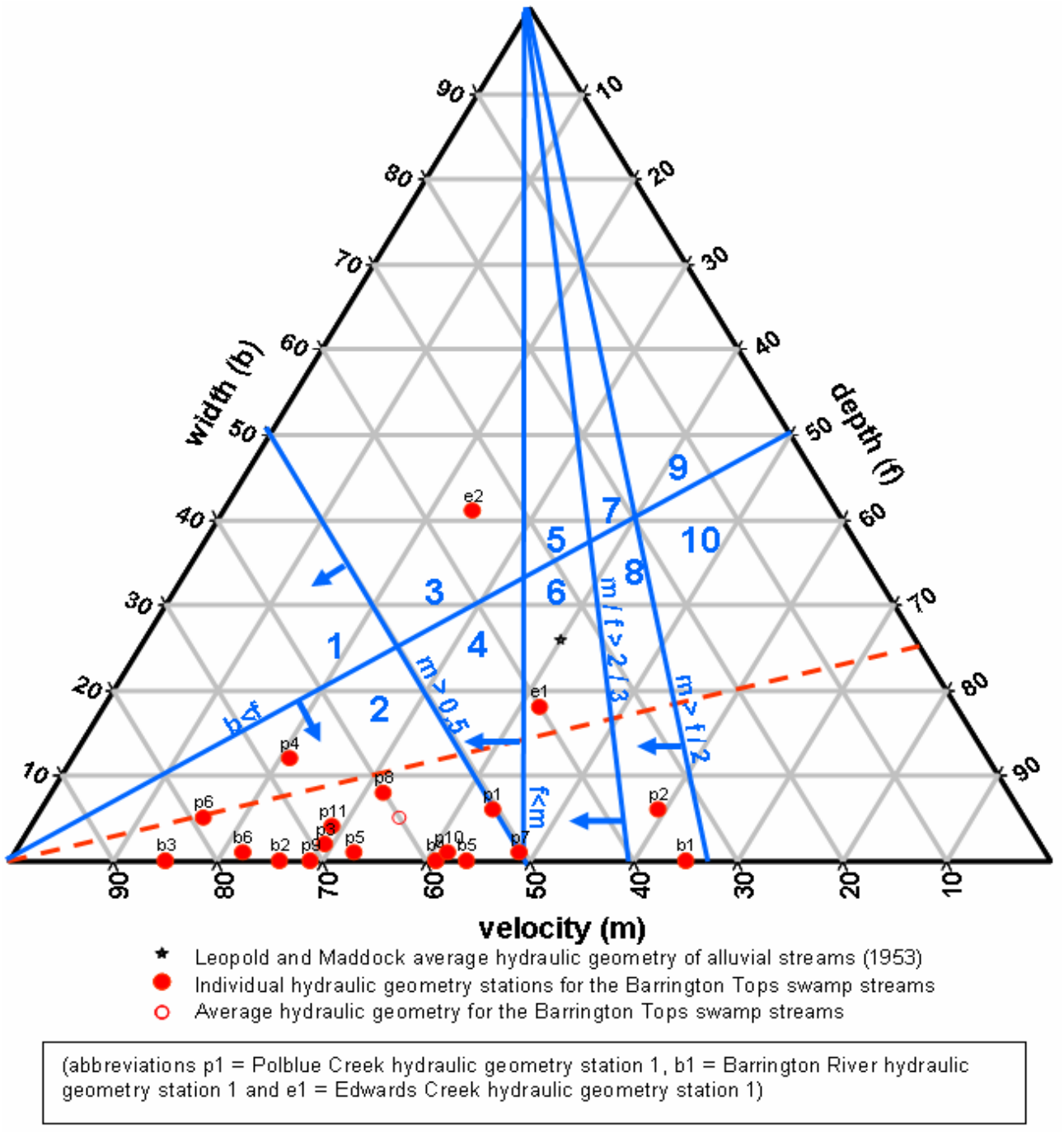

Figure 3.8 Ternary graph of at-a-station hydraulic geometry exponents from the Barrington Tops swamp channel stations (red dots) and the average values (open red dot). A black star illustrates the average result for alluvial channels based on the findings of Leopold and Maddock (1953). The red dashed line indicates stations (below it) at which b is les than 1/3 of f. Modified from Rhodes (1977).

Channel geometry

The symmetry and shape of the Barrington swamp channel cross-sections physically account for low width exponents. Only Stations E1 and E2, which are Type 6 and Type 3 channels, respectively, deviate from this characteristic. They are asymmetrical in cross-section (Figure 3.5) owing to the presence of bedforms, a point to be considered in more detail in Chapter 4. The asymmetry of the cross-sections clearly determines their higher b values, as increasing discharge fills a wider proportion of the channel bed before encountering the vertical channel banks. Similar channel geometry was observed in several wetland streams across North America by Jurmu and Andrle (1997) and Jurmu (2002). Narrow and deep, steep-sided channels are typical of wetland environments.

Sediment load

Sediment load in the Barrington swamp channels was not measured and probably could not easily be because both bedload and suspended load are both so low. Even at close to bankfull flow, the Barrington swamp channels carried so little suspended load that the water remained essentially clear. As a consequence, the bed could be observed and this showed virtually no movement of the bed material during such flows. However, the division $b < f$ implies a predominance of suspended load over bedload. This is probably the effect of strong bank vegetation rather than suspended load. The channels are very narrow and deep, with average width/depth ratios of 2.2, closely approximating the optimal geometry of 2 for the most efficient transport of sediment free water in rectangular channels (Chow, 1973). Stations E1 and E2 support this conclusion by being very different in form; they are wider and shallower with width/depth ratios of 6.5 and 7.1, respectively, and they possess large bedforms, indicative of there having been, at least in the past, some bedload transport (see Chapter 4). However, the majority of stations present extremely low width-depth ratios and width exponents. Huang et al. (2004) suggested that, despite such narrow geometries being theoretically optimal for sediment free rectangular channels, insufficient bank strength in natural channels would likely limit their occurrence. The Barrington swamp channels, with their well vegetated banks, provide for the first-time natural channel data that support their findings.

Bank strength.

The banks of the study channels are nearly vertical in profile and are comprised of dense vegetative matter in their upper portion, below which is up to 1.5m of blocky to smooth peat with variable densities of intruding roots (see Chapter 2). The bank geometry of some estuarine channels are also vertical, owing to high silt and clay content rather than vegetative support, and have resulted in similarly low width exponents (Myrick and Leopold, 1963) (Figure 3.7).

Schumm (1960) used silt/clay bank sediment ratios (M) to assess bank stability. When applied here, M was calculated in reverse, using bankfull width-depth ratios to produce *theoretical* silt/clay ratios in a manner similar to that used for sod channel banks by Zimmerman et al. (1967). These values are presented in Table 3.3 and range from 14 in broad, shallow sections up to 143 in narrow, deep sections. An average M value of 76, resembles high silt and clay content, similar to Zimmerman et al. (1967) observations. But despite apparent variations in bank sediment composition represented by varying M values for the Barrington swamp channels, it is not variation in bank composition or strength, provided by either vegetation or sediment characteristics, which determines the variations in the Barrington hydraulic geometry exponents. The hydraulic erodibility of stream banks is difficult to determine quantitatively on most streams (e.g. Millar and Quick, 1993; Abernethy and Rutherfurd, 1998, 2000, 2001), because of the problems experienced in obtaining appropriate hydraulic erodibility measurements. Such a measure of erodibility is particularly problematic on the Barrington Tops streams because they run very full much of the time. Field observations of the highly consistent bank sediment and vegetation along the length of each swampy channel suggest that bank strength is a relatively constant value. But while the banks are resistant, so too are the stream beds. In places the latter are made of cohesive clays whereas elsewhere they appear to be formed of a lag of coarse cobbles, possibly of periglacial origin, or even of bedrock (see Chapter 2).

The depth of deformable swamp material above the basement material varies, thereby limiting the depth that channels can attain at different stations. Figures 3.9 and Figure 3.10 illustrate how the depth of swamp material varies with the depth of channel distance downstream. At most stations, channel depth is the same as the depth of deformable swamp

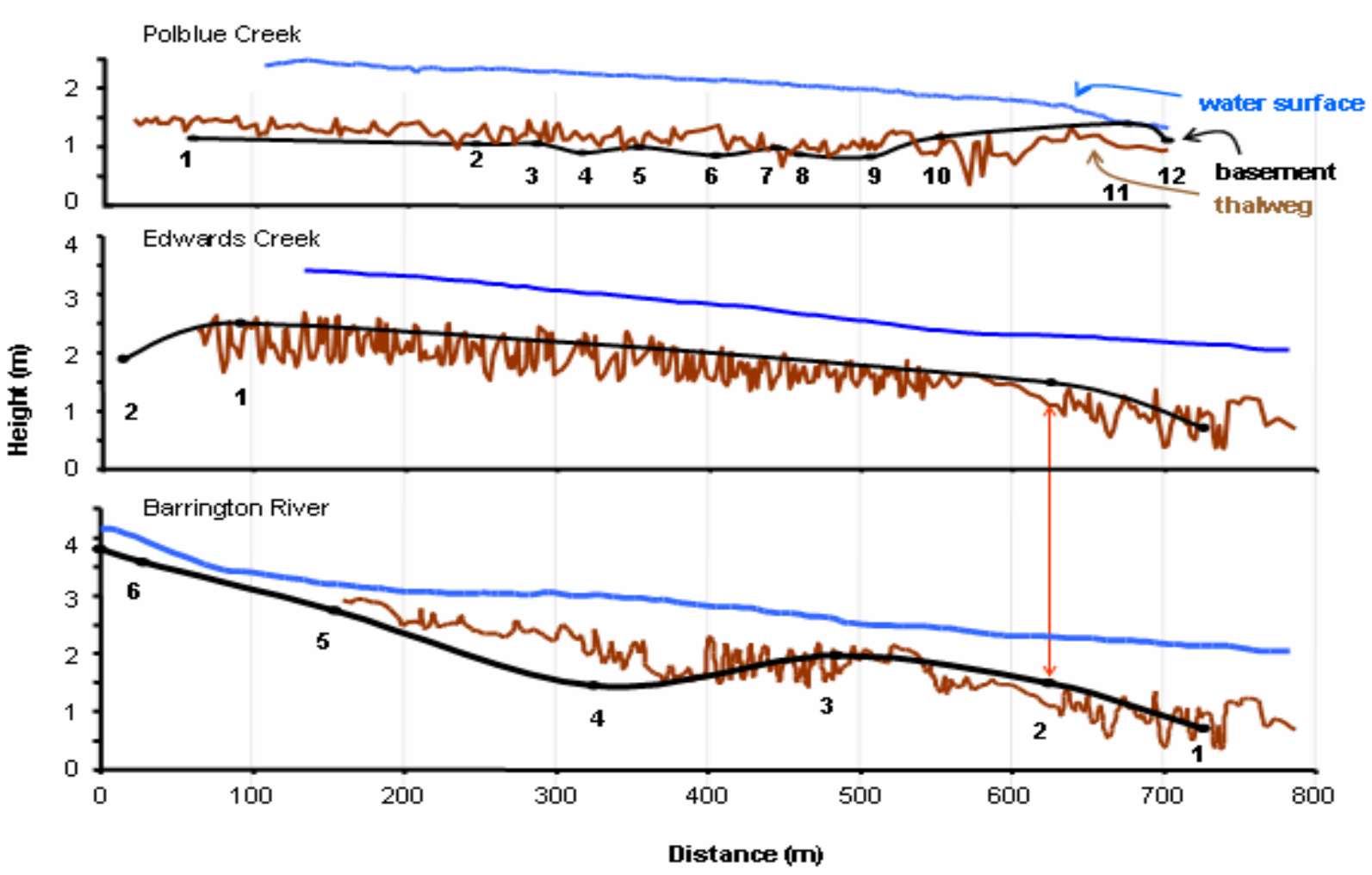

Figure 3.9 Long profiles of each studied channels, including the channel thalweg, bankfull water surface and basement depth, the latter interpolated between hydraulic geometry stations which are indicated by black numbers. The red arrow marks the confluence between Edwards Creek and the Barrington River.

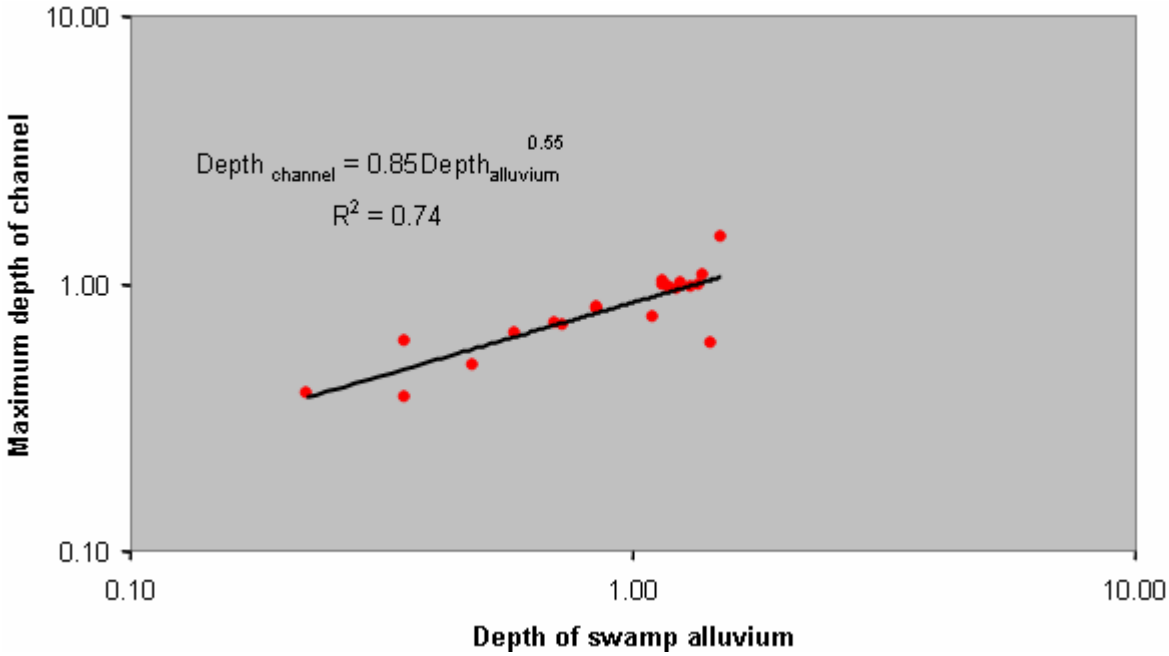

Figure 3.10 This figure illustrates a clear power-form relationship between the depth of swamp alluvium (peat), averaged for each station bank datum, and the maximum channel depth.

material, within the range of measurement error (approximately ±0.1m), resulting from a very uneven, tussocky swamp surface. Several stations, however, have incised into the basement material and these stations, P11&12 and B4, B5 and B6, are located at the entry and exit points of the swamps; they have correspondingly high stream powers (Table 3.2) and therefore have been able to cut down through the confining basement sills at the exit of the swamps. Here the channel sections are wide and shallow, whereas where the peat is deeper, the channels, in the absence of bedload, are narrower and deeper.

(ii) f < m (Δ depth < Δ velocity) & (iii) m > 0.5 (Δ velocity > 0.5) on the Rhodes diagram

This part of Rhodes (1977) diagram defines channels where velocity increases more rapidly than depth (f < m) and indeed where velocity accommodates more than 50% of the increase in discharge (m > 0.5). The rate of change in velocity is closely related to flow competence. Competence is defined as the maximum size of the material that the flow can transport and the changing competence of a cross-section is a function of the ratio of the rates of change of depth and velocity with increasing discharge (Wilcock, 1971). Wilcock found that increases in flow competence were facilitated through higher rates of increase in velocity

than depth, and Leopold and Maddock (1953) found that narrow and deep channels are more conducive to suspended sediment transport.

For the Barrington swamp stations, with the exception of just four locations (E1, E2, P2 and B1), the exponent m is greater than 0.5. In other words, rapid increases in velocity accompany increases in discharge at most cross-sections. P7 lies almost on this line (Figure 3.8) and together with Stations E1, E2, P2 and B1 they provide some idea of what may influence this parameter. As the Manning equation shows, increased velocity is achieved by increasing slope and even more so by increasing depth, and as slope can be assumed to increase slowly with increasing at-a-station discharge (Leopold and Maddock, 1953), increases in depth and commensurate marked decreases in flow resistance (Hicks and Mason, 1998) are the most likely causes for rapid increases in at-a-station velocity.

(iv) m/f > 2/3 on the Rhodes diagram

This portion of Rhodes (1977) diagram (Figure 3.8) includes stations which decrease in roughness with increasing discharge. All the study channels satisfy this condition with the exceptions of B1 and P2. The distances of the plotted stations to the left of this line illustrate the extent to which their roughness decreases and indeed the Barrington swamp channels tend to decrease more rapidly than most other alluvial channels that have been studied. Only Stations P2 and B1 increase resistance with increasing discharge and Stations E1, E2, P1 and P7 decrease roughness only slightly, illustrated by their y and p values (see Figure 3.4 and Table 3.2). All four locations have large bedforms.

An explanation for these velocity and roughness characteristics lies in their cross-sectional shape, bedforms and bed-boundary material. In narrow and deep channel reaches, which are most of the stations, the frictional resistance of the channel boundary rapidly decreases with only slight increases in depth (and associated hydraulic radius), resulting in rapid increases in velocity with discharge and hence high m values. In wide, shallow reaches the effects of boundary resistance are not so easily overcome. The considerable skin resistance provided by large cobbles on the bed at Stations P11&12 and B5&6 at low flow are more easily overcome with increasing flow stage than is the resistance from the large bedforms (see Chapter 4), present at Stations E1, E2, B1 and P2, all of which are also wide and

shallow. Bedforms exert considerable resistance on the flow at stages up to bankfull (Simons and Richardson, 1966) and velocity therefore increases more slowly through sections that have these forms. It appears that bedforms are an important feature of flow resistance in those channels that are supplied with mobile sediment, whereas cobble lags only provide significant resistance at low flow, consistent with Rhodes (1977) original interpretation.

Coupled with the implications for increased hydraulic efficiency with increasing discharge, described above, the condition $f < 0.5 < m$ also dictates that channel cross-sections must exhibit very high bank strengths for this condition to persist.

(v) m > f/2 (Δvelocity > ½ Δdepth) on the Rhodes diagram

This last remaining division of the ternary diagram (Figure 3.8) delineates cross-sections in which Froude number increases with increasing discharge from those which do not. The Barrington swamp streams all display increasing Froude number with discharge, implying that, given sufficient bedload of a transportable calibre, a variety of bedforms are theoretically capable of forming in these channels. At bankfull the maximum Froude number for all stations is only 0.27 (Table 3.2). It is unlikely, therefore, that critical flow is experienced at any cross-section, and bedforms are therefore limited to those that occur only in the lower flow regime.

3.5.1.3 At-a-station summary

Adjustments in flow width, depth and velocity at-a-station in the Barrington swamp streams have been directly related to variations in discharge and also to the available depth of swamp alluvium, as is evidenced by high r^2 values for power relations between these parameters (Figure 3.4 and Figure 3.10, respectively). From their position on Rhodes (1977) ternary graph, adjustments in width, depth and velocity can also be interpreted as responding to uniformly high bank strength and stability. However, while there is almost no active bedload transport, in some places deformable, unconsolidated bed material has modified the channel geometry and resistance to flow. Consistent with the assertions of Ferguson (1986) regarding sediment transport and flow dynamics, the *physical controls* on hydraulic geometry are high bank strength and variations in the depth of swamp alluvium,

or more specifically the location of basement basalt lobes, and the *hydrological controls* are the calibre and quantity of sediment supplied.

In the absence of significant bedload, the Barrington swamp channels (both the smaller Polblue and the larger Barrington channel systems) have developed average width/depth ratios of 2.2 (Table 3.2 and Figure 3.5) through sections with sufficient alluvium depth for adjustment, which are almost identical to those theorised by Chow (1973) as ideal for efficient channel flow without bedload. These results also support the concept of maximum flow efficiency (Huang et al., 2004) whereby channels adjust to minimise their boundary friction for a given quantity of bedload, lending support to their theory of principal of minimum energy (PME) for adjustable channels. Owing to the unusual conditions for its occurrence in the case of sediment free water in natural channels, it has until now been an untested theory.

In sections with limited depth of adjustable swamp material the average width/depth ratios are approximately 8.0. In two Edwards Creek sections with a sufficient depth of swamp to form deeper cross sections, the presence of large unconsolidated bed features of coarse sand and fine gravel, has caused relatively large average width-depth ratios of 6.8 (see Chapter 4). These results indicate that, even in swamp streams with resistant banks, channel cross-sections can adjust when there is a limited depth to the swamp or when sediment is, or has been, available for bedform development.

3.5.2 Bankfull hydraulic geometry discussion

Leopold and Maddock (1953) obtained bankfull (downstream) hydraulic geometry exponent values for b, f and m (width, depth and velocity) of 0.50, 0.40 and 0.10 for mid-western United States streams. In contrast, Myrick and Leopold (1963) obtained values of 0.76, 0.2 and 0.05 for small tidal estuaries and Tooth and McCarthy (2004) obtained wetland-stream values of 0.45, 0.21 and 0.34 for the Maunachira River and 0.83, -0.01 and 0.18 for the Okavango-Nqoga River. The Barrington swamp channel dataset does not compare well with any of these datasets. The low r^2 values suggest that the changes in bankfull channel geometry and associated flow hydraulics in the Barrington swamp

channels are not strongly related to any increase in bankfull discharge. Further comparisons with existing models for bankfull hydraulic geometry are of little value but site specific considerations do present some interesting possible interpretations.

3.5.2.1 Limitations on depth adjustment

An explanation suggested by Wharton (1995) for poor depth (f) r^2 values is that, due to the presence of bed features, channel depth varies so dramatically in a given reach that an average value for a given reach is probably inadequate. However, most of the Barrington streams do not have large depth variability due to bedforms. A more likely explanation for the poor correlation between increasing bankfull discharge and channel depth is the limited and variable depth of deformable swamp material. The swamps have formed in upland catchments, above basin outlet sills formed of coarse basalt cobbles and granite boulders. In such basins the depth of swampy alluvium increases downstream, decreasing again towards the downstream exit sill. The beds of the swamp channels are comprised mostly of basement material underlying the peat (Figure 3.11). In addition, lobes or ridges of a cobble basement occasionally extend out from the basin side beneath the swamps and into mid-basin channel reaches, causing localised reductions in the depth of deformable swamp material within which the channels can form.

Figure 3.10 has illustrated that the depth of swamp alluvium is closely related to at-a-station and bankfull hydraulic geometry. The degree of depth adjustment in these channels is similar to that observed in estuarine channels, resulting in similarly low downstream depth (f) values. Sediment deposition at the mouths of estuarine channels and low slopes, caused by their inherent proximity to base level, probably do much to limit such values compared to those in typical alluvial channels (~0.4) (Leopold and Maddock, 1953).

Figure 3.11 A section of the Barrington River illustrating cobble basement material, not transported by the current flow regime. Note the undercut bank. Channel width is approximately 1m and flow is from left to right.

Figure 3.12 illustrates the control of the depth of swamp alluvium very clearly for the bankfull case. It plots changes in width, depth and velocity at bankfull flow for each station against the corresponding depths of alluvium. The results illustrate clear power relationships of decreasing width, increasing depth and decreasing velocity with increasing depth of swamp alluvium, with corresponding r^2 values of 0.17, 0.55 and 0.34, respectively. While still only moderately well correlated, with width remaining relatively weak, these r^2 values are an improvement over the downstream hydraulic geometry relationship r^2 values of only 0.14, 0.01 and 0.20, respectively.

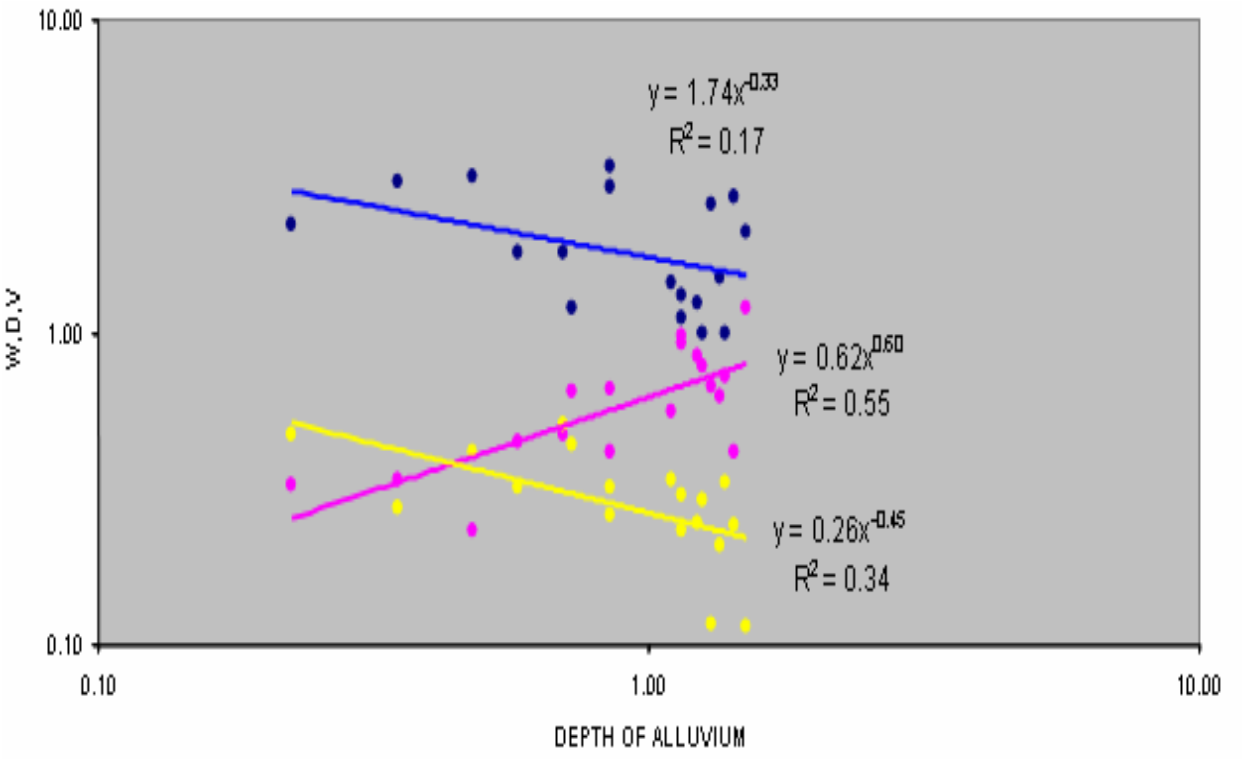

Figure 3.12 The depth of swamp alluvium at hydraulic geometry stations in relation to bankfull width, depth and velocity. Blue is width, purple is depth and yellow is velocity.

Zimmerman et al. (1967) documented that narrower channels are maintained in sod rather than in forested settings and that in the Sleepers River in North America there was no downstream increase in width until catchment areas exceeded ~13km^2. From this they concluded that small streams are subject to exaggerated bank vegetation influences through the provision of either high bank strength or increased roughness imposed on the flow. The contributing areas of the Barrington swamp channels do not exceed 13km^2.

The high effective strength of vegetated channel banks, as a result of the increased tensile strength of roots (Smith, 1976; Millar and Quick, 1993; Abernethy and Rutherfurd, 1998, 2000, 2001; Simon and Collison, 2002) or the protection of the bank through the provision of bank roughness by vegetation (Kutija and Hong, 1996; Simon and Collison, 2002) is now well documented. Recent research has specifically focused on the particularly high bank-strength afforded by "wet-meadow vegetation" (Micheli and Kirchner, 2002a, 2002b) and has concluded that channel banks possessing wet-meadow vegetation produced bank

erosion rates only one tenth of those for banks without wet-meadow vegetation. Smith (1976) very convincingly demonstrated that banks with an effective root mat can be 20 000 times more resistant than those with the same sediment composition but lacking such a root mat.

The exaggerated effect of bank vegetation in small channels is clearly evident in the Barrington swamp channels. Increasing downstream discharge does not cause a notable response in channel width, as evidenced primarily by the low correlation with this parameter (Figure 3.6).

3.5.2.2 Resultant response of velocity to restricted width and depth adjustment

The effects of limited adjustment in width and depth to increasing bankfull discharge results in a similarly limited adjustment between discharge and the rate of change in velocity. Only Polblue Creek has the semblance of a systematic variation in velocity, with an exponent (m) of 1.53 and an r^2 value of 0.58 (Figure 3.6). Such a high exponent illustrates the ability of the boundary materials to resist sharp increases in velocity. These channels are primarily depth-limited and may otherwise respond to increasing discharge by increasing their width, however high bank strength means that width changes too are severely limited. Hence the increasing downstream discharge is accommodated mostly by an increase in velocity, with very little subsequent erosion or channel enlargement.

3.6 At-a-station and bankfull hydraulic geometry conclusions

At-a-station and bankfull hydraulic geometry analyses have both shown the limitation on channel depth adjustment caused by shallow depths of deformable swamp material. In the at-a-station case, this limitation has necessitated the widening of the channel through shallow reaches of the swamp. In the downstream case it has been identified as the primary independent control on variations in width, depth and velocity exponents (Figure 3.12), having a more clearly defined impact than bankfull discharge.

Despite the constraint of swamp depth through many channel reaches, at-a-station hydraulic geometries display a variety of results. The vast majority of stations display width

exponents approaching, or equalling, zero. The resulting adjustments to increasing discharge through these stations are predominantly accommodated by increases in velocity. The implications for channels with such well-defined vertical banks, rapid increases in flow velocity and low width-depth ratios are that they must have highly stable banks and a very limited supply of bedload. These implications are consistent with the theoretical model of Huang et al. (2004), in which width/depth ratios of 2 indicate both the most efficient hydraulic section and the achievement of MFE for sediment free water.

It is significant that both the larger Barrington channel system and the smaller Polblue system have each attained average width/depth ratios approaching 2. This demonstrates that despite relatively shallow swamp depths, the channels of both swamps have developed equivalent and optimal geometries. Bankfull flows were witnessed many times during each field season and display remarkably even confinement along the channel lengths. As described in Chapter 1, swamp vegetation is highly dependant on water table height. Once the channels attained optimal cross-sections through the vertical accretion and growth of the *inset floodplains* (described in Chapter 2), further swamp growth may have been limited by bankfull stage height. This is demonstrated by rapid growth of the *inset floodplain* from ~800BP - 660BP, followed by only slow growth since, as described in Chapter 2. Therefore, while cobble lobes might control channel morphology over some reaches by allowing only shallow depths of swamp material to accumulate, the swamp height is probably controlled more by channel dimensions through the remaining reaches of the channelled swamps.

The majority of reaches in the Barrington swamp streams have very little bedload. Along many reaches, particularly along much of the Barrington River and Polblue Creek, the bed consists of eroded clay or has a cobble lag with clasts far larger than can be moved by contemporary flows. At other locations, especially at Stations E1 and E2 on the Edwards River, large bedforms of coarse sand and granules occur, but even at high flows there is almost no bed sediment movement visible through the clear water. While there must be, or have been at times, some bedload in transport for the construction of these bedforms, it appears that even at bankfull flow the bed is relatively stable, poised close to the threshold

for incipient motion. With their large bedforms, Stations E1 and E2 exhibit lower velocity exponents and higher width exponents. Bedforms appear to result in more moderate velocity exponents, even up to high stage. In contrast, skin resistance provided by the channel boundary through narrower, deeper, vertical sided sections is rapidly overcome by increasing stage.

While Stations E1 and E2 exhibit large bedforms, several locations along the Barrington swamp streams exhibit a range of bedforms including riffle-like and dune-like features, and subdued point bars. The presence of these features raise further questions in relation to channel adjustment; what sorts of bedforms have developed to influence the hydraulic geometry exponents and what function do they serve in relation to sediment transport, flow resistance and flow through meander bends? These questions are addressed in the following chapters.

Chapter 4 Bed features

4.1 Introduction

The preceding chapter on hydraulic geometry has outlined the optimality of most Barrington Swamp channel cross-sections for the transport of essentially sediment-free water. Although these streams appear to transport almost no bedload under conditions up to bankfull flow (nor any significant suspended load), they do exhibit bedforms including riffle-like and bar-like features. The adjustments of the bedforms and planforms of these channels to such maximally efficient cross-sections are the focus of the next two chapters.

Maximally efficient channel cross-sections for sediment-free water, by definition, provide low levels of energy dissipation, as evidenced by high velocity exponents (m values) with increasing discharge. However, for channels to be stable they must consume energy in excess to that required for equilibrium sediment transport and flow, consistent with both the concept of maximum flow resistance (Eaton et al., 2004) and the principal of minimum energy (PME) (Huang et al., 2004). In conjunction with planform and cross-sectional adjustment, bed features determine a significant portion of any resistance applied to open-channel flow (Leopold et al., 1960; Simons and Richardson, 1966; Bray, 1982; Prestegaard, 1983; McLean et al., 1999; Millar, 1999a; Lawless and Robert, 2001), thereby regulating flow velocity and sediment transport (Church et al., 1998). Because of the intimate relationship between bed features and flow resistance (Simons and Richardson, 1966), bed morphology is a very important consideration in the investigation of channel-energy adjustment. Indeed, Eaton et al. (2004; pp.524) state *"... form* (bedform) *roughness represents a powerful potential adjustment of the system."*

Knowledge of established relationships between channel bed-morphology, geometry and flow is reviewed in the following section to provide a context for the presence of particular bed features in the Barrington swamp channels. These features are then identified in the study streams and related to channel and flow dimensions to determine whether they can be classed as bedforms or barforms. Their morphology is then used to quantify the effect on flow and sediment transport.

4.2 Typical bed feature morphology

It is useful here to try to distinguish between bedforms and barforms, as they are associated with different scales of channel adjustment. However, in the Barrington streams the distinction is not always obvious. The following summary of existing knowledge of bed- and barforms details the morphologic characteristics and the hydrologic and formative processes of each.

4.2.1 Bedform characteristics

Bedforms are broadly classified into lower (Fr < 1) and upper (Fr > 1) regime features, the former of which are most common in natural channels (Simons and Richardson, 1966). Subsequent research has suggested that upper regime bedforms (anti-dunes) can form under Froude numbers much less than 1, with increasing effective depth (flow depth / mean grain size) corresponding to a decreasing transitional Froude number (Carling and Shvidchenko, 2002). Carling and Shvidchenko (2002) collated extensive data on the transitional Froude numbers in fine gravel channels and found that the transition in bedforms could occur over a wide range of values, from Fr 0.5 to 1.8. However they also found a more typical value of 0.84, below which gravel dunes can potentially form (Carling, 1999). In the Barrington swamp streams, no standing waves were observed at even the largest discharges and Froude numbers reached a maximum of only ~0.27 at bankfull (Table 3.3). As a consequence it is unlikely that upper regime forms exist in these streams and such forms will not be considered further here.

Lower regime forms exhibit relatively high resistance to flow and low bedload discharges. As they progress from ripples, to ripples on dunes, to dunes, with increasing depth and velocity of flow, resistance coefficients increase correspondingly (Simons and Richardson, 1966). The most common bedforms found in natural channels under sub-critical flow conditions are dunes (Simons and Richardson, 1966).

Ripples range in amplitude (height) up to 0.06m and in wavelength up to 0.61m, whereas dunes range from these values up to 16m and 100m, respectively (Carling, 1999), or occasionally even larger (Miall, 1996). However dunes are not just large ripples as the two

forms behave in fundamentally different ways. Dunes are scaled to the depth of flow; an increase in flow depth over a dune can cause an increase in flow resistance and an increase in dune amplitude, whereas an increase in flow depth over a ripple will always result in a decrease in flow resistance (Simons and Richardson, 1966). Dune amplitudes are roughly scaled to flow depth with a ratio of 0.2 (Allen, 1982; Carling and Orr, 2000) and dune-wavelengths to flow-depth ratios of approximately six (Yalin, 1992). Dunes usually form in medium sands up to fine gravel (Best, 1996) and usually on gradients up to 1% (Clifford, 1993), above which pools and riffle tend to form.

The *magnitude* (Prestegaard, 1983) or *steepness* (Robert, 2003) of a bed feature is defined as its amplitude/wavelength. This is the inverse of the *vertical form index* that was first investigated by Bucher (1919) (in Miall, 1996, pp.20). Ripples have average steepness values of 0.12 (Baas, 1999), whereas dunes are relatively low and normally range between 0.03-0.06 (Kostaschuk and Villard, 1996), with a maximum of 0.08 observed by Carling (1999) for gravel dunes. A link between barform amplitude and wavelength has also been long recognised (e.g. Hey and Thorne, 1986; Robert, 1990), and their steepness typically falls around 0.01, though Carling and Orr (2000) recently observed an upper steepness limit of 0.03. Feature steepness therefore varies from the lowest to the highest in the order riffles (0.01-0.03) to dunes (0.03-0.06) to ripples (average 0.12).

4.2.2 Barform characteristics

Barforms include pools, riffles and point bars (Best, 1996) and are often synchronised with channel planform. Pools are usually found at the concave bank of meandering channels with point bars attached to the convex bank of bend apices, whereas riffles commonly occur between successive pools. However, pools and riffles are not exclusively features of meandering channels, also being found in straight (Keller, 1972) and braided channels (Ashmore, 1991).

Leopold et al. (1964) and Keller and Melhorn (1978) first related channel width to barform wavelength and Keller and Melhorn (1978) found that the dominant wavelength of pool-pool sequences ranges between 5 and 7 channel widths, a range subsequently supported by

numerous researchers (e.g. Richards, 1982). However, recent work by Carling and Orr (2000) obtained a different result in the River Severn where the riffle-crest wavelength was predominantly 3 channel widths. Following this observation, they sought relationships between pool-riffle spacing and parameters other than width and found it to be related to flow depth, ranging from 7 to 18. They also expressed riffle amplitude as a fraction of flow depth and found it ranged from 0.151 to 0.223. Carling and Orr (2000) likened these results to the dune relationships of the many studies collated by Allen (1982). Based on this, they suggested that the formation of riffles and dunes should not be attributed to exclusively different processes. Although Robert (2003) argued that caution should be applied in the interpretation of Carling and Orr's (2000) results because of their use of different devices on the exceptionally large River Severn to those that had previously been used to collect data, the overlap of riffle and dune wavelengths should not be overlooked. Indeed, the analysis below on the very small Barrington streams also demonstrates ambiguity and overlap in the definitional characteristics of bed features.

4.2.3 Summary of bed feature attributes

In summary, bedforms are fundamentally linked to flow properties such as velocity and depth of flow, whereas barforms are generally scaled to the physical channel dimensions, such as channel width and planform (Jackson, 1976). Bedforms are considered fast-response features that adjust to changes in sediment and water supply during a single flow event (Simons and Richardson, 1966; Best, 1996), whereas pools and riffles (barforms) adjust over the longer term, often in conjunction with planform development (Keller and Melhorn, 1978), and may persist in location for many decades or longer (Dury, 1970). Bedforms are generally considered more transport-limited than supply-limited than are pools and riffles (Montgomery and Buffington, 1997). Such generalisations are appropriate for most studies, however, the recent work by Carling and Orr (2000) has demonstrated overlap in the flow-form relations between riffles and dunes, implying that a less rigid distinction between each feature may be more appropriate.

4.2.4 Flow resistance, shear stress and bed sediment transport

While the definition of bed and bar features may be somewhat arbitrary, the influence that both exert on the flow and bed sediment transport can be quantified using their steepness values (amplitude / length). Bedload transport capacity is directly related to the shear stresses acting on a channel bed. The du Boys shear stress equation is often used to estimate this, however, Robert (1990) compared empirically derived shear stress data estimated using the inner-layer velocity profile with the du Boys shear stress estimates and illustrated the gross overestimation caused by the latter approach. Such overestimation is caused by the equation comprising the sum of several shear components whereas only the shear acting on the bed is responsible for bed sediment transport. The other components of the total shear must be removed to obtain realistic estimates of transporting competence (Robert, 1990). In an effort to determine the effects of bedform development on sediment transport competence in the Barrington swamp channels, the proportion of the total shear that is actually exerted on the bed will be considered later in this chapter.

4.3 Bed features of the Barrington swamp channels

4.3.1 Bed feature identification

In the Barrington swamp streams, the bed features appear complicated and it is not possible to distinguish easily between bedforms and barforms. Because of the small scale of the channels, what would clearly be bedforms in larger channels appeared to be scaled to the physical dimensions of the channels. A consistent method is required here to identify and label these features and to then describe their morphology.

4.3.1.1 Methodology

The longitudinal profiles of the Barrington River and Edwards and Polblue Creek beds were surveyed using a Sokkia Total Station. The surveys followed the thalweg of the channel, rather than the centreline, as it was the morphology of the bedforms along the deepest part of the channel that were of interest. Data points were collected at irregular intervals corresponding to discernable changes in bed topography. Because of this the bed levels could be linearly interpolated between these inflection points.

A differencing analysis technique was employed to identify the bed features prior to the subsequent calculation of their amplitude and wavelength (O'Neill and Abrahams, 1984). The technique is an improvement on the regression technique (Richards, 1976) as it identifies features superimposed on sequences of positive or negative residuals (O'Neill and Abrahams, 1984) and allows bed features within an extended depression or hump to be identified as discrete, alternating units, rather than their being classified as single, long pools or riffles as would be the case if the regression technique were used. The differencing technique requires that data be equally spaced, so a Matlab script was used to linearly interpolate the bed elevation survey data at both 1m and 2m intervals to create two separate datasets for each channel (Appendix 3), (1-2m being approximately the bankfull width) (O'Neill and Abrahams, 1984). As average channel width is difficult to define, and as the bed fluctuations may be better identified using *either* the 1m or 2m dataset, both were used for comparison of the results in the initial stages of analysis.

The differencing technique can only be applied to datasets of similarly scaled bed features, so that each of the channel surveys were divided into sections based on clear changes in bedform wavelength and amplitude (Figure 4.1). In addition, several reaches were identified as plane-bedded, lacking rhythmic undulation in bed topography along their lengths (Montgomery and Buffington, 1997). These reaches were removed from all analyses and are identified in Figure 4.1. Following these subdivisions, the resulting sub-datasets possessed more consistent bedform wavelength and amplitude with linear trends. The resulting sub-sets are presented in Figure 4.1 and include: “Barrington River Upper”, “Middle” and “Lower”, “Edwards” Creek and “Polblue Creek Upper” “Middle” and “Lower”.

Differences in elevation between equally spaced successive points along a linearly detrended channel thalweg survey were calculated, following which the standard deviation (SD) of these differences were calculated. A series of peaks and troughs in the channel long profile were then identified as successive elevation-point sets whose differences multiply to give negative values: i.e. [(–) elevation difference] X [(+) elevation difference] = (-) result (in this case a trough) (and vice-versa) and were therefore peaks or a troughs. A threshold

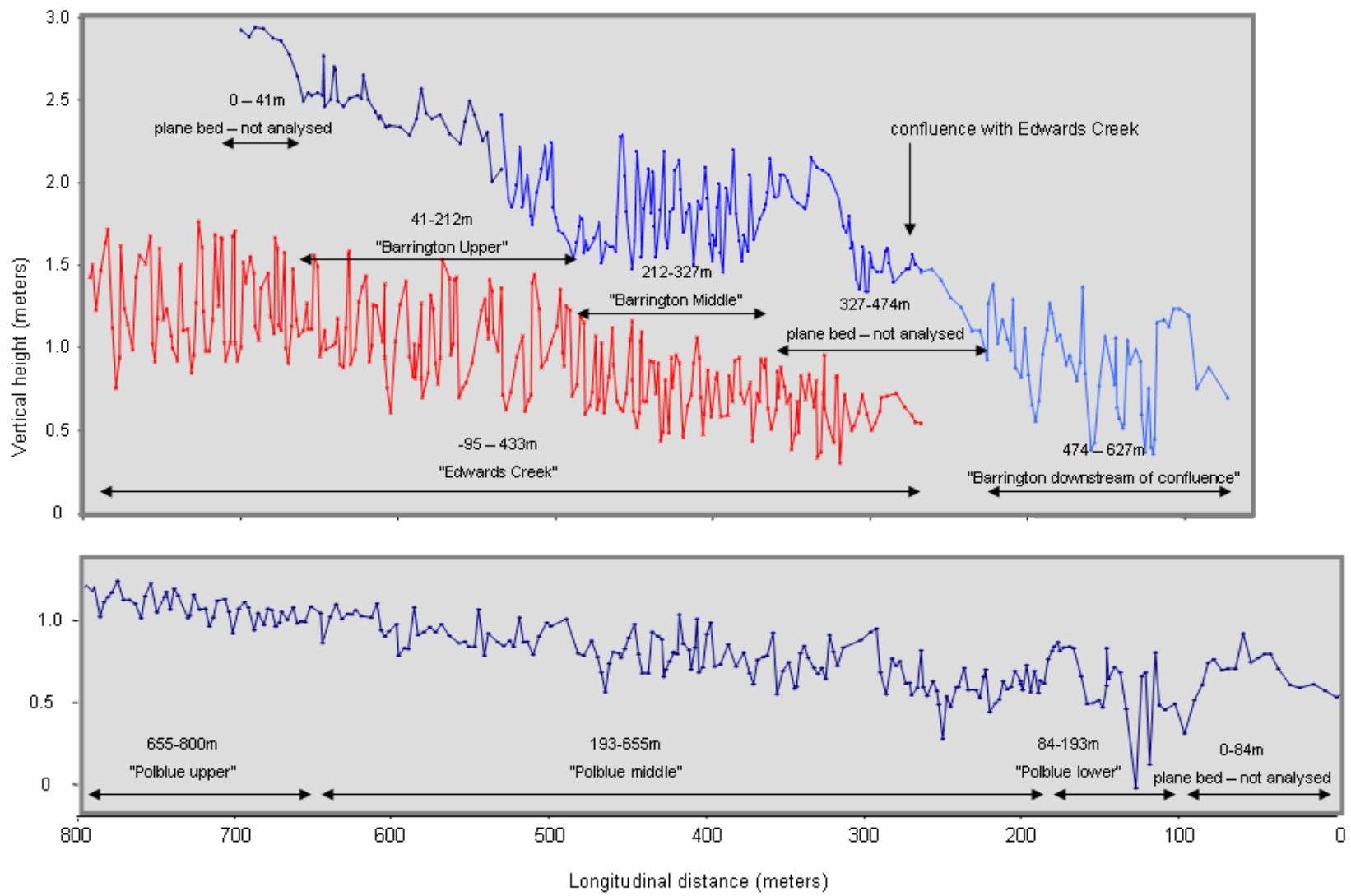

Figure 4.1 Divisions of the bed long profiles for a) Barrington River and Edwards Creek and b) Polblue Creek

(T) is set with which to choose those points that qualify as bed features. O'Neil and Abrahams (1984) found that T = 0.75SD was the most successful filter in identifying pools and riffles where data point spacing equalled the approximate channel width. Subsequent peaks and troughs were tested for absolute elevation differences greater than 0.75SD of the last identified feature and then accepted if this criteria was satisfied. A Matlab script was used to apply this procedure (Appendix 4).

4.3.1.2 Results

The results from both the 1m and 2m spaced dataset, differencing-technique bed-form analysis are presented in planform view in Figure 4.2 and their summary statistics are presented in Table 4.1. Figure 4.3 illustrates the identified bed-form locations in comparison with the original, non-systematically sampled long profile data.

4.3.2 Bed feature amplitude and wavelength calculations

The features identified for both the 1m and 2m spaced datasets were analysed to determine their wavelengths and amplitudes. These results could then be considered, in conjunction with feature-planform relations, to determine the most prominent bed features to consider in the analysis of bed feature-flow interactions.

4.3.2.1 Methodology

Bedform amplitude and wavelength were calculated using peak-peak and trough-trough spacing (wavelength) and peak-trough heights (amplitude), with resulting statistics for both the 1m and 2m datasets. In Figure 4.2 the bed-feature wavelengths and amplitudes are presented as histograms, similar to Keller and Melhorn (1978) and O'Neill and Abrahams (1984), and the modal values are discussed where they are clear and the mean values when they are not. Figure 4.3 highlights an important feature of the differencing analysis technique; due to the rigidity of re-sampling at 1m and 2m intervals, the technique did not necessarily define the real maximum or minimum heights of these features. The bed-feature amplitude statistics resulting from this analysis must, therefore, be considered minimum values.

4.3.2.2 Results

Barrington River

The Barrington River Upper reach shows no clear modal values for bed morphology wavelength for either the 1m or 2m datasets, for which there were 18 and 17 features, respectively. However, the bedform amplitudes of these same datasets illustrate convincing modes of 0.3m and 0.2 m, respectively

Through the Barrington River Middle reach, immediately downstream of Barrington River Upper, 24 and 16 features were identified for the 1m and 2m datasets, respectively, with corresponding feature wavelength modes of 4 and 4-5 channel widths, respectively, and a convincingly high frequency for both wavelength modes. Both datasets also illustrate clear modal bed-feature amplitudes of 0.5m, with the 1m dataset identifying a second mode at 0.2m.

The Barrington River Lower reach has bed morphology wavelength modes of 4 and 6 channel widths from a total of 22 and 15 features for the 1m and 2m datasets, respectively, however, only the 1m dataset shows a convincing mode for amplitude, at 0.5m.

Edwards Creek

Along the 530m of the Edwards Creek that was analysed, a large number of bed features were identified: 112 for the 1m dataset and 70 for the 2m dataset. Modal values for the wavelength of these features were 2 channel widths for the 1m dataset and 5-6 channel widths for the 2m dataset. Feature amplitudes of 0.3-0.5m and 0.4-0.5m were identified in the 1m and 2m datasets, respectively.

Polblue Creek

The Polblue Creek Lower reach presented no modal value for either the bed-feature wavelength or amplitude from the 1m or 2m datasets, which identified 11 and 7 features, respectively.

The analysis of the Polblue Creek Middle reach resulted in the identification of 74 and 57 features for the 1m and 2m datasets, respectively, and shows a clear mode of 6 channel

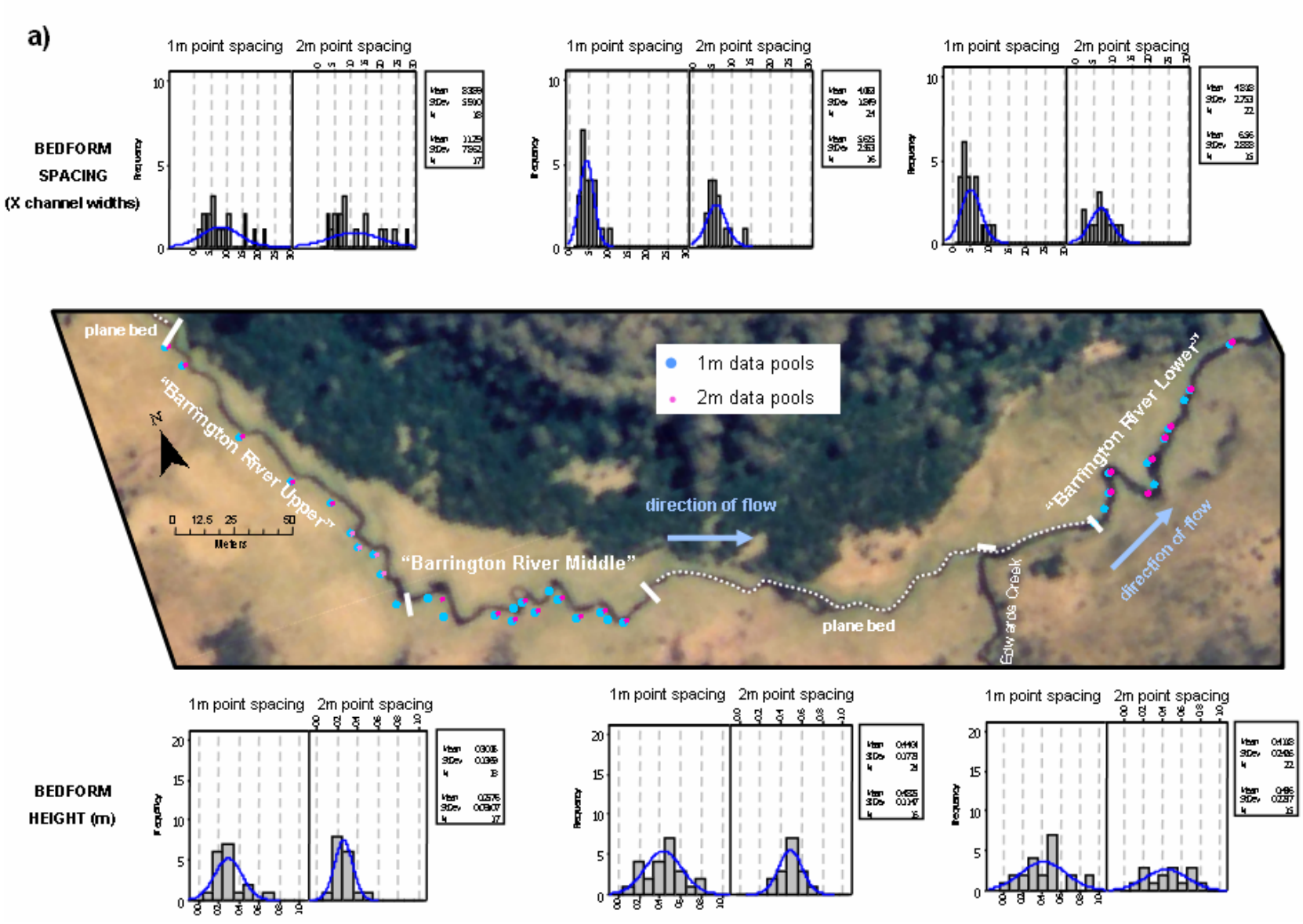
a)
BEDFORM SPACING (X channel widths)
1m point spacing
2m point spacing
Frequency
plane bed
"Barrington River Upper"
"Barrington River Middle"
"Barrington River Lower"
1m data pools
2m data pools
direction of flow
direction of flow
plane bed
Edwards Creek
N
0 12.5 25 50
Meters
BEDFORM HEIGHT (m)

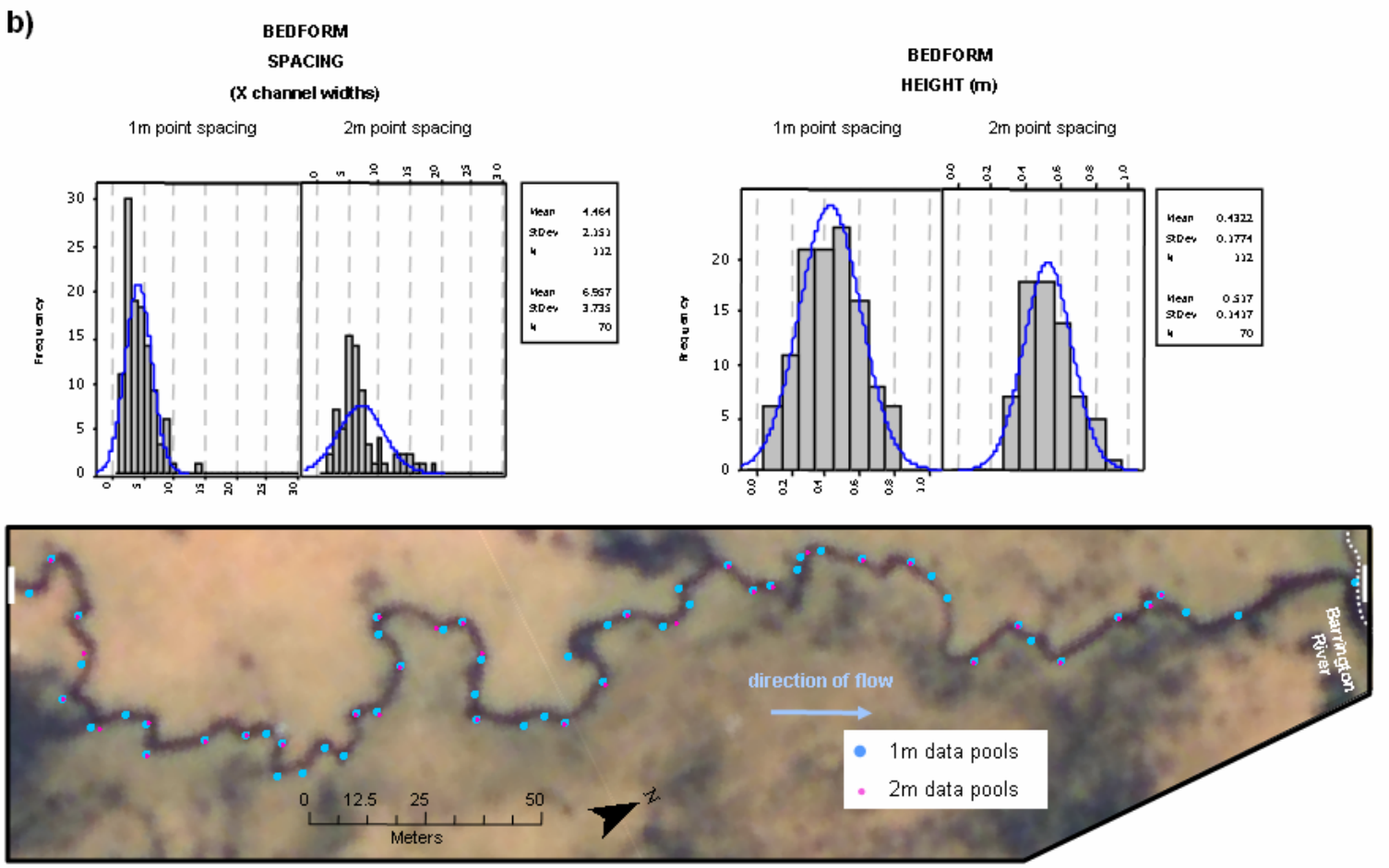

Figure 4.2 Aerial view of 1m and 2m dataset bedform analysis results with histograms of bed-feature wavelength and amplitude for (a) Barrington River, (b) Edwards Creek and (c) Polblue Creek.

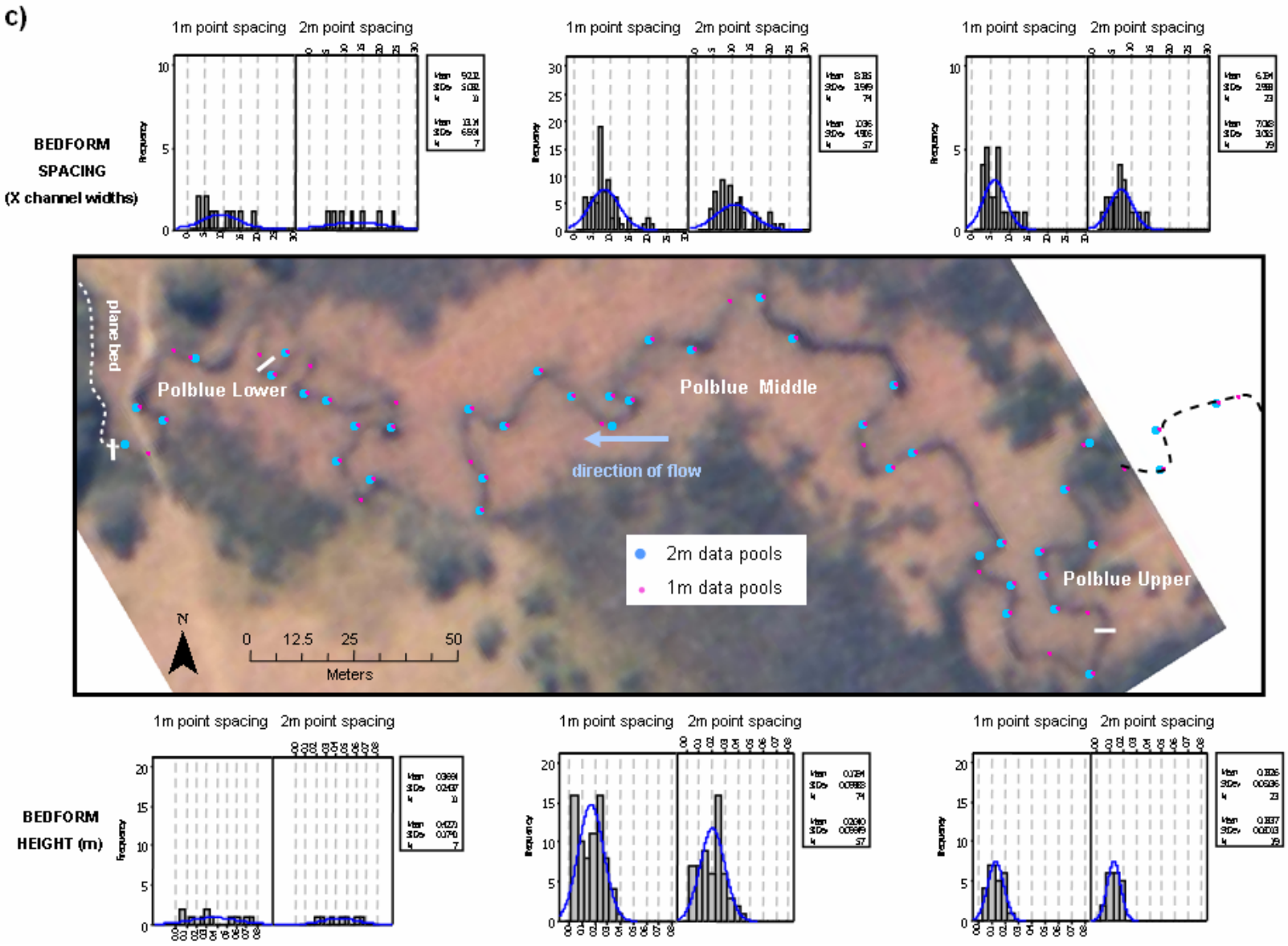
c)
BEDFORM SPACING (X channel widths)
1m point spacing
2m point spacing
plane bed
Polblue Lower
Polblue Middle
Polblue Upper
direction of flow
2m data pools
1m data pools
N
0
12.5
25
50
Meters
BEDFORM HEIGHT (m)

Table 4.1 Summary of bed feature analysis results

	distance (m)	width (m)	wavelength (channel widths)		amplitude (m)		% expected pools		% not planform pools		selected dataset	steepness	average flow depth (m)	wavelength / average flow depth	amplitude / average flow depth
			mean	mode	mean	mode	1m	2m	1m	2m					
Barrington															
Upper	41-212	2	11	8	0.26	0.20	53	60	20	22	2m	~	0.91	24	0.22
Middle	212-327	2	6	4-5	0.48	0.50	90	90	31	11	2m	0.06	1.42	8	0.35
Up & Mid	41-327	2					68	72	26	17	2m				
Lower	474-627	2.5	7	6	0.44	none	78	89	36	38	2m	0.03	1.29	14	0.34
Edwards	-100-415	2	4	2	0.52	0.45	90	67	16	3	1m	0.11	1.00	8	0.45
Polblue															
Upper	655-800	1.8	7	4&6	0.14	0.10					1m	0.01	1.00	13	0.10
Middle	193-655	1.5	10	6	0.20	0.25 & 0.10	91	80	7	7	1m	0.03 & 0.01	1.06	14	0.24 & 0.09
Lower	84-193	1.5	9	none	0.37	none					1m	~	0.88	15	0.42

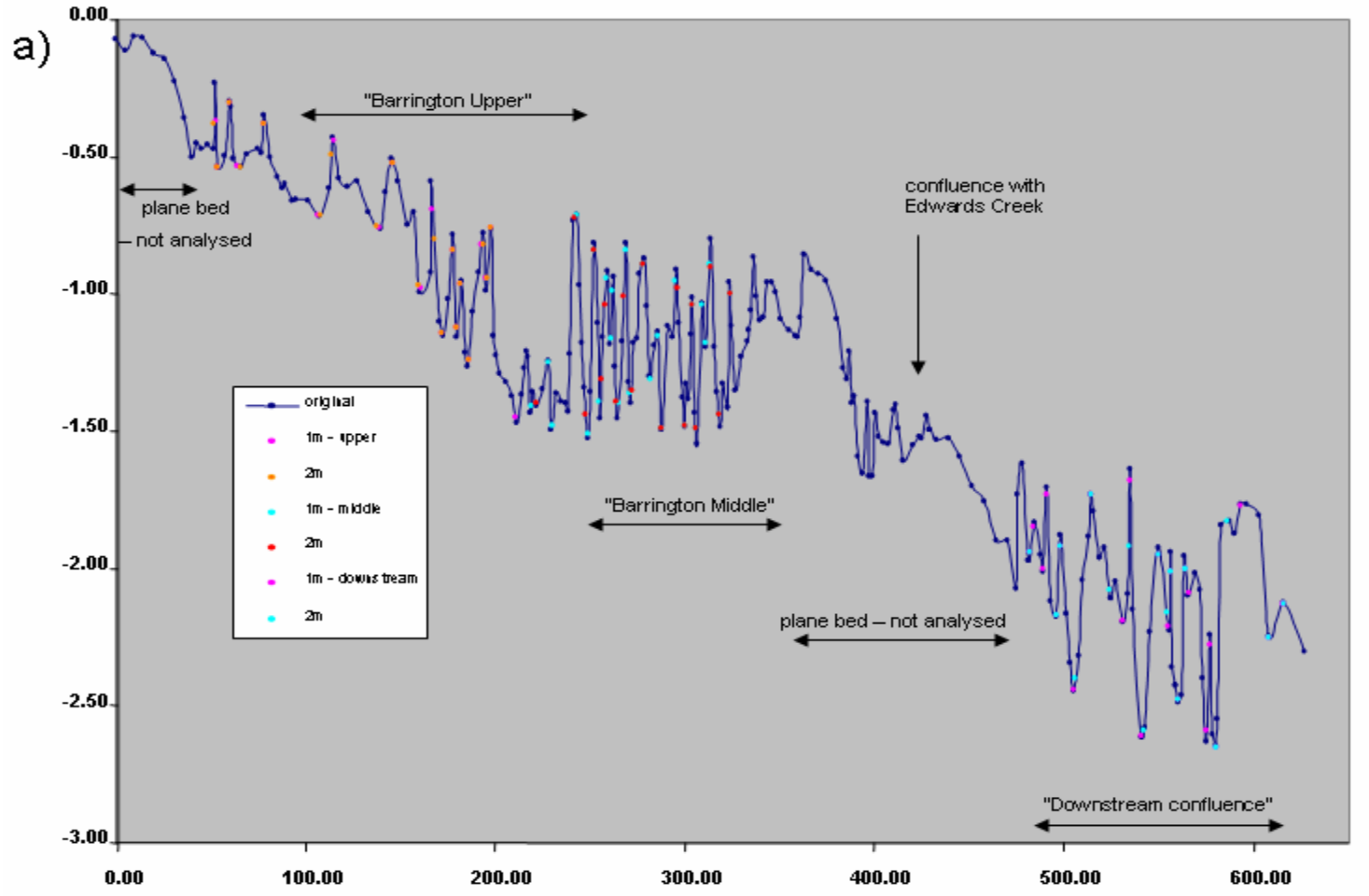

Figure 4.3 Longitudinal illustration of the bed feature analysis results, both 1m and 2m datasets compared with original datasets for (a) Barrington River, (b) Polblue Creek and (c) Edwards Creek (over page).

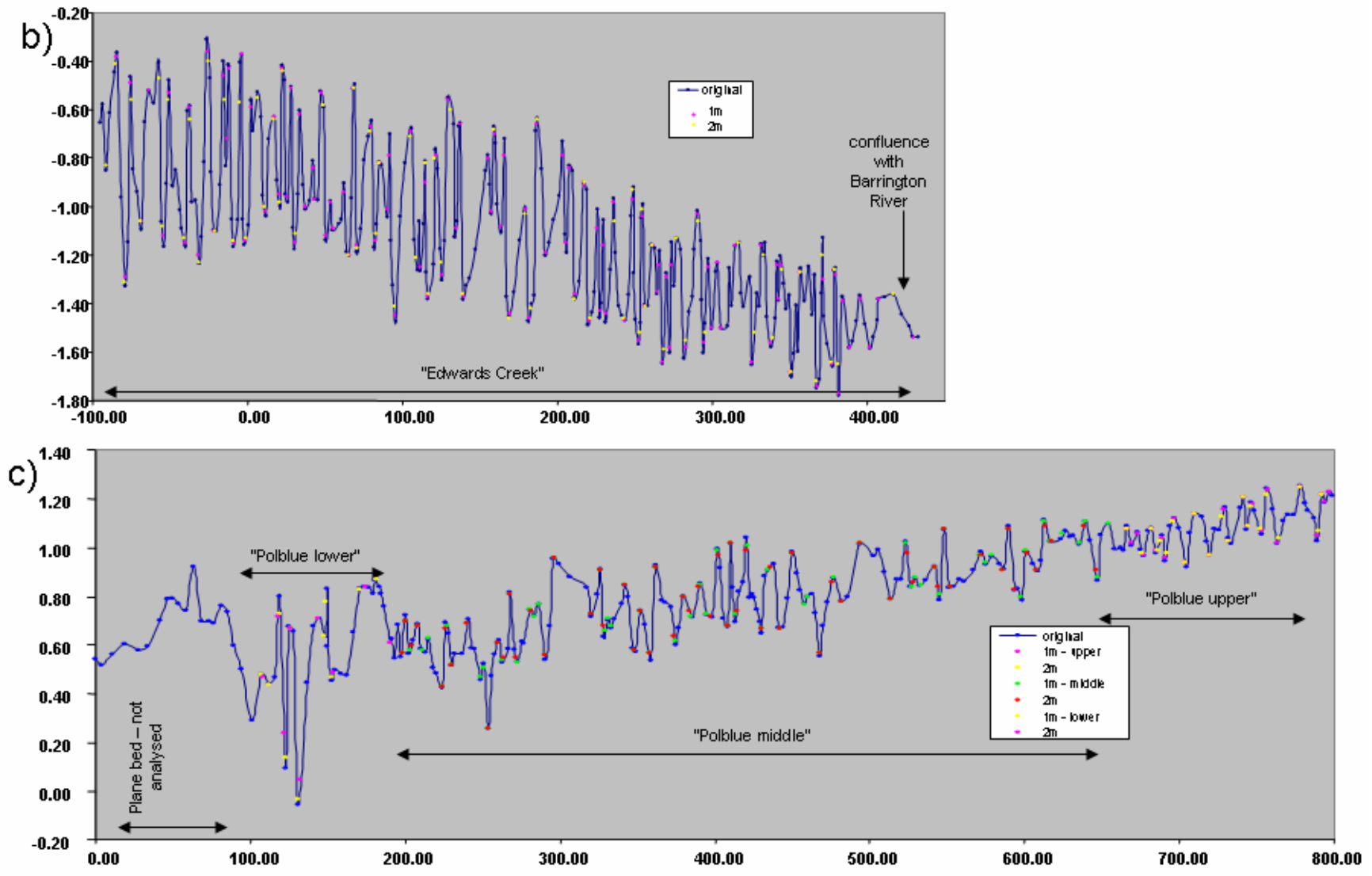
b)
-0.20
-0.40
-0.60
-0.80
-1.00
-1.20
-1.40
-1.60
-1.80
-100.00
0.00
100.00
200.00
300.00
400.00
orighal
1m
2m
confluence with Barrington River
"Edwards Creek"
c)
1.40
1.20
1.00
0.80
0.60
0.40
0.20
0.00
-0.20
0.00
100.00
200.00
300.00
400.00
500.00
600.00
700.00
800.00
"Polblue lower"
"Polblue upper"
"Polblue middle"
Plane bed – not analysed
orighal
1m - upper
2m
1m - middle
2m
1m - lower
2m

width wavelengths for the former and a less convincing mode of 7 for the latter. However, both datasets illustrate clear bed-feature amplitude modes of 0.25m, with an additional mode of 0.05m for the 1m dataset. The Polblue Creek Upper reach 1m and 2m datasets identified 23 and 19 features respectively, and both resulted in feature spacing mode values of 6 channel widths, with the 1m dataset having identified modal feature amplitudes of 0.1m and the 2m dataset identified an equally strong mode of 0.15m.

4.3.2.3 Summary

For the datasets Barrington River Middle, Edwards Creek and Polblue Creek Middle, the 1m spaced datasets identified *lower amplitude* bed-features additional to those identified using the 2m dataset and in all analyses the 1m datasets identified *additional* features to those identified from the 2m dataset (Figure 4.2 and Figure 4.3). Shorter longitudinal survey increments identify greater numbers of smaller-magnitude bed-features illustrating, rather importantly, that the scale of the survey increment dictates the scale of the features that will be identified.

Bed features identified in the Barrington River Upper and Polblue Creek Lower reaches are not scaled consistently with channel width, and do not have persistent amplitudes, for either the 1m or 2m datasets. These reaches flow over pre-fluvial cobbles and basement clay and their bed features have probably not have formed in response to contemporary fluvial processes (see Chapter 2).

The range of modes for bed-feature wavelength for all datasets lie between 4 and 7 channel widths in all analyses, with the exception of a wavelength of 2 channel widths for the 1m dataset on Edwards Creek. Such consistent scaling of bed features with channel width strongly suggests their identification as pools and riffles (Keller and Melhorn, 1978) and encourages further consideration of their distribution in the channel in relation to channel planform.

4.3.3 Bed morphology and planform relations

Field observations suggested that the largest pools were usually located on channel bends, consistent with another wetland stream examined by Jurmu and Andrle (1997). The bed

features that bound such pools were sometimes very steep and produced visible turbulence in the flow, observed as boils, and were clearly defined by the alignment of ribbon-weed at various levels in the flow (see Chapter 6). The spacing of bed features is scaled approximately to the physical dimensions of the channel, in multiples of 4-7 channel widths. If the most dominant bed features are planform related, then it is these features that are of primary interest to this study and which are sought for identification and quantification. This is because they combine with planform adjustments to produce large scale turbulence and therefore high levels of flow resistance. Indeed, Lewin and Brewer (2001) have found that bedforms may be inextricably linked to channel pattern generation, thereby emphasising the co-dependence of the two morphological adjustments. Channel planform will now be used to determine the most prominent bed features using both the 1m and 2m datasets for each reach.

4.3.3.1 Methodology

A dataset was created whereby pools were "expected" at channel bend apices. By allocating expected depressions at these locations, and comparing these with the actual identified depression locations, the relationship between planform and bed features from each of the 1m and 2m datasets were assessed. The datasets which most accurately represented the planform "expected" (i.e. bend located) depressions were selected for bed morphology characterisation for the subsequent flow depth, steepness and flow resistance analyses.

In Figure 4.3 it may not appear that the points indicating pools are located on channel bends. However, the differencing technique which identified these points stipulated neither the midpoint nor the deepest/shallowest point in any bed feature. It must be appreciated that the pools extend for considerable distances up- and downstream from these specific pool-identification points, thereby incorporating pools at the position of many of the bends. The simultaneous consideration of both the planform and long profile figures (Figure 4.2 and Figure 4.3) therefore allowed relations between bed features and planform to be identified.

4.3.3.2 Planform – bed feature relations and dataset selection

Figure 4.4 illustrates the success of both the 1m and 2m datasets in identifying pools at bend locations. In all channel reaches over 68% of the expected bend pools were

successfully identified using both the 1m and 2m spaced dataset analyses. If this success rate is indicative of the identification of the most significant pools, then the most useful datasets are the 1m spaced datasets for reaches Edwards Creek (90%) and Polblue Creek (all three reaches) (91%) and the 2m datasets for the Barrington River Upper and Middle (grouped reaches) (72%) and Barrington Lower (89%). The wavelengths and amplitudes of these features are summarised in Table 4.1. These results support the identification of the swamp channel-bed features as predominantly pools and riffles. The reason for the somewhat different success rates in the different reaches for the 1m and 2m datasets is that the bed features are predominantly scaled to channel dimensions, including width *and* meander wavelength. As previously explained, channel widths vary between 1m and 2m and are therefore best represented by one or other datasets in different reaches. Furthermore, lower meander wavelengths produce bedforms at closer intervals. Polblue Creek and Edwards Creek are more sinuous than the Barrington River and bedforms are therefore more closely spaced than the channel width relations would otherwise predict.

Figure 4.4 also illustrates the percentage of pools that were identified which do not correspond with the expected bend locations (i.e. those pools occurring along straight reaches). While pools associated with bends are expected, the datasets selected for ongoing consideration corresponded with pools not related to planform equalling 17% for the Barrington River Upper and Middle, combined, 38% for the Barrington River Lower, 16% for Edwards Creek and 7% for Polblue Creek (all three reaches). While most channel bends correspond with pool locations, pools can also occur along straight reaches of channel (Keller, 1972). However, the high number of non-planform related pools in the Barrington River downstream reach (38%) requires further explanation. Through this reach the Barrington River flows over granite boulders with b axes up to 1m, and it is this pre-fluvial substrate that often dictates “riffle” locations. The identified pools are not true flow-generated pools and are, unsurprisingly therefore, inconsistent in amplitude and spacing and frequently unrelated to channel planform.

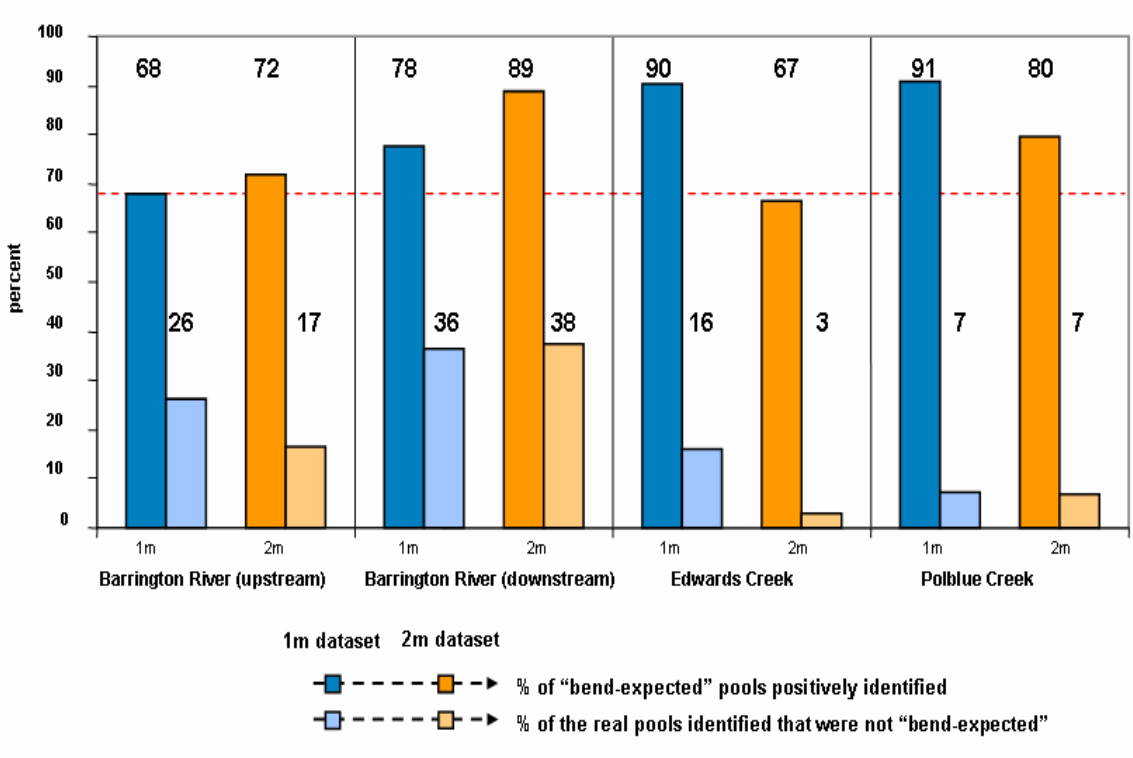

Figure 4.4 Success of the 1m and 2m datasets in identifying expected pools and the percentage of pools identified that were not planform related. The red dashed line indicates the 68% of expected pools successfully identified using both the 1m and 2m datasets. Numbers indicate the % values for each column.

4.3.4 Bed feature and flow depth relations

The amplitudes and wavelengths of the bed features through each of the reaches were calculated for the selected 1 or 2m datasets, based on the planform association technique described above. Their amplitudes and wavelengths vary greatly, however, for comparison of their ratios between reaches they can be standardised by scaling them to bankfull flow-depth. Different ratios are characteristic of dunes and riffles and these results may aid further in, 1. the classification of the Barrington swamp channel bedforms, and 2. understanding their role in channel processes.

4.3.4.1 Methodology

The average water depth was calculated by linearly regressing both the water surface and bed long profiles through each channel reach, thereby providing equations for each in the form $y = mx + b$. The most upstream and downstream extent of each reach provided

distance values (x) which were inserted into the regression equations to determine the regressed bed and water surface heights (y) at these locations. The difference in height between these two sets of water and bed elevations at each measurement point were averaged to determine the average flow depth through each channel reach (Figure 4.5). Average flow depth was then compared with bed-feature amplitude.

In order to determine bed-feature amplitude to average flow depth relations, modal bed feature amplitude values were used. However, due to unclear modal values for the bed features in Polblue Creek Lower and the Barrington River Lower (see Figure 4.2), mean values were used instead for their analyses.

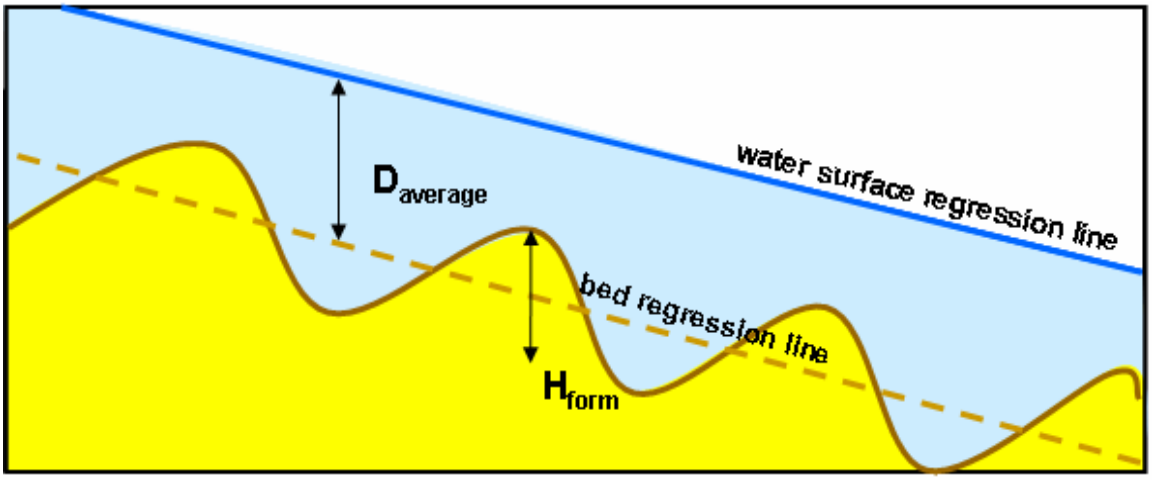

Figure 4.5 Calculation of reach averaged flow depths, using the regression technique

Owing to data errors resulting from either Total Station reading errors in failing light or a slipping survey staff reflector, the water surface long profile along Polblue Creek could not be extended through the Polblue Creek Upper reach. The modal bed-feature amplitude as a percentage of average pool depth was, therefore, not able to be calculated for this upper dataset. However, as it is useful for both comparison with other reaches and completeness of the Polblue Creek bed analysis, it was approximated based on the adjoining dataset (Polblue Creek Middle) with an estimated flow depth of 1m. While the estimated 1m depth

of flow is only approximate, the bedform data is real and the ratio between the two is likely to be only slightly affected (perhaps even less so than variations in the localised flow depth and bedform amplitudes).

4.3.4.2 Results

The results of the relationship between the modal amplitudes and wavelengths of bed features and average flow depths are presented in Table 4.1 (page 105).

Bed-feature amplitude to flow-depth relations ratios are 9% for the smaller of the bimodal amplitudes (0.10m mode) in Polblue Creek Middle and 24% for the larger mode (0.25m mode), an estimated 10% (0.10m mode) for Polblue Creek Upper, 22% (0.20m mode) for Barrington River Upper, 34% (0.44m mean) for Barrington River Lower, 35% (0.50m mode) for Barrington River Middle, 42% (0.37m mean) for Polblue Creek Lower and 45% (0.52m mode) for Edwards Creek. Due to the smoothing of the bed survey data caused by re-sampling at 1m and 2m intervals, these amplitudes should be considered to be minimum modal values.

Bed feature wavelength to flow depth ratios vary from 8 (Barrington Middle and Edwards Creek), 13-15 (Polblue Creek all reaches and Barrington Lower) up to 24 through the Barrington River Upper reach.

4.3.4.3 Summary

With the exception of Polblue Creek, the channel bed-features in these swamps present very high ratios of amplitude to flow depth, with Edwards Creek approaching 50%. This is a reach average and more extreme individual examples were observed in the field, as illustrated in Figure 4.6, where the ratio would be in the order of 80%. Such high ratios exceed those documented for both dunes and riffles (Allen, 1982; Carling and Orr, 2000). However their wavelength to flow depth relations provide more definitive results; all reaches exceed the ratio of 6 that is most usual for dunes (Yalin, 1992) and, with the exception of Barrington Upper reach, fall within the range of 7-18, a range recently observed for riffles in the River Severn (Carling and Orr, 2000). The inconsistency of the Barrington River Upper reach may lie in its coarse cobble substrate which could not be deformed by the present flow regime.

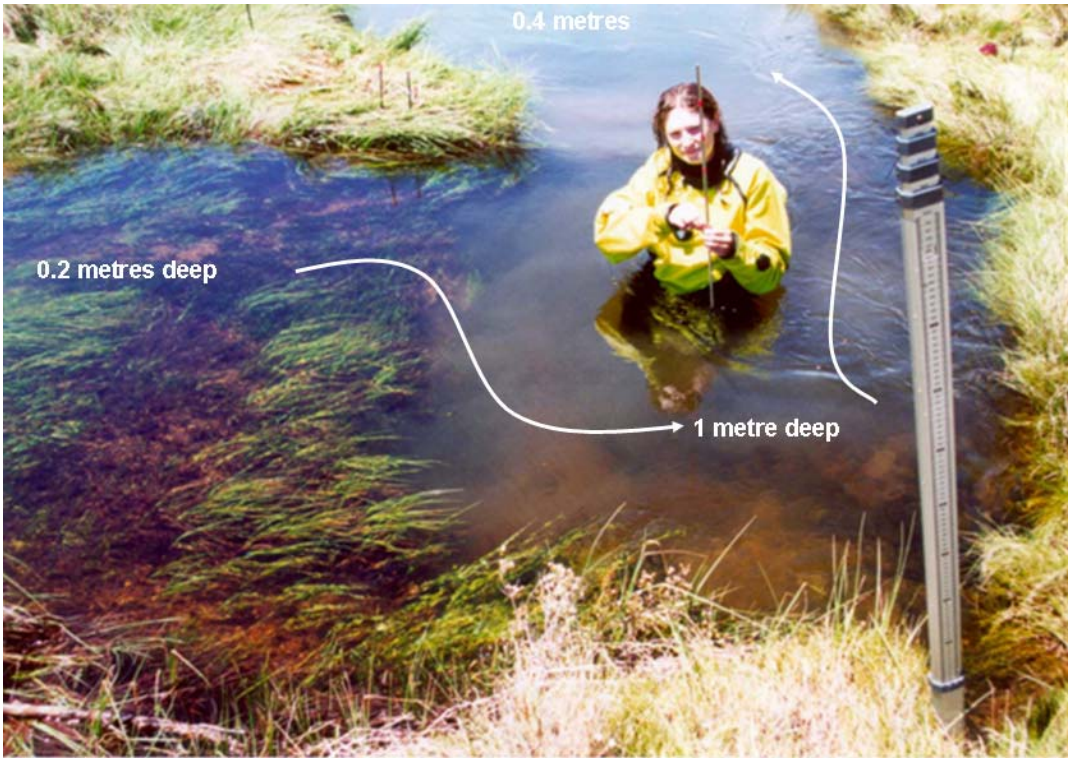

Figure 4.6 Highly variable bed topography through a bend in Edwards Creek. Flow is from left to right and person is standing upright.

A point of particular interest is that the lowest wavelength-to-depth ratios occur in reaches with the highest feature amplitude to average flow-depth ratios; Edwards Creek and Barrington Middle. This relationship will be considered in greater detail in the following section.

4.3.5 Bed feature steepness

Distinct values of bed-feature steepness have been attributed to ripples (0.12) (Baas, 1999), dunes (0.03-0.08) (Kostaschuk and Villard, 1996; Carling, 1999) and riffles (0.01-0.03) (Carling and Orr, 2000), as the interaction between feature steepness, flow resistance and bed-sediment transport necessarily determines that each value should be relatively distinct. The following section quantifies bed-feature steepness in the Barrington Tops streams to aid in the classification of these features, and to allow for the later quantification of their influence on possible bed-sediment transport.

4.3.5.1 Methodology

Modal values of bed-feature amplitudes and wavelengths were used to calculate reach-average steepness values.

4.3.5.2 Results

Low steepness values between 0.01 and 0.03 were observed along Polblue Creek and the Barrington River Lower reaches. The steepest bed features occurred along the Barrington River Middle (0.06) and Edwards Creek (0.11). This result is illustrated in Figure 4.7 in which modal amplitudes and wavelengths for reach averaged bed features are illustrated schematically in comparison with one another.

4.3.5.3 Bed feature steepness summary

The steepness values of Polblue Creek and the Barrington River Lower reaches are consistent with those cited elsewhere for riffles (Carling and Orr, 2000). However, the Edwards Creek and Barrington River Middle reaches are much steeper than in all other reaches and are more consistent with ripple values (Baas, 1999). Dunes and riffles with such steepness values are highly unusual. Once again, the morphology of the bed features in these two reaches defies simple classification as riffles, dunes or ripples.

4.3.6 Bed morphology summary

Along Polblue Creek bed features are almost entirely linked to planform (91%), are of low amplitude (<0.25 m), extend up to just 24% of the average bankfull flow depth and their wavelengths are also scaled to 13-15 times the flow depth. They are not steep (steepness <0.03) and their wavelength is scaled to between 4 and 8 times channel width; all of these characteristics are strongly suggestive of their being pool-riffle sequences (Leopold et al., 1964; Keller and Melhorn, 1978; Richards, 1982; Carling and Orr, 2000). The small number of non-planform related features identified (7%) appear to be bedforms such as dunes, superimposed on riffles.

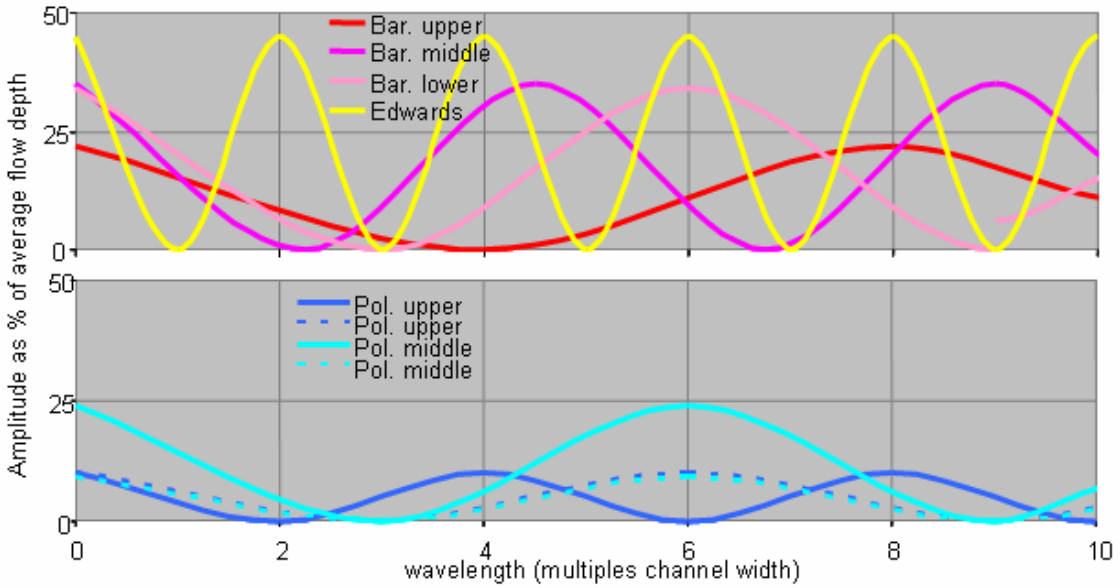

Figure 4.7 A schematic comparison between bed-feature wavelength and amplitude by reaches using modal values: (a) Edwards Creek and Barrington River subsets and (b) Polblue Creek subsets. The greatest amplitude, shortest wavelength (steepest) reaches are Edwards Creek (yellow) and Barrington River Middle (purple) (a).

On the Barrington River most bed features are also associated with planform; 72% along the combined Upper and Middle reaches, rising to 89% along the Lower reach. However, 38% of the identified pools in the downstream reach are not planform related. Bed-feature steepness is high, ranging from 0.03 to 0.06, suggesting that they could be classed as dunes. Their protrusion 34-42% into the average bankfull flow depth is also higher than normal riffles. While their steepness values are higher than those usually documented for pool riffle morphology, and more consistent with those for dunes, their wavelengths range from 4 to 8 times channel width and eight times the average flow depth, highly consistent with pool riffle morphology (e.g. Keller and Melhorn, 1978; Carling and Orr, 2000). As a consequence, their definition causes some ambiguity.

Edwards Creek bed features are strongly linked to planform with 90% of expected bend pools identified and only 16% of the identified pools not located on bends, suggesting that, in this respect at least, they are behaving essentially as pools and riffles. However they also display a very high steepness (0.11) and their height is 45% of the average bankfull flow depth; these values far exceed those expected for pools and riffles, being more consistent

with dunes. Wavelengths of only two times channel width are consistent with neither riffles nor dunes, and depth-wavelength ratios of eight support their identification as riffles. As with those along the Barrington River, the identification of these features as simply dunes or riffles is not possible.

Bed features along all Barrington swamp stream datasets are closely related to channel planform and are strongly scaled to channel width. Their scaling to both width and planform suggests that they are pool-riffle features, despite their sometimes uncharacteristically large vertical component and steep amplitude-to-wavelength values.

Owing to physical constraints along the Barrington River Upper, Barrington River Lower and Polblue Creek Lower channel reaches, bed-feature morphology is not systematic. At the entry and exit of the channels to the swamps, represented by the Polblue Creek Lower and Barrington River Upper reaches, the channels flow through shallow peat over coarse cobble basement (Figure 3.11); these sections of channel are also not entirely alluvial and pool locations are partly determined by the location of clusters of cobbles on the pre-fluvial substrate. Dunes can theoretically reach amplitudes up to mean flow depth and provide the highest resistance to flow of all lower regime bedforms (Simons and Richardson, 1966) but, while considerable scatter is evident in this relationship, the ratio more typically falls around 20% of flow depth (Allen, 1982). Riffle amplitudes have only recently been related to flow depth by Carling and Orr (2000). On the River Severn they found that they are from 7-18% of the depth. While this single set of values cannot be considered a general rule, the values of 45 and 35% for the Barrington and Edwards bed features, respectively, well exceed values for both riffles and dunes.

In summary, it is likely that while these larger bed features in the Barrington swamp streams are planform related and are scaled to channel dimensions, their interaction with immediate flow at any specific point in the channel is more closely related to that exhibited by dunes. Therefore, the large bed undulations identified along the Edwards Creek and Barrington River Middle reaches, which are related to both planform and channel dimensions as is consistent with riffles, have steepness and amplitude relations more consistent with dunes. These features that combine the properties of **du**nes and ri**ffles** will

be referred to in this study as *duffles*. All other reaches are either plane bedded or possess riffles. Dunes are not recognised as existing here other than in a hybrid form with riffles.

The comparison between modal bed-feature amplitude and wavelength through all channel reaches in Figure 4.7 illustrates that Edwards Creek *duffles* possess the greatest amplitude and shortest wavelength relative to average flow depth and channel width, respectively, followed by the Barrington River Middle reach. Polblue Creek has the smallest riffles of all channels. Reaches of channel with *duffles* are conceivably experiencing very high levels of flow resistance, while those with only riffles are experiencing much less.

The significance of the formation of *duffles* lies in their influence on channel flow. In straight, wide sections of gravel bed channels, form roughness can account for between 50 and 75% of flow resistance, with feature steepness positively related to their flow resistance (Prestegaard, 1983). Very steep *duffles* may lie in the upper region of this range, or even exceed it. The influence of *duffles* and riffles on bed-sediment transport in the Barrington swamp channels will be quantified in the following section.

4.4 Bed features and shear stress

Shear stress, measured in N/m^2, is a measure of the force from flowing water that is exerted on the flow boundary. Some of this force is responsible for bed-sediment transport, however, of the total shear stress only a fraction results in bed-sediment transport. This fraction can be determined by first examining the resistance elements in a channel. Total flow resistance is measured using Darcy-Weisbach's f:

$$f = \frac{8gRS}{U^2}$$

where g is gravity, R is the hydraulic radius (defined as wd/(2d + w) in rectangular channels), S is the water surface slope and U is the downstream velocity component of the flow. However, at least two resistance components sum to provide the total flow resistance (f) in straight reaches; grain roughness f' and form roughness f'' (Einstein and Banks, 1950). Form resistance can comprise up to 90% of the total (Millar, 1999b). In narrow and

deep channels, a significant third resistance element (f''') is provided by the channel banks and should be included in considerations of total flow resistance (Knight et al., 1984). Spill resistance can also be important in supercritical flow and in the vicinity of bank irregularities (Leopold et al., 1960), but in the straight reaches of channel examined here in which flows do not exceed Fr > 0.27, it provides little of the total flow resistance. Internal distortion resistance is another form of resistance, important in channel bends and considered in later chapters (Chapters 5 and 6), but is not relevant in the straight reaches of channel that are examined in *this* chapter. Bedload transporting resistance is another component of total flow resistance in channels which transport sediment (Gao and Abrahams, 2004), but is considered to contribute little in these clear-flowing channels.

It follows from these considerations of resistance that total shear stress is, in a relatively straight channel, the sum of grain, form and wall shear stress components, in the form:

$$\tau_0 = \tau' + \tau'' + \tau'''$$

(Einstein and Barbarossa, 1952). Of these three shear components, only grain shear determines the bedload transporting competence of the flow (Einstein and Barbarossa, 1952; Carson, 1987). Therefore, the greater the resistance provided by channel banks (wall resistance) and bedforms, the lower the bedload transporting competence of the flow. The following section outlines an attempt to quantify both the effect of form ratio and bedforms on sediment transport and the ability of the flow to transport its bedload.

4.4.1 Methodology

Total shear stress (τ_0) is calculated using the equation:

$$\tau_0 = \rho g R S$$

where ρ is water density (~1000 kg/m^3 at 4°C), and provides a reach average of the total shear stress acting on a cross-section. To calculate the grain shear stress, and therefore the bedload transporting competence of the flow, it remains to calculate the form and wall

shear components; the effective grain shear stress can be calculated by subtracting the wall (τ''') and form (τ'') shear stress components from the total shear stress:

$$\tau' = \tau_0 - (\tau'' + \tau''')$$

4.4.1.1 Estimating wall (bank) shear stress

Knight et al. (1984) examined flow in smooth rectangular channels and produced an empirical equation to estimate wall shear as a percentage of the total shear force ($\%SF_w$) using the equation:

$$\%SF_w = e^{\alpha}$$

whereby

$$\alpha = -3.230 \log_{10}(\frac{w}{d} + 3) + 6.146$$

As it was developed for plane beds in flumes, wall shear stress is computed as a percentage of the total shear stress prior to considerations of form shear.

Recent studies (e.g. Yang and Lim, 1998; Guo and Julien, 2005), have confirmed the accuracy of this equation. However it was produced and subsequently tested in smooth, rectangular channels; in natural channels with rough boundaries and varying wall and bed roughness's, it may provide an underestimate.

4.4.1.2 Estimating form shear stress

McLean et al. (1999) related the resistance provided by dunes to dune height and flow velocity and Robert (2003) has suggested the application of this relation to riffles to determine their resistance to flow. McLean et al. (1999) proposed that form shear stress (τ'') can be calculated using the equation:

$$\tau_0'' = 0.5 C_d (h/l) \rho U_R^2$$

where h/l is the bedform steepness and where C_d equals 0.19, if U_R (the reference velocity) is measured at 1 bedform height above the crest of the bedform. They empirically derived the value of C_d which was found to calculate form drag within an error of ±15%. This constant increases in value and error as the reference velocity (U_R) height approaches the bed (crest of the bedform) and decreases in value and error as the reference height moves away from the bed.

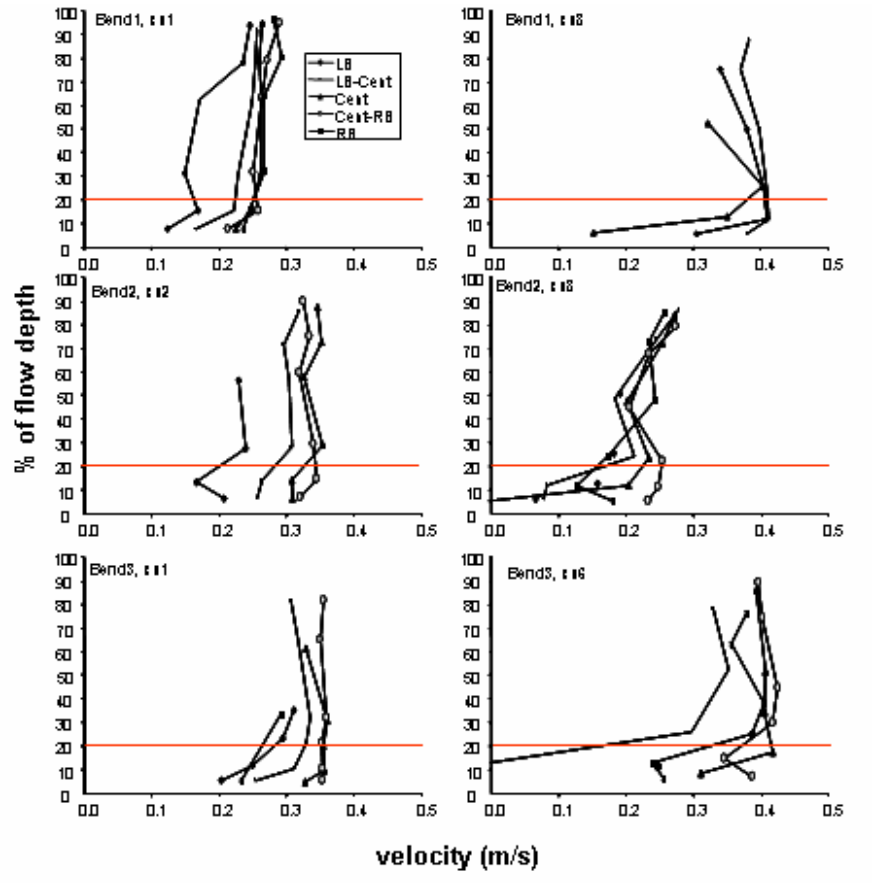

Figure 4.8 Sample velocity profiles from intensive flow data collection from cross-sections at the entry and exit of Polblue Creek, Bends 1, 2 and 3 (See Chapter 6). These profiles are from cross-sections at the entry and exit of each of these bends, but are used to illustrate typical velocity profiles. The inner boundary layer height approximates 20% of the flow depth in each profile, which in turn approximates the height at which velocity equals the average cross-sectional, bankfull velocity and therefore represents U_R, the reference velocity for form shear stress calculations.

Reach averaged steepness values and average bankfull flow velocity through each station were used to represent h/l and U_R in the application of this equation in this thesis. This

height is intended to represent the velocity at the height of the mean thickness of the internal boundary layer. Figure 4.8 illustrates example velocity profiles for Barrington swamp channel sections. These are near-vertical, and as such the velocities at the intended reference height (U_R (McLean et al., 1999)) are well approximated by the average flow velocity at bankfull, calculated in Chapter 3.

The resulting estimates of form, wall and bed shear provide values for comparison of energy consumption by bedforms and the resultant sediment transport competence between stations. The absolute values are only estimates and must be considered as such. These estimates can, however, be used more specifically to examine the relative adjustments in the sediment transporting ability of the flow in response to shear consumption by bedforms.

4.4.1.3 Comparing critical and grain shear stresses

Critical shear stress is that shear required to initiate the transport of a sediment particle of a given diameter. Using the calculations outlined above, the grain shear remaining after the removal of the wall and form shear components can therefore be viewed in relation to this critical shear stress to determine the potential for sediment entrainment by the flow. Shields (1936) produced an equation for calculating critical shear stress (τ_c), based on the representative sediment diameter (d), sediment (ρ_s) and water (ρ) density, gravity (g) and a dimensionless constant (θ_c), usually referred to as the *dimensionless critical shear stress* (Gordon et al., 2004). His equation takes the form:

$$\tau_c = \theta_c g d(\rho_s - \rho)$$

Shields originally proposed that a constant value of $\theta_c = 0.056$ was appropriate, however, the value has since been found to vary from 0.01 to in excess of 0.1 as a function of the configuration of the bed surface (e.g. armouring, imbrication and packing) and fluid properties (Gordon et al., 2004). Grayson et al. (1996) provides a summary table, synthesising several other more specific studies, which presents θ_c values pertaining to various stream bed conditions. Over uniform materials or well settled beds, θ_c values range from 0.035-0.065, whereas close-packed beds with particles in the voids in between range from 0.065-0.10. Most stations in the Barrington swamp channels appeared to have “well

settled" beds and were allocated values of 0.045 and the D_{50} was used to represent d, whereas *duffle* features were typically armoured and were therefore considered to have "well settled" to "close packed beds" and were allocated θ_c values of 0.065. Further support for the selection of these values come from recent modelled relations between dimensionless critical shear stress and channel width/depth ratios by Eaton et al. (2004); they produced θ_c values approximating 0.05 for width/depth ratios of ~2.5, in channels with near vertical (80°) banks (representative of high bank strength). The Barrington swamp channels have somewhat steeper banks, but probably very similar θ_c values. Parker (1982) found that in armoured channels, the D_{50} grain size of the armoured layer was the most appropriate grain size to use in the calculation of critical shear stress. Bed samples from the Barrington swamp channels included both surface *and* subsurface materials and the D_{90} grain size on *duffle* crests was considered the best approximation of Parker's D_{50} armoured-bed recommendation (his samples were from *only* the armoured layer). In this way, critical shear to grain shear comparisons were used to determine the mobility of channel bed material.

The use of the Shields critical shear stress equation only provides information on the movement, or otherwise, of bed material, with no detail of the bedforms that might be expected to develop. The bedform existence diagram of Best (1996) relates grain size to shear stress estimates with resulting bedform types; this is useful in the consideration of bedform development and the subsequent effect of bedforms on estimates of total and grain shear stresses. Therefore, this diagram was also used to examine the effects of wall and form shear on reducing bedform developing capacity.

4.4.1.4 Bed material grain size determination

Grab-samples were collected at low flow stages from the bed using a sample bottle mounted on a pole at hydraulic geometry stations and from *duffles* through Edwards Bends 1 and 2 and Barrington Bend 1 (detailed in Chapter 6); the device was inserted into the bed to include surface and subsurface material and carefully raised in an upright position to prevent sediment loss.

Through Polblue Creek and the Barrington River Lower and Upper reaches, the channel bed was comprised mainly of basement material with alluvial bed sediment deposited on these materials as discontinuous units, which did not necessarily span the whole cross-section. Along the Barrington River Middle reach and the entirety of Edwards Creek, the *duffles* usually spanned the entire width of the cross-section. Where there were clear variations in sediment size across a cross-section, multiple samples were collected.

Samples were oven dried at 55°C, weighed, immersed in calgon solution for 24 hours and placed in ultrasonic baths for up to 2 hours during that 24 hour period. The samples were then wet sieved through a 63µm sieve to separate the silt and clay particles from the coarser fraction. Both the wash and the coarse fractions were then collected, dried at 55°C and re-weighed. The coarse fractions (>63µm) were then shaken through nested sieves at half phi intervals from 66µm to 8mm for 10 minutes. The resulting grain size fraction weights were entered into the GRADISTAT grain size analysis program (Blott and Pye, 2001) which calculated a variety of grain size statistics, including those designed by Folk and Ward (1957). Both the Folk and Ward method of grain size analysis, and the GRADISTAT program, were recently detailed and given a positive review by Blott and Pye (2001).

Either the D_{50} or D_{90} grain size statistics obtained by the GRADISTAT program were used in subsequent analyses. The D_{50} was used in the majority of cases, however, as described above, bed armouring was observed on the *duffles* along Edwards Creek. While the extent of armouring varied along this channel, the D_{90} values provided results that were probably more consistent with field observations of the surface materials along these reaches than did the D_{50} values which, owing to the collection method, were more representative of the subsurface fine sediments. Sediment descriptions, sorting, skewness and kurtosis were obtained using the Folk and Ward (1954) method within GRADISTAT.

4.4.2 Results

4.4.2.1 Shear stress components

The total, wall, form and grain shear stress estimates for each hydraulic geometry station are presented in Table 4.2.

Form shear stress varies from 0-23% of the total shear through Polblue Creek, 0-18% through the Barrington River and between 40 and 43% on Edwards Creek. The most significant shear stress attributed to bedforms is through the reaches possessing *duffles* where form shear contributes between 18 and 43% of the total shear stress.

Low width/depth ratio locations are subject to substantial wall shear losses and the formula used to calculate this parameter (Knight et al., 1984) is very sensitive to channel width/depth ratio. Along Polblue Creek between 19 and 62% of the total shear is exerted on the channel banks; narrower stations experience wall shear stresses at the higher end of this range. The Barrington River Middle and Downstream reaches are also quite narrow and their banks receive between 25 and 52% of the total shear. The Barrington River Upstream Stations, B5 and B6, are much wider and shallower and their banks are subjected to only 9 and 14% of the shear, respectively.

When the form and wall shear stress components are removed from the total shear, grain shear accounts for between 18 and 91% of the total shear. Those stations with either moderately narrow and deep cross-sections or with *duffle* bedforms exert large shear forces on either the banks or the water column and only moderately wide stations with no significant bedforms exert much of their shear stress on the channel bed (e.g. P11, P2, B1, B2, B5 and B6). With the exception of P2, those stations that exert much of their shear stress on the channel bed flow over pre-fluvial basement cobbles underlying shallow depths of alluvium. Clearly, either low width/depth ratios or high bed deformity reduces the available grain shear acting on the bed.

4.4.2.2 Grain size

Sample grain size statistics are summarised in Table 4.2, and their ratios are illustrated on, the gravel-sand-mud ternary plot in Figure 4.9. Bed sediments ranged in texture from sandy-mud to gravel (Folk, 1954), were typically bi- or uni-modal and poorly to very poorly sorted (Folk and Ward, 1957).

Table 4.2 Shear stress and grain size calculations for all hydraulic geometry stations and Edwards Creek and Barrington River bend samples. Highlighted station samples are considered suspended load.

site	total shear stress	Form shear stress	% of total	wall shear stress	% of total	grain shear stress	% of total	D_{50} (mm)	D_{90} (mm)	sediment description	modality	sorting	critical shear - D50	critical shear - D90	critical shear
p1	6.69	0.20	2.94	2.94	43.92	3.56	53.14	0.14	0.40	very fine sand	unimodal	very poor	0.10	0.29	0.10
p2 1/2	3.02	0.11	3.64	0.96	31.81	1.95	64.56	0.05	0.23	very coarse silt	unimodal	poor	0.04	0.17	0.04
p2 2/2	3.02	0.11	3.64	0.96	31.81	1.95	64.56	0.16	0.48	fine sand	unimodal	poor	0.12	0.35	0.12
p3 1/2	2.09	0.27	13.10	1.27	60.75	0.55	26.15	3.38	8.30	very fine gravel	bimodal	poor	2.46	6.05	2.46
p3 2/2	2.09	0.27	13.10	1.27	60.75	0.55	26.15	1.56	8.59	coarse sand	trimodal	very poor	1.14	6.26	1.14
p4 1/2	4.04	0.94	23.26	2.37	58.53	0.74	18.21	0.4	2.50	medium sand	bimodal	poor	0.29	1.82	0.29
p4 2/2	4.04	0.94	23.26	2.37	58.53	0.74	18.21	2.52	2.02	fine sand	bimodal	very poor	1.84	1.47	1.84
p5	4.47	1.03	22.97	2.40	53.56	1.05	23.48	no bed sediment							
p6	4.90	0.70	14.31	2.77	56.58	1.43	29.11	3.13	9.57	very fine gravel	bimodal	very poor	2.28	6.97	2.28
p7	4.31	0.97	22.40	1.79	41.49	1.56	36.11	0.51	1.23	coarse sand	unimodal	moderate	0.37	0.90	0.37
p8	4.72	0.85	18.08	2.95	62.44	0.92	19.47	0.02	0.21	coarse silt	bimodal	poor	0.01	0.15	0.01
p9	5.36	0.66	12.33	3.21	59.82	1.49	27.86	1.65	6.01	very coarse sand	polymodal	poor	1.20	4.38	1.20
p10	9.13	1.25	13.69	4.63	50.75	3.25	35.55	0.06	1.54	very fine sand	bimodal	very poor	0.04	1.12	0.04
p11	12.81	0.00	0.00	2.45	19.13	10.36	80.87	no bed sediment							
b1	7.46	0.00	0.00	1.84	24.63	5.62	75.37	no bed sediment							
b2	7.26	0.00	0.00	2.29	31.51	4.97	68.49	no bed sediment							
b3 1/2	3.83	0.65	17.05	2.00	52.32	1.17	30.63	0.48	1.57	medium sand	bimodal	very poor	0.35	1.14	1.65
b3 2/2	3.83	0.65	17.05	2.00	52.32	1.17	30.63	2.06	9.16	very coarse sand	trimodal	very poor	1.50	6.67	9.64
b4	9.96	1.81	18.17	3.02	30.32	5.13	51.51	5.03	8.52	fine gravel	unimodal	poor	3.66	6.21	3.66
b5	2.16	0.00	0.00	0.19	8.98	1.97	91.02	no bed sediment							
b6	2.95	0.00	0.00	0.42	14.07	2.54	85.93	no bed sediment							
e1 1/3	6.22	2.50	40.24	1.23	19.80	2.48	39.96	0.2	0.43	fine sand	unimodal	moderate	0.15	0.31	0.45
e1 2/3	6.22	2.50	40.24	1.23	19.80	2.48	39.96	0.07	0.25	very coarse silt	unimodal	poor	0.05	0.18	0.26
e1 3/3	6.22	2.50	40.24	1.23	19.80	2.48	39.96	0.15	0.41	fine sand	unimodal	poor	0.11	0.30	0.43
e2 1/2	6.31	2.73	43.21	1.15	18.24	2.43	38.55	0.19	0.95	fine sand	bimodal	very poor	0.14	0.69	1.00
e2 2/2	6.31	2.73	43.21	1.15	18.24	2.43	38.55	0.02	0.16	coarse silt	unimodal	poor	0.01	0.12	0.17

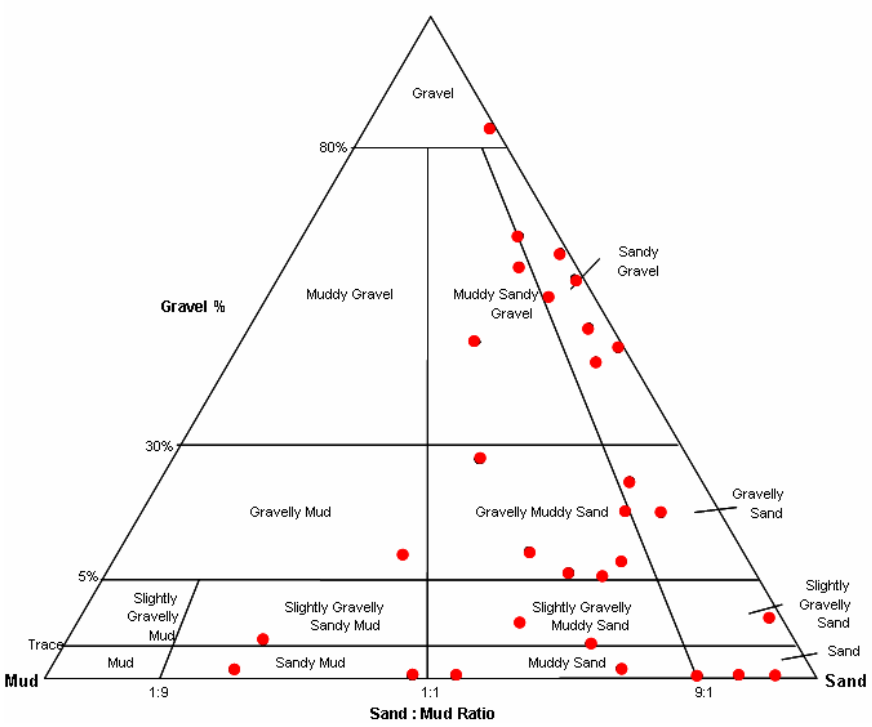

Figure 4.9 Grain size fractions for all Barrington swamp channel hydraulic geometry and bend samples.

4.4.3 Critical versus grain shear stress

Figure 4.10 illustrates the grain shear stress, after the removal of the wall and form shear components from the total, in comparison with critical shear stress. Stations which plot above the line have insufficient grain shear for the initiation of particle motion, and those below the line exceed the critical shear values.

Sites with insufficient grain shear include Polblue Creek samples P3 (1&2/2), P4 (2/2) and P6, Edwards Creek Bends 1&2 samples IV and V, Barrington River sample B3 (1&2/2) and Barrington Bend 1 samples I, II & IV.

Polblue Stations P3, P4 and P6 have the lowest width/depth ratios of all Barrington swamp channel-stations: 1.28, 1.39 and 1.5, respectively, exceeded only by Station P8 which has a ratio of 1.20, but which possessed only wash-load on its bed (D_{50}~0.02mm). In addition, Barrington River Station B3 also lacks sufficient grain shear and likewise has a very low width/depth ratio of 1.76. While Figure 4.10 indicates insufficient grain shear stresses for

bed sediment entrainment at these stations, their at-a-station hydraulic geometry exponents for velocity are extremely high; 0.68 at P3, 0.67 at P4, 0.78 at P6 and 0.85 at B3. The explanation may lie in considerations of wall shear stress estimates which are based heavily on width/depth ratio, and which are possibly over-predicting this component of the shear stress in excessively narrow channel sections such as these. At bankfull or slightly over-bank discharges, what little bedload there is must indeed be transported through Polblue stations P3, P4 and P6 and Barrington station B3 for these locations show no sign of significant sediment accumulation on their beds.

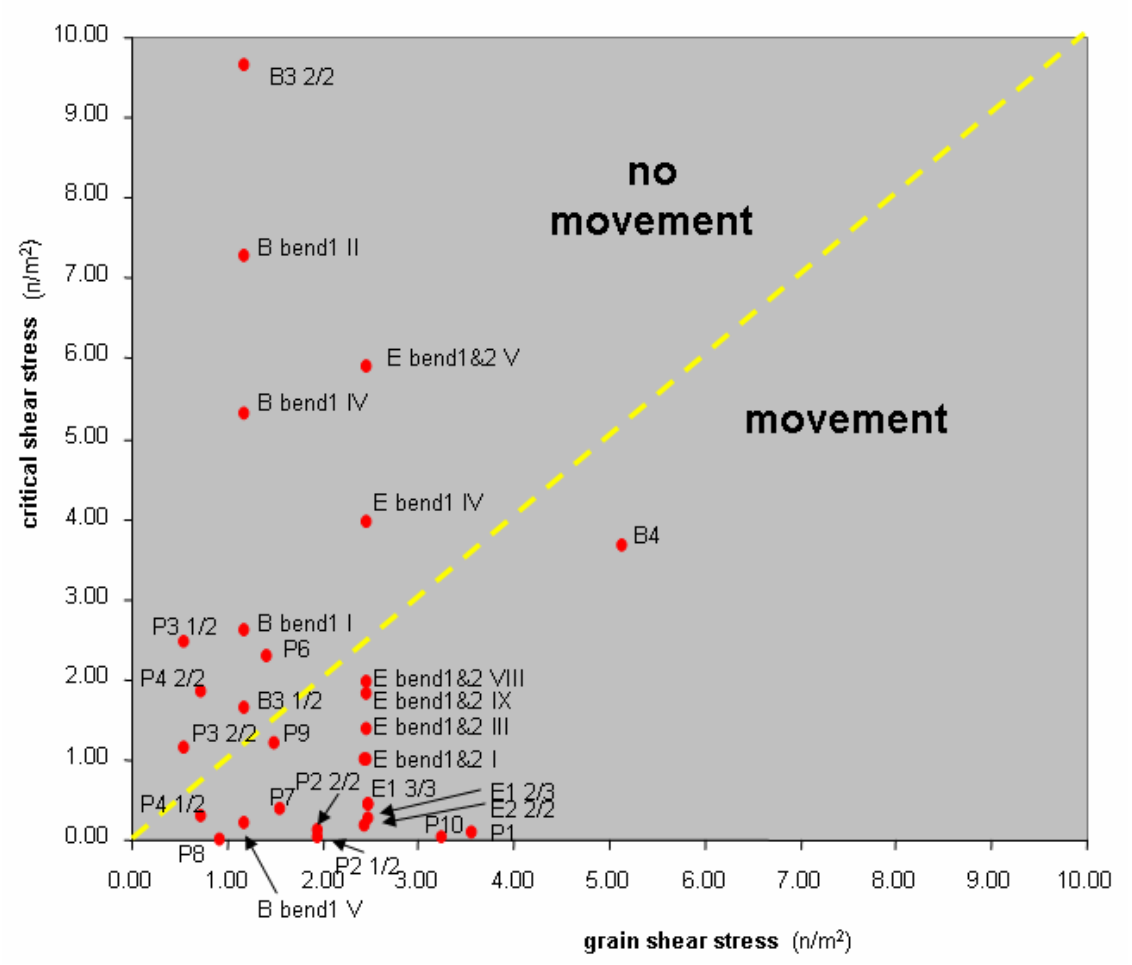

Figure 4.10 Grain versus critical shear stress for all bed samples from hydraulic geometry stations and bends. Points below the yellow line represent stations where grain shear stress exceeds critical shear stress. P is Polblue Creek, B is Barrington River, E is Edwards Creek. I, II, III etc. are multiple samples collected from each bend.

The remaining stations that plot with insufficient grain shear for sediment entrainment were collected from locations with large bed-material deposits (i.e. bedforms). While this would seem to indicate a necessity for sufficient grain shear for sediment entrainment at some point in time, this does not appear to currently be the case.

The samples which plot with sufficient grain shear for sediment motion, are highlighted in Table 4.2. These samples are all finer than medium sand and some may be skewed to the finer end by suspended sediments deposited during the falling stage of high flows.

In summary, those sites that are illustrated as having sufficient shear stress for sediment transport by this plot are actually devoid of significant bedforms. Their deposits, where present, are sheet veneers across a resistant basement material. Paradoxically, those stations theoretically capable of sediment transport have not formed bedforms, and those that are not theoretically capable have them. The bedform existence diagram of Best (1996) is suited to the interpretation of these results and is considered in detail in the following section.

4.4.4 Shear stress-bedform relations

Best (1996) synthesised the results of many studies to produce a bedform existence diagram relating du Boys shear stress, grain size and resulting bedforms. The total and grain shear stress for the D_{50} or D_{90} grain sizes for each Barrington swamp channel station are presented in comparison with Best's bedform divisions in Figure 4.11. This diagram primarily illustrates the effect of bedforms on sediment transport. When the wall and form shear stresses are removed from the total shear stress, and the same sites are replotted, the effect is a reduced capacity for the flow to produce large scale bed features replaced by an increased capacity for ripple formation and lower stage plane beds. The same sites that plot in the region of insufficient grain shear for bed sediment entrainment in Figure 4.10 also plot in the "no movement" region of this graph. Such a correlation between the results of

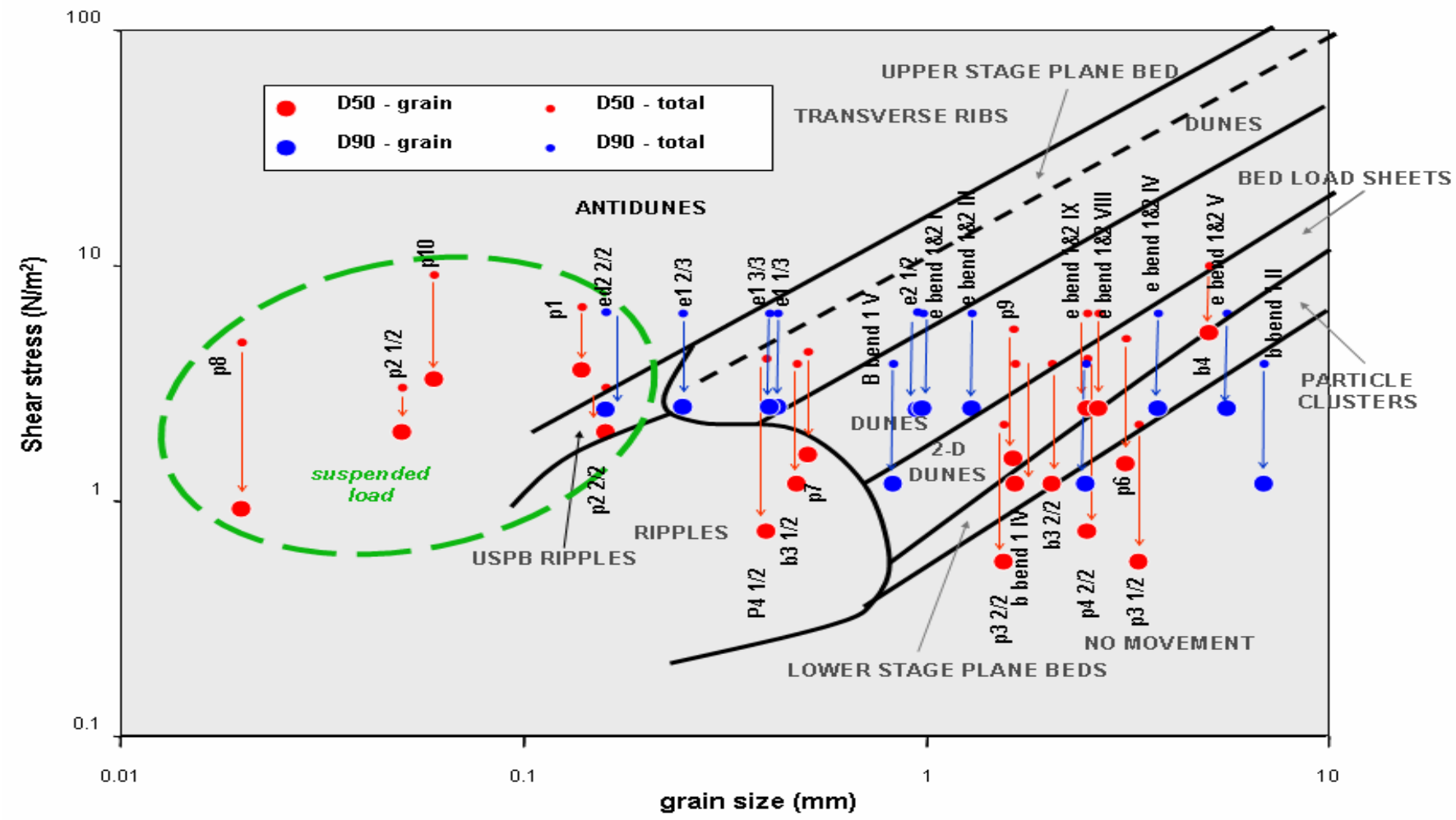

Figure 4.11 A comparison between total shear stress (small dots) and grain shear stress (larger dots) with grain size. Arrows link data from the same stations. The prefixes P (Polblue Creek), B (Barrington River) and E (Edwards Creek) are followed by the station number and then the sample number / total number of samples for that section. Modified from Best (1996).

these two separate graphs is encouraging and necessitates more detailed inspection. The implications for the shear stress and resulting bedform adjustments on the grain size – shear stress plot of Best (1996) are considered separately for each channel in the following sections.

Polblue Creek

Based on the total shear stress and D_{50} grain size, Polblue Creek is capable of producing a range of bedforms, from ripples, to dunes and bedload sheets (Figure 4.11). The previous section has determined that the bed of Polblue Creek typically presents pool-riffle morphology and the lack of bedforms must therefore be attributed to very limited sediment supply and the capacity of the flow to move most of the limited bed material completely through. Even when the form and wall shear components are removed from the total shear, most Polblue Creek stations are capable of transporting their bed material. Sites P1, P2 P8 and P10 have only scattered suspended load on their beds which has settled out following flows, and are therefore not considered further for bedform development. Sites P3, P4 and P6 are exceptions in that they plot as though grain shear can produce "no movement". These stations have particularly low width/depth ratios (1.28, 1.39 and 1.5, respectively) and it may be that the equation used to estimate wall shear stress (Knight et al., 1984) overestimates the losses of total shear to wall friction in extremely low width-depth ratio channels and thereby cause underestimation of the grain shear stress. The bed sediment was observed to be present as only sheet-like veneers over the basement material at these stations and not as slugs or bedforms.

Barrington River

The Barrington River Upper reach is represented by Station B4. Figure 4.11 illustrates that, considering the total shear stress, this reach is capable of forming dunes but when only the grain shear is considered this capability reduces to only being able to form cluster particles and bedload sheets; pool-riffle bed morphology was identified through this reach using the *differencing* analysis technique, described in an earlier section of this chapter. Site B3 possesses *duffle* bedforms through its reach, but not actually at the station cross-section. Figure 4.11 illustrates how the total shear stress at this station is capable of forming dune bedforms, but the removal of both the wall and form shear reduces bedforming ability

considerably, to the point where it can only form ripples and two-dimensional dunes and lower stage plane beds. Furthermore, bed vegetation makes these forms even more stable.

Barrington River at Bend 1 contains a full *duffle*-pool-*duffle* sequence with bed armouring on the *duffle* crests. With the exception of B1 Sample II, which plots just below the plane bed region of the graph, samples in this bend plot initially in the region of dunes when the total shear is considered, but move to two-dimensional dunes, lower stage plane beds or no movement regions of the graph when only the grain shear stress is considered.

Edwards Creek

The armouring of the bed along Edwards Creek required that the D_{90} grain size be used to assess shear stress-grain size relations. Stations E1 and E2 exhibit total shear capable of forming antidunes and dunes, however, low bankfull flow Froude numbers dictate that only lower flow regime forms should be present. When the wall and form shear are removed from the total shear, the resultant grain shear is barely sufficient to form dunes through E1 and the region is one of more conservative ripple formation. Similarly, E2 approaches a lower region of the plot, but still appears capable of forming dunes. Form shear stress comprises 40 - 43% of the total shear stress. Clearly, the *duffle* features in this channel provide major resistance to flow and markedly reduce the sediment transporting, and hence bedform developing capacity of the channel, but apparently do not eliminate dune-forming ability.

Sediment samples from the *duffle* crests in Edwards Creek Bends 1&2 *duffles* are much coarser than those through stations E1 and E2. Plotted on Figure 4.11, and when the total shear is considered, the stresses are capable of forming dunes, however, their ability to form bed features reduces grain shear to that capable of maintaining only lower stage two dimensional dunes or lower stage plane beds with no movement. The supply and movement of sediment is obviously very limited. It is likely that while the hydraulic geometry stations located in the straighter reaches may experience the gradual migration of bedforms through their reaches, in bends where flow resistance is higher, the *duffle* features are stationary. While bed sediment is transported gradually through these bends, the sediment does not accumulate on *duffles* and hence the *duffles* do not migrate.

4.4.5 Bed feature and shear stress summary

Using the bedform existence diagram of Best (1996) to view bedform development capacity, the shear exerted on the channel walls and consumed by bedforms combine to dramatically reduce the shear available for subsequent sediment movement in an environment of very limited bed-sediment supply. Along Edwards Creek and the Barrington River, shearing forces are focused on the essentially stable but also very large bedforms, whereas along Polblue Creek the very narrow and deep cross-sections ensure that a considerable proportion of the total shear is exerted on the channel banks. From the sediment transport perspective, the reduction of total shear stress by that exerted on the walls and/or the bedforms in these channels is very considerable. In particular, very narrow and deep stations and those with *duffle* bed features experience greatly reduced grain shear and sediment transporting capacity. This, in combination with very limited sediment supply, results in highly stable bedforms.

4.5 Barrington swamp bed-feature summary

The formation of *duffles* along Edwards Creek and the Barrington River middle reach can be partially explained using the proposed sediment supply - transport model of Montgomery and Buffington (1997) in conjunction with considerations of high bank strength. Montgomery and Buffington (1997) suggested that, due to increased sediment supply and decreased transport capacity, a continuum in bed-feature type occurs from pools and riffles to dunes and ripples.

Reaches of Barrington swamp channels mostly lacking in alluvial bed material include Polblue Creek and Barrington River Upper. They possess pools formed predominantly as scours within the basement material; only small quantities of alluvial material form occasional long, low riffles. These reaches must be profoundly supply limited (Montgomery and Buffington, 1997) (transport capacity of the flow exceeds sediment supply) as their bed shear stress values suggest that, given sufficient transportable bedload, ripple and dune features would develop. Along the reaches of Edwards Creek and Barrington River Middle that possess bed material (fine gravel and coarse sand), but no

visual evidence of significant sediment transport occurring, bed features are particularly large; *duffles* are closely spaced and occupy 45% and 35% of the average flow depths in each channel, respectively. Here it appears that dune-like features have developed, consistent with the bedform existence diagram of Best (1996). However, unlike dunes which typically migrate downstream (Simons and Richardson, 1966), *duffles* are essentially fixed in position and are strongly influenced by the presence of bends. The implications for this are that traditional scaling rules applied distinctly to pools and riffles (their wavelength to channel width) and dunes (their wavelength and amplitude to channel width) may actually overlap.

Duffles are associated with the tightest bends and are the largest bedform features observed in these channels, closely followed by those in straighter reaches present at several of the hydraulic geometry stations. Although bedload flux was not measured in this study, as stated previously, the lack of suspended load resulted in clear water at bankfull through which little or no bedload transport was observed. The sediment that was and possibly is still supplied to the channels, and which has formed these sometimes relatively large bed features, appears to have been only sufficient for their formation, probably over a relatively long time. Sediment supply would seem to be insufficient to instigate significant bedload transport and associated bedform migration. Consideration of the total shear that is exerted in the channel other than on the bed appears to provide supporting evidence. Once the shear stress components that are not responsible for sediment transport are deducted from the total, the ability of the flow to transport the bedload is much reduced. These results are consistent with those of Church et al. (1998) which demonstrated significantly reduced sediment transport following the formation of surface grain structures. Furthermore, the critical shear stress required for sediment transport in narrow channels has been shown to be higher than that in wider ones, owing to dampened turbulence in the former (Carling, 1983). This would imply even less bed mobility in the Barrington swamp channels than that indicated by their position on Best's (1996) diagram. The primary effect of *duffles* in these streams appears, therefore, to be the creation of considerable flow resistance. The degree of turbulence that they generate in the form of the large separation zones on their lee sides orchestrates this resistance (Chapter 6).

As shown in Chapter 6, *duffles* in bends are associated with highly developed secondary currents and large turbulent eddies, features that appear inconsistent with low rates of sediment transport and stable channels. However, the exceptionally high bank strengths provided by dense root mats and peat are able to maintain stability. Furthermore, the presence of ribbon-weed that, in places, grows on the surfaces of the barforms presumably reduces near bed velocities and hence grain shear stress.

These channels are narrow and deep with relatively low wetted perimeters and therefore in cross-section offer highly efficient conduits for transporting water (Chapter 3). However, large bedforms and stable banks, both protected by vegetation, mean that a balance can be maintained because a great deal of this conserved energy can be expended as turbulence without generating significant scour and sediment transport. The result is the "meandering" of flow in both the vertical (bedform) and lateral (planform) planes. The effect on the flow patterns are examined in detail in the following two chapters.

4.6 Conclusions

In Chapter 3, highly efficient channel flow through most hydraulic geometry stations was implied by exceptionally high velocity exponents and very low width exponents. One purpose of the present chapter is to identify how an adjustment of channel energy conditions occurs through the development of bed features.

The bedforms identified along the Polblue Creek Middle and Upper and the Barrington River Upper reaches are pools and relatively low amplitude riffles. These bed features provide limited flow resistance and imply that the channels are supply limited as, according to critical shear - available grain shear relations, most hydraulic geometry stations have the required critical shear stresses for the entrainment of their scant bedload. Through these reaches, width/depth ratios are very low and flow resistance is primarily provided by the channel banks. In very low width/depth ratio stations, bank or wall resistance appears significant and severely reduces the sediment transporting ability of the channels. Despite the resisting effects of their confining channel banks, high velocity exponents indicate

increasingly high flow efficiency with increasing discharge and it must be concluded that the strength of the channel banks is sufficient to resist these flow forces.

In Edwards Creek and the Middle reach of the Barrington River, sediment supply has, at some stage or over a long enough period, been sufficient to have constructed very large bedforms. Because in their form they are intermediate between dunes and riffles, they have been termed *duffles*. *Duffles* are associated with the tightest bends and are scaled to channel dimensions such as planform and width, consistent with pool-riffle sequences, but they are also very steep features, more consistent with mobile bedforms such as dunes. High bank strengths, directly implied from hydraulic geometry investigations (Chapter 3), and aquatic vegetation and sediment armouring of their beds has ensured the stability of these bed features despite the large turbulent flow structures that they produce. Their effect on sediment transport is to introduce considerable form resistance and greatly reduce the shear stress available for bed material entrainment and transport. Once formed, the *duffles* are partly protected by aquatic vegetation growing on the bed.

The apparent lack of sediment supply and the armouring and partial vegetative cover of the *duffles* indicate that these bedforms are probably very vulnerable to disturbance. Loss of bed armouring or disturbance of the vegetation could result in greatly increased mobility of the bed sediment, as subsurface materials are more easily entrained by the available grain shear stresses available. Because these catchments do not have a ready supply of sediment, disturbance to *duffles* would very likely result in a decrease in flow resistance and a concomitant increase in bed, and possibly bank, erosion.

Chapter 5 Channel sinuosity and assessment of grade

5.1 Introduction

Channel planform simply describes the planimetric view of a river channel. It is essentially synonymous with channel pattern, although the latter implies a related set of processes associated with each pattern type. Channel pattern is broadly classified into straight, meandering, braided (Leopold and Wolman, 1957) and anabranching types (Smith, 1981). Anabranching is not present in the channels of the Barrington swamps. However, a short unstudied length of the Barrington River has exposed cobble bars at low flow and could be described as braided. Along the majority of reaches, the Barrington channels are either straight or meandering.

Using the concept of minimum stream power, Bettess and White (1983) described how channel planform adjusts from straight to meandering (to braided) as a function of the balance between the *regime slope*, defined as that slope required for the equilibrium transport of the supplied sediment, and valley slope. Channels in which regime slope equals valley slope are straight, whereas valley slopes in excess of the required regime slope will result in either meandering or braiding planforms. While any number of paths could be taken between two points Langbein and Leopold (1966) proposed the theory of minimum variance to suggest that the most probable path between two points for a river with excess gradient is a uniformly meandering one, whereby the stream power per unit length of stream is most evenly distributed. Therefore, channels meander for two reasons, both of which directly impact on channel energy: 1. to reduce channel slope, (Langbein and Leopold, 1966; Bettess and White, 1983) and 2. to provide bend flow resistance through the development of secondary circulation and turbulent flow structures (Leopold et al., 1960; Langbein and Leopold, 1966), thereby facilitating the most probable distribution of channel energy in accordance with the theory of minimum variance (Langbein and Leopold, 1966). The more sinuous the channel, the greater the reduction in slope (potential energy) and the greater the loss of (kinetic) energy due to internal distortion of the flow through bends. In fact, Leopold et al. (1960) found that bend flow resistance could provide twice that of skin resistance. Eaton et al. (2004) concurred, stating that with increased sinuosity the

importance of reach-scale form resistance increases. Direct estimations of bend-flow energy losses due to flow structures in bends are not the focus of this chapter, however, examples of flow through a number of the Barrington swamp channel bends are detailed in the next chapter.

Huang et al. (2004) described how optimal cross-sections for maximum flow efficiency (MFE) can provide excess energy to the system, necessitating the adjustment of channel planform to consume this energy and any other that is surplus to MFE and channel stability (equilibrium). Eaton and Church (2004) suggest that channel slope adjustment is the primary means by which a channel can adjust its energy and that it will precede any other means of channel energy (flow-resistance) adjustment. In this chapter, the effect of channel slope adjustment and the provision of flow resistance by meandering are considered collectively, using the sinuosity index (defined below). Bedforms, investigated in Chapter 4, were found to provide considerable flow resistance in the vertical plane and this resistance is essentially represented by their dimensionless steepness values (height/wavelength). If the combined effects of planform and bedform as resistance elements are considered in comparison with the depth to width ratio as a measure of flow efficiency (Chapter 3), a systematic relationship might be expected and is investigated below.

In alluvial settings channel planform has been shown to adjust to energy conditions (essentially stream power in the form of discharge and slope), thereby attaining equilibrium (Leopold and Wolman, 1957). In a study particularly relevant to the narrow, deep Barrington streams, Parker (1976) found that channel planform can also be differentiated using the relationship between cross-sectional geometry and the channel's slope / internal energy balance ratio (slope/Froude number). Planform existence diagrams delineating between straight, meandering and braided channels have been produced by Leopold and Wolman (1957) and Ackers (1982), and Parker (1976), and Schumm (1985) suggested that channels which plot inconsistently with these divisions may indicate a propensity for change and hence inherent instability. However, unique controlling conditions might allow channels to plot in anomalous positions on these graphs *and* to maintain stability. The

adjustment of channel planform in response to high bank strength, low sediment supply and limited depths of swamp material is examined here.

5.2 Planform and slope methods

The degree to which a channel meanders can be expressed by its *sinuosity*, which is the length of the channel relative to the length of valley through which the channel flows. Sinuosity (P) is determined using the index:

$$P = \frac{channel\_length}{valley\_length}.$$

A crucial step in defining P is in the selection of an appropriate length of channel or valley over which to measure the channel to valley length ratio. Through trial and error it became apparent that too short a length of channel would provide a low local sinuosity and too long a length of channel would average out otherwise observed variations in sinuosity. For this reason a length of 50m of channel, corresponding to roughly 20 to 30 times channel width, was measured along the channel path for Polblue Creek. Longer lengths of 100m were selected for the Barrington River and Edwards Creek as their alluvial channel belt was less sinuous. This length corresponded to roughly 30 to 50 times their channel widths. Starting at one end of the water surface survey reach in each case, P was calculated for the overlapping section lengths 0m to 50m, 25m to 75m, 50m to 100m and so on. The average of the two P values calculated over any station was deemed indicative of the channel sinuosity associated with that point.

Sinuosity results were simplified into four divisions for the Barrington River, two for Edwards Creek and five for Polblue Creek (Figure 3.3). The detailed 50m and 100m overlapping sections were used to aid in the determination of boundary positions for breaks in sinuosity.

To test for a defined relationship, channel flow efficiency represented by the dimensionless depth-width ratio, and flow resistance represented by product of the dimensionless P and dimensionless bedform steepness, were regressed against each other. If greater cross-

sectional efficiency is balanced by increased flow resistance (the product of sinuosity and bedform development), a relationship should be apparent.

The use of two planform existence diagrams, one a comparison between channel slope and discharge (Leopold and Wolman, 1957; Ackers, 1982) and the other a comparison between form ratio (d/w) and the slope/Froude number ratio (Parker, 1976)) requires the division of P values into planform types. The division between straight and meandering channels is commonly defined as 1.5 (Leopold and Wolman, 1957), a value adopted here to enable consistent comparisons with previous work.

To obtain accurate channel-slope data, the bankfull water surface was surveyed along each reach of channel using a SOKKIA Total Station. Successive points were located between 5 and 10 m apart, primarily at bend apices but also where bends were further than this apart along the intervening straight reaches. Slope was then calculated for individual reaches demarcated by clear changes in slope. These divisions are also illustrated in Figure 3.3.

5.3 Planform results

5.3.1 Sinuosity and slope

The sinuosity of each channel reach is presented in Table 3.2 and in Figure 3.3. Channel reaches range from straight ($P < 1.05$), through partly meandering ($1.05 < P < 1.5$) to meandering ($P > 1.5$) (Brice, 1964), bearing in mind that, for comparison with earlier graphical comparisons, all values less than 1.5 are plotted here as straight.

The Barrington River is the straightest overall, with sinuosities (P) between 1.07 and 1.36. Polblue Creek is also relatively straight along its lower reach, with a value of only 1.14. The remainder of Polblue Creek and all of Edwards Creek are more sinuous, with values of between 1.41 and 1.98. While the Barrington swamp channels appear to be highly sinuous in aerial photographs, these values are not exceptionally high by world standards. This is partly because the meander train, inset within the broader swamp, wanders across the valley floor. It was therefore considered inappropriate to measure valley length along the broad valley curve through the within-valley swamp. The ‘valley path’ that was used is the *inset*

floodplain that itself has a winding path within which the channel meanders. This is illustrated in the aerial photos (Figure 3.3). Channel bankfull water surface slopes for each reach are summarised in Table 3.2. Slope ranges from 0.0007 to 0.0052 along Polblue Creek, is constant at 0.002 along Edwards Creek and ranges from 0.0007 to 0.0034 along the Barrington River.

5.3.2 Flow efficiency – resistance balance

A relationship between the proposed flow-resistance term, the product of P and bedform steepness, and the proposed flow-efficiency term, depth-width ratio, is presented in Figure 5.1. The two Edwards Creek stations, for reasons discussed below, plot as outliers on this graph, but if they are removed from the dataset, the Barrington River and Polblue Creek stations illustrate a linear relationship with an r^2 of 0.50. Cross sectional efficiencies of the channel stations are positively related to their associated measures of flow resistance, at a rate of 0.06 times efficiency.

Stations that plot in the lower left region of the graph are located at entry and exit points of the swamps – they are wide and shallow with low cross-sectional efficiency. Their planforms are straight and they have only subtle bedforms. Stations toward the right hand side of the plot experience greater cross-sectional hydraulic efficiency and the channel response is an increase in sinuosity or bedform development, or both. The outlying positions of E1, E2 and B3 illustrate additional resistance provided by steep *duffle* bedforms. In the case of these three stations, large bedforms combine with a sinuous planform to significantly counteract the cross-sectional efficiency of the channel. However, the position of the two Edwards stations so high in Figure 5.1 may also be exaggerated because the resistance surrogate on the y axis gives an equal weighting to sinuosity and bedform steepness. These two sites have the steepest bedforms in this study but, as stated earlier, Leopold et al. (1960) found that boundary resistance is significantly less important than bend flow resistance. Therefore, these two sites may simply be illustrated with exaggerated “resistance”, represented by the product of bedform steepness and P.

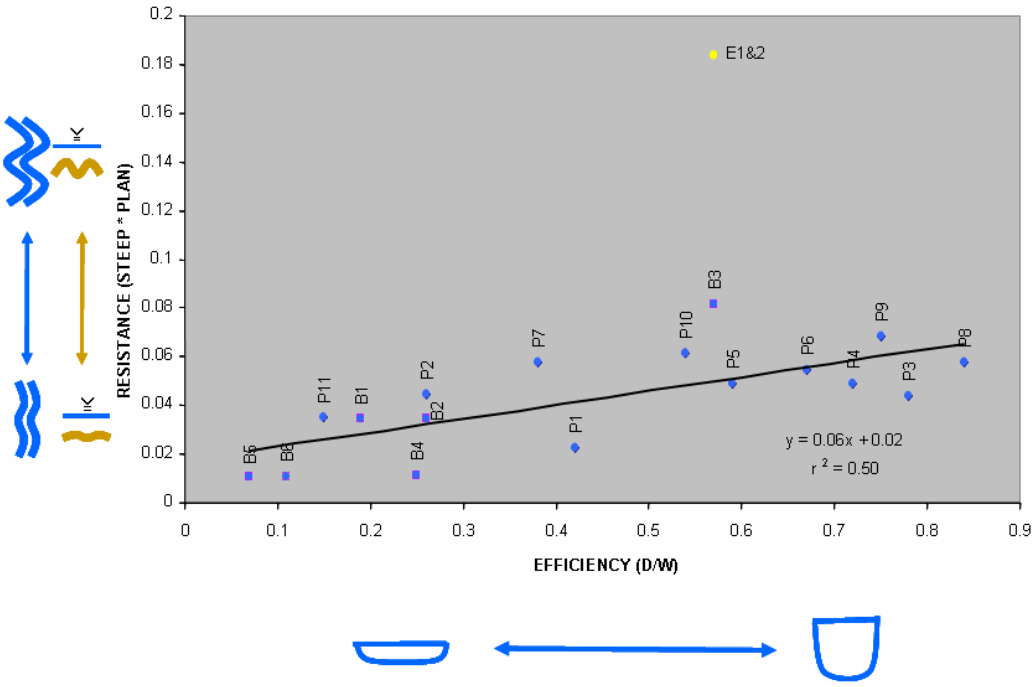

Figure 5.1 Channel flow efficiency, represented by depth - width ratio, versus the product of the bedform steepness and channel sinuosity resistance elements.

5.3.3 Planform existence diagrams

The Barrington swamp channels do not conform well to the meandering and straight zones in the slope/discharge Leopold/Wolman/Ackers plot (Figure 5.2). Only three straight reaches, from a total of nine, are successfully located on the graph, but they are accompanied by one meandering reach. Many sections of channel are not meandering, contrary to the expectation given by their energy setting. Indeed, two straight channel stations plot particularly high, even approaching the braided region of the graph. A lack of correspondence to this simple bivariate relationship is perhaps not surprising. Others have found that the conditions that differentiate channel pattern are more diverse than just slope and discharge (e.g. Ferguson, 1987; Tooth and McCarthy, 2004; Tooth and Nanson, 2004).

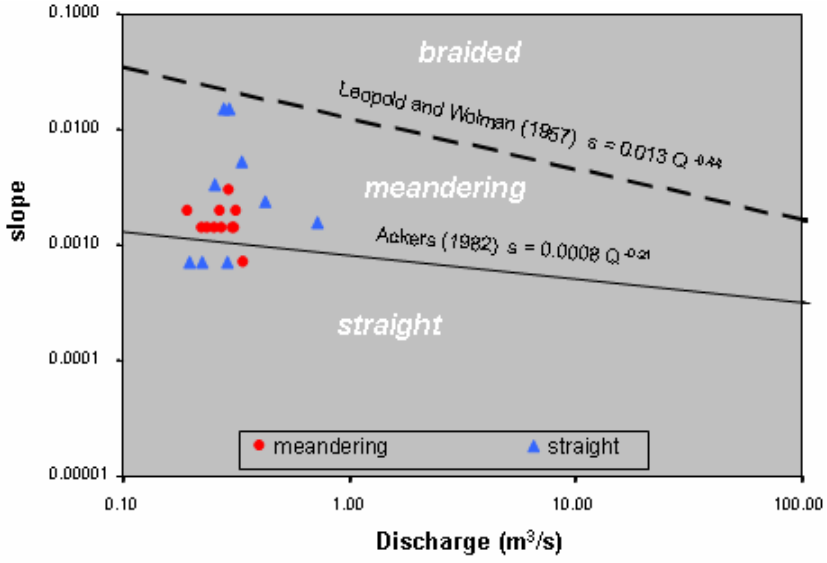

Figure 5.2 The discharge to slope plot of Leopold and Wolman (1957), modified by Ackers (1982) and here extended to lower discharge values than originally presented. Plotted stations represent both straight and meandering channel stations from the Barrington swamps.

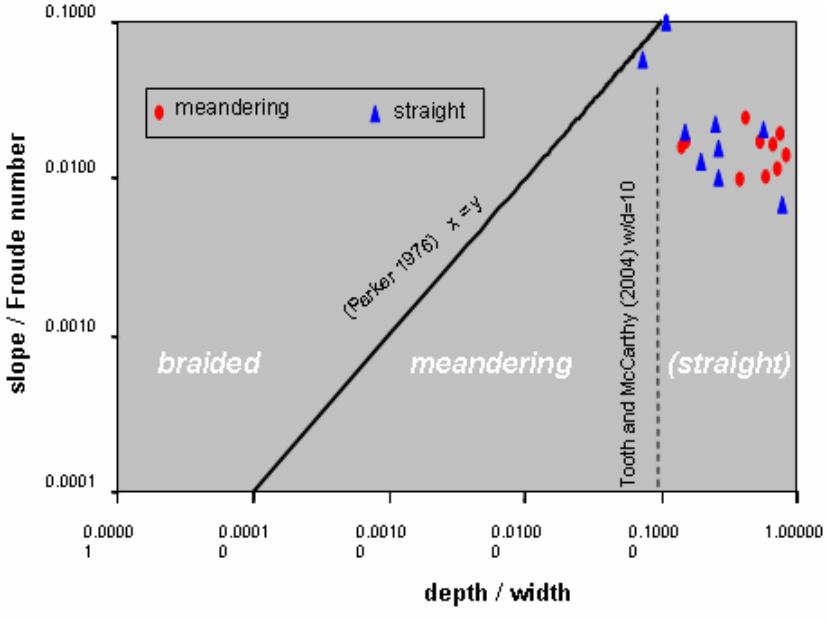

Figure 5.3 Parker's (1976) plot of form ratio versus slope-Froude number to distinguish between braided, meandering and straight channel planform. Barrington swamp channels, both straight and meandering, plot primarily to the right of the vertical division at d/w = 0.1, where only straight channels are usually found.

More interesting is that the Barrington swamp channels do not conform to Parker's (1976) slope/Froude number to depth/width plot. In the Okavango swamp channels, Tooth and McCarthy (2004) attributed the failure of the Leopold/Wolman/Ackers plot and the success of the Parker (1976) planform delineation for their own data to Parker's use of a combination of morphological (depth-width) and hydrological (slope-Froude number) attributes. This plot should ideally differentiate between braided, meandering and straight channel planforms. However, with only one exception, all Barrington stations plot within the zone of straight channels (Figure 5.3). The one station that does plot in the meandering region of the graph is actually straight. It appears that channel cross-sectional geometry, represented by the form ratio, and energy balance, represented by the channel slope/Froude number ratio, do not exclusively determine channel planform. Barrington swamp streams, whether straight or meandering in planform, have excessively low width/depth ratios for their energy setting (s/Fr).

5.4 Planform discussion

Previous chapters have concluded that the Barrington swamp channels have hydraulically efficient cross sections and very limited sediment transport. This makes for an interesting comparison between them and the wide shallow channels with mobile beds used to construct the planform existence diagrams by Wolman and Leopold (1957) and Parker (1976).

The inability of the discharge / slope Leopold-Wolman-Ackers plot to delineate between straight and meandering channels in the Barrington swamps suggests that exceptionally resistant, well-vegetated banks result in channel bank strengths beyond the range of those used to develop the discriminating boundaries on the plot. Their diagram represents self-forming channels in relatively unconsolidated material, very different to the Barrington swamp channels. Furthermore, Figure 3.10 showed that the depth of swamp alluvium is also an important factor in determining the cross-sections of these swamp channels. At the entry and exit of the swamps, in addition to several valley margin locations specifically along the Barrington River, the channels flow over valley-basement, with very little overlying peat or alluvial material. Here, the channels are unable to deepen and their beds

are comprised of coarse cobbles that form the basement of the swamp at these locations. These cobbles provide rough beds that consume flow energy; hence the channels straighten and steepen.

The depth-width versus slope-Froude number plot developed by Parker (1976) and used by Tooth and McCarthy (2004) to separate meandering from straight channels in the Okavango does not apply to the Barrington swamp streams. Parker's (1976) division of meandering and straight channels at depth-width ratios of 0.1 was supported by Tooth and McCarthy (2004) in the Okavango Wetland channels which transport an abundant sandy bedload in the form of well developed bedforms. As recognised by Schumm (1960) and then Fergusson (1987) for the Leopold and Wolman (1957) bivariate relationship, bed material can have a profound impact on just where in the relationship different channel patterns will lie. Parker's (1976) plot assumes sediment transport to be operating in self-forming alluvial channels and at rates controlled by channel slope and the Froude number. The inconsistencies between the position of the Barrington swamp channels and Parker's plot may be attributed to the demonstrated absence of sediment in the swamp channels (Chapter 3 and Chapter 4). The Barrington swamp channels must consume channel excess energy by means other than bedform resistance; planform adjustment is an important option.

Tooth and McCarthy (2004) emphasised the importance of sidewall drag in well vegetated, particularly narrow channels where secondary currents can be suppressed. They argued that sidewall drag centres the zone of maximum velocity, thereby protecting the channel banks from scour and meander development. However, their explanation does not apply here. As will be shown in Chapter 6, the Barrington swamp channels experience high shear stresses along the channel boundaries. Furthermore, secondary currents, far from being suppressed by the bank vegetation, are pronounced, even under conditions where w/d ratios are much less than those for the Okavango. The occurrence of straight channels in the Barrington swamps and in the Okavango wetlands under much higher energy settings than the Leopold-Wolman-Ackers slope-discharge plot would predict, and the apparent imbalance between depth-width and slope-Froude plot of Parker for the Barrington examples, are

likely to be a product of bank strength. The high bank strengths of the Barrington swamp channels, as discussed in Chapter 3, allow narrow, deep, hydraulically efficient cross sections to form and remain stable, even in the absence of bedform development that might otherwise moderate flow energy. In the case of the Okavango, the presence of more flexible banks formed of abundant reeds and peat, but with well developed energy-consuming bedforms, could explain the maintenance of straight channels there.

Given the planform adjustments just described, and the cross-sectional (Chapter 3) and bedform (Chapter 4) adjustments outlined earlier, it remains to determine whether the Barrington swamp channels have attained equilibrium. This will be considered using Mackin's (1948) concept of adjustments in channel slope leading to a graded or equilibrium condition.

5.5 An assessment of channel equilibrium

Entropy is a thermodynamic quantity representing the amount of energy in a system that is no longer available for doing work (Leopold and Langbein, 1962; Chorley and Kennedy, 1971) and considers the distribution of available energy within a system. The principle was first applied to fluvial environments by Leopold and Langbein (1962), in an effort to produce definitive equations for the solution of hydraulic geometry through the application of two principles: least work and maximum probability. They stated that (pp.11 and pp.7, respectively):

> *"the 'equilibrium profile' of the graded river is the profile of maximum probability and the one in which entropy is equally distributed"*

and that

> *"the most probable distribution of energy exists when the rate of gain of entropy in each interval of length along the river is equal".*

Over an unconstrained length of channel they concluded that the most likely form is exponential in long profile, however, over a more moderate length of stable channel, that is neither aggrading (which might cause backwater effects) nor degrading, it follows that the

energy of an equilibrium river, (which is represented by the energy grade line and *approximated* by the bankfull water surface slope), should be evenly distributed and represented by a straight line. Mackin (1948) stated that the length of channel constituting a graded (equilibrium) system need not be a fixed length. In the present study the graded condition is considered within the channelled reaches of each swamp that lie between constrictive lobes of shallow basement material, as it is these reaches, and their interaction with the swamp, that have the ability to self-adjust as equilibrium systems. The presence or otherwise of such straight equilibrium water-surface slopes are investigated here for the Barrington streams. Water surface long-profiles are the result of adjustments in a range of variables and are not necessarily straight in bedrock systems (Hack, 1957), nor do localised deviations from straight profiles represent localised disequilibrium (Leopold et al., 1964). However, in self-adjusting channels and unconstrained environments it follows that the smoother the energy gradient line, the more closely the whole system approaches equilibrium (Leopold and Bull, 1979).

5.5.1 Water surface slope methods

To calculate reach channel slopes the irregularly spaced bankfull water surface long profile survey data were re-sampled at 10m intervals using the same Matlab script that was applied to the bedform analysis data (Appendix 3).

If the Barrington River, Edwards Creek and Polblue Creek water surface slopes were regressed along their entire surveyed lengths, the resultant analysis would have implied a lack of grade. This is due to the presence of lobes of basement cobble material which in places extend out from the valley margins beneath the swamp and limit the depth to which overlying channels can form and therefore the degree to which these reaches of channel are free to adjust. The Barrington River and Edwards Creek long profiles were therefore divided into three sections consisting of the Barrington River upstream of its confluence with Edwards Creek (Barrington River Middle and Upper), downstream of its confluence with Edwards Creek (Barrington River Lower) and Edwards Creek. The Polblue Creek dataset was divided into three subsections, the single analysed dataset extending through

the middle section of its surveyed extent. These divisions were based on the location of major cobble lobes.

The resulting sub-datasets were then linearly regressed and their residual values used to assess the achievement of grade. An r^2 value close to unity indicates a system close to a graded condition.

5.5.2 Water surface slope results and interpretation

The longitudinal water surface regression results are presented in Figure 5.4. All water surface regressions indicate r^2 values between 0.97 and 0.99.

The entire study reach for over 460m of Edwards Creek shows a water surface slope with an almost linear relationship and an r^2 of 0.99. The 180m reach of the Barrington River downstream of its confluence with Edwards Creek also presents a very even water surface profile with an r^2 value of 0.98, and the middle reach of 370m of Polblue Creek has a remarkably constant gradient with an r^2 value of 0.99. However, upstream of its confluence with Edwards Creek, 530m of the Barrington River (Middle and Upper reaches) is somewhat variable with an r2 value of 0.97. The Barrington River Upper flows through very shallow peat over basement material and is not free to adjust uniformly.

These channels, generally, have remarkably uniform water surface profiles over several hundreds of metres. With sufficient freedom to adjust, it appears that swamp channels can achieve graded long profiles indicative of equilibrium conditions. This is particularly well illustrated by Polblue Creek which lacks large bedforms and which has therefore adjusted primarily through planform adjustment. Figure 5.5 illustrates the longitudinal profile of Polblue Creek, measured along the channel thalweg and bankfull water surface. The variations in channel sinuosity, valley width, channel width/depth ratio, depth of swamp material and valley slope along these same reaches are also illustrated. As the valley slope increases and valley width decreases in a downstream direction, the channel becomes increasingly sinuous until the depth of alluvium decreases to a depth in which a

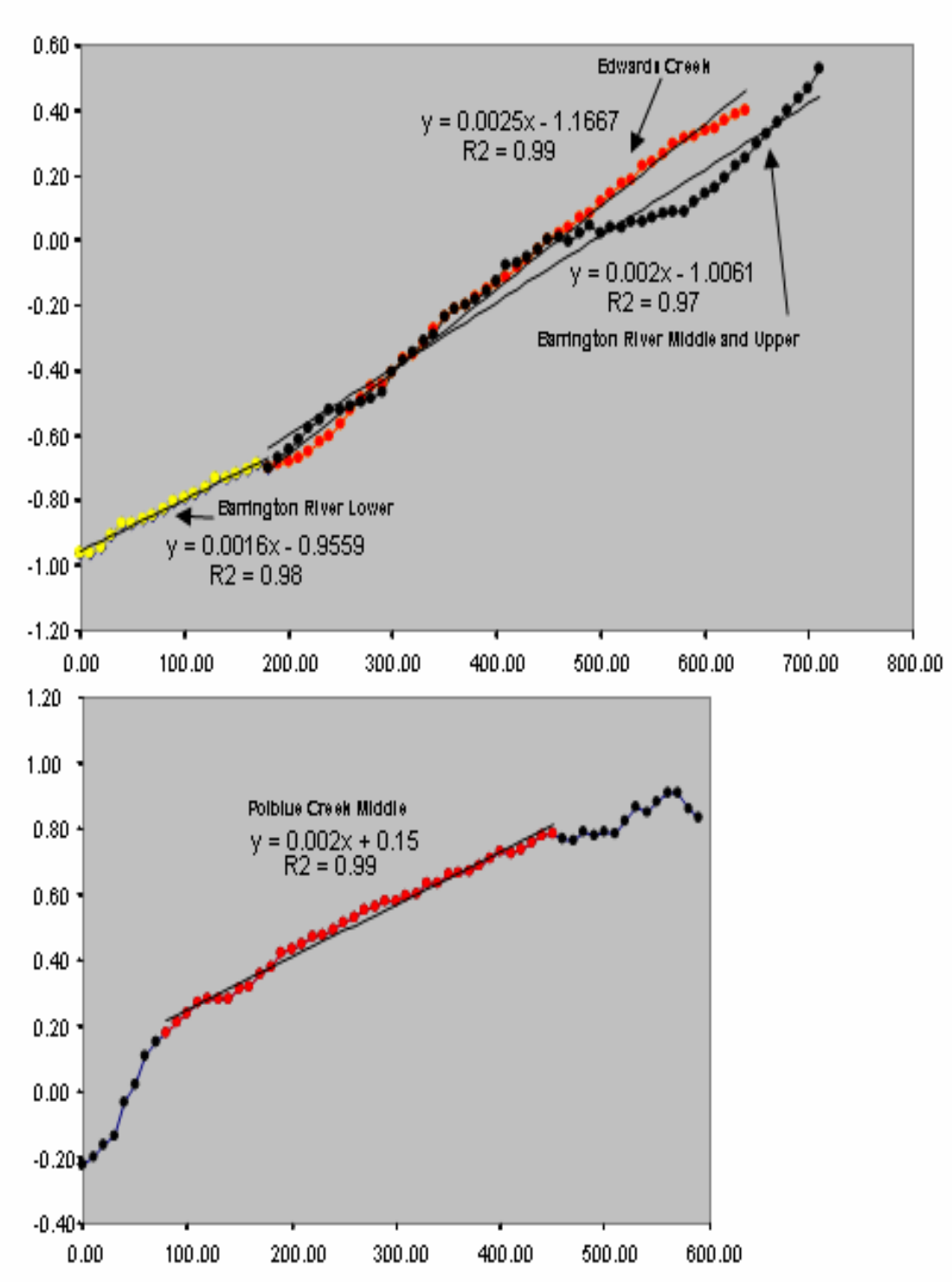

Figure 5.4 Assessment of grade through linear regression of water surface slopes a) Edwards Creek and Barrington River and b) Polblue Creek.

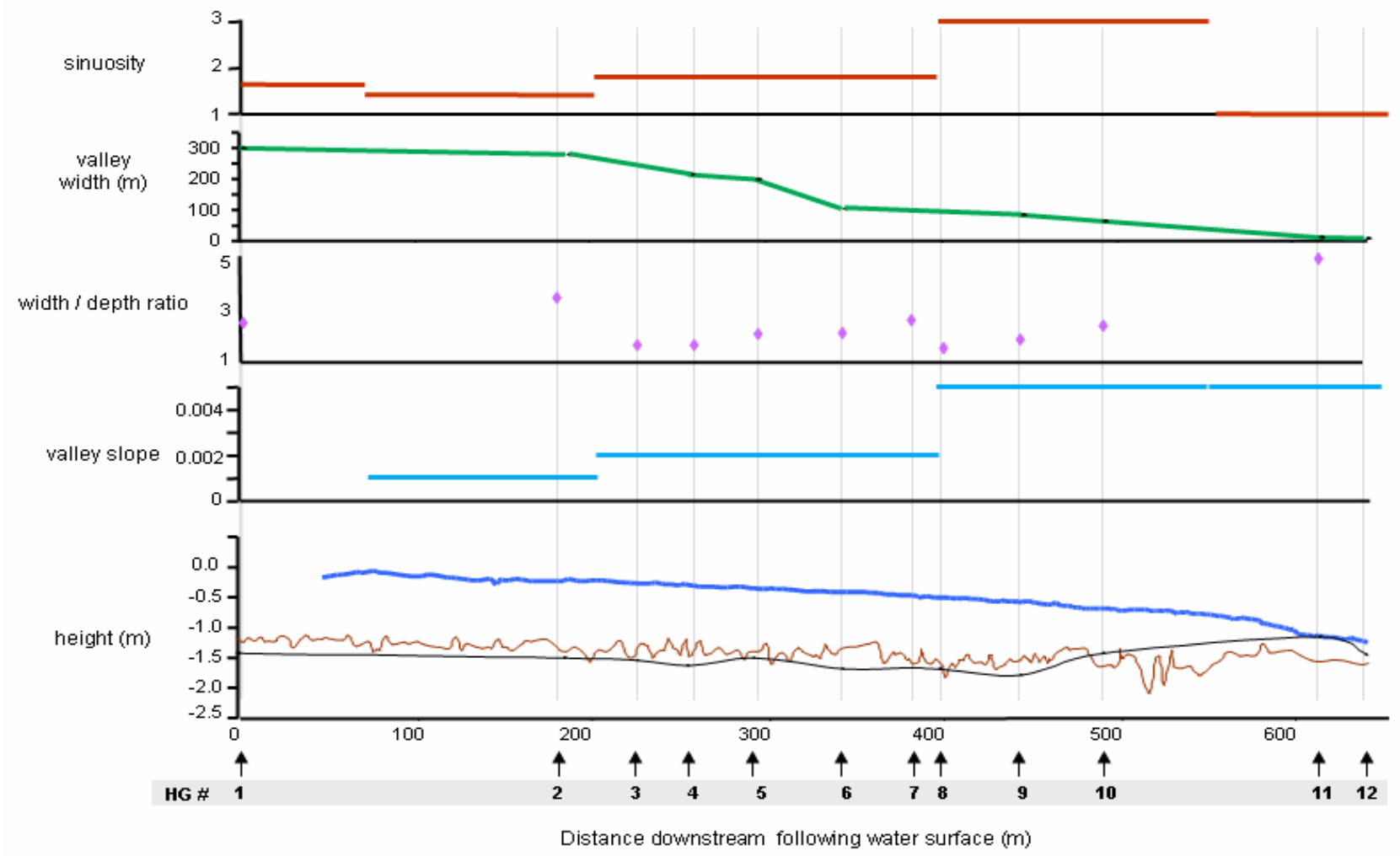

Figure 5.5 Longitudinal profile of Polblue Creek, illustrating reach averaged sinuosity, valley width and valley slope (calculated using straight-line distance between bankfull water surface points). The bottom plot illustrates the surveyed channel thalweg (brown line), water surface (blue line) and basement (black line) and hydraulic geometry stations (HG) are marked along the x-axis. Width/depth ratios for these stations are illustrated on the middle plot.

sinuous planform cannot be maintained. The channel widens and straightens and the flow passes over cobble basement material. The longitudinal water surface profile of this same channel (Polblue Creek), illustrated in Figure 5.4, indicates that the adjustments in channel cross-section, bedforms and particularly planform have been sufficient for the attainment of equilibrium.

5.6 Channel adjustment conclusions

Through the Barrington swamps the narrow, deep and steep-banked channels provide optimal conditions for the hydraulically efficient flow of sediment free water, consistent with the principal of minimum energy. The development of meanders in the Barrington swamp channels appears to have been sufficient, in the absence of bedforms in most instances, for the attainment of channel stability. Leopold et al. (1960, pp.131 and pp.132, respectively) stated that:

> *"a river which is deficient of bed material of large enough size to stabilise a straight channel may become stabilised in an irregular channel merely by creating random bank projections"*

and that:

> *"the meander form may represent one of the channel patterns to which the above generalisation applies, only the random bank projections are replaced by somewhat symmetrical channel curves".*

However, in the higher stream power channels (Edwards Creek and Barrington River) sediment must have been supplied at some time in the past, or has accumulated slowly, for *duffle* bedforms to develop. Bedforms ranging from negligible (in most instances) to extreme in magnitude indicate a tendency for the channels to form flow resisting elements in the vertical plane where sediment is sufficient to do so and where additional resistance is required for channel stability in higher stream power systems. Furthermore, a variety of channel sinuosities have developed, from nearly straight to meandering, thus illustrating freedom for these channels to adjust in the lateral plane where necessary to achieve equilibrium. However, the presence of exceptionally tightly curving and stable meander

bends at many locations (Chapter 6) indicate that the banks of the Barrington streams must be sufficiently resistant to erosion to maintain stability. Channels with more mobile banks would presumably erode and release sediment, form bedforms and consume energy more evenly between the bed and the distortion of flow in bends.

Graded water-surface long profiles over hundreds of metres in channels with almost no bedforms (Polblue) as well as in higher stream power channels with exceptionally large bedforms (*duffles* – Edwards and Barrington channels), suggests that planform is closely integrated with other flow resisting elements. Equilibrium channels can clearly form, and be maintained, in these densely vegetated and highly erosion-resistant swampy environments. How the bend flow structures that are produced by these morphologically unusual channels contribute to significant levels of flow resistance, and to the development of these swamp- channel morphologies, is the subject of the next chapter.

Chapter 6 Time averaged flow structures in bends with unusual geometry

6.1 Introduction

The channels flowing through the Barrington swamps have very little sediment load. With what little is available some have formed stable and often armoured bedforms, as described in Chapter 4. The combination of cross-sections that are highly efficient for the conveyance of water (Chapter 3) with very little sediment load means that considerable surplus energy must be consumed by other means. As discussed in Chapter 3, surplus energy is that in excess of the energy required to maintain a stable (equilibrium) channel form with the water and sediment that is supplied. Leopold et al. (1960, pp.131-132) suggested that under the condition of insufficient sediment of a suitable calibre to form bed features, channel stability *can*, nonetheless, be achieved largely through sinuous planform development. Aerial photographs of the Barrington swamp channels (Figure 3.3) illustrate sinuous planforms and tight bends (r_c/w as low as 0.6).

The most immediate reduction of channel energy by meander planform development is achieved by the resulting decrease in the energy grade line, caused by extension of the flow path. This was considered in Chapter 5 (Figure 5.1) through the use of the sinuosity index (P), which was also used to roughly represent comparative differences in bend-flow resistance. More specifically, bend-flow resistance is caused by *internal distortion* of the flow resulting from the shearing of flow lines and the increased bank resistance. Some *spill* resistance can be caused by water surface slope variations resulting from channel flow interaction due to bend geometry. Resistance elements create additional eddies that interfere with the primary flow and therefore consume energy (Leopold et al., 1960). However, flow conditions are further complicated by the creation of secondary currents which minimise flow distortion and the resistance to flow that would otherwise result from shearing of the flow lines parallel to the boundary of a bend (Bagnold, 1960). Circulation strength is maximised and energy losses from shearing are minimised in bends with radius of curvature to width ratios of about 2-3 (Bagnold, 1960). This range of values coincides

with those most commonly observed in natural channels (Hickin and Nanson, 1975; Hickin, 1978; Hickin and Nanson, 1984) supporting Bagnold's initial notion that secondary currents develop to minimise flow resistance and are successful in doing so in the majority of documented bends.

Regardless, however, secondary currents cause energy losses through the creation of eddy driven flow turbulence and distortion resistance that is additional to that which would occur in a straight channel (Bagnold, 1960). These losses can be greatly increased by the turbulence created in regions of separated flow (Bagnold, 1960; Markham and Thorne, 1992). It is not the intention of this chapter to quantify bend-flow energy losses in the Barrington swamp channels, but rather to document the flow structures that interact with the unusual geometry of the channels and to thereby infer such energy losses.

Polblue Creek, Barrington River and Edwards Creek each have very low width-depth ratios, very steep banks and very tight bends. The Barrington River and Edwards Creek have also developed *duffle* bedforms (Chapter 4). Furthermore, large concave bank embayments, termed meander pools by Alford et al. (1982), have developed at many bend apices and as yet, no comprehensive studies have examined the flow fields that form within them, the conditions which lead to their development or what effect they may have on the flow. Comparison of bend flow structures resulting from such unusual channel morphologies in channels both with and without *duffles* provide insights into the complex flow conditions that can form in very narrow and deep channels carrying very little sediment.

This chapter investigates bend flow in the meanders of the Barrington swamp channels, including flow structures and shear stress distribution. Because bend-flow is a complex topic it is essential to review the literature on bend-flow patterns, before presenting and interpreting the Barrington data presented later in the chapter.

6.1.1 Pool-riffle maintenance and bend flow patterns

Shear stress distribution determines both the rates of bank erosion (e.g. Bathurst et al., 1979) and the patterns of sediment transport (e.g. Hooke, 1975). Much work has suggested

that processes which operate in straight channels lead to the development of channel bends (e.g. Leopold and Wolman, 1957; Keller, 1972; Lewin, 1976) as pools and riffles forming in straight channels can lead to the formation of variable bank erosion and hence the development of meandering planform. Flow structures in straight channels may therefore be present in meandering channels, albeit in distorted form.

Pool-riffle maintenance along straight reaches has received considerable attention and several models have been proposed. The velocity, or shear stress, reversal hypothesis (Gilbert, 1914; Leopold et al., 1964; Keller, 1971) is the most oft-quoted, in which pool flow velocities are purported to increase more rapidly with stage than those over riffles, and then to exceed them during bank full flows. Recent modelling (Booker et al., 2001) and field observations in straight reaches (Milan et al., 2001) have found support for this model. However, Clifford (1993) proposed an alternative theory involving particle queuing and which is based on the kinematic wave theory of Langbein and Leopold (1968). In the particle queuing model sediment particles accumulate on riffles and become more structured. As a result they require higher critical shear stresses to mobilise and are less capable than pool sediments of being transported by the flow. Alternatively, Wilkinson et al. (2004) recently observed and modelled one-dimensionally flow through a straight pool-riffle sequence and found that, with increasing flow stage, the region of maximum shear stress shifted from the lee to the stoss side of riffles. They described this as a *phase-shift*.

Whether pools and riffles in straight reaches are maintained by velocity or shear stress reversals or shifts, pool-riffle maintenance in bends differs somewhat from that in straight reaches, as the secondary currents produced by bend geometry can significantly influence patterns of velocity and shear stress. Some debate has focused on the importance of secondary currents in determining bend flow sediment transport (Hooke, 1992), for tight bends have significant secondary flow strength that can equal primary currents (Markham and Thorne, 1992). While the magnitude of secondary currents may not in themselves necessarily cause shear stresses of any great consequence (Bridge and Jarvis, 1976), they still play a major role in controlling the location of channel-bend sediment transport and bend migration.

A general model of bend shear stress distribution was proposed by Dietrich et al. (1979) in which the region of maximum bed shear stress shifts from near the inner bank at the bend entry to near the outer bank at the bend exit. Maximum shear stresses in bends are associated with both the location of the maximum velocity filament (MVF) and with regions of down welling (Bathurst, 1979). Bathurst et al. (1979) found that the development of secondary currents, in the form of outer bank cells of reverse rotation (see below), can enhance down-welling and therefore bed shear-stresses. Furthermore, Hey and Thorne (1975) described a mechanism by which pools and riffles could form and maintain in both straight and curved reaches. In the case of adjacent, independently rotating helices, converging flow near the bed and consequent diverging flow near the water surface over riffles encourages sediment deposition and the reverse pattern in pools encourages scour.

Bend-entry patterns of flow have also been acknowledged as a primary control over bend-flow patterns. Prus-Chacinski (1956), for example, examined patterns of bend entry flow for channels with varying geometries and found that, owing to the sensitivity of these patterns to entry flow currents, the number of resultant patterns seemed almost infinite. However, some consistencies in general bend flow patterns have been widely documented and are described below.

Markham and Thorne (1992) formalised three main regions of bend flow which facilitate discussion of general flow patterns and variations in this pattern (Figure 6.1): the *inner* region, over the point-bar, the *mid-channel* region, which is positioned over the thalweg, and the *outer* region, extending up to two channel depths from the concave (outer) bank (Thorne et al., 1985).

6.1.1.1 Inner bend flow region

The *inner* region of bend flow is dominated by shoaling over the point which causes outward flow of the whole water column (Hickin, 1978; Dietrich and Smith, 1983) (Figure 6.1), although return flow across the point bar surface at bankfull flow in a bend with constant width-stage relations has also been reported (Thorne et al., 1985). Flow separation can develop within the downstream flank of this inner region (Leeder and Bridges, 1975), particularly in tight bends (Markham and Thorne, 1992). In very tight bends the MVF can

move inwards, up and over the point bar, causing higher shear stresses and erosion of the point bar (Hickin, 1978). The lack of point bar development in the Barrington swamp channel bends are suggestive of an inward movement of the MVF.

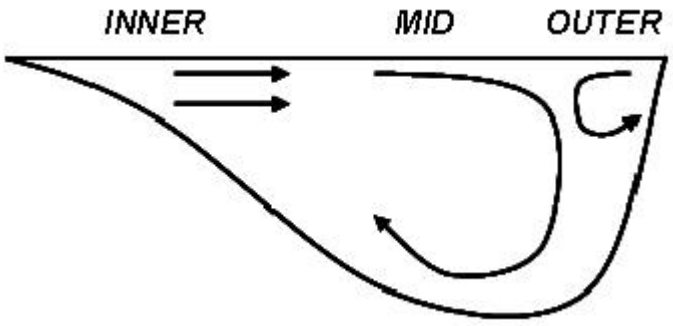

Figure 6.1 Regions of bend flow and general patterns of secondary currents. Modified from Markham and Thorne (1992)

6.1.1.2 Mid-channel bend flow region

As flow moves through a bend, centrifugal and pressure forces combine with boundary friction to produce secondary currents. Centrifugal (or, more correctly, tangential) forces cause superelevation of the water surface towards the outside bank, the height of which (Z) is a function of flow velocity (v), channel width (w), the radius of curvature to width ratio (r_c/w) and gravity (g), and takes the form:

$$Z = \frac{v^2 w}{g r_c}$$

(Leopold et al., 1960). The elevated water surface results in a pressure gradient across the channel and through the water column. Near the water surface, the centrifugal force usually exceeds the pressure gradient force and flow is directed outward, whereas near the bed the pressure gradient forces dominate and, encouraged by flow retardation resulting from bed friction (Prus-Chacinski, 1955; Bagnold, 1960; Bridge and Jarvis, 1976), the flow is directed inward over the bed. The pattern thus produced is one of outward flow at the surface, downward flow towards the bed near the outside bank and inward flow over the

channel bed (Prus-Chacinski, 1955), the process of which has been termed *skew induced* secondary flow or *helical* flow (Bathurst et al., 1979) (Figure 6.1).

The helical flow in the *mid-channel* region persists through all flow stages and through bends of varying geometries (Prus-Chacinski, 1955, 1956; Hey and Thorne, 1975; Hooke, 1975; Hickin, 1978; Dietrich and Smith, 1983; Thorne et al., 1985). This region of flow is perhaps the most consistent in structure of any of the three bend-flow regions. Helical flow strength, however, is strongly influenced by channel geometry and flow hydraulics. It is enhanced by low bend radius of curvature to width ratios (Hickin, 1978; Bathurst, 1979), high flow velocities (Hooke, 1975), low bank roughness (Thorne and Furbish, 1995), high width-depth ratios (Bathurst, 1979), point bar presence (Dietrich and Smith, 1983) and high flow stages (Hooke, 1975). It is also initiated earlier in the bend in narrow and deep channel sections, in which it also dissipates more rapidly (Choudhary and Narasimhan, 1977). Contradictory conditions for the development of helical flow exist in the Barrington swamp channels, in which low w/d ratios, tight bends, lack of point bars and high bank roughness's may produce unusual helical flow patterns and strengths.

6.1.1.3 Outer bend flow region

Both Bathurst et al. (1979) and Powell (1998) have provided thorough descriptions of the processes that lead to the development of an *outer* bank cell, upon which the following description is based. As flow moves into a bend, bend geometry and centrifugal forces drive flow towards the outside bank, causing it to stagnate and super elevate. The weight of the superelevated water can drive a downward flow along the boundary where the stagnated water (*outer* bank flow) meets with the main flow cell (*mid-channel* flow). The cell of reversed helicity is thus formed against the concave bank (Figure 6.1). At the junction of these opposing cells, flow converges and the MVF is forced toward the bed where it diverges and results in high bed shear stresses (Hey and Thorne, 1975; Thorne et al., 1985). Sharper bends and higher velocities cause enhanced superelevation of the water surface and drive larger outer bank cells with greater associated bed shear-stresses (Bathurst et al., 1979; Markham and Thorne, 1992). Steep banks appear to be necessary for the development of this cell (Thorne and Rais, 1983), and Bathurst et al. (1979) found that its formation was suppressed in wide, shallow bends. Furthermore, Bathurst et al. found that in

the absence of outer bank cell development, bed shear stresses may not develop significant peaks and, in the absence of a strong outer bank cell, maximum bed shear stresses are instead associated with the MVF, consistent with the original observations of Hooke (1975). Hey and Thorne (1975) suggested that, even in the absence of field data recording this small cell, the location of the MVF and zone of bedload transport away from the outer bank supports its existence. Steep banks and narrow and deep cross-sections in the Barrington swamp channels are ideal for the formation of this cell, and patterns of velocity and shear stress through these bends should indicate its existence.

6.1.1.4 Flow separation

Flow separation is the response of flow to abrupt changes in channel geometry. Here the flow lines diverge and this can cause the flow and channel boundaries to separate. Separation zones can develop at either convex (e.g. Leeder and Bridges, 1975; Ferguson et al., 2003) or concave (e.g. Hickin, 1978; Nanson and Page, 1983; Andrle, 1994) banks or in the lee of bedforms (Yalin, 1971), and their development can influence channel stability.

Convex-bank flow separation zones generally form in the lee of point bars, where channel depth increases as the channel boundary curves away from the flow (Markham and Thorne, 1992). Outer-bank flow separation occurs as a result of water superelevation at the outer bank, causing stalling and separation (Markham and Thorne, 1992). Both can alter the radius of curvature/width and width/depth ratio (Leopold et al., 1960), reducing the latter by up to 50% (Leeder and Bridges, 1975), thereby causing reduced flow resistance. Both inner and outer bank regions of flow separation often develop in tight bends (Hickin, 1978; Andrle, 1994; Hodskinson and Ferguson, 1998) and their influence on secondary currents, shear stress distribution and channel migration are therefore of particular interest in the very tight channel bends of the Barrington swamps.

Flow separation also forms near the bed in the lee of dunes. Bedform resistance correlates positively with overall flow resistance and was used in Chapter 4 to calculate the shear stresses attributed to bed features. Shear lines form where the separated flow interacts with the main flow and large turbulent eddies emanate from both this region and from where the shear line intersects with the bed (Best, 1996). Shear stresses are maximised along the shear

line, but also at the point of reattachment to the physical channel boundary, and are responsible for large instantaneous increases in shear stress and sediment transport (Kostaschuk and Church, 1993). These flow structures are visible at the surface as kolks or boils (Yalin, 1992) and were frequently observed at high discharges in the bends of the Barrington swamp channels. The *duffle* bedforms of the Barrington River and Edwards Creek, while clearly planform related, are morphologically similar to dunes and therefore their resultant flow structures are likely to correspond with these features.

There is an absence of data on flow through bends with bedforms of the magnitude observed in some of the Barrington channels. As described in Chapter 4, *duffles* are very steep, provide resistance to flow at all flow stages and are likely to have a pronounced effect on bend flow. This chapter examines flow structures that result from the interaction of low and high amplitude bedforms with tight meander bends and narrow and deep channels. The importance of these relates to both the development of the channels as well as to their contemporary morphology and processes.

6.2 Barrington bend geometries

The aerial photographs of the Barrington swamp channels, presented in Figure 3.3, illustrate their sinuous planforms with some very tight bends. The radius of curvature to width ratio (r_c/w) is used to provide a dimensionless representation of bend curvature comparable between channels of any scale.

The radius of curvature is measured as the radius of a circle passed through the centreline of a channel bend (Goudie, 1990), however such straightforward application is only possibly in bends with regular sine-curve geometry, which the Barrrington swamp channels do not have. In this study channel widths through the bends were sometimes highly variable. Hence an arc of curvature was passed through the mid-point of the channel at he entry and exit cross-sections in each bend, located immediately upstream and downstream of skew (bend) induced secondary currents. In addition, the arc ideally passed through the centreline of the channel at the bend apex. The approach taken to measure r_c/w is therefore a morphodynamic, rather than a simple geometric, one.

The existence of secondary currents could be recognised visually from the alignment of ribbon weed on the bed of the channel. Average widths of all the cross-sections examined through the bends were used to define bend channel width.

In such narrow channels as those of the Barrington Tops swamps, channel bed topography through a bend plays a major role in influencing bend flow patterns. The reach-averaged bedform steepness values from Chapter 4 were used to represent this parameter, and a variety of bend geometries representing varying bend tightness and bedform steepness were identified.

6.2.1 Bend geometry results

A total of seven bends, spanning radius of curvature to width ratios from 0.6 to 2.4 and bedform steepness from 0.03 to 0.11 (Table 6.1), and these bend locations are indicated in Figure 3.3. Barrington Bend 2 is located in a reach that is essentially plane bedded (Chapter 4). However, the bend itself is not plane-bedded (unlike much of the reach that it is located in) and to also enable its comparison with the other studied bends it was allocated a realistically low bedform steepness value of 0.03, representative of pool-riffle bed morphology (e.g. Polblue Creek). The resulting spread of bend tightness and bedform steepness is illustrated in Figure 6.2, which shows that a variety of bends with *tight and steep*, *tight and flat* and *open and flat* geometries were selected for detailed bend flow examination. Interestingly, despite seeking to locate bends and bedforms that were *open and steep*, no examples were identified, suggesting a causal link between bend geometry and bedform development.

Table 6.1 Bend geometry and flow stage comparisons. Q_{bf} represents bankfull discharge.

Bend #	r_c/w	steepness	% Q_{bf}
Polblue Bend 1	2.4	0.03	60-68
Polblue Bend 2	2.2	0.03	80-88
Polblue Bend 3	1.2	0.03	88-100
Barrington Bend 1	0.7	0.06	90-100
Barrington Bend 2	1.35	*(0.03)*	53-58
Edwards Bend 1	0.6	0.11	64-81
Edwards Bend 2	0.6	0.11	42-48

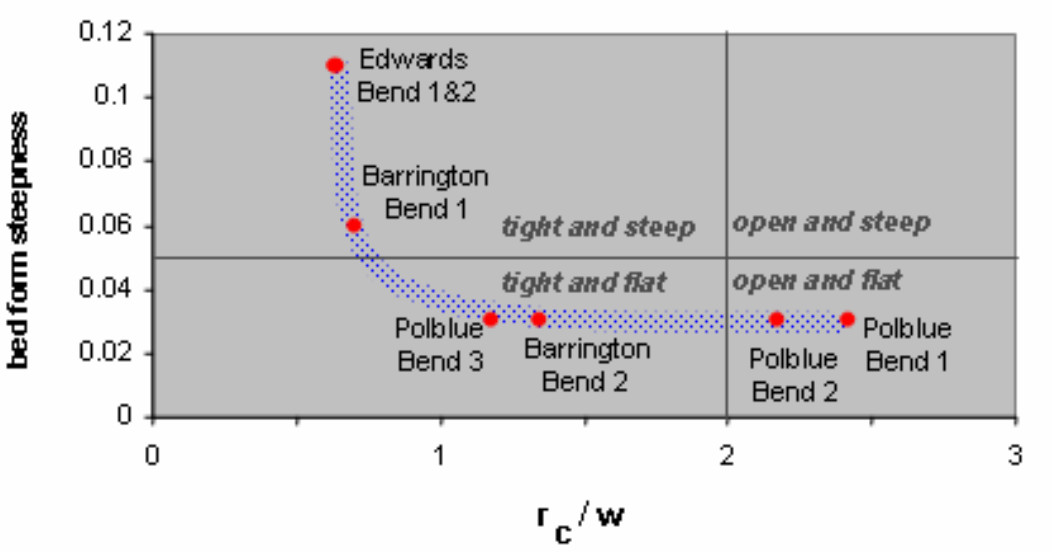

Figure 6.2 Channel geometry comparisons for all bends in which flow field data was collected. Note the absence of *open and steep bend* examples. The trend line highlights the tendency for bedform steepness to increase with decreasing r_c/w (increasing tightness), once r_c/w decreases below approximately 1.

In addition to the tight planform and varying bed undulations, several bends have developed embayments at their concave banks and of the intensively studied bends, this was most pronounced in Barrington Bend 1.

6.3 Bend flow in the Barrington swamp channels

6.3.1 Methods of flow data collection and processing

The discharge of channel flow through each bend varied from 42% - 100% of bankfull and ranges through each bend are presented in Table 6.1. This range resulted from the rapid rise and fall of the hydrographs in association with rainfall during the measurement periods (Chapter 1).

Current data was collected using an OTT C2 current metre for three Polblue Creek bends, and with three NORTEK Vector Current Metres, referred to as Acoustic Doppler Velocimeters (ADV's), for the four Barrington River and Edwards Creek bends.

Cross sections were oriented perpendicular to the outside bank (e.g. Frothingham and Rhoads, 2003). As these channels are so narrow it was considered that this angle could be consistently and accurately estimated in the field.

In previous studies of secondary flows in bends, the direction of these flows has been related to either the mean flow direction (e.g. Chow, 1973) or to the longitudinal direction of the channel (e.g. Frothingham and Rhoads, 2003). Chow (1973, pp.12) defined secondary flow as

> *"the movement of water particles on a cross-section normal to the longitudinal direction of the channel".*

Frothingham and Rhoads (2003) argue that this approach is appropriate if it is the interaction of the flow with the bend geometry that is of interest. It was therefore unnecessary to rotate the cross section orientation perpendicular to mean flow direction based on averaged directional data from either each individual vertical set of measurements (Rozovskii 1957; Bathurst et al. 1977), or the mean flow direction for the entire cross section (Hickin 1978).

The limited size of the channels at narrow or shallow cross-sections sometimes inhibited the collection of large datasets of flow measurements. However, the flow through such cross-sections was largely two-dimensional and, for the purposes of this study, did not require more detailed investigation.

6.3.1.1 Collection of two-dimensional flow data

An OTT C2 was mounted on a vertical rod and aligned with the direction of maximum velocity. This direction was measured using a ribbon tied to the back of the OTT, which flowed in the maximum current direction (Figure 6.3a), a technique very similar to that used by Bridge and Jarvis (1976). The operator stood above the instrument, on an aluminium plank placed perpendicular to the outside bank, and the current speed was recorded for 40-60 seconds. The angle of the ribbon from the perpendicular cross section (0° for flow towards the left bank through to 180° for flow towards the right bank, through to 270° for upstream flow) was measured using a clear plastic protractor, through which the angle of the ribbon was observed. The water was clear and did not inhibit the observation

of the ribbon. Primary and secondary current magnitudes were derived by resolving the maximum velocity into primary and secondary flow magnitudes.

6.3.1.2 Collection of three-dimensional flow data

Three dimensional flow data were collected using three ADV's, mounted on a vertical rod and positioned on the downstream side of the aluminium plank. The plank, in turn, was placed perpendicular to the outside bank between the end datum for each cross section (Figure 6.3b). The instruments were manually deployed using Vector software operated from a laptop computer. Each instrument was deployed for between 60 and 120 seconds, however only the first 40 to 60 seconds of each record was utilised, depending on data quality. Data were filtered by allowing signal to noise ratios (SNR's) of <10, correlation scores of >70, a velocity range of ±1 m/s and acceleration between instantaneous velocity measurements of no more than that which could be attributed to gravity (9.8m/s). Further details of the ADV devices and data cleaning are provided in Appendix 5.

6.3.1.3 Method for calculating shear stress distribution in bends

Grain (bed) shear stress estimates were calculated in Chapter 4 using the Du Boys equation in conjunction with wall and form shear estimates. In this chapter, more precise distribution of bed shear stress in channel bends was of interest and required a different approach. Direct shear stress approximation provides the most suitable estimate of the forces acting on a particle of sediment and it is therefore the preferred technique for determining sediment transport potential (Grayson et al., 1996). The Law of the Wall technique is one such method of direct shear stress measurement, and is derived and defined in Appendix 6. When applied here, Law of the Wall shear stress calculates the slope of the regression line from the lowest point beneath 20% of the flow depth to the origin (τ_{LP}). While this specific technique is not encouraged for obtaining absolute values of shear stress, it was considered that values obtained in the bends were reliable for comparison relative to one another.

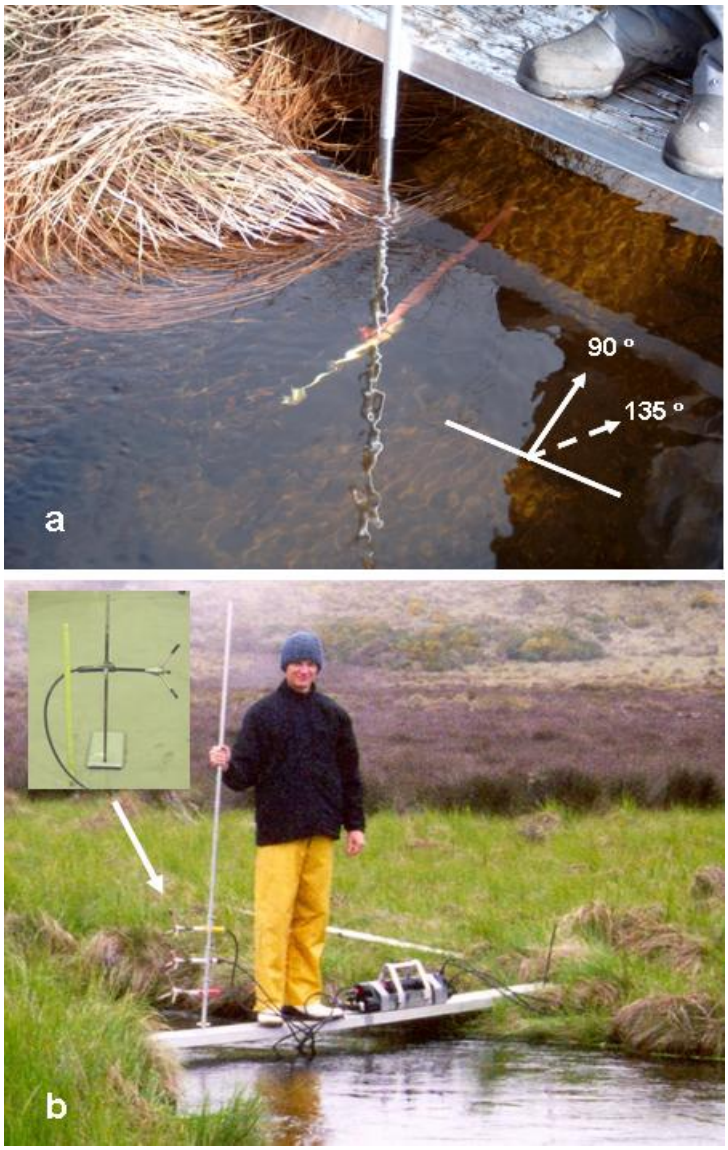

Figure 6.3 a. OTT current meter and b. ADV deployment at near bankfull. The ADV was deployed and data collected using a laptop computer, (out of view).

6.3.2 Bend flow patterns for the Barrington swamp channels

Patterns of primary and secondary flow for each of the bends are presented as a series of cross-sections which also include sketch maps of the surface bed-material distribution. Vertical velocity profiles for each cross section are also presented from which the shear stress distributions are derived. Estimates of shear stress calculated using the Law of the Wall are compared in Table 6.2 with those derived in Chapter 4 (du Boys). The values provided by each technique compare well and confirm their value in terms of relative

accuracy from site to site, despite concessions made in the application of the Law of the Wall.

Bend flow patterns are considered in two separate categories: 1. those bends with gentle bed relief (Figure 6.4 to Figure 6.6) and 2. those bends with steep bed relief (Figure 6.7 to Figure 6.9).

6.3.2.1 Gentle bedform bends

These bends were measured using the OTT C2 current meter, with attached ribbon and therefore provided only two-dimensional flow data (the vertical component is not measured).

Table 6.2 Shear stress values: total and grain values calculated for hydraulic geometry (HG) stations nearest the studied bends (from Chapter 4) and those calculated using the Law of the Wall for single data-points in each bend. Units in N/m^2. Maximum and range values provided by the τ_{LP} technique are provided for comparisons between the techniques.

Bend #	Values for nearby HG stations		Law of the Wall derived shear stress	
	τ_{TOTAL}	τ_{GRAIN}	$\tau_{LP\ -\ MAX}$	τ_{LP}- dominant
Polblue Bend 1	2.1 / 4.0	0.6 / 0.7	1.5	0.1 - 0.5
Polblue Bend 2	4.5	1.1	1.8	0.5 – 1.5
Polblue Bend 3	4.9	1.4	2.4	1.0 – 1.5
Barrington Bend 1	3.8 / 7.3	1.2 / 5.0	11.7	0.5 – 4.0
Barrington Bend 2	7.5	5.6	7.4	1.0 – 2.0
Edwards Bend 1	6.3	2.5	1.0	0.5 – 1.0
Edwards Bend 2	6.3	2.5	3.2	0.1 – 0.5

Polblue Creek Bend 1

Velocity distribution at the entry of this bend was very uniform, both vertically and laterally (Figure 6.5), and there was very little secondary circulation (Figure 6.4a). Bed shear stress at the bend entry, however, was strongly skewed toward the outer bank (Figure 6.6) but became minimal through Sections 4 to 6, where the flow boundary broke away from both the bed *and* the banks and the velocity profiles became more irregular. By Section 5, moderate secondary circulation was developed, with outward flow near the surface and some weak inward flow over the low, sandy point-bar (Figure 6.4a). Return flow up this bar was strengthened in Section 6, before the channel contracted in Section 7

and secondary flow almost entirely ceased. The dominant MVF moved from near the surface of the water column at bend entry (Sections 3 and 4), toward the middle region mid-way through the bend (Section 6) and towards the bed at the exit (Section 8). The maximum bed shear stress declined was located near the outside bank in the entrance of the bend then declined rapidly through the middle of the bend. However, it rose slightly in intensity and followed a central path through much of the remainder of the bend, probably as a result of the outer bank flow separation zone forcing it away from the bank, but did not regain its initial strength until the bend exit (Section 8).

Polblue Creek Bend 2

At the bend entry, the MVF and maximum shear stress were positioned towards the outside bank but in Section 2 both became centred and more evenly distributed, where the region of maximum shear stress in the bend was located. The vertical velocity profiles illustrate two, vertically-stacked MVF's through the centre of the channel in Section 2 (Figure 6.5), however the scale of the isovels in Figure 6.4b do not illustrate these features. Skew-induced secondary currents developed at Section 3 and flow was weakly directly toward the outer bank. The velocity profiles became more complex through Sections 4 to 6 as full helical flow progressively strengthened and flow interacted with a low sandy point-bar. A small region of separated flow developed at the bed in Section 4 and persisted through Section 5. Bed shear stresses were minimal through these sections, as the dominant MVF was located near the surface (Figure 6.5). A region of separated, upstream-directed flow also developed at the outer bank in Section 4 and persisted through Section 5 before dissipating. A new region of separated flow directed upstream developed at the inner bank of Section 6 and became attached to the bank at Section 7. Vertically stacked MVF's developed again through Sections 6 - 8 (Figure 6.5). Bed shear stress increased again from Section 6 and secondary currents were directed weakly inward, then weakly outward through Sections 7 and 8, respectively. A region of maximum shear stress developed in Sections 6 to 8 near the concave bank where the

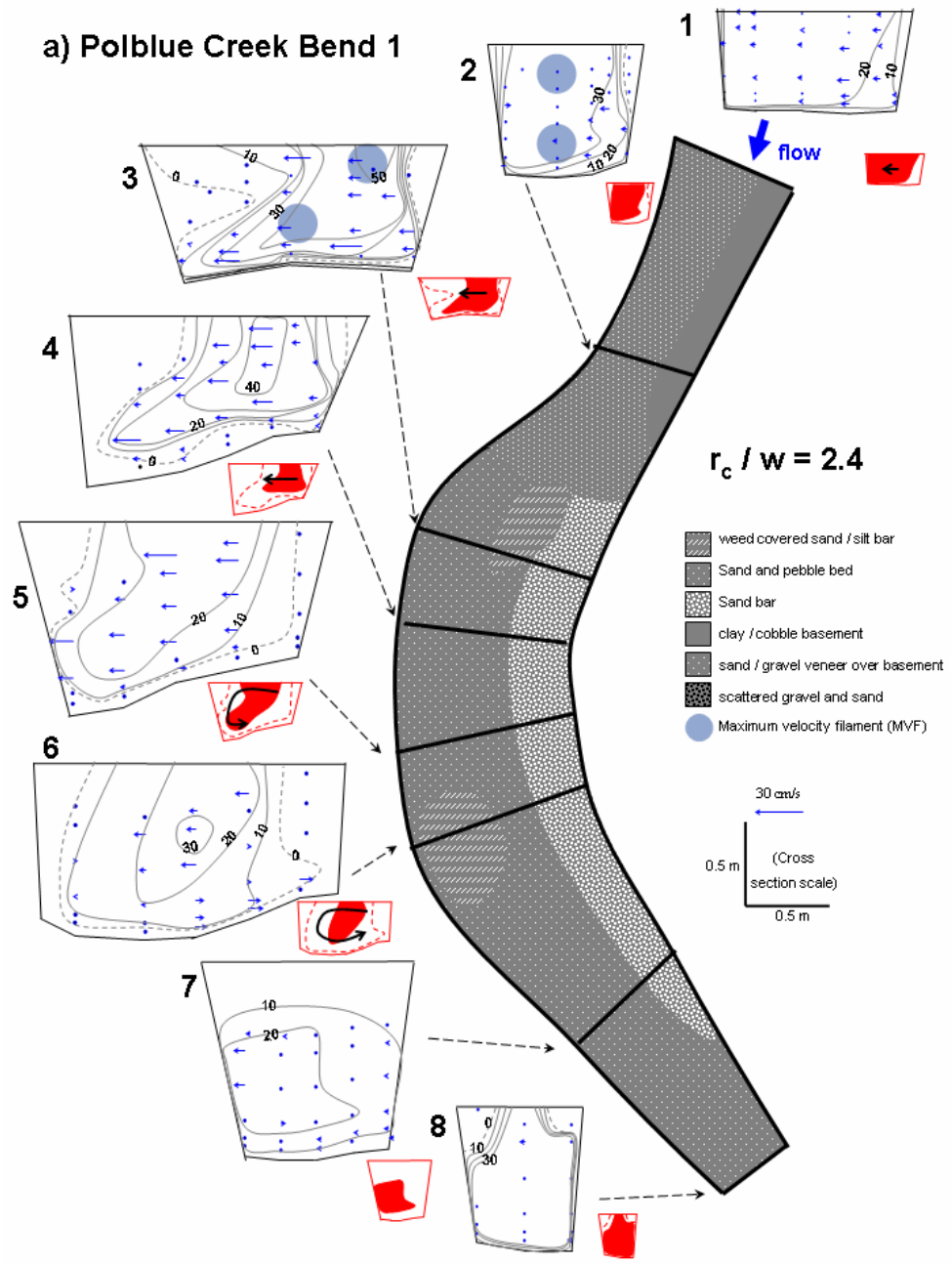

Figure 6.4 Polblue Creek primary and secondary flow and MVF patterns, a. Bend 1 (this page) b. Bend 2 and c. Bend 3. Primary currents are indicated by the isovels (contours) and secondary currents are indicated by vectors (arrows). Flow separation is indicated by grey shaded regions where flow was clearly directed upstream, or by dashed grey lines where flow was essentially stationary within the zone. Diagrammatic illustrations show the MVF in red and separated regions of the flow are indicated by dashed red lines or red and white striping. Black arrows on these diagrams indicate generalised patterns of secondary currents. Isovel intervals are 10cm/s. Paired MVF's are indicated by shaded blue-grey circles.

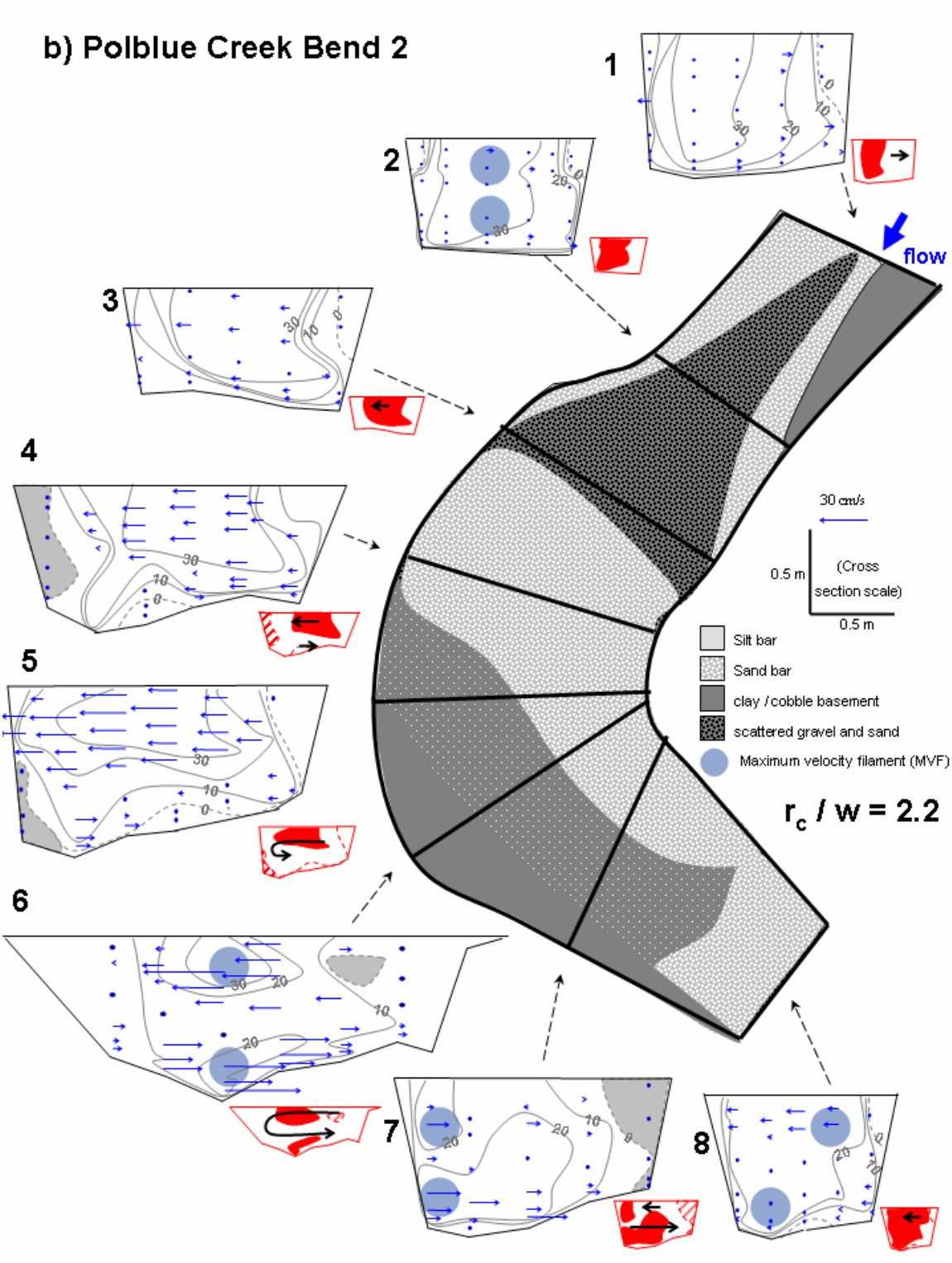

Figure 6.4 (continued)

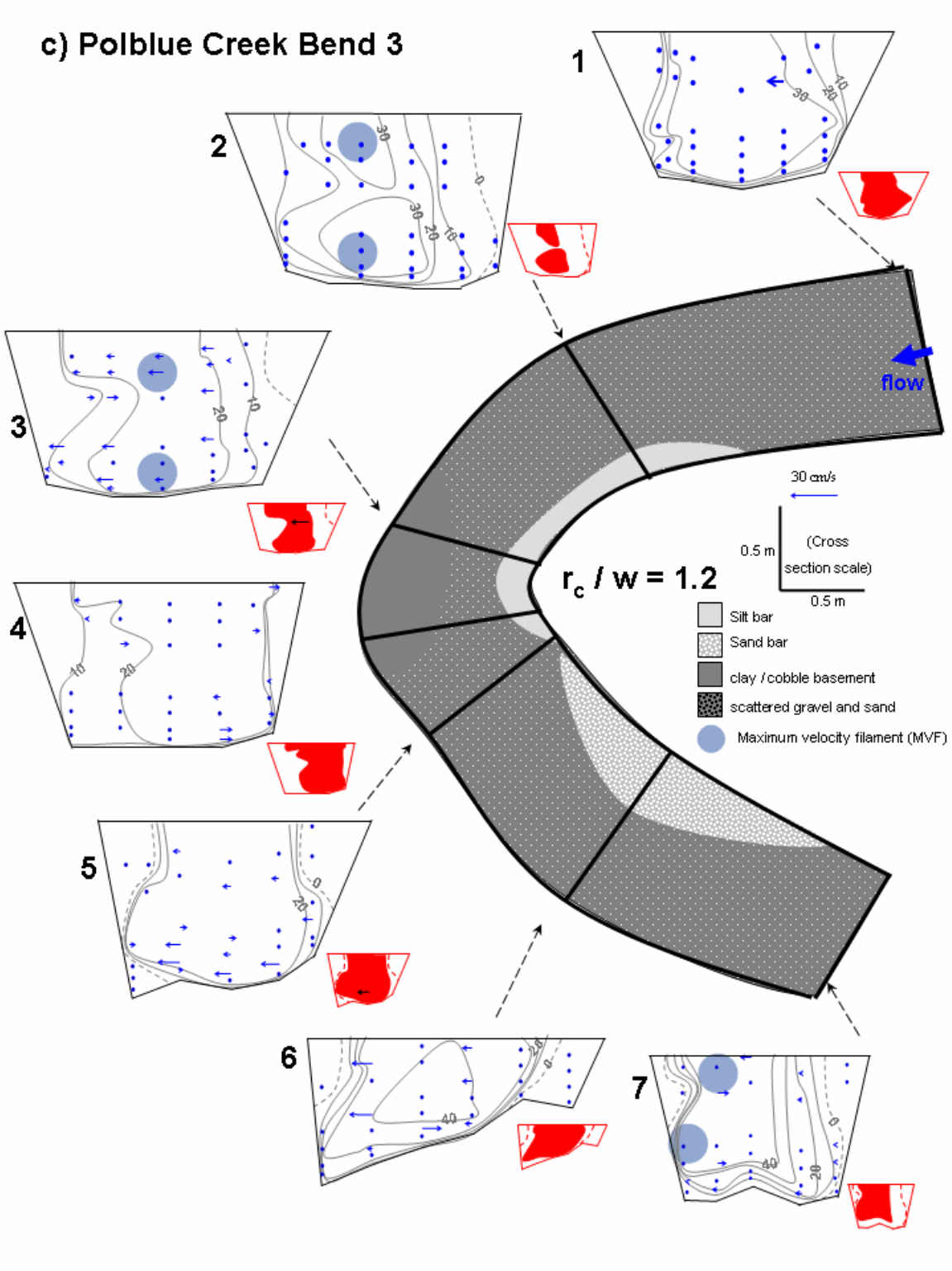

Figure 6.4 (continued)

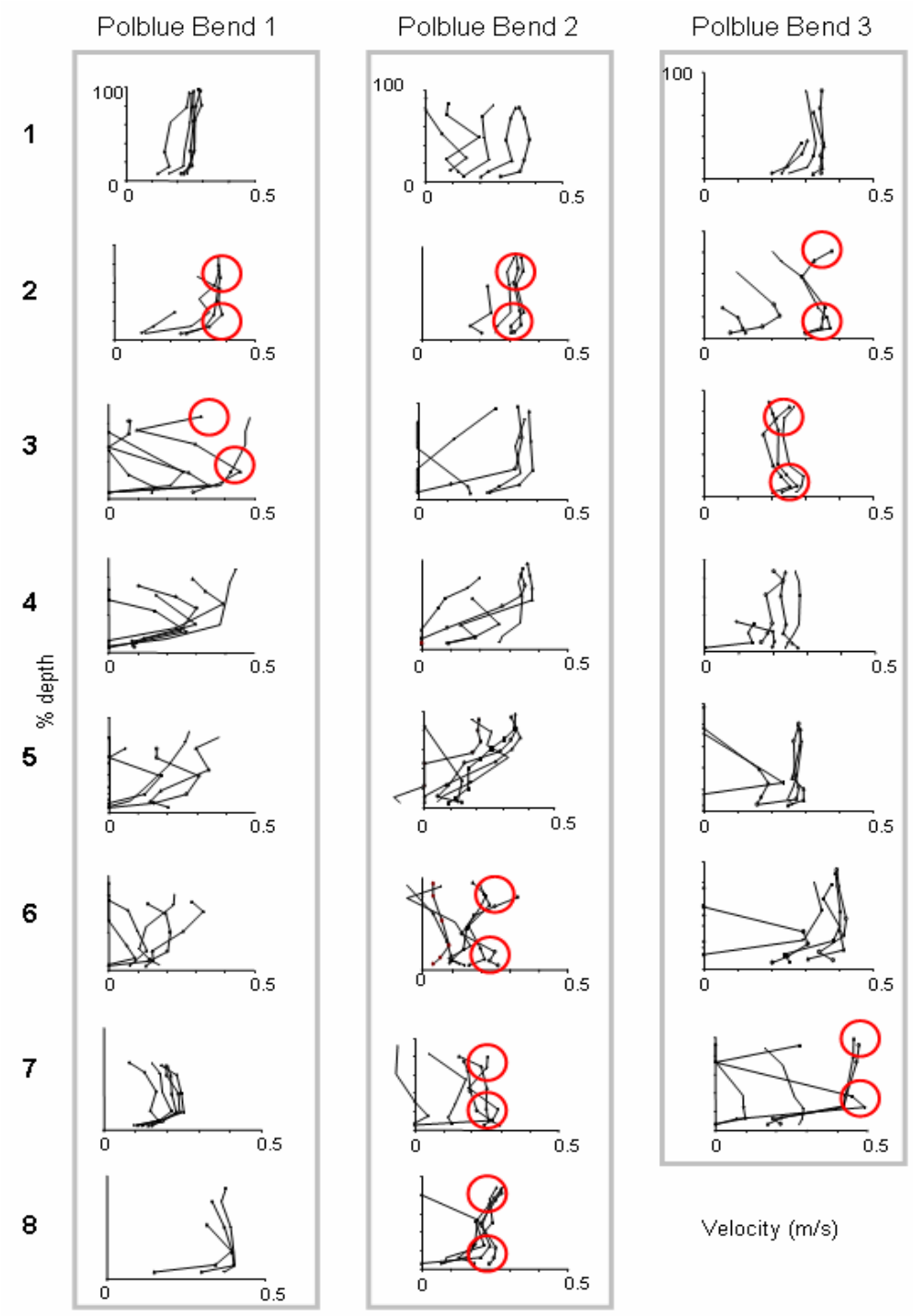

Figure 6.5 Velocity profiles for all Polblue bend flow measurements. Profiles are ordered from Section 1 through each bend down the page. Stacked MVF's are indicated by red circles and sections numbers are indicated at the left of the figure.

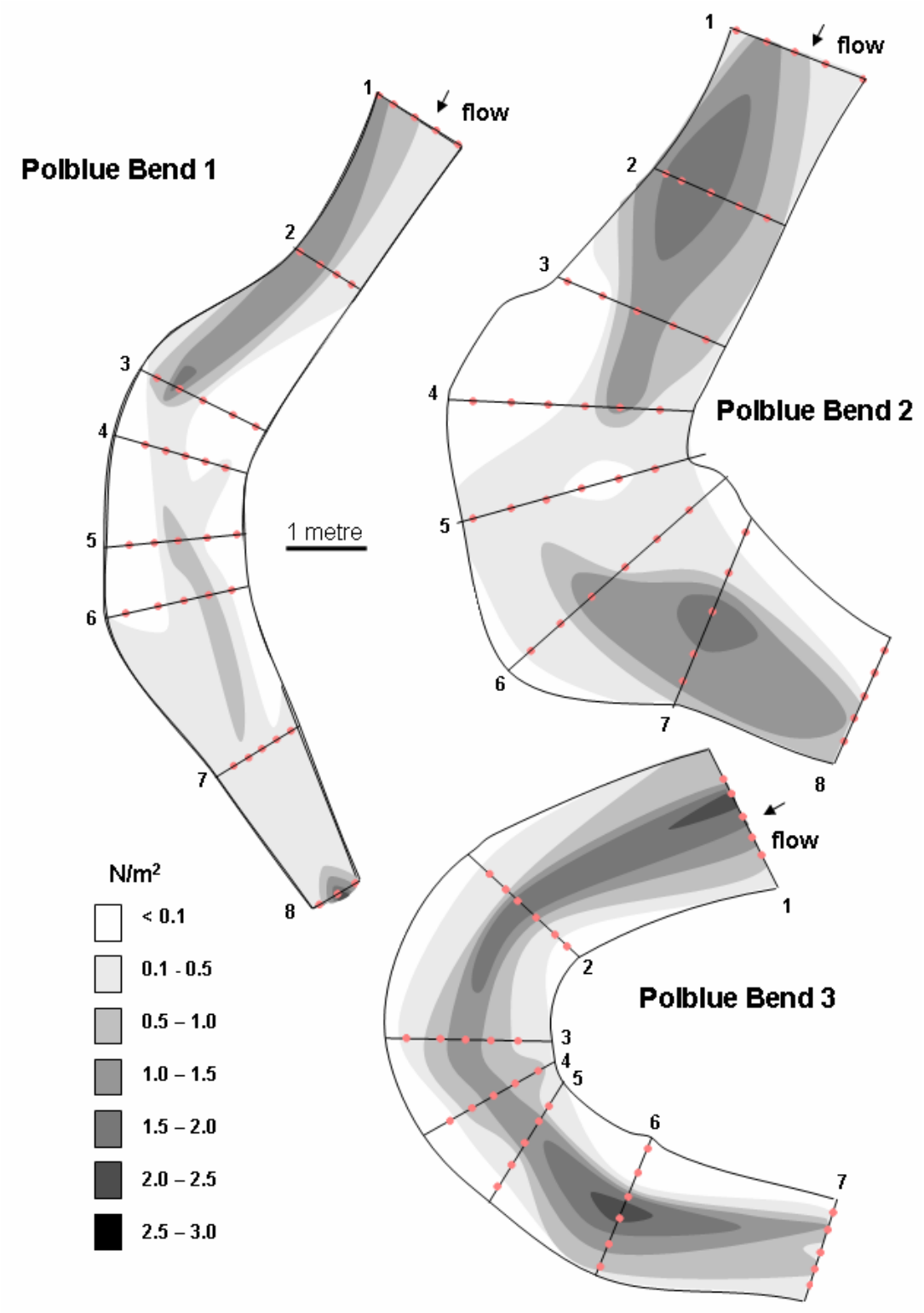

Figure 6.6 Shear stress in the three Polblue bends, calculated using the Law of the Wall (τ_{LP}).

region of concave bank flow separation (formed in the preceding cross-sections) reattached to the channel bank.

Polblue Creek Bend 3

Flow in Section 1 of this bend was very evenly distributed, in terms of both velocity and downstream components (Figure 6.4c). Maximum shear stresses were also centrally located here, with the MVF's splitting into two vertically stacked units in Sections 2 and 3 (Figure 6.5). In the latter, flow was directed weakly outwards away from a very low silty sand-bar. Immediately past the apex of the bend (at Section 4, Figure 6.4c) almost no secondary currents were evident and flow velocities were evenly distributed vertically and laterally. Significant secondary currents failed to develop through the remainder of the bend, however, slight outward flow over a sandy point bar occurred at Section 6. Vertically stacked MVF 's redeveloped at Section 5 (Figure 6.5), then returned to a more evenly distributed region of velocity through Section 7. A sandy point bar downstream of the bend apex directed flow weakly outwards through Section 6 and a small separation zone developed above this feature. The path of the maximum shear stress followed the centreline of the channel through this bend (Figure 6.6). It was not until Section 6 that slightly higher shear stresses extended to the outer bank before becoming confined to the channel centreline again in Section 7.

Summary of results for bends with gentle bedforms

Several characteristics of these three bends are worthy of reiteration:

- They have each developed point bars, limited in both lateral and vertical extent.
- At bend entry, secondary circulation was not strong and by the bend exit the influence of bend geometry on secondary currents had waned. In other words, flow entered and exited these bends with minimal secondary motion. In addition, velocity profiles at the entry and exit of each bend are remarkably uniform, vertically and laterally.
- As flow moved into each bend, secondary currents became directed toward the concave bank. In Bends 1 and 2, this effect increased through the bends, with helical flow

developing over the point bar. In contrast, secondary circulation in the tightest bend (Bend 3) did not develop, with flow aligning approximately with the channel margins.

- In Bends 2 and 3, the vertical velocity profiles (Figure 6.5) indicated the existence of two, vertically stacked MVF's at the entry and exit cross-sections with velocity higher in the one nearer the bed in each case.

- In Bends 1 and 2, large separation zones developed at both the bed and the banks, significantly reducing the cross-sectional area of downstream flow.

- The MVF and regions of maximum shear stress passed centrally through all three bends, until past the bend apices where they tended to move to the outside bank. In Bends 1 and 2, separated flow at both the bed and outer bank forced the MVF to a central position well above the bed in the second half of the bend and bed shear stresses were significantly reduced in this region.

6.3.2.2 Steep bedform bends

These bends were measured using the ADV's to provide information on three-dimensional flow patterns. These bends have larger bedforms (*duffles*) and flow is therefore more responsive in the vertical dimension. Therefore, the flow is more appropriately measured using devices capable of measuring more complex currents.

Barrington River Bend 1

Flow entering Bend 1 was comprised of two adjacent MVF's, with secondary currents rotating such that flow converged at the bed and diverged near the surface. Adjacent MVF's were maintained through Section 3 (Figure 6.8). At this section, flow passed over the crest of a *duffle* and bed shear stress was maximised beneath the adjacent MVF's. Flow also developed a helical motion at this section and, owing to the development of complicated secondary circulation, the velocity profiles became increasingly complex from here through the remainder of the bend.

Flow plunged into a large pool at Section 4, with secondary currents strongly directed toward the bed, generating high shear stresses (Figure 6.9). An upstream directed, counter-

rotating zone of separated flow with a velocity in excess of -0.1m/s formed at the outer bank at this cross-section and persisted through Section 5. The separated region of flow ensured that the MVF and maximum shear stress were centrally positioned and that the primary flow cell maintained a low width-depth ratio, thus reducing the boundary for active flow in the channel by over 30%. Between Sections 5 and 6, a wavering surface line of eddies, here termed an *eddy line*, was observed. Downstream of the eddy-line at Section 6 the pattern of secondary circulation of the flow was mostly reversed compared to that at Section 5, such that surface flow was directed toward the inner bank. A separation zone with flow in an upstream direction formed adjacent to the inner bank. Near the outer bank, a much smaller helical-flow cell persisted with the same rotation as that upstream in Section 5. Inward flow dominated nearly all of Section 7, but with weak outward flow immediately above a pronounced point bar. For the first time in the bend, the MVF and maximum bed shear were located near the outer bank and asymmetric velocity and shear stress distributions persisted through the exit of the bend (Section 8) where flow returned to two, albeit weak, MVF's of reverse rotation that converged at the bed and diverged at the surface, similar to that in Section 1 at the entry of the bend.

Barrington River Bend 2

The velocity of flow entering Bend 2 was evenly distributed, with uniform velocity profiles and weakly rotating surface flow toward the inner bank. The MVF was also depressed below the surface and the region of maximum shear stress was closer to the inner bank. At Section 2 secondary circulation was weak and somewhat confused, and it was not until Section 3 that a clear pattern of outward flow through the entire water column became evident. Until the bend exit, however, vertical velocity profiles remained remarkably uniform.

The regions of maximum velocity and maximum shear stress remained close to the inner bank from the bend entrance to the bend apex where secondary currents became directed outward towards the concave bank. Some return flow across the upward inclined bed was evident near the thalweg, immediately downstream of the sand riffle where a small region of separated flow developed (Section 5). At Section 5 the MVF became a more diffuse region but shifted across the channel to approach the outer bank, but by Section 6 it had

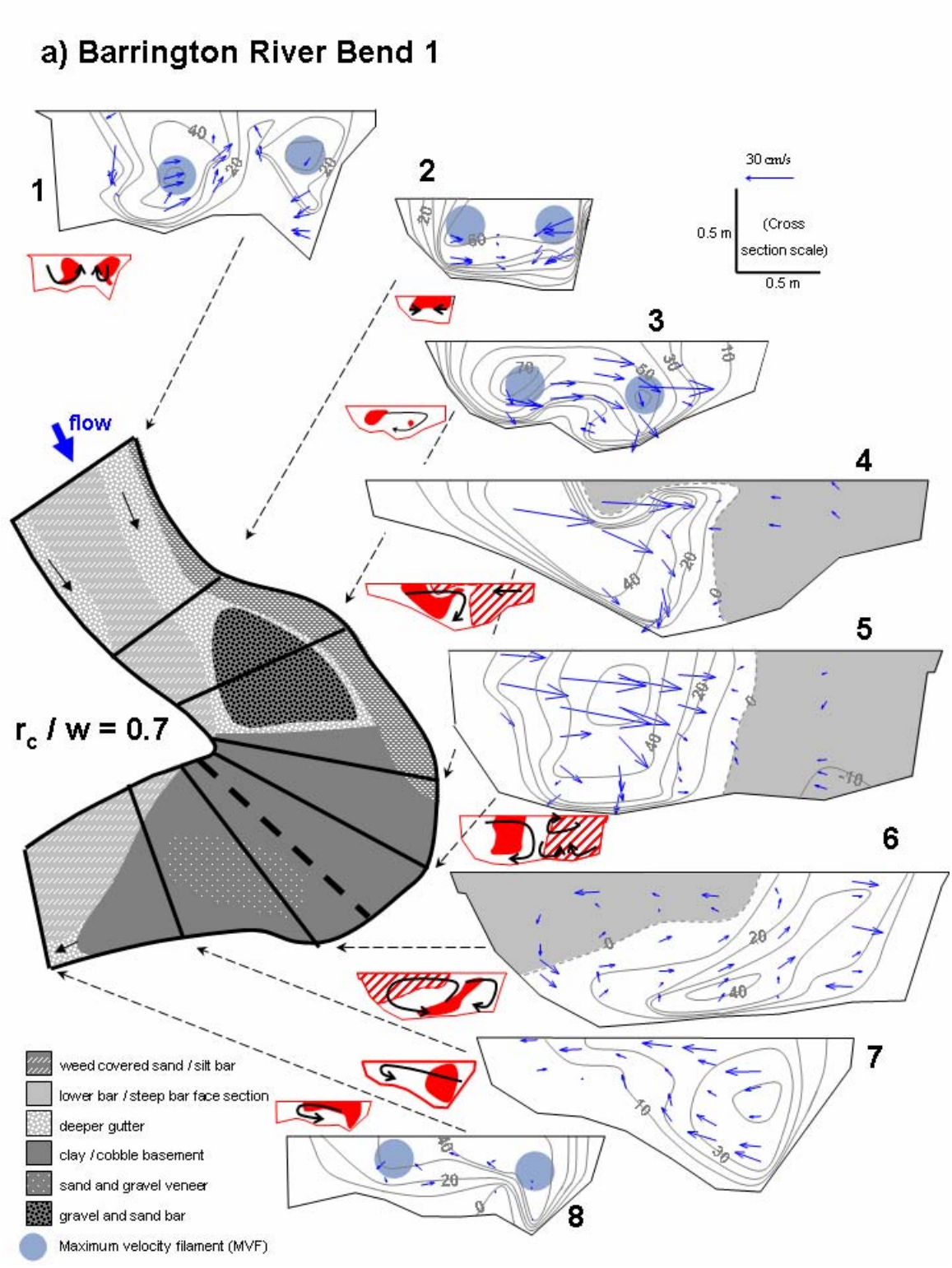

Figure 6.7 (caption on following page)

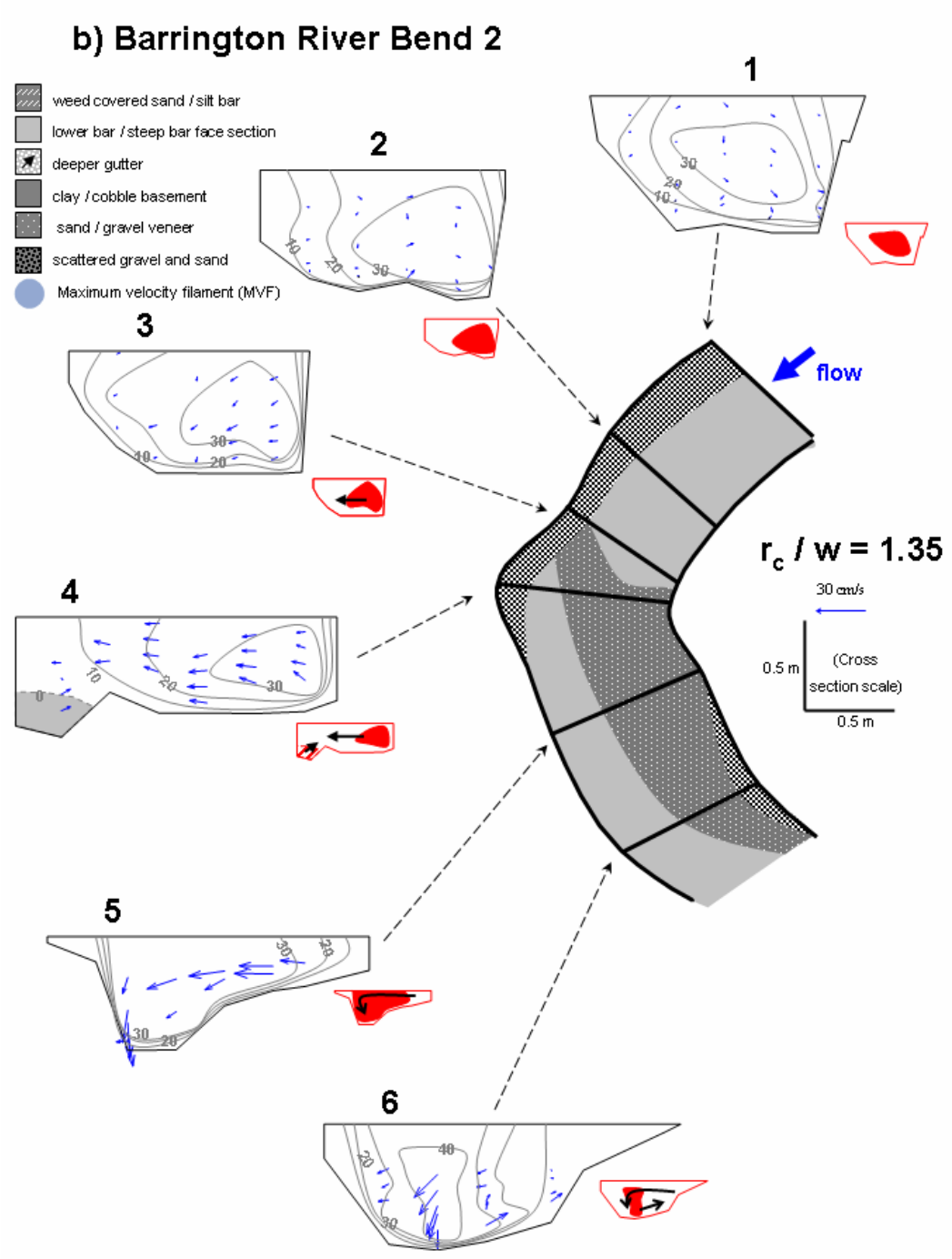

Figure 6.7 Barrington River primary and secondary flow and MVF patterns, a. Bend 1 b. Bend 2 (this page) and Edwards Creek c. Bend 1 and d. Bend 2. Diagrammatic illustrations show the MVF in red and separated regions of the flow are indicated by dashed red lines or red and white striping. Black arrows on these diagrams indicate generalised patterns of secondary currents. Contour intervals are 10cm/s. Paired MVF's are indicated by shaded blue-grey circles.

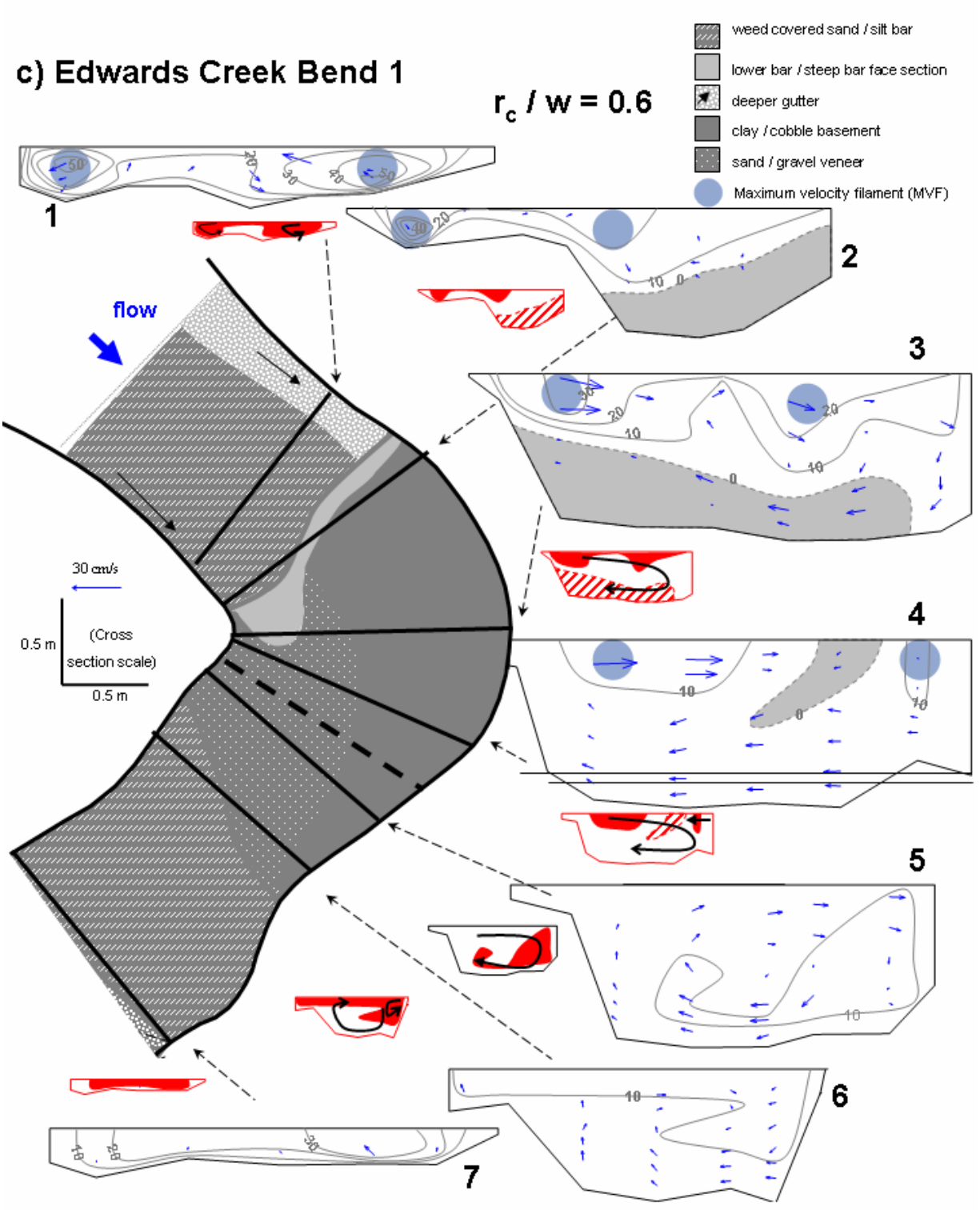

Figure 6.7 (continued)

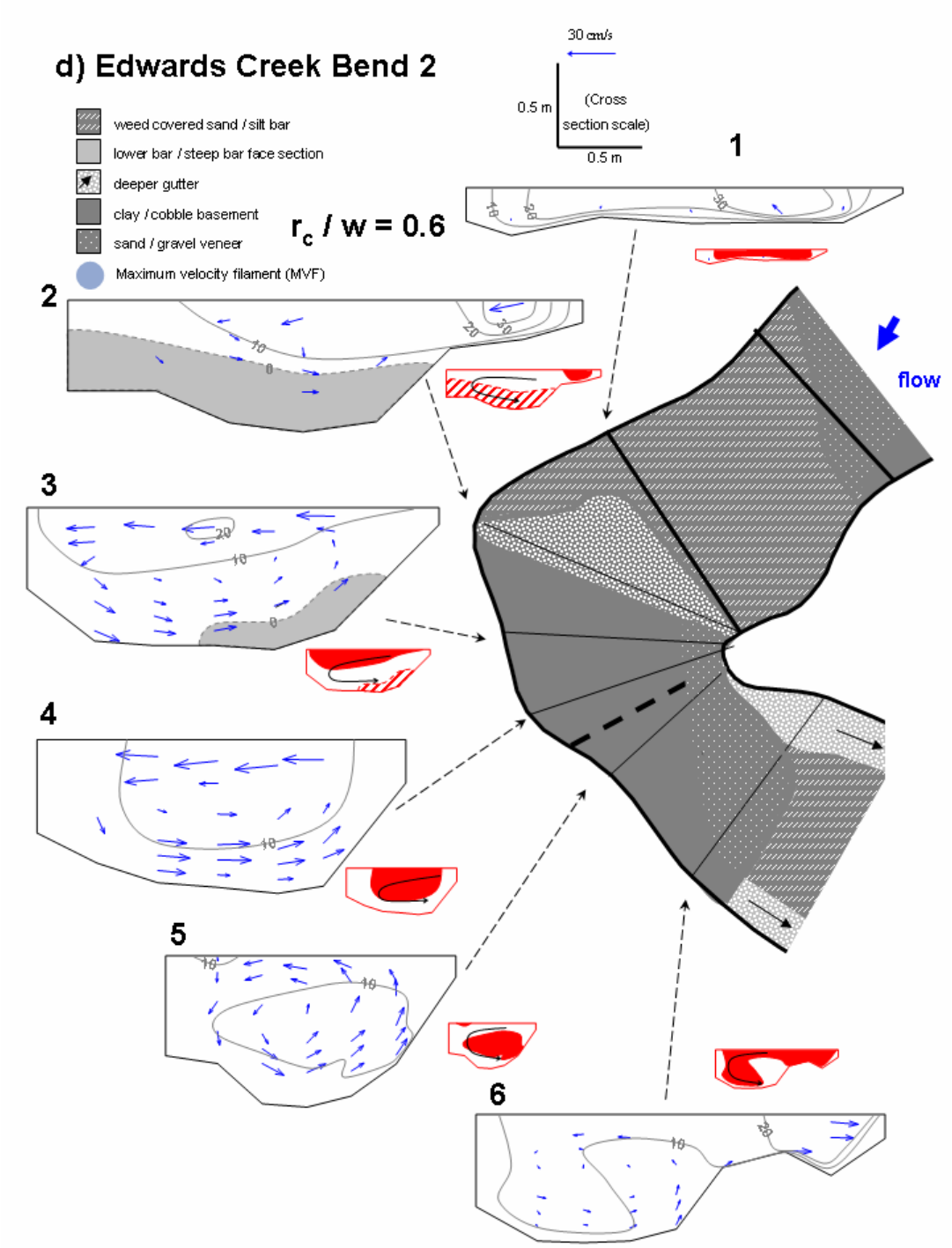

Figure 6.7 (continued)

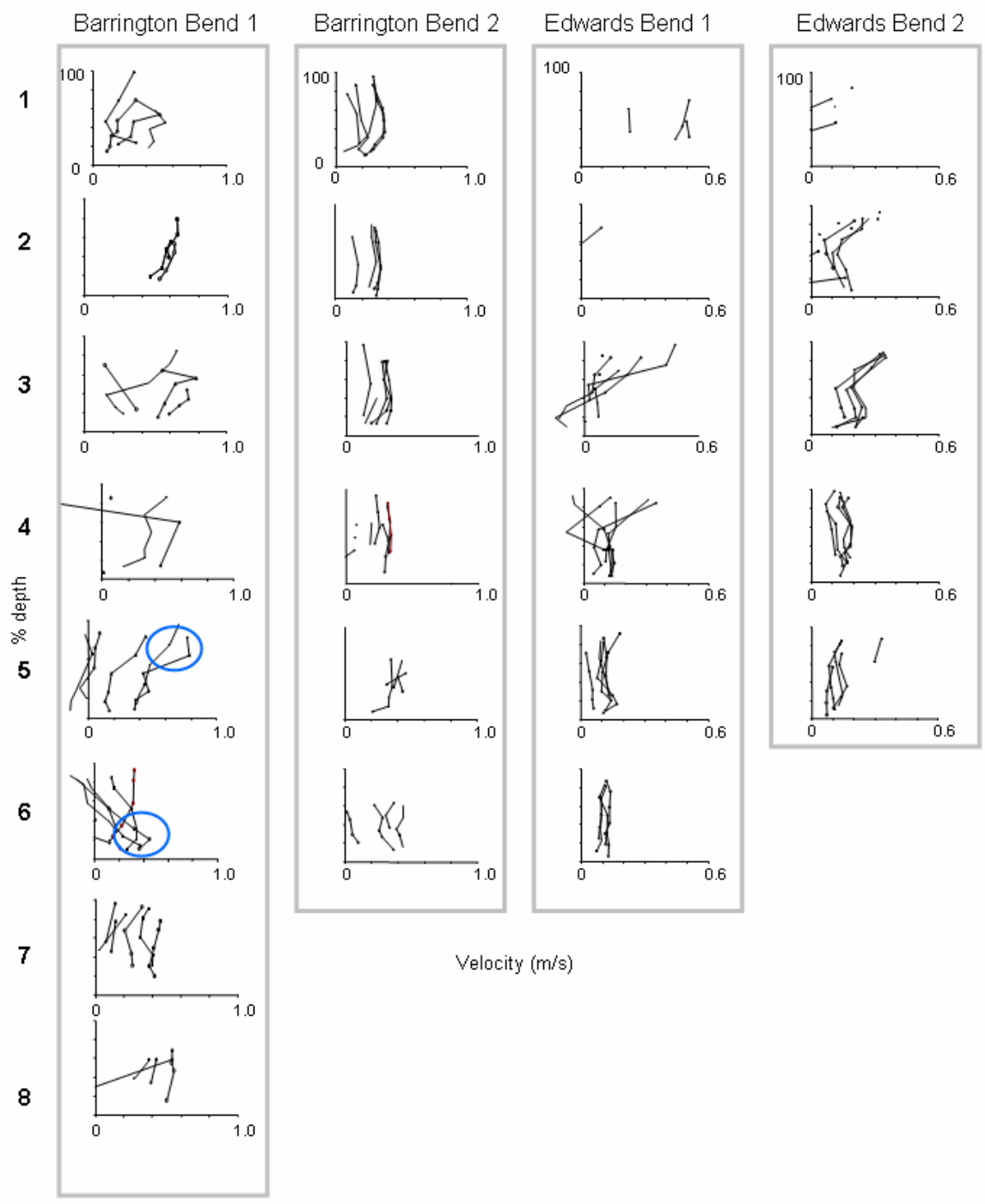

Figure 6.8 Velocity profiles for all Barrington River and Edwards Creek bend flow measurements. Profiles are ordered from Section 1 through each bend down the page, as indicated at the left of the figure. Note the change in the vertical position of the MVF from Sections 5 to 6 in Barrington Bend 1 (circled in blue).

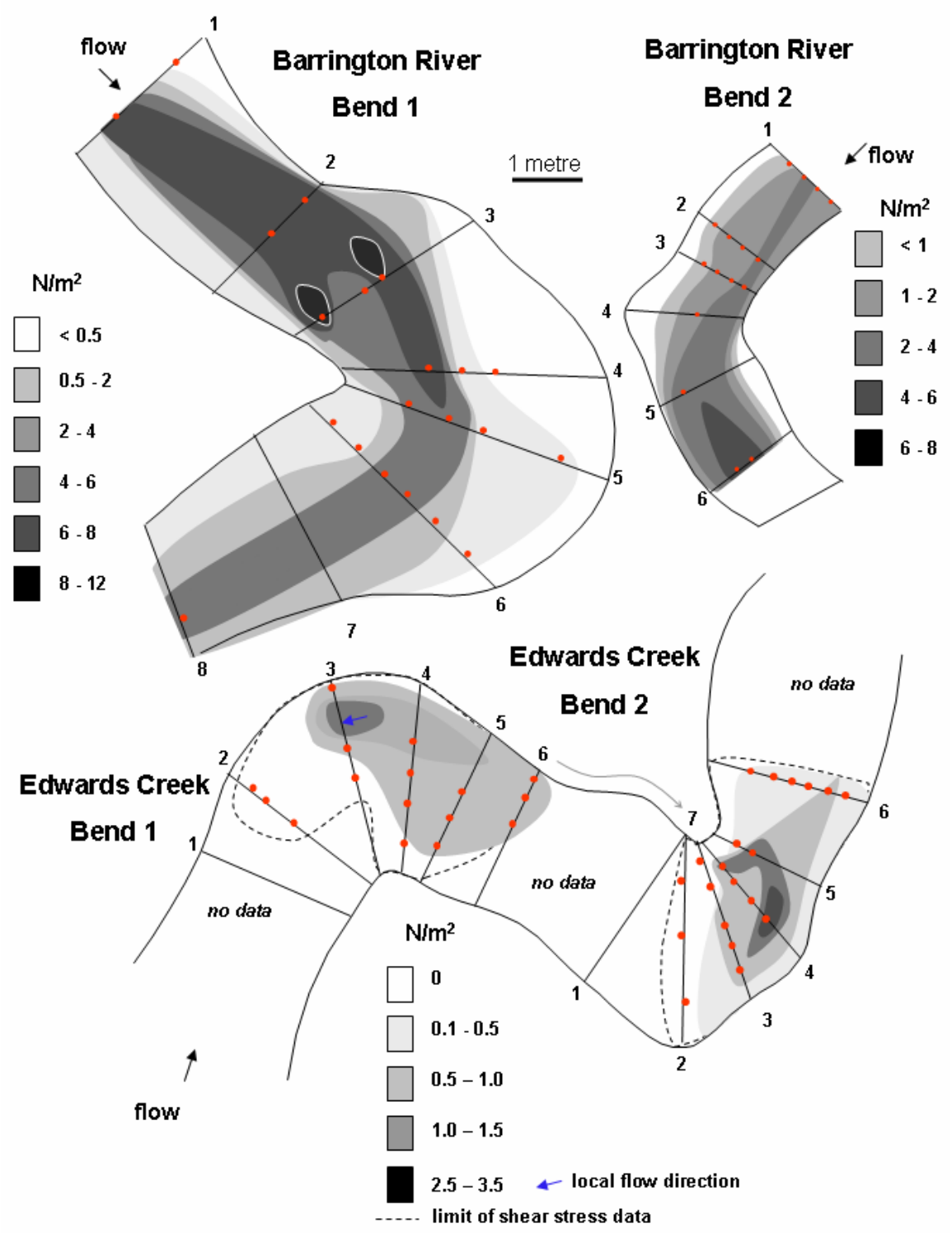

Figure 6.9 Shear stress in the four Edwards Swamp bends, calculated using the Law of the Wall.

returned to a more central position. It was not until this cross-section that inward flow over the point bar was well developed, but this may be more apparent than real due to a lack of near-bed velocity data obtainable using the large ADV instruments.

Edwards Creek Bend 1

Entry flow to Bend 1 was very shallow as it flowed over a *duffle* crest and secondary circulation was weak. Shear stress was conceivably high, but a lack of near bed velocity data prohibited its estimation. The velocity data, however, indicates that the maximum shear stress would likely be associated with the two MVF cells, one located near each bank (Figure 6.7c). Immediately downstream, at Section 2, flow plunged into a large pool and the outer filament of maximum velocity expanded to fill much of the cross-section. A large separation zone in the lee of the *duffle* extended across the bed of the pool up to half of the flow depth and towards the outer bank. It was not until Section 3 that significant helical flow developed, with outward flow near the surface and inward and upstream (separated flow) flow near the bed. Somewhat surprisingly shear stress values for the pool reached maximum values at this cross-section, however they were directed upstream within a large, bed-attached separation zone (Figure 6.9). Helical flow strengthened in Section 4, where a small region of reversed flow was also present near the surface on the outer side of the channel centreline, with the helical flow continuing into Sections 5 and 6. An armoured sand-gravel point bar was evident in Section 6, and weakened secondary currents persisting over the bar. There was also a small region of flow away from the outer bank near the surface of the concave bank, possibly indicative of a small reverse cell. The region of maximum shear stress followed the outer bank through the pool (Figure 6.9), but was unable to be estimated over the *duffle* crests because of the shallow flow and the size of the ADVs. Higher velocities near the *duffle* surface at the outer bank (Figure 6.7c) indicate that the maximum shear stress was likely to follow the same path.

Edwards Creek Bend 2

Bend 2 lies immediately downstream of Bend 1 and shares Section 7 (Figure 6.7d) (Section 1 for this bend). Flow through Section1 was shallow, with little secondary motion and only one region of maximum velocity near the inner bank where shear stress was presumably at a maximum. Flow plunged into a large pool and Sections 2 and 3 illustrate pronounced

helical motion and a substantial separation zone at the bottom of the pool (Figure 6.7d). Helical flow strength increased markedly at Section 4, as did bed shear stress (Figure 6.9), and between Sections 4 and 5 an eddy-line was observed. Secondary currents weakened in Section 5 as flow moved through this part of the bend. In addition, the MVF redeveloped near the inner bank of this bend, in contrast to the pattern through Edwards Bend 1, immediately upstream, and in contrast to Barrington River Bend 1.

Summary of results for bends with steep bedforms

There are several important aspects of flow through these sharp bends with steep bed topography:

- With the exception of those at, or immediately downstream of, bend apices, vertical velocity profiles were remarkably uniform.

- Where the entry conditions are shallow they tend to consist of flow with a MVF on each side of the channel which can be associated with a weak secondary circulation helix. Where the entry conditions are deeper, paired helices may occur or alternatively flow can consist of very little secondary circulation and a single MVF.

- All four bends developed strong helical motion with their circulation strength roughly proportionate to the steepness of the bed topography. Bends with *duffles* followed by a deep pool produced more pronounced helicity compared to more consistently deep bends (Barrington River Bend 2). The "point-bars" in these bends had inward flow over their stoss faces.

- Pronounced eddy-lines were observed in those bends with *duffle* bedforms; in one of these (Barrington Bend 1), the helical motion in the flow reversed direction immediately downstream of this line.

- Separation zones formed in all bends and were most extensive in those with *duffle* bedforms. These separation zones could form near the bed (all bends), near the surface (Barrington Bend 1 and Edwards Bend 1) or near either the inside and outside bank (Barrington Bend 1).

- Separation zones obstruct up to half the cross-sectional area, greatly confining the zone of active flow. They alter the passage of the MVF and hence bed shear stress in each bend. Just where they form is a complex issue but appears to be the product of the bend shape and the magnitude and shape of the bedforms.

- While obtaining flow data near the boundary proved difficult due to the size of the ADV's, limited data points indicated the possible existence of a small outer-bank cell of reverse rotation in Edwards Bends 1. In Barrington Bend 1, the large region of flow separation at the outer bank may be an enlargement of smaller such features elsewhere. The outer bank cell rotated in a reversed direction to the helix in the main flow.

6.4 Discussion

Owing to the variations and complexity of flow behaviour in each of the seven bends examined, the following discussion focuses on discrete regions and features of the resultant bend flow patterns.

6.4.1 Bend entry flow patterns

As raised in the introductory section of this chapter, bend flow patterns are very sensitive to bend-entry flow patterns and the result is an almost infinite combination of resultant flow patterns (Prus-Chacinski, 1956). Bend flow entry conditions in the Barrington swamp channels vary between narrow and deep and wide and shallow; the former have remarkably even distributions of flow velocity and the latter are more skewed.

The traditional riffle-flow model proposed by Hey and Thorne (1975) advocates converging flow cells at the bed over riffles, and a reversal of this motion at bend apices. However, Tooth and McCarthy (2004) found that the low width/depth ratios and rough channel margins characteristic of some swamp channels can suppress secondary currents and thus may encourage more even distributions of velocity and shear stress. Entry cross-sections at all Polblue Creek bends and Barrington River Bend 2 are narrow and deep and have very uniform vertical velocity profiles, a fairly even distribution of the velocity laterally and almost no secondary currents. However, vertically stacked MVF's were either present at the bend entry or formed through these bends, but were not observed to rotate

independently in the manner described by Hey and Thorne (1975) for lateral cells over riffles. Furthermore, unlike the findings here, their model did not describe separate MVF's associated with each cell of opposing secondary motion. Low width/depth ratio channels, such as Polblue Creek, with overhanging, trailing grasses, produce pipe-like cross-sections. Stacked MVF's most likely result from a zone of maximum velocity developing within the lower "pipe-flow" region with another forming near the free surface where flow resistance is minimised.

In contrast, wider and shallower examples of bend entry cross-sections where flow passes over *duffle* crests had laterally unevenly-distributed flow velocities and variable patterns of secondary currents. In Barrington Bend 1, two adjacent MVF's counter-rotated, consistent with Hey and Thorne's (1975) divergent riffle-bed flow observations. Edwards Bend 1 also had two adjacent MVFs at the bend entry but both flowed weakly towards the inner bank at the surface and toward the outer bank at the bed. In Edwards Bend 2 the flow was skewed toward a single MVF at the inner bank, consistent with the observations of Whiting and Dietrich (1993) for large amplitude meanders, but the flow had little secondary motion. Counter-rotating cells have been supposed to completely dissipate between successive bends of reversed orientation (Hey and Thorne, 1975; Markham and Thorne, 1992), however, the model does not advocate paired MVF's associated with these counter-rotating cells. With the exception of Barrington Bend 1, the observed patterns here of secondary flow motion through the relatively wide, shallow bend entry cross-sections are not consistent with the riffle flow models developed elsewhere.

Thorne and Hey (1982) described the development of vertically stacked counter-rotating cells of flow over riffles in wide channels at low flows. The upper cell persisted as a remnant of the skew induced secondary currents in the upstream bend and the basal cell was purported to develop in response to *macro-bar* forms and expanded to dominate the flow by the time it entered the next bend. In earlier work, Chacinski and Francis (1952) and Toebes and Sooky (1967) both found that in narrow and deep flume-channels, similar cells can be laterally adjacent. However, none of these models of paired cells can explain the MVF's described in the Barrington bends, as the MVF's did not independently rotate in the

manner these models describe. Thorne and Hey (1982) documented fundamental changes in secondary flow patterns over riffles with increased discharge, and Parsons (2002) measured laterally adjacent MVF's flowing over a riffle in a bend entry cross-section which had a very similar planform geometry to Barrington Bend 1, but which he attributed to local channel anomalies.

The paired MVF's over the Barrington swamp channel bend riffles and *duffles* may be the result of local bend geometry anomalies, consistent with Parson's suggestion (2002), or the result of variations in secondary flow patterns with changing flow stage. However, the similarity between flow patterns in Parson's bend flow study and those in the Barrington channels suggest that something more systematic may be involved.

6.4.2 Helical flow and patterns of shear stress distribution

Full helical flow is usually limited to the channel thalweg (Hickin, 1978; Dietrich and Smith, 1983; Markham and Thorne, 1992), as point bars cause shoaling over their surfaces and force the flow outwards, over and away from the bar toward the concave bank. However, similar to the *sinuous canaliforms* described by Brice (1984), very few of the bends examined in the Barrington swamp channels had significant point bars, and therefore flow was forced toward the outer bank by tangential (centrifugal) forces rather than shoaling. As a consequence, very strong helicity developed across the entire width of the channel. These results were consistent with the work of Thorne et al. (1985), in which they observed helical flow motion across much of the channel width, including return flow near the bed over the point bar.

Rather than the lateral confinement of helical flow to near the thalweg, helical flow was sometimes *longitudinally* confined. In the two Polblue bends in which helical flow developed, the flow maintained little secondary motion and became two-dimensional by the bend exit, consistent with the rapid dissipation of helical motion observed by Choudhary and Narasimhan (1977) in their flume study of narrow, deep channels. In contrast, in Edwards Bends 1 and 2 and Barrington Bend 2, helical motion was maintained well past the bend exit and over the following *duffle* crest. In stark contrast to all other bends studied, in Barrington Bend 1 helicity *spontaneously* reversed its motion across a very short reach of

channel. While the physical processes to cause such a reversal are not fully understood (see section 6.4.6), the effect must be a remarkable degree of internal shear in such a bend.

Patterns of bed shear stress through these study bends show a marked response to bend shape. Bed shear stress rapidly reduced though bend apices, coincident with the development of maximum flow helicity, and then increased further downstream as flow returned to predominantly two-dimensional patterns (Figure 6.6 and Figure 6.9). In these regions of narrow, deep bend pools, significant energy losses were presumably occurring via turbulent shearing through the water column, rather than as a result of frictional losses at the bed. However, the association between very tight bends and the occurrence of *duffle* bedforms indicates co-dependence. It may be the large turbulent flow structures that result from very tight bends either scour the bed at the pool apex and deposit this material almost immediately downstream, forming *duffles,* or the energy consumed in tight bends reduces the sediment transporting capacity of the flow and results in the immediate deposition of sediment from the water column on the bed and thereby forming a *duffle*. Either way, it is clear from Figure 6.2 that only the very tightest bends have *duffle* bedforms. Despite an extensive investigation of bends in the study area, no examples of open bends with large bedforms were found.

6.4.3 Interactions between MVF's, flow separation and outer bank cells

Until the bend exits, MVF's maintained central paths through all of the studied Barrington swamp channel bends. In accordance with Markham and Thorne's (1992) model, the outer filament of laterally paired MVF's always dissipated. Consistent with Dietrich et al. (1979) bend shear distribution model, in all cases, it was not until flow was past the bend apex that the MVF approached the outer bank, and in Edwards Creek Bends 1 and 2 the MVF's dissipated before approaching any bank, reforming at the exit of each bend.

The paths of the MVFs were clearly controlled by large envelopes of separated flow. In the lee of *duffles*, separated flow formed close to the bed, similar to separation zones in the lee of dunes (Yalin, 1992; Kostaschuk and Villard, 1996), preventing shear from acting on the bed in these regions. Separated flow extended to half the flow depth in the lee of these *duffles* and, in Polblue Bends 1 and 2, very thin layers of separated flow developed in the

lee of lower amplitude riffle forms. In just over half of the bends, flow separation developed against the *outer* banks and varied from less than 10% of the channel width, in Polblue Bend 3, up to more than 30% in the case of Barrington Bend 1, somewhat short of the 50% observed by Leeder and Bridges (1975) at the *inner* bank of open bends with uniform width. In Barrington Bend 1, the geometry was such that the channel widened significantly at its apex, a characteristic that has been both observed (Nanson and Page, 1983; Andrle, 1994) and modelled (Hodskinson and Ferguson, 1998) in bends with concave bank flow separation. Furthermore, the removal of the point bar was shown by Hodskinson and Ferguson (1998) to enhance concave-bank flow separation. Consistent with these observations, Barrington Bend 1 has no point bar and a large region of concave bank flow separation.

Secondary flow patterns within regions of separated flow varied between bends. In the lee of the Edwards Creek *duffles*, flow was directed upstream and towards the inner banks (Figure 6.7c and d). In the Polblue Bends, the outer bank regions of flow separation had almost no discernable flow patterns (Figure 6.4). In Barrington Bend 1, the outer bank flow separation was particularly complex. In the upstream region of this zone, rotation of the flow in a reverse manner to the primary flow caused convergent flow at the water surface and divergent flow at the bed, similar to the cells of reversed rotation observed at steep outer banks in numerous other studies (e.g. Hey and Thorne, 1975; Hooke, 1975; Bathurst et al., 1979; Thorne and Rais, 1983; Thorne et al., 1985), except here at a much larger scale (Figure 6.7a). Immediately downstream, the pattern increased in complexity with an inner bank zone of separation developing secondary flow toward the inner bank near the surface and towards the bed at the bank.

Small helices of reversed rotation at the outer banks have been proposed as both important bank stabilisation features, as they divert the MVF and regions of maximum shear stress away from the outer bank (Bathurst et al., 1979), and as destabilising features which enhance outer-bank flow turbulence where the separated flow reattaches to the physical bank (e.g. Leeder and Bridges, 1975; Markham and Thorne, 1992). In Barrington Bend 1, the scale of this cell is such that there can be no doubt of its protection of the outer bank

from scour and redirection of the maximum shear stress and MVF away from the bank within the bend to a point further downstream. The only other observed outer bank helical cell was in Edwards Bend 1, where limited data indicated flow outward, and toward the channel centre-line, from the concave bank near the water surface, and implied the presence of such a cell.

6.4.4 Concave bank embayments

Many of the bends along Polblue Creek, the Barrington River and Edwards Creek have developed pronounced concave bank embayments in which separated regions of flow have formed (Figure 6.4, Figure 6.7 and Figure 6.10). In tight bends in other wetland channels, Jurmu and Andrle (1997) identified similar features, in which lily-pads were growing and fine sediments accumulating. Andrle (1994) measured the flow field through one such bend, at near bankfull flow (Figure 6.11a), and observed consistent patterns of surface flow at various stages from low to bankfull in this and other bends. The pattern he observed closely paralleled that measured in Barrington Bend 1 (Figure 6.11b) and Andrle considered a counter current (separated flow) could both form, and maintain, this region of the channel. In low gradient coastal plain streams across the United States Alford et al. (1982) identified 57 bends with these features. He measured bankfull flows through these bends, found only weak downstream currents, and hence proposed that their development must occur during the fall stage of overbank flood flows, when substantial water gradients, and therefore erosive forces, develop. The following explanation describing the formation of concave bank embayments builds on that proposed by Andrle (1994), with the addition of further factors.

Hickin's (1978) model of bend evolution describes how bends migrate until their radius of curvature to width ratios reduce to approximately 3, when flow becomes increasingly directed toward the concave bank, causing scour and bank erosion. Outer-bank flow separation ensues and causes increased turbulence and more rapid, but localised, retreat of the bank at the point at which the primary flow reattaches to the physical channel boundary (Markham and Thorne, 1992), until a localised embayment forms. More extensive flow separation develops within this zone, against the outside bank. At this stage of bend development, the MVF can move back towards the centreline of the channel. Shear stresses

are then either redirected to a point further downstream on the concave bank, or to the inner bank over the point bar, or both, depending on the specifics of bend geometry (Markham and Thorne, 1992). Whether the embayment aggrades as a concave bench and encourages inward migration of the bend (Nanson and Page, 1983; Parker, 1996) or maintains its depth (Alford et al., 1982; Andrle, 1994), depends on several factors.

Figure 6.10 Barrington Bend 1: an example of a concave bank embayment with flow separation (indicated by dashed white line) and a concave bank bench on its upper limb (bound by solid white line – presently covered by flow). Flow is from top to bottom left.

It is proposed here that the Barrington swamp channel bends with concave bank embayments evolve to very low r_c/w ratios, following Hickin's model, then either remove or fail to form point bars owing to the shifting of the MVF to the inner bank or a lack of sediment with which to do so. They then create increasingly larger embayments as the channel migrates or retreats towards the inside bank, consistent with the observations of Andrle (1994) in similar bends. But the Barrington swamp channel bend embayments have relatively weak shear stresses, more consistent with the observations of Alford et al. (1982) than Andrle (1994), and therefore they should be infilling and developing concave bank benches. However, insufficient sediment supply presumably allows the embayments to maintain their depth and width for a long time.

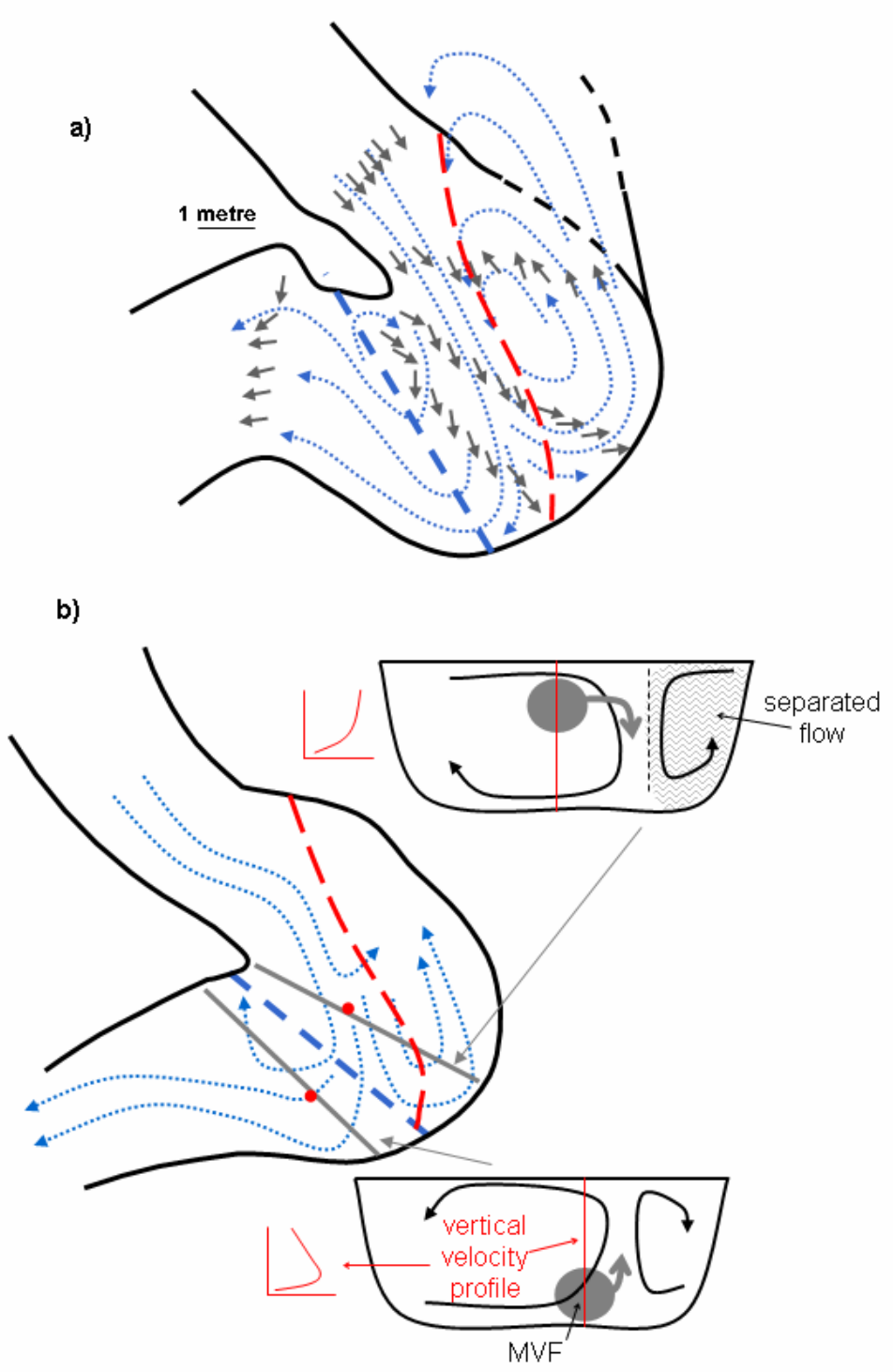

Figure 6.11 Flow through bends with concave bank embayments: a. modified from Andrle (1994; Figure 5). Black arrows represent measured near-surface flow vectors and blue lines are sketches of surface flow patterns; b. Barrington River Bend 1 compiled from data presented in Figure 6.7a. The straight, dashed blue line indicates the expected (a) and observed (b) eddy-lines and the red dashed line indicates the region of flow separation.

The results from Chapter 3 and Chapter 4 showed that these channels lack significant amounts of either suspended or bed load and Andrle (1994) considered a similar explanation for such embayments in Connecticut swamp environments. While fine materials and aquatic plants were observed in most embayments in the Barrington swamp channel bends, the low rate of sediment supply has also ensured that accretion in these regions is a slow process. Indeed, it appears there may even be sufficient flow within some embayments to prevent fine sediment that does move into the region from being deposited, in support of Andrle's theory (1994). Nevertheless, Barrington Auger Transect 5 (illustrated in Figure 2.3) demonstrates concave-bank bench accretionary deposition within much of the outer bank floodplain and thus implies some lateral adjustment of the channel system by inward channel migration. However, most of this material is organic with minor fining upwards sediment composition and it is therefore likely that vegetation growth determines subsequent sedimentation within these regions.

The Barrington swamp channel-bends continue to direct the MVF toward the downstream end of the concave bank embayments. Here the primary flow reattaches to the physical channel bank and turbulence is expected to be maximised, leading to elongated concave bank embayments. Such features were illustrated earlier in Figure 3.3.

6.4.5 Secondary circulation strength

Hickin (1978) showed how secondary circulation strength is inversely related to r_c/w; tighter bends have stronger circulation. Bathurst et al. (1979) found that circulation strength is also a function of the interactions between the flow and the point bar and that it responds to flow stage by first increasing, until mid flow stages, then decreasing toward bankfull as the point bar becomes submerged and the effective radius of curvature to width ratio of the bend increases. Previous work in flumes (Shukry, 1950; Choudhary and Narasimhan, 1977) has also shown that in channels with fixed curvature, secondary circulation can decrease with increased discharge. The Barrington swamp channel bends lack significant point bars and some have fixed curvature through flow-stage variations. It is therefore possible that at more moderate flow stages, these bends may also exhibit stronger secondary circulation than they do at near-bankfull.

Because bend flows were measured at Barrington Tops at a variety of stages (Table 6.1), measures of secondary circulation strength are thus not appropriate to compare with one another *quantitatively*, in the manner applied by Hickin (1978), however a *qualitative* comparison can be made. In the simplest bends that exhibit only low amplitude bedforms (Polblue Bends 1, 2 and 3) decreasing r_c/w results in a marked increase in secondary circulation from Bend 1 to Bend 2. However, Bend 3, the most tightly curving, shows little secondary current development (Figure 6.4c). The mechanics leading to the decrease in secondary circulation strength in Polblue Bend 3, and hence the mimicking of a free-vortex (irrotational) flow (Shukry, 1950), can be considered by investigating the elements that lead to the helical motion of flow in bends; tangential (centrifugal) force (resulting in superelevation of the water surface) and bed friction. The extent of superelevation of flow in a bend is a product of variations in radius of curvature, flow velocity and width. Polblue Bend 3 maintains a low width/depth ratio, until the bend exit where the channel widens slightly and some secondary motion of the flow is observed. Low widths and moderate velocities suppress superelevation of the water surface, despite low r_c/w ratios. Furthermore, owing to the constant low width/depth ratio of the channel through this bend, bank friction far exceeds bed friction (see Chapter 4 for shear stress partitioning) and may act to further inhibit the superelevation of the flow by keeping the vertical velocity profiles relatively uniform (Figure 6.5). Because superelevation of flow is one of the main drivers, its suppression will inhibit the development of secondary currents. Furthermore, narrow and deep channels, with a greatly reduced proportion of their boundary resistance at the bed, are not expected to develop secondary current strengths of the magnitude observed in wider channels (Bathurst, 1979; Tooth and McCarthy, 2004).

Indeed, Figure 6.5 shows that the vertical velocity profiles in Polblue Bend 3 to be remarkably uniform. Secondary currents will only form where there is a marked difference in the surface and near-bed velocities. In the absence of secondary circulation, the flow becomes closer to being irrotational than rotational (Shukry, 1950), and the MVF follows the law of conservation of angular momentum and moved towards the inside of the bend, as is the case in this bend.

6.4.6 Bend flow helicity reversal

An example of a *spontaneous* reversal in flow helicity was observed in Barrington Bend 1 (Figure 6.7a). In this bend, flow first developed very strong clockwise helical motion, presumably enhanced by the shallower depth of flow and the steep geometry of the *duffle* bedform, approaching the concave bank at an acute angle. An eddy-line formed approximately as an extension into the pool of the right bank, but slightly downstream, and formed a boundary between the normal and reversed flow helicity conditions to anti-clockwise. Similar eddy-lines in the Edwards Bends 1 and 2 also appear to be a result of rapid reductions in the strength of secondary currents between adjacent channel cross-sections either side of the bend apices, although in the Edwards bends the helices did not actually reverse direction.

As already stated, high velocities and low r_c/w ratios enhance flow superelevation in bends, but low turbulence and shearing consume energy and reduce flow velocity, thereby reducing the force available to maintain superelevated flow. At bankfull flow, Barrington Bend 1 exhibited very pronounced secondary currents, and the ADV data indicated very high levels of turbulence. As flow enters this bend, high velocities cause the flow to superelevate. Flow collides with a large region of separated flow (Figure 6.7a, Sections 4 and 5) and presumably consumes a great deal of energy in the creation of turbulence and shearing of flow along this boundary. Velocities at this point are reduced (compare Sections 5 to 7, Figure 6.7a) and, as the separated region of the flow at the outside of the bend is dissipated, flow expands to fill much of the cross-section. As a consequence a major component of the force that drives superelevation upstream of the bend apex is lost. Water is therefore superelevated, but with a reduced force available to maintain its superelevation. Furthermore, the MVF at this point dives to the channel bed (Figure 6.7a) as the outer cell and main cell converge near the surface and dive toward the bed. The superelevated surface flow near the outside bank, under the influence of gravity, flows back toward the inner bank, especially at the surface. Retardation of bed flow by boundary friction slows the near-bed flow and, encouraged by the MVF near the channel bed, flow near the bed becomes directed toward the outer bank. The result is a complete reversal of the direction of flow helicity within this bend.

Support for the helicity reversal model proposed above is provided by several studies. Hodskinson and Ferguson (1998) observed abrupt reversals of surface flow direction near the apex of a tight bend at sub-bankfull flow. Parsons (2002) used a 3-D model to predict sub-bankfull flow through a bend with a large concave bank pool (although he did not define it as such), and his results also indicated reversals of flow helicity near the bend apex. However, at bankfull flow the modelled pattern of helicity reversal in that bend was not complete in that only surface flow reversed its direction. His model also illustrated a water surface elevation difference between the inner and outer bank across a 4m wide bend apex of approximately 0.28m, and he described intense shearing between the primary and the separated flow.

New and particularly relevant work supporting the helicity reversal model described above is that by Corney et al. (in review). Their study modelled and experimentally demonstrated very unusual bend flows in submarine channel bends and demonstrated that the helical flows were in the reverse direction to the circulation observed in rivers. They attributed this result to the unusual velocity profiles in these channels where the MVF's occurred near the bed, rather than near the surface as would normally be the case for sub aerial flow conditions. Tangential (centrifugal) forces, which normally dominate surface flow and cause superelevation at the outside bank, were maximised near the bed and drove the flow outward and up the outer bank, thereby causing helical motion in reverse to that in sub-aerial bends. The plunging MVF located near the bed in Barrington Bend 1 could drive a similar mechanism for reversing flow helicity mid-way through this bend.

6.5 Conclusions

The narrow, deep and variable bed morphologies of the Barrington swamp channels enables the study of flow in meander bends under very different conditions to the relatively wide, shallow cross-sections that characterise most meander bend entry and apex cross-sections. Furthermore, high bank strengths and armouring have enabled some unusually large bedforms to develop and be maintained. These circumstances have resulted in bend flow patterns with several remarkable characteristics:

- Bend entry flow patterns varied between all bends. The narrow and deep cross-sections tended to exhibit even velocity distributions and little secondary circulation at bend entries or exits. In contrast, the wider and shallower entry cross-sections (located at *duffle* or riffle crests) exhibited more skewed velocity patterns and some rotation of paired MVF's. With the exception of Barrington Bend 1, the rotation of these MVF's were not consistent with riffle or inflection point flow models (Hey and Thorne, 1975; Thorne and Hey, 1982) as they converged near the surface, rotated in the same direction or did not rotate much at all.

- With the exception of Polblue Bend 3, helical flow became fully developed across each of the bend apices that were examined. Large point bars, which might otherwise cause shoaling (and hence outward) flow over their surfaces, have not developed in the Barrington swamp channels and helical flow patterns therefore also extended across the full extent of bend apices.

- In the narrow and deeper Polblue Creek, helical flow developed and dissipated rapidly within the bends, in accordance with the observations of Choudhary and Narasimhan (1977) in flume channels. In contrast, in the high amplitude bed topography and wider and shallower cross-section bends of Edwards Creek and the Barrington River, flow helicity persisted until past each bend exit. This emphasises the importance of bed friction in contributing to the formation of secondary currents.

- In contrast to the results of Hickin (1978), the tightest bend with low amplitude bedforms (Polblue Bend 3) did not develop significant secondary currents. This is probably because the low width/depth ratios and limited bed friction reduces the vertical flow velocity imbalance required to generate secondary currents. This result is consistent with the findings of Bathurst (1979) and Choudhary and Narasimhan (1977), in which wider cross-sections with considerable bed friction encourage helical motion of the flow.

- Outer bank cells of reversed rotation were observed in one bend (Barrington Bend 1), and inferred in one other (Edwards Bend 1) by outward directed vectors near the water

surface at the concave bank. A lack of near-bank flow data may be responsible for the very few observations of these reverse rotation cells, as steep banks are highly conducive to their development.

- *Duffle* bedforms were found in association with only the tightest bends. Their occurrence appears, therefore, to be the result of either intense bed and bank erosion at the bend apex with subsequent sediment transport from only the bend to the following *duffle*, or the inability of the flow to maintain sediment transport once turbulent energy losses associated with bend flow interactions reduce flow velocities immediately past the bend apices.

- Separation zones associated with the outer bank and bedform flow dictate the path of the MVF and the distribution of shear stress in the Barrington swamp channel bends. Bank-attached flow separation redirected maximum shear stresses toward the channel centreline, until the bend exits. Here, bed-attached separated zones formed in the lee of bedforms and reduced boundary shear stresses near the apices of bends. Furthermore, these locations coincided with the region of maximum flow helicity in each bend.

- The outer bank cell of reverse rotation in Barrington Bend 1 takes the form of a large separated zone within the outer bank embayment. Highly turbulent energy losses resulting from the interaction of the main flow within this separated region of flow combines with the suppression of the MVF toward the bed to drive a complete reversal of flow helicity through the downstream half of this bend. The effect of the MVF being located very near the bed in bend flow, and the subsequent effect on the forces that drive bend-flow secondary circulation, has been documented to drive reverse helicity in both flume and model analyses of submarine flumes (Corney et al., in review). Reversals in *surface* flow patterns similar to this have also been documented in bends with similar geometries to that in Barrington Bend 1 (Andrle, 1994; Hodskinson and Ferguson, 1998; Parsons, 2002).

- In contrast to the model proposed by Alford (1982), whereby concave bank embayments (or *circular meander pools)* were purported to develop at (or following)

overbank flows, it is proposed here that they have developed via the bend evolution model proposed by Hickin (1978), which was also suggested by Andrle (1994) for similar circular meander pools. Bends become increasingly tight, then cease to migrate outward as the MVF moves inward and erodes the point bar. Owing to a lack of sediment supply, the development of concave bank benches, which might be expected to form against the upstream limb of the concave banks in such tight bends (Nanson and Page, 1983), has not occurred. The MVF is directed to the concave bank downstream of separated flow regions that have developed in these embayments, leading to the elongation and enlargement of these features. Sediment supply limitations severely impede the subsequent accretion of such embayments.

The patterns of bend flow described above explain the presence and persistence of some unusual channel planform and bedform morphologies, largely unique to swamp channels. The hydraulic efficiency of these swamp channel cross-sections, afforded by high bank strengths and low sediment supply (Chapter 3), are balanced by turbulent energy losses caused by both *duffles* and riffles, in combination with relatively tight bends.

Chapter 7 Discussion and conclusions

This thesis has examined three streams flowing through two upland swamps on a sub-alpine plateau near the central coast of New South Wales. Such streams are not common in an Australian context; however, the unusual form and behaviour of these channels provide opportunities for the research of fundamental stream processes.

In some swamps, channel development is a catastrophic response to system disturbance (Young, 1983, 1986a, 1986b; Hope, 2003). However, this study challenges the application of this concept to the Barrington swamps and demonstrates that their channels have probably persisted in a similar form for the last ~1ka, indicative of both channelled system longevity and stability (equilibrium).

How the streams have adjusted toward equilibrium was considered at several different time scales, beginning with their development over the longer-term and ending with *instantaneous* measurements of bend flow. Within the range of these two temporal extremes, adjustments were also considered through hydraulic geometry, bedform and planform analyses. Importantly, each of these analyses builds upon the other and emphasis was placed on their linkages. From Chapter 2 through Chapter 6, not only were temporal scale adjustments considered, but also the spatial scale adjustments, initially broad-scale and finally fine-scale. Adjustments over both these scales were then assessed in the context of the equilibrium channel condition, revealed by uniform water surface gradients. It is appropriate to reconsider the stated objectives in the context of these results.

7.1 Addressing the objectives

Several objectives were defined in Chapter 1 and are restated and summarily addressed below, before a discussion of more specific outcomes is provided.

Objective 1. Assess the evolution and stability of the channel corridors within the swamps

The stability of the channelled condition of Edwards and Polblue Swamps was determined using both radiocarbon and palynological evidence. This data indicated likely incision of the swamps at ~1200BP and 800BP, and 1000BP, respectively, and the probable

persistence of channelled conditions since this time. Hydrological data also indicated balanced and intimate exchanges in the water table between the contemporary channels and their adjacent swamps. Channel flow stage-height conceivably limits swamp floodplain growth rates and height, closely mimicking the control imposed by overbank deposition in more conventional alluvial channels, thereby emphasising the likely control of channel dimensions on swamp height, rather than the reverse.

Mechanisms for floodplain development were investigated using both stratigraphic interpretation and bend flow-field data collection. Rapid vertical accretion/growth of the *inset floodplains* in response to likely channel incision, and slow concave bank bench accretion since have been identified as mechanisms for floodplain development in these swamp systems.

Objective 2 Describe interactions between channel geometry and flow in these narrow and deep, sediment-deficient channels

& Objective 3. Describe bed adjustments in such narrow, sediment-deficient channels

Channel adjustments to flow conditions were quantitatively investigated by analysing their hydraulic geometry, bed morphologies and channel planforms. Hydraulic geometry was shown to be constrained by several parameters: channel widths are constrained by unusually high bank strengths and channel depths are, in places, limited by the depth of swamp alluvium overlying basement material. Furthermore, a lack of sediment supply imposes a limitation on bedform development. As a consequence, the channels have developed narrow and mostly deep cross-sections with high velocity exponents and, despite depth limitations through some reaches, the channels were largely able to develop width/depth ratios approximating 2-3. Despite the resultant high velocity exponents, and shear stresses in excess of those required to mobilise bed and bank material, planforms and bedforms were essentially stable as a result of particularly resistant bank vegetation and bedform armouring. The achievement of equilibrium channel conditions indicated the success of channel self-adjustment in attaining stability.

Objective 4. Describe the planform adjustments and bend-flow characteristics in systems with such narrow and deep, tightly curving bends

The formation and maintenance of several peculiar swamp channel-bend morphologies were described and associated with unusual patterns of bend flow. The inability of flow to develop helical motion in one particularly tight bend, and the complete reversal of flow helicity in another mid-way through the bend, were documented and related to particular bedform and planform geometries. Flow patterns through particularly tight bends, which were bound by steep bedforms called *duffles,* were described and the development of concave bank meander pools were described by measuring flow fields.

7.2 Specific outcomes

The specific outcomes of the thesis are divided into four broad categories, which are addressed separately below.

Evolution of the Barrington swamp channel corridors

Swamp channel longevity associated with frequent bankfull flows imply stability (equilibrium). Radiocarbon dating and palynological data determined either the incision of previously unchannelled swamps ~1000 BP, or the contraction of previously large channels starting at this time, and their subsequent relative stability.

Present-day flow hydrographs illustrate diurnal fluctuations, indicative of intimate flow exchanges between the channels and swamp water tables. These fluctuations are the result of water being drawn into the floodplain by swamp vegetation during the hours when evapotranspiration is at a maximum rate and minimisation of this process at night (Todd, 1964). While there is a moderated release of water from these systems most of the time, the *implication* is that a balance exists between the channels and the swamps, indicative of their co-evolution and mutual stability.

Constraints on organic-alluvial channel adjustment and resulting extremes in channel morphology.

Similarities between the morphology of the Barrington swamp channels and alluvial channels in other environments directly imply that self-adjusting fluvial mechanisms *must*

operate in both (Jurmu and Andrle, 1997; Jurmu, 2002) which facilitate their adjustment toward stability (equilibrium) (Mackin, 1948).

Several constraints influence channel adjustment in these swamp systems: depth limitations are, in several places, imposed by finite peat thickness above basement material, but in many places the channels are narrow and deep; width limitations are imposed by high bank strength and the constrictive growth of vegetation; and sediment supply limitations from well forested headwater streams prevent the ongoing development and migration of bedforms. The resultant narrow and deep channel geometries produce rapid increases in velocity with discharge.

Low width/depth ratios approximating two are hydraulically ideal for conveying sediment-free water (Huang et al., 2004), conditions consistent with the geometry and low sediment supply in the Barrington swamp streams. Hydraulically efficient channels with very little sediment load could result in surplus energy and unstable systems, if not countered by bedform and planform adjustments and resilient channel boundaries.

Bedform and planform adjustment in swamp channels

In most of the channel reaches examined, insufficient sediment load has limited the development of flow resisting bedforms. However, complex planforms and semi-permanent bed features generate large scale turbulent structures and sufficient flow resistance to maintain stability. Dense root mats provide high bank strengths that are central to the maintenance of channel form. Such strong banks and aquatic plant growth on the bedforms that have developed can withstand the intense turbulence, created by the lateral (planform) and vertical (bedform) flow undulations, maximised during high discharges.

Velocities increase markedly with stage through most reaches but in the relatively high stream power Edwards Creek and Barrington River the development of unusually large bedforms (*duffles*) and complex planforms have moderated velocity exponents. Cross-sections with *duffles* exhibit more modest velocity exponents illustrating that these bed features limit sediment transport capacity and channel erosion.

Duffles are defined as bed features with both dune and riffle characteristics. Their positions are predominantly determined by channel planform, consistent with riffles (Keller and Melhorn, 1978) but their amplitudes are scaled to both flow depth, consistent with both dunes (Simon and Thorne, 1996) and riffles (Carling and Orr, 2000), and with channel width, again consistent with riffles (Keller and Melhorn, 1978). Furthermore, their steepness values exceed those exhibited by either dunes *or* riffles, but are more consistent with ripples (Baas, 1999). These ambiguities suggest overlap in both the definition and function of these bed features.

While in most cases the critical shear stresses for the sub-surface sediments of *duffles* are exceeded by the flow at bankfull, their surfaces are armoured. The persistence, and the consequent stability of these reaches of channel, is dependent on the maintenance of these armoured surfaces and on the strength of the vegetated banks. Furthermore, the magnitude (steepness) of *duffles* are such that their contribution to flow resistance and the reduced shear stress significantly reduces the capacity of the flow to transport sediment, as illustrated using Best's (1996) shear stress - grainsize bedform existence diagram. As bed features they appear to be attuned to minimising sediment transport and channel erosion.

Unusual bend flow characteristics resulting from extremes in channel morphology

Very low width-depth ratios, high sinuosity and varying magnitude bedforms have produced both unusual bend geometries and bend flow patterns. Owing to their discrete character, these are best addressed in point form.

- Sediment supply limitations have inhibited point bar development and greatly altered the flow that would otherwise shoal over such surfaces (Hickin, 1978; Dietrich and Smith, 1983; Markham and Thorne, 1992). The Barrington swamp channels are able to develop full helical motion across the entire width of most bend apices. The suppression of helical motion in Polblue Bend 3, the only exception to full apex-flow helicity, is attributed to its unusually constant width and its extremely low width-depth ratio. These characteristics are contrary to those that enhance the development of secondary circulation (Bathurst, 1979) and appear to override the low radius of curvature/width ratio that would otherwise promote the formation of such currents (Hickin, 1978).

- Sediment supply limitations combined with unusually high bank strengths enable the development of particularly tight meander bends, often in association with a feature common to swamp channels (e.g. Alford et al., 1982; Ingram, 1983; Andrle, 1994): a concave bank embayment, termed a *circular meander pool* by Andrle (1994). These features have developed as bends evolve lower radii of curvature/width ratios, and the MVF is drawn inwards and away from the concave bank, in the manner described by Hickin (1978). *Concave bank benches* that might otherwise form in the upstream limbs of these bends (Nanson and Page, 1983) are limited from doing so in these swamp channels by low sediment supply rates. The result is the persistence of concave bank embayments in many bends, with separated flow, and the deposition of only scant point bar deposits.

- Flow separation developed at the outer banks of most channel bends and at the inner banks of some bends, in response to tight and irregular planforms. Large separation zones also developed in the lee of *duffles*, consistent with those that form in the lee of dunes (Yalin, 1971). The significance of these separation zones is twofold: the shifting away of maximum shear stresses and hence the protection of the channel boundaries adjacent to these regions, and the large energy losses resulting from the turbulent eddies that develop in association with them (e.g. Best, 1996). These energy losses are important for countering highly efficient channel flows resulting from low width-depth ratio swamp-channel cross-sections.

- A reversal in bend flow helicity mid-way through one bend was attributed to its unusual morphology; it is bound by *duffles*, has a large concave bank *circular meander pool* and a very low r_c/w ratio. High turbulent energy losses result from the interaction of the main flow with the separated flow at the concave bank, a condition probably enhanced by both *duffle*-flow interactions and surface flow convergence. These drive the MVF towards the bed, a position that has been shown to drive helicity reversals in both flume and model research through *entire* submarine channel bends (Corney et al., in review). Reversals in surface flow patterns similar to this have also been documented in other studies with similar bend geometries (Andrle, 1994; Parsons, 2002).

7.3 Management implications

It has been demonstrated that the Barrington Tops channels and their swamps are highly unusual, equilibrium features. The concept of the *stable channelled swamp* is a relatively new one (e.g. Jurmu and Andrle, 1997; Jurmu, 2002) and their uniqueness and picturesque character mark them as worthy of conservation. Furthermore, the moderated release of flow from these upland catchments, resulting from the intimate exchanges of water between the channels and the adjacent swamps, has consequences that are more widespread; downstream reaches of channel benefit, both ecologically and possibly economically, from the base flows that these environments provide (Mitsch and Gosselink, 1986).

This research has demonstrated that the cross-sectional form of these swamp channels results in highly efficient flow conduits with velocities that increase sharply with increasing stage. The stability of such velocity-responsive swamp channels is dependent on two major factors; high bank strength, provided by vegetation, and bedform strength, provided by sediment armouring and aquatic vegetation. The preservation of these two controlling parameters is integral to the continuing stability of both the channels and swamps. If *duffle* bedforms were to erode through the loss of armouring, sediment supply limitations would inhibit their redevelopment. This research suggests that there would be a marked reduction in flow resistance, resulting in the destabilisation of the channel geometry. Likewise, the loss or significant alteration of riparian vegetation would have major implications for bank and bed strength and would also encourage changes in channel form and swamp hydrology. A feedback between stable, equilibrium channels and the surrounding swamps is evident; there cannot be one without the stability of the other and the disruption of either would likely be to the detriment of both.

Present threats to bedform armouring and channel vegetation are numerous. Evidence of feral animals such as horses and pigs include recently grazed swamp vegetation, dung heaps, well formed tracks and over-turned soil (caused by rooting pigs). These modifications threaten both the integrity of the armoured *duffle* surfaces, on which the horses tread, and the swamp surfaces, on which horses and pigs graze and form animal-tracks.

The notion of the vulnerability of channelled swamps is partly challenged by their land-use history. Sporadic summer grazing of the swamps until the 1960's (Randell et al., 2003) did not cause their destruction and suggests that these systems may, in fact, be more resilient than they might otherwise appear. Certainly, periods of fire and drought over the preceding ~1ka years of their existence must have occurred and has not resulted in their destruction. Perhaps the risk to these systems lies in some combination of the effects of drought, fire and feral animals.

7.4 Further research

Several results from this thesis suggest lines for further investigation.

- Evidence for a reversal of flow helicity mid-way through a meander bend on the result of just Barrington Bend 3 could be improved by documenting further examples. While other studies have documented similar reversals in surface flow at sub-bankfull (Parsons, 2002) or bankfull (Alford et al., 1982) flows in bends with *meander pools*, this study provides strong evidence for the reversal of subsurface flows as well. The measurement of three-dimensional flow fields through at least one other bend would be desirable. This would enable the probable mechanism that drives the reversal (primarily the plunging maximum velocity filament) to be more rigorously assessed.

- Shear stress calculations derived from the application of the Law of the Wall to near-bed velocity measurements could be further improved by applying the Turbulent Kinetic Energy (TKE) approach to near-boundary data points obtained using the Acoustic Doppler Velocimeters (ADV's) (Kim et al., 2000; Biron et al., 2004). Some of the data obtained in this study are suited to the application of this technique; however, the cumbersome size of the ADV's prohibited many near-bed and near-wall deployments. Both additional and suitable existing data could be analysed using this technique. These calculations would also further substantiate the shear stress estimates derived in this study from the Du Boys shear stress partitioning and would enable wall shear stresses to be directly measured and compared with those estimated by Knight et al. (1984) in flume channels.

- Aerial photographs and field evidence illustrate many examples of meander cut-offs in Edwards Swamp through which the Barrington River and Edwards Creek flow. The source of sediment for *duffle* bedform development in these same channels remains undetermined. As there is currently very little sediment moving through these channels it is proposed here that the *duffles* formed either: 1) rapidly from the sediment released during planform adjustments and they provided the flow resistance required to stabilise the channels at this time or, 2) more slowly through the gradual accretion of the limited amount of bedload available. Recent developments in optically stimulated luminescence quartz dating enable relatively young deposits to be dated (Olley et al., 2004; Thompson et al., in press) and this technique may be suitable for application in these swamp channel deposits.

- Channelled swamps have only recently been either morphologically described (this study, Jurmu and Andrle, 1997; Jurmu, 2002) or modelled in terms of their evolution (this study). As swamp geomorphology effects the palynology of distal swamp cores within a swamp by altering the entire swamp water table and hence the swamp vegetation, swamp geomorphology (including channel presence) may have significant implications for palynological interpretations (Young, 1986a). Not all palynological changes need be climatically induced. Further research linking the palynology and geomorphology of channel tracts within a swamp and distal cores from the same swamp could determine if different interpretations would arise.

References

Abernethy B, Rutherfurd ID. 1998. Where along a river's length will vegetation most effectively stabilise stream banks? *Geomorphology* **23**(1): 55-75.

Abernethy B, Rutherfurd ID. 2000. The effect of riparian tree roots on the mass-stability of riverbanks. *Earth Surface Processes and Landforms* **25**(9): 921-937.

Abernethy B, Rutherfurd ID. 2001. The distribution and strength of riparian tree roots in relation to riverbank reinforcement. *Hydrological Processes* **15**(1): 63-79.

Ackers P. 1982. Meandering channels and the influence of bed material. In *Gravel-bed rivers: Fluvial processes, engineering, and management*, Hey RD, Bathurst JC, Thorne CR (eds). John Wiley and Sons: Chichester; 389-421.

Alford JJ, Baumann RH, Lewis A. 1982. Circular meander pools. *Earth Surface Processes and Landforms* **7**(2): 183-188.

Allen JRL. 1982. *Sedimentary structures: their character and physical basis*. Elsevier Scientific Publishing Company: Amsterdam.

Andrews ED. 1984. Bed material entrainment and hydraulic geometry of gravel-bed rivers in Colorado. *Geological Society of America Bulletin* **95**(3): 371-378.

Andrle R. 1994. Flow structure and development of circular meander pools. *Geomorphology* **9**(4): 261-270.

Ashley GM, Zeff ML. 1988. Tidal channel classification for a low-mesotidal salt marsh. *Marine Geology* **82**(1-2): 17-32.

Ashmore PE. 1991. Channel morphology and bed load pulses in braided gravel-bed streams. *Geografiska Annaler* **73A**(1): 37-52.

Australian Standard 3778.3.1. 1990. *Measurement of water flow in open channels Part 3.1: Velocity-area methods - measurement by current meters and floats (Identical with ISO 748:1997)*, Standards Australia, Sydney.

Baas JH. 1999. An empirical model for the development and equilibrium morphology of current ripples in fine sand. *Sedimentology* **46**(1): 123-138.

Bagnold RA. 1960. Some aspects on the shape of river meanders. *United States Geological Survey Professional Paper* **282E**: 135-144.

Barrows TT, Stone JO, Fifield LK. 2004. Exposure ages for Pleistocene periglacial deposits in Australia. *Quaternary Science Reviews* **23**(5-6): 697-708.

Bathurst JC. 1979. Distribution of boundary shear stress in rivers. In *Adjustments of the fluvial system: A proceedings volume of the tenth annual Geomorphology symposia series held at Binghamton, New York, September 21-22, 1979,* Rhodes DD, Williams GP (eds), Kendall/Hunt Publishing Company: Iowa; 95-116.

Bathurst JC. 1993. Flow Resistance through the Channel Network. In *Channel Network Hydrology*, Beven K, Kirkby MJ (eds). John Wiley and Sons: New York; 69-98.

Bathurst JC, Thorne CR, Hey RD. 1979. Secondary flow and shear stress at river bends. *Journal of the Hydraulics Division American Society of Civil Engineers* **105**(10): 1277-1295.

Best J. 1996. The fluid dynamics of small-scale alluvial bedforms. In *Advances in fluvial dynamics and stratigraphy*, Carling PA, Dawson MR (eds). John Wiley and Sons Ltd.: Brisbane; 67-125.

Bettess R, White WR. 1983. Meandering and braiding of alluvial channels. *Proceedings of the Institution of Civil Engineers, Part 1: Design and Construction* **75**: 525-538.

Bettess R, White WR. 1987. Extremal hypotheses applied to river regime. In *Sediment transport in gravel bed rivers*, Thorne CR, Bathurst JC, Hey RD (eds). John Wiley and Sons Inc.: Chichester; 767-789.

Biron PM, Lane SN, Roy AG, Bradbrook KF, Richards KS. 1998. Sensitivity of bed shear stress estimated from vertical velocity profiles: the problem of sampling resolution. *Earth Surface Processes and Landforms* **23**: 133-139.

Biron PM, Robson C, Lapointe MF, Gaskin SJ. 2004. Comparing different methods of bed shear stress estimates in simple and complex flow fields. *Earth Surface Processes and Landforms* **29**(11): 1403-1415.

Blench T. 1952. Regime theory for self-formed sediment-bearing channels. *Transactions of the American Society of Civil Engineers* **117**: 383-400,401-408.

Blott SJ, Pye K. 2001. GRADISTAT: a grain size distribution and statistics package for the analysis of unconsolidated sediments. *Earth Surface Processes and Landforms* **26**(11): 1237-1248.

Booker DJ, Sear DA, Payne AJ. 2001. Modelling three-dimensional flow structures and patterns of boundary shear stress in a natural pool-riffle sequence. *Earth Surface Processes and Landforms* **26**(5): 553-576.

Bowler JM, Hope GS, Jennings JN, Singh G, Walker D. 1976. Late Quaternary climates of Australia and New Guinea. *Quaternary Research* **6**: 359-394.

Bradley WC, Fahnestock RK, Rowekamp ET. 1972. Coarse sediment transport by flood flows on Knik River, Alaska. *Geological Society of America Bulletin* **83**(5): 1261-1284.

Bray DI. 1982. Flow resistance in gravel-bed rivers. In *Gravel-bed rivers: Fluvial processes, engineering, and management*, Hey RD, Bathurst JC, Thorne CR (eds). John Wiley and Sons Ltd: Chichester; 109-137.

Brice JC. 1964. Channel patterns and terraces of the Loup Rivers in Nebraska. *United States Geological Survey Professional Paper* **422D**: D1-D41.

Brice JC. 1984. Planform properties of meandering rivers. In *River meandering: Proceedings of the conference rivers '83, New Orleans,* Elliot CM (ed), American Society of Civil Engineers: New York; 1-15.

Bridge JS, Jarvis J. 1976. Flow and sedimentary processes in the meandering River South Esk, Glen Clova, Scotland. *Earth Surface Processes* **1**: 303-336.

Brierley GJ, Fryirs K, Outhet D, Massey C. 2002. Application of the River Styles framework as a basis for river management in New South Wales, Australia. *Applied Geography* **22**(1): 91-122.

Brierley GJ, Fryirs KA. 2005. *Geomorphology and river management: Applications of the River Styles framework.* Blackwell Publishing: Malden.

Brooks AP, Brierley G. 2002. Mediated equilibrium: the influence of riparian vegetation and wood on the long-term evolution and behaviour of a near-pristine river. *Earth Surface Processes and Landforms* **27**: 343-367.

Bucher WH. 1919. On ripples and related sedimentary surface forms and their palaeogeographic interpretation. *American Journal of Science* **47**: 149-210, 241-269.

Carling PA. 1983. Threshold of coarse sediment transport in broad and narrow natural streams. *Earth Surface Processes and Landforms* **8**(1): 1-18.

Carling PA. 1999. Subaqueous gravel dunes. *Journal of Sedimentary Research* **69**(3): 534-545.

Carling PA, Orr HG. 2000. Morphology of riffle-pool sequences in the River Severn, England. *Earth Surface Processes and Landforms* **25**(4): 369-384.

Carling PA, Shvidchenko AB. 2002. A consideration of the dune : antidune transition in fine gravel. *Sedimentology* **49**(6): 1269-1282.

Carson MA. 1987. Measures of flow intensity as predictors of bedload. *Journal of Hydraulic Engineering, American Society of Civil Engineers* **113**(11): 1402-1421.

Chacinski TM, Francis JRD. 1952. Discussion of, On the origin of river meanders, P. W. Werner. *Transactions of the American Geophysical Union* **33**(5): 771-774.

Chorley RJ, Kennedy B. 1971. *Physical geography, a systems approach*. Prentice Hall: London.

Choudhary UK, Narasimhan S. 1977. Flow in 180 degrees open channel rigid boundary bends. *Journal of the Hydraulics Division* **103**(6): 651-657.

Chow VT. 1973. *Open-channel hydraulics*. McGraw-Hill Book Company: Singapore.

Church M. 1992. Channel Morphology and Typology. In *The Rivers Handbook*Blackwell Scientific Publications: Oxford; 126-143.

Church M, Hassan MA, Wolcott JF. 1998. Stabilizing self-organised structures in gravel-bed stream channels: field and experimental observations. *Water Resources Research* **34**(11): 3169-3179.

Clifford NJ. 1993. Differential bed sedimentology and the maintenance of riffle-pool sequences. *Catena* **20**(5): 447-468.

Cohen TJ, Nanson GC. in prep. Mind the gap: valley deposits and independant proxy climate data identifying the Holocene hypsithermal period of enhanced flow regome in southeastern Australia.

Corney R, Peakall J, Parsons DR, Elliott L, Amos K, Best J, Keevil G, Ingham D. in review. The orientation of helical flow in curved channels. *Sedimentology*.

Dietrich WE, Smith JD. 1983. Influence of the point bar on flow through curved channels. *Water Resources Research* **19**(5): 1173-1192.

Dietrich WE, Smith JD, Dunne T. 1979. Flow and sediment transport in a sand bedded meander. *Journal of Geology* **87**: 305-315.

Dodson JR. 1987. Mire development and environmental change, Barrington Tops, New South Wales, Australia. *Quaternary Research* **27**(1): 73-81.

Dodson JR, Greenwood PW, Jones RL. 1986. Holocene forest and wetland vegetation dynamics at Barrington Tops, New South Wales. *Journal of Biogeography* **13**(6): 561-585.

Dodson JR, Myers CA. 1986. Vegetation and modern pollen rain from the Barrington Tops and Upper Hunter River regions of New South Wales. *Australian Journal of Botany* **34**(3): 293-304.

Dodson JR, Roberts FK, Salis TD. 1994. Palaeoenvironments and human impact at Burraga Swamp in montane rainforest, Barrington Tops National Park, New South Wales, Australia. *Australian Geographer* **25**(2): 161-169.

Dury GH. 1970. A re-survey of part of the Hawkesbury River, New South Wales, after one hundred years. *Australian Geographical Studies* **8**(2): 121-132.

Eaton BC, Church M. 2004. A graded stream response relation for bed load-dominated streams. *Journal of Geophysical Research* **109**: F03011, doi:10.1029/2003JF000062.

Eaton BC, Church M, Millar RG. 2004. Rational regime model of alluvial channel morphology and response. *Earth Surface Processes and Landforms* **29**(4): 511-529.

Einstein HA, Banks RB. 1950. Fluid resistance of composite roughness. *Transactions of the American Geophysical Union* **31**(4): 603-610.

Einstein HA, Barbarossa NL. 1952. River channel roughness. *Transactions of the American Society of Civil Engineers* **117**: 1121-1146.

Emmett WW, Wolman MG. 2001. Effective discharge and gravel-bed rivers. *Earth Surface Processes and Landforms* **26**(13): 1369-1380.

Eriksson MG, Olley JM, Kilham DR, Wasson RJ. 2002. Late Holocene aggradation and incision in the Naas River, Australian Capital Territory - preliminary findings. In *Regolith and landforms in eastern Australia*, Roach IC (ed). Cooperative research Centre for Landscape Environments and Mineral Exploration (CRC LEME): Canberra; 24-27.

Eyles RJ. 1977a. Birchams Creek: the transition from a chain of ponds to a gully. *Australian Geographical Studies* **15**(2): 146-157.

Eyles RJ. 1977b. Changes in drainage networks since 1820, Southern Tablelands, N.S.W. *Australian Geographer* **13**(6): 377-386.

Ferguson RI. 1986. Hydraulics and hydraulic geometry. *Progress in Physical Geography* **10**(1): 1-31.

Ferguson RI. 1987. Hydraulic and sedimentary controls on channel pattern. In *River channels: environment and process*, Richards KS (ed). Blackwell: Oxford; 129-158.

Ferguson RI. 1994. Critical discharge for entrainment of poorly sorted gravel. *Earth Surface Processes and Landforms* **19**(2): 179-186.

Ferguson RI, Parsons DR, Lane SN, Hardy RJ. 2003. Flow in meander bends with recirculation at the inner bank. *Water Resources Research* **39**(11): 1322,DOI:10.1029/2003WR001965.

Folk RL. 1954. The distinction between grain size and mineral composition in sedimentary-rock nomenclature. *Journal of Geology* **62**: 344-359.

Folk RL, Ward WC. 1957. Brazos River bar [Texas]: a study in the significance of grain size parameters. *Journal of Sedimentary Petrology* **27**(1): 3-26.

Frothingham K, Rhoads B. 2003. Three-dimensional flow structure and channel change in an asymetrical compound meander loop, Embarras River, Illinois. *Earth Surface Processes and Landforms* **28**(6): 625-644.

Fryirs K, Brierley G. 1998. The character and age structure of valley fills in Upper Wolumla Creek catchment, South Coast, New South Wales, Australia. *Earth Surface Processes and Landforms* **23**(3): 271-287.

Galloway RW. 1963. Geomorphology of the Hunter Valley. *CSIRO Australian Land Research Series* **8**: 91-102.

Galloway RW. 1965. Late Quaternary climates in Australia. *Journal of Geology* **73**: 603-618.

Gao P, Abrahams AD. 2004. Bedload transport resistance in rough open-channel flows. *Earth Surface Processes and Landforms* **29**: 423-435.

Garofalo D. 1980. The influence of wetland vegetation on tidal stream channel migration and morphology. *Estuaries* **3**(4): 258-270.

Gilbert GK. 1914. The transportation of debris by running water. *United States Geological Survey Professional Paper* **86**: 1-263.

Goodwin P. 2004. Analytical solutions for estimating effective discharge. *Journal of Hydraulic Engineering* **130**(8): 729-738.

Gordon ND, McMahon TA, Finlayson BL, Gippel CJ, Nathan RJ. 2004. *Stream hydrology: An introduction for ecologists*. John Wiley and Sons Ltd.: Chichester.

Gore AJP. 1983. Introduction. In *Mires: Swamp, bog, fen and moor*, Gore AJP (ed). Elsevier Scientific Publishing Company: Amsterdam; 1-34.

Goudie A. 1990. *Geomorphological techniques*. Unwin Hyman: Sydney.

Grayson RB, Argent RM, Nathan RJ, McMahon TA, Mein RG. 1996. *Hydrological recipes: Estimation techniques in Australian hydrology*. Cooperative Research Centre for Catchment Hydrology: Clayton, Victoria.

Guo J, Julien PY. 2005. Shear stress in smooth, rectangular open-channel flows. *Journal of Hydraulic Engineering* **131**(1): 30-37.

Hack JT. 1957. Studies of longitudinal profiles in Virginia and Maryland. *United States Geological Survey Professional Paper* **294B**: 49-97.

Hey RD, Thorne CR. 1975. Secondary flows in river channels. *Area* **7**(3): 191-195.

Hey RD, Thorne CR. 1986. Stable channels with mobile gravel beds. *Journal of Hydraulic Engineering* **112**(8): 671-689.

Hickin EJ. 1978. Mean flow structure in meanders of the Squamish River, British Colombia. *Canadian Journal of Earth Science* **15**(11): 1833-1849.

Hickin EJ. 1984. Vegetation and river channel dynamics. *Canadian Geographer* **28**(2): 111-126.

Hickin EJ, Nanson GC. 1975. The character of channel migration on the Beatton River, north-east British Columbia, Canada. *Geological Society of America Bulletin* **86**(4): 487-494.

Hickin EJ, Nanson GC. 1984. Lateral migration rates of river bends. *Journal of Hydraulic Engineering* **110**(11): 1557-1567.

Hicks DM, Mason PD. 1998. *Roughness characteristics of New Zealand rivers: A handbook for assigning hydraulic roughness coefficients to river reaches by the "visual comparison" approach*. National Institute of Water and Atmospheric Research Ltd.: Christchurch.

Hodskinson A, Ferguson RI. 1998. Numerical modelling of separated flow in river bends: Model testing and experimental investigation of geometric controls on the extent of flow separation at the concave bank. *Hydrological Processes* **12**(8): 1323-1338.

Hoey TB, Bluck BJ. 1999. Identifying the controls over downstream fining of river gravels. *Journal of Sedimentary Research* **69**(1): 40-50.

Hooke JM. 1992. Discussion of: Geomorphology of gravel-bed river bends. In *Dynamics of gravel-bed rivers*, Billi P, Hey RD, Thorne CR, Tacconi P (eds). John Wiley and Sons: Chichester; 450-452.

Hooke RLB. 1975. Distribution of sediment transport and shear stress in a meander bend. *Journal of Geology* **83**(5): 543-565.

Hope GS. 2003. The mountain mires of southern New South Wales and the Australian Capital Territory: their history and future. In *Celebrating mountains: Proceedings of an International Year of Mountains conference, Jindabyne, Australia,* Janet Mackay and Associates (ed), Australian Alps Liason Committee: Canberra; 67-79.

Hope GS, Chokkalingam U, Syaiful A. 2005. The stratigraphy and fire history of the Kutai Peatlands, Kalimantan, Indonesia. *Quaternary Research* **64**(3): 407-417.

Huang HQ, Chang HH, Nanson GC. 2004. Minimum energy as the general form of critical flow and maximum flow efficiency and for explaining variations in river channel pattern. *Water Resources Research* **40**(4): DOI:10.1029/2003WR002539.

Huang HQ, Nanson GC. 1997. Vegetation and channel variation; a case study of four small streams in southeastern Australia. *Geomorphology* **18**: 237-249.

Huang HQ, Nanson GC. 1998. The influence of bank strength on channel geometry: an integrated analysis of some observations. *Earth Surface Processes and Landforms* **23**: 865-876.

Huang HQ, Nanson GC. 2000. Hydraulic geometry and maximum flow efficiency as products of the principle of least action. *Earth Surface Processes and Landforms* **25**(1): 1-16.

Huang HQ, Nanson GC, Fagan SD. 2002. Hydraulic geometry of straight alluvial channels and the principal of least action. *Journal of Hydraulic Research* **40**(2): 152-160.

Huang HQ, Warner RF. 1995. The multivariate controls of hydraulic geometry: a causal investigation in terms of boundary shear distribution. *Earth Surface Processes and Landforms* **20**: 115-130.

Hughes PJ, Sullivan ME. 1981. Aboriginal burning and Late Holocene geomorphic events in eastern N.S.W. *Search* **12**(8): 277-278.

Ingram HAP. 1983. Hydrology. In *Mires: Swamp, bog, fen and moor*, Gore AJP (ed). Elsevier Scientific Publishing Company: Amsterdam; 67-158.

Jackson RG. 1976. Unsteady-flow distributions of hydraulic and sedimentologic parameters across meander bends of the lower Wabash River, Illinois-Indiana USA. In *International symposium on unsteady flow in open channels,* University of Newcastle-upon-Tyne, England, Stephens HS, Hemmings SK (eds), BHRA Fluid Engineering: Cranfield;

Jurmu MC. 2002. A morphological comparison of narrow, low-gradient streams traversing wetland environments to alluvial streams. *Environmental Management* **30**(6): 831-856.

Jurmu MC, Andrle R. 1997. Morphology of a wetland stream. *Environmental Management* **21**(6): 921-941.

Keller EA. 1971. Areal sorting of bed-load material: the hypothesis of velocity reversal. *Geological Society of America Bulletin* **82**(3): 753-756.

Keller EA. 1972. Development of alluvial stream channels: a five stage model. *Geological Society of America Bulletin* **83**(5): 1531-1536.

Keller EA, Melhorn WN. 1978. Rhythmic spacing and origin of pools and riffles. *Geological Society of America Bulletin* **89**(5): 723-730.

Kemp J. 2005. Mis-use of hydraulic geometry to estimate palaeochannel discharges: sinuous Late Pleistocene rivers in the Riverine Plain, SE Australia (abstract). In *The fluvial system - Past dynamics and controls, 16-22 May 2005, Bonn, Germany*, 33.

Kim SC, Friedrichs CT, Maa JPY, Wright LD. 2000. Estimating bottom stress in tidal boundary layer from Acoustic Doppler Velocimeter data. *Journal of Hydraulic Engineering* **126**(6): 399-406.

Knight DW, Demetriou JD, Hamed ME. 1984. Boundary shear in smooth rectangular channels. *Journal of Hydraulic Engineering* **110**(4): 405-422.

Knighton AD. 1975. Variations in at-a-station hydraulic geometry. *American Journal of Science* **275**(2): 186-218.

Knighton AD. 1998. *Fluvial forms and processes: A new perspective*. Arnold: London.

Knighton AD, Nanson GC. 1994. Flow transmission along an arid zone anastomosing river, Cooper Creek, Australia. *Hydrological Processes* **8**(2): 137-154.

Kostaschuk RA, Church M. 1993. Macroturbulence generated by dunes: Fraser River, Canada. *Sedimentary Geology* **85**(1-4): 25-37.

Kostaschuk RA, Villard P. 1996. Flow and sediment transport over large subaqueous dunes: Fraser River, Canada. *Sedimentology* **43**(5): 849-863.

Kutija V, Hong HTM. 1996. A numerical model for assessing the additional resistance to flow introduced by flexible vegetation. *Journal of Hydraulic Research* **34**(1): 99-114.

Lacey G. 1930. Stable channels in alluvium. *Minutes of the Proceedings of the Institution of Civil Engineers* **229**: 259-292.

Langbein WB. 1964. Geometry of river channels. *Proceedings of the American Society of Civil Engineers* **90**(Part 1): 301-312.

Langbein WB, Leopold LB. 1966. River meanders - theory of minimum variance. *United States Geological Survey Professional Paper* **422-H**: H1-H15.

Langbein WB, Leopold LB. 1968. River channel bars and dunes - theory of kinematic waves. *United States Geological Survey Professional Paper* **422-L**: L1-L20.

Lawless M, Robert A. 2001. Scales of boundary resistance in coarse-grained channels: turbulent velocity profiles and implications. *Geomorphology* **39**(3-4): 221-238.

Leeder, Bridges. 1975. Flow separation in meander bends. *Nature* **253**(5490): 338-339.

Leopold LB, Bagnold RA, Wolman MG, Brush(Jnr) LM. 1960. Flow resistance in sinuous or irregular channels. *United States Geological Survey Professional Paper* **282D**: 108-134.

Leopold LB, Bull WB. 1979. Base level, aggradation and grade. *Proceedings of the American Philosophical Society* **123**(3): 168-202.

Leopold LB, Langbein WB. 1962. The concept of entropy in landscape evolution. *United States Geological Survey Professional Paper* **500A**: A1-A20.

Leopold LB, Maddock T. 1953. The hydraulic geometry of stream channels and some physiographic implications. *United States Geological Survey Professional Paper* **252**: 1-58.

Leopold LB, Wolman MG. 1957. River channel patterns: braided, meandering and straight. *United States Geological Survey Professional Paper* **282-B**: 39-85.

Leopold LB, Wolman MG, Millar JP. 1964. *Fluvial processes in geomorphology*. W.H. Freeman and Company: San Francisco.

Lewin J. 1976. Initiation of bed forms and meanders in coarse-grained sediment. *Geological Society of America Bulletin* **87**(2): 281-285.

Lewin J, Brewer PA. 2001. Predicting channel patterns. *Geomorphology* **40**: 329-339.

Lindley ES. 1919. Regime channels. In *Proceedings of the Punjab Engineering Congress,* India, 63-74.

Mackin JH. 1948. Concept of the graded river. *Geological Society of America Bulletin* **59**(5): 463-511.

Makridakis S, Wheelwright SC, Hyndman RJ. 1998. *Forecasting: Methods and Applications*. John Wiley and Sons: Brisbane.

Markham AJ, Thorne CR. 1992. Geomorphology of gravel-bed river bends. In *Dynamics of gravel-bed rivers*, Billi P, Hey RD, Thorne CR, Tacconi P (eds). John Wiley and Sons: Chichester; 433-456.

McDonald RC, Isbell RF, Speight JG, Walker J, Hopkins MS. 1990. *Australian soil and land survey field handbook.* Inkata Press: Melbourne.

McLean SR, Wolfe SR. 1999. Spatially averaged flow over a wavy boundary revisited. *Journal of Geophysical Research* **104**(C7): 15742-15753.

McLean SR, Wolfe SR, Nelson JM. 1999. Spatially averaged flow over a wavy boundary revisited. *Journal of Geophysical Research* **104**(C7): 15743-15753.

Miall AD. 1996. *The geology of fluvial deposits: sedimentary facies, basin analysis, and petroleum geology*. Springer-Verlag: Berlin.

Micheli ER, Kirchner JW. 2002a. Effects of wet meadow riparian vegetation on streambank erosion 1. Remote sensing measurements of streambank migration and erodibility. *Earth Surface Processes and Landforms* **27**(6): 627-639.

Micheli ER, Kirchner JW. 2002b. Effects of wet meadow riparian vegetation on streambank erosion 2. Measurements of vegetated bank strength and consequences for failure mechanics. *Earth Surface Processes and Landforms* **27**(7): 687-697.

Milan DJ, Heritage GL, Large ARG, Charlton ME. 2001. Stage dependant variability in tractive force distribution through a riffle-pool sequence. *Catena* **44**(2): 85-109.

Millar RG. 1999a. Grain and form reistance in gravel-bed reaches. *Journal of Hydraulic Research* **37**(3): 303-312.

Millar RG. 1999b. Theoretical regime equations for mobile gravel-bed rivers with stable banks. *Geomorphology* **64**: 207-220.

Millar RG, Quick MC. 1993. Effect of bank stability on geometry of gravel rivers. *Journal of Hydraulic Engineering* **119**(12): 1343-1363.

Mitsch WJ, Gosselink JG. 1986. *Wetlands*. Van Nostrand Reinhold Company Inc.: New York.

Montgomery D, R., Buffington JM. 1997. Channel-reach morphology in mountain drainage basins. *Geological Society of America Bulletin* **109**(5): 596-611.

Myrick RM, Leopold LB. 1963. Hydraulic geometry of a small tidal estuary. *United States Geological Survey Professional Paper* **422-B**: B1-B18.

Nanson GC, Croke JC. 1992. A genetic classification of floodplains. *Geomorphology* **4**(6): 459-486.

Nanson GC, Page KJ. 1983. Lateral accretion of fine-grained concave benches on meandering rivers. In *Modern and ancient fluvial systems*, Collinson JD, Lewin J (eds). Blackwell: Oxford; 133-143.

National Parks and Wildlife Service. 2005. *http://www.nationalparks.nsw.gov.au, Department of Environment and Conservation*, accessed 10th September 2005.

Nortek AS. *unpublished*. *Vector current manual user manual* Sandvika, Norway.

Offenberg AC. 1967. Tamworth 1:250,000 Geological Series Sheet SH 56-13. New South Wales Geological Survey, Sydney.

Olley JM, Pietsch T, Roberts RG. 2004. Optical dating of Holocene sediments from a variety of geomorphic settings using single grains of quartz. *Geomorphology* **60**: 337-358.

O'Neill MP, Abrahams AD. 1984. Objective identification of pools and riffles. *Water Resources Research* **20**(7): 921-926.

Osterkamp WR. 1979. Invariant power functions as applied to fluvial geomorphology. In *Adjustments of the fluvial system: a proceedings volume of the tenth annual Geomorphology symposia series held at Binghamton, New York, September 21-22, 1979,* Rhodes DD, Williams GP (eds), Kendall/Hunt Publishing Company: Dubuque, Iowa; 33-54.

Pain CF. 1983. Geomorphology of the Barrington Tops area, New South Wales. *Journal of the Geological Society of Australia* **30**(1-2): 187-194.

Park CC. 1977. World-wide variation in hydraulic geometry exponents of stream channels: an analysis and some observations. *Journal of Hydrology* **33**(1-2): 133-146.

Parker G. 1976. On the cause and characteristic scales of meandering and braiding rivers. *Journal of Fluid Mechanics* **76**(3): 457-480.

Parker G. 1996. Some speculations on the relation between channel morphology and channel-scale structures. In *Coherent flow structures in open channels*, Ashworth

PJ, Bennett SJ, Best JL, McLellend SJ (eds). John Wiley and Sons: Chichester; 423-458.

Parsons DR. 2002. Flow separation in meander bends. PhD Thesis, University of Sheffield.

Pickup G. 1976. Alternative measures of river channel shape and their significance. *Journal of Hydrology (NZ)* **15**(1): 9-16.

Pickup G, Warner RF. 1976. Effects of hydrologic regime on magnitude and frequency of dominant discharge. *Journal of Hydrology* **29**(1): 51-75.

Powell DM. 1998. Patterns and processes of sediment sorting in gravel-bed rivers. *Progress in Physical Geography* **22**(1): 1-32.

Prestegaard KL. 1983. Bar resistance in gravel bed streams at bankfull stage. *Water Resources Research* **19**(2): 472-476.

Proser [sic] IP. 1987. The history of Holocene alluviation in the southeastern highlands of Australia. *Search* **18**: 201-2.

Prosser IP, Chappell J, Gillespie R. 1994. Holocene valley aggradation and gully erosion in headwater catchments, south-eastern highlands of Australia. *Earth Surface Processes and Landforms* **19**(5): 465-480.

Prus-Chacinski TM. 1955. Helical flow in open channel bends, *The Dock and Harbour Authority*, London.

Prus-Chacinski TM. 1956. Patterns of motion in open-channel bends. *Institution of Water Engineers* **10**(5): 420-426.

Randell F, Ellsmore D, Messner A, Brown I, Bubb G, Low, Hooke. 2003. *Contextual history for the Barrington Tops National Park and heritage action statements for five huts within the park*, NSW National Parks and Wildlife Service, Messner A.

Rhodes DD. 1977. The b-f-m diagram: graphical representation and interpretation of at-a-station hydraulic geometry. *American Journal of Science* **277**(1): 73-96.

Rhodes DD. 1987. The b-f-m diagram for downstream hydraulic geometry. *Geografiska Annaler* **69A**(1): 147-161.

Rice S. 1999. The nature and controls on downstream fining within sedimentary links. *Journal of Sedimentary Research* **69**(1): 32-39.

Richards KS. 1973. Hydraulic geometry and channel roughness - a non-linear system. *American Journal of Science* **273**(10): 977-896.

Richards KS. 1976. Channel width and the riffle-pool sequence. *Geological Society of America Bulletin* **87**(6): 883-890.

Richards KS. 1982. *Rivers: Form and process in alluvial channels*. Methuen: London.

Robert A. 1990. Boundary roughness in coarse-grained channels. *Progress in Physical Geography* **14**(1): 42-70.

Robert A. 2003. *River processes: An introduction to fluvial dynamics*. Arnold: London.

Roberts J, Engel B, Chapman J. 1991. Camberwell 1:100,000 geological sheet 9133. New South Wales Geological Survey, Sydney.

Rosgen DL. 1994. A classification of natural rivers. *Catena* **22**(3): 169-199.

Roy AG, Buffin-Belanger T, Lamarre H, Kirkbridge A. 2004. Size, shape and dynamics of large-scale turbulent flow structures in a gravel-bed river. *Journal of Fluid Mechanics* **500**: 1-27.

Schumm SA. 1960. The shape of alluvial channels in relation to sediment type. *United States Geological Survey Professional Paper* **352B**: 17-30.

Schumm SA. 1985. Patterns of alluvial rivers. *Annual Review of Earth and Planetary Sciences* **13**: 5-27.

Schumm SA, Khan HR. 1972. Experimental study of river patterns. *Geological Society of America Bulletin* **83**(6): 1755-1770.

Shields A (ed) 1936. *Anwendung der Anlichkeitsmechanik und der Turbulenzforschung auf die Geschiebebewegung*, Translated by W.P. Ott and J.C. van Uchelen, California Institute of Technology, Pasadena, California, USA.

Shukry A. 1950. Flow around bends in an open flume. *Transactions of the American Society of Civil Engineers* **115**: 751-779.

Simon A, Collison JC. 2002. Quantifying the mechanical and hydrologic effects of riparian vegetation on streambank stability. *Earth Surface Processes and Landforms* **27**(5): 527-546.

Simon A, Thorne CR. 1996. Channel adjustment of an unstable coarse grained stream: Opposing trends of boundary and critical shear stress, and the applicability of extremal hypotheses. *Earth Surface Processes and Landforms* **21**(2): 155-180.

Simons D, Richardson EV. 1966. Resistance to flow in alluvial channels. *United States Geological Survey Professional Paper* **422J**: J1-J61.

Smith DG. 1976. Effect of vegetation on lateral migration of anastomosed channels of a glacial meltwater river. *Geological Society of America Bulletin* **87**(6): 857-860.

Smith DG. 1981. Aggradation of the Alexandria-North Saskatchewan River, Banff Park, Alberta. In *Fluvial geomorphology: A proceedings volume of the fourth annual geomorphology symposia held at Binghamton, New York, September 27-28, 1973,* Morisawa M (ed), Allen and Unwin: London; 201-219.

Smith JD, McLean SR. 1977. Spatially averaged flow over a wavy surface. *Journal of Geophysical Research* **82**(12): 1735-1746.

Smith ND, Perez-Arlucea M. 2004. Effects of peat on the shapes of alluvial channels: examples from the Cumberland Marshes, Saskatchewan, Canada. *Geomorphology* **61**(3-4): 323-335.

Southern W. 1982. Late Quaternary vegetation and environments of Jackson's Bog and the Monaro Tablelands, New South Wales. Masters Thesis, Monash University.

Stanley S, De Deckker P. 2002. A Holocene record of allochthonous, aeolian mineral grains in an Australian alpine lake; implications for the history of climate change in southeastern Australia. *Journal of Limnology* **27**(2): 207-219.

Stapleton KR, Huntley DA. 1995. Seabed stress determinations using inertial dissipation method and the turbulent kinetic energy method. *Earth Surface Processes and Landforms* **20**: 807-815.

Sutherland FL, Fanning CM. 2001. Gem-bearing basaltic volcanism, Barrington, New South Wales: Cenozoic evolution, based on basalt K-Ar ages and zircon fission track and U-Pb isotope dating. *Australian Journal of Earth Sciences* **48**(2): 221-237.

Sutherland FL, Graham I. 2003. *Geology of the Barrington Tops Plateau: Its rocks, minerals and gemstones, New South Wales, Australia*. The Australian Museum Society: Sydney.

Sweller S, Martin HA. 2001. A 40,000 year vegetation history and climatic interpretations of Burraga Swamp, Barrington Tops, New South Wales. *Quaternary International* **83-85**: 233-244.

Tabata KK, Hickin EJ. 2003. Interchannel hydraulic geometry and hydraulic efficiency of the anastomosing Columbia River, southeastern British Columbia, Canada. *Earth Surface Processes and Landforms* **28**(837-852): 837-852.

Thompson C, Rhodes E, Croke J. in press. Bed material storage in mountain stream morphologies assessed using optically stimulated luminescence dating. *Geomorphology*.

Thorne CR, Hey RD. 1982. Discussion of, channel bars in gravel-bed rivers by M. Church and D. Jones. In *Gravel-bed rivers: Fluvial processes, engineering, and management*, Hey RD, Bathurst JC, Thompson A (eds). Wiley-Interscience: Chichester; 332-334.

Thorne CR, Rais S. 1983. Secondary current measurements in a meandering river. In *River meandering: Proceedings of the conference rivers '83, New Orleans,* Elliott CM (ed), American Society of Civil Engineers: New York; 675-686.

Thorne CR, Zevenbergen LW, Pitlick JC, Rais S, Bradley JB, Julien PY. 1985. Direct measurements of secondary currents in a meandering sand-bed river. *Nature* **316**(6022): 746-747.

Thorne SD, Furbish DJ. 1995. Influences of coarse bank roughness on flow within a sharply curved river bend. *Geomorphology* **12**(3): 241-257.

Todd DK. 1964. Groundwater. In *Handbook of applied hydrology : A compendium of water-resources technology*, Chow VT (ed). McGraw-Hill: New York; 13/1-55.

Toebes GH, Sooky AA. 1967. Hydraulics of meandering rivers with flood plains. *Journal of the Waterways and Harbors Division, Proceedings of the American Society of Civil Engineers* **93**(WW2): 213-236.

Tooth S, McCarthy TS. 2004. Controls on the transition from meandering to straight channels in the wetlands of the Okavango Delta, Botswana. *Earth Surface Processes and Landforms* **29**(13): 1627-1649.

Tooth S, Nanson GC. 2004. Forms and processes of two highly contrasting rivers in arid central Australia, and the implications for channel pattern discrimination and prediction. *Geological Society of America Bulletin* **116**(7/8): 802-816.

Tweedie AD. 1963. Climate of the Hunter Valley. *CSIRO Australian Land Research Series* **8**: 62-70.

Vandergoes MJ, Prior CA. 2003. AMS dating of pollen concentrates - a methodological study of Late Quaternary sediments from South Westland, New Zealand. *Radiocarbon* **45**(3): 479-491.

Wahl TL. 2000. Analyzing ADV data using WinADV. In *Joint conference on water resources engineering and water resources planning and management,* Minneapolis, Minnesota,

Ward RC. 1967. *Principles of hydrology*. McGraw-Hill: London.

Wharton G. 1995. Information from channel geometry-discharge relations. In *Changing river channels*, Gurnell AM, Petts G (eds). John Wiley and Sons: Chichester; 325-346.

Whiting PJ, Dietrich WE. 1993. Experimental studies of bed topography and flow patterns in large-amplitude meanders 2. mechanisms. *Water Resources Research* **29**(11): 3615-3622.

Wilcock DN. 1971. Investigation into the relations between bedload transport and channel shape. *United States Geological Society of America Bulletin* **82**(8): 2159-2176.

Wilkinson SN, Keller RJ, Rutherfurd ID. 2004. Phase-shifts in shear stress as an explanation for the maintenance of pool-riffle sequences. *Earth Surface Processes and Landforms* **29**(6): 737-753.

Wolman MG, Miller JP. 1960. Magnitude and frequency of forces in geomorphic process. *Journal of Geology* **68**(1): 54-74.

Yalin MS. 1971. On the formation of dunes and meanders. *Proceedings of the 14th international congress of the International Association for Hydraulic Research* **3**(C13): 1-8.

Yalin MS. 1992. *River mechanics*. Pergamon: Oxford.

Yang S-Q, Lim S-Y. 1998. Boundary shear stress distributions in smooth rectangular open channel flows. *Proceedings of the Civil Engineers Water, Maritime and Energy* **130**: 163-173.

Young ARM. 1983. Upland swamps (dells) on the Woronora Plateau, N.S.W. PhD Thesis, University of Wollongong.

Young ARM. 1986a. The geomorphic development of dells (Upland Swamps) on the Woronora Plateau, N.S.W., Australia. *Zeitschrift fur Geomorphologie* **30**(3): 317-327.

Young ARM. 1986b. Quaternary sedimentation on the Woronora Plateau and its implications for climatic change. *Australian Geographer* **17**: 1-5.

Zeff ML. 1988. Sedimentation in a salt marsh - tidal channel system, southern New Jersey. *Marine Geology* **82**: 33-48.

Zeff ML. 1999. Salt marsh tidal channel morphometry: applications for wetland creation and restoration. *Restoration Ecology* **7**(2): 205-211.

Zimmerman RC, Goodlett JC, Comer GH. 1967. The influence of vegetation on channel form of small streams. In *Symposium on River Morphology,* Belgique, International Union of Geodesy and Geophysics and International Association of Scientific Hydrology (ed), International Association of Scientific Hydrology; 255-275.

Zoete T. 2000. Vegetation survey of the Barrington Tops and Mount Royal National Parks for use in fire management. *Cunninghamia* **6**(3): 511-578.

Appendix 1

FLOW HYDROLOGY DATA ANALYSIS TECHNIQUE

This appendix describes the processing of the water level data that was used in Chapter 1 to describe the daily water level fluctuations. The data collected using the Andeera Water Level Recorders include flows resulting from several rainfall events during each measurement period. A lack of concurrent temperature and rainfall data limited data analysis techniques to a simple time-series decomposition.

Time series decomposition

To separate the stage hydrograph and sub-daily fluctuations in flow, datasets comprising several weeks of stage data for both the Barrington River and Polblue Creek were initially analysed using both additive and multiplicative decomposition approaches. This approach is based on the theory that:

$$\text{Data} = \text{pattern} + \text{error}$$

$$\text{Pattern} = f\,(\text{St}, \text{Tt}, \text{Et})$$

where: St = seasonality

Tt = the trend cycle

Et = error (or remainder)

(Makridakis et al., 1998). The dataset is assumed either multiplicative or additive in nature: if multiplicative, the amplitude of seasonality is expected to increase with increasing magnitude; if additive, the amplitude of seasonality should not vary with magnitude:

Multiplicative:

$$Yt = S_t \,.\, T_t \,.\, E_t$$

Additive:

$$Yt = S_t + T_t + E_t$$

For the datasets examined, neither of these conditions were entirely satisfied, as the amplitude of seasonality *decreased* with increasing magnitude, the inverse of what is expected of a multiplicative dataset. For this reason, both the multiplicative and additive approaches were undertaken.

Using the Minitab statistics program, whole datasets (Figure 1.9) were detrended using centred 24-hour moving averages, in an effort to minimalise the complicating influence of rainfall. The residuals were then decomposed to determine the seasonal component of each dataset. Poor results were obtained using this method and partial datasets were therefore selected; these were also indicated in Figure 1.9. They were chosen visually, on the basis of consistency in trend, consistent with Grayson et al. (1996, p55) recommendation, that "any statistical test (of trend) should be preceded by graphical analyses" and who therefore encourage dataset visualisation prior to the application of analysis techniques. Using this visual technique it was determined that linear detrending was suitable for the decomposition of the selected flow sub-datasets.

Decomposition error estimates

Results were derived for three partial datasets (two from the Barrington River dataset and one from Polblue Creek) creating six additive and multiplicative decompositions. The accuracy of the resulting forecasts were assessed by calculating the root-mean squared deviation (RMSD) and mean absolute percentage error (MAPE), each of which are standard statistical techniques. The inability of the MAPE to represent error as a fraction of the total model range resulted in an inability to comprehend the reliability of the model, both within and between datasets of varying mean value. Therefore in addition to the standard statistical calculations, the error of the resulting seasonals was also expressed

using the RMSD as a fraction of the seasonal range and is termed the *seasonal reliability* (SR). It is comparable between datasets with differing mean values. The following formulae represent the derivation of each of these results:

$$\text{RMSD} = \sqrt{\frac{1}{n}\sum_{t=1}^{n} e_t 2}$$

$$\text{MAPE} = \frac{1}{n}\sum_{t=1}^{n}\left|\text{PE}_t\right|$$

$$SR = \frac{RMSD}{(seasonal range)} \times 100$$

The RMSD and SR results for each decomposition are presented in Table A1.1. These scores were used to determine which of the forecasts were appropriate for describing the hydrology of each channel.

Table A1.1 Error scores for partial series decompositions for summer water level recorder data.

RMSD	**multiplicative**	**additive**
Barrington 2003	0.01	0.01
Polblue 2003	-	0.01
SR		
Barrington 2003	16.10	23.79
Polblue 2003	-	18.12

Selected seasonal trends

Only additive model error scores were obtained for each subset as the multiplicative approach resulted in unintelligible seasonal trends in the Polblue subset. The multiplicative approach was therefore not pursued for data analysis. The additive decomposition method produced reliable seasonality with errors of ±0.01m (RMSD) and SR scores of <24% for the two Barrington River subsets, averaged, and the single Polblue subset; these are illustrated in Figure 1.9.

Appendix 2

POLLEN DATA

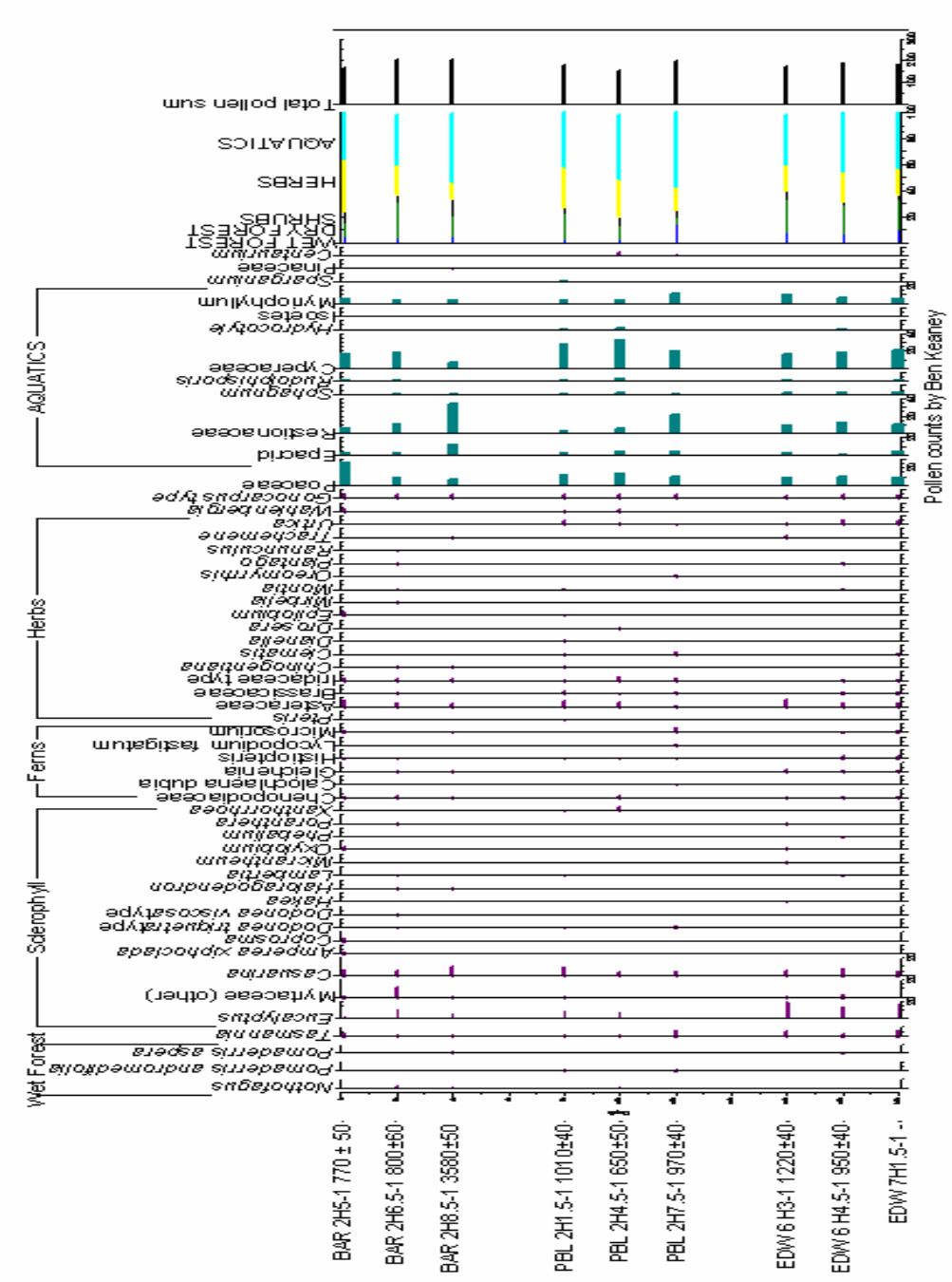

Appendix 3

MATLAB SCRIPT “resample_long”

A Matlab script to resample randomly spaced longitudinal profile data at given intervals.

In this case the resampling interval is 1metre.

```
load pollong.txt;
[m,n]=size(pollong);
inc=1;
dd=diff(pollong(:,1));
ind=find(dd == 0);
new_dist=pollong(1,1):inc:pollong(m,1);
new_ht=interp1(pollong(:,1),pollong(:,2),new_dist);
plot(pollong(:,1),pollong(:,2))
hold on
plot(new_dist,new_ht,'r.')
data=[new_dist' new_ht'];
save 'pollong_new1m' data -ascii
```

Appendix 4

MATLAB SCRIPT "Pools_riffles.mod"

A Matlab script for calculating the SD of the differences in elevation of consecutive points in a long profile, then determining changes in the sign of the product of consecutive points (i.e. peaks or troughs), then using 0.75 SD as a minimum difference between consecutive peaks and troughs to identify them as pools or riffles.

```
load conlong.txt;
x=conlong(:,1);
y=conlong(:,2);
plot(x,y)
b=y(2:end)-y(1:end-1);
% differences
c=b(2:end).*b(1:end-1);
% negative values => local max or min
i=find(c<=0); % indices of negative values in c
extremay = y(i+1);
% values corresponding to indices of negative values in c
extremax = x(i+1);
SD=std(conlong);
Standdev=0.75.*SD(3);
% using the 0.75 SD tolerance suggested by O'Neil and Abrahams - can use 0.5, 1 and 1.25
peakdiff=extremay(2:end)-extremay(1:end-1);
j=1;
k=1;
while extremax(j) < extremax(length(extremax))
sum=0
while(abs(sum) < Standdev & j <= length(peakdiff));
   sum=sum+peakdiff(j);
   j=j+1;
end
xp(k)=extremax(j);
yp(k)=extremay(j);
k=k+1;
end
hold on
plot(xp,yp,'r.');
data=[xp' yp'];
save 'conporif' data -ascii
```

Appendix 5

ACOUSTIC DOPPLER VELOCIMETER (ADV) DATA PROCESSING

ADV's use the doppler effect to measure flow velocity. An ADV transmits short pulses of sound of known pitch then records the altered pitch of the echo that reflects off sediment or organic particles moving with the flow (Nortek, *unpublished*). The difference between the transmitted and received pitch is converted into velocity components for each dimension (X, Y and Z) via three receivers. The technique has potential problems resulting from inadequate quantities of suspended particles, or the passing of particularly large objects such as debris or fish. Anomalies in the record resulting from such inaccuracies were filtered from the dataset using the *Signal to Noise Ratio* (SNR), which measures the signal strength to noise strength ratio, and the *correlation scores*. These determine the strength of the signal that is transmitted to that which is received.

Further errors can result from setting an inappropriate velocity range. The range is set to minimise noise; higher velocities record greater errors and it is important to set the expected velocity to not much more than the maximum velocity that is expected. However, if flow velocities exceed this range, *aliasing* may result whereby the ADV *overranges* and records a change in sign but the same velocity (Wahl, 2000). Aliasing is not evidenced by SNR or correlation values and cannot be filtered using these parameters; it was necessary to check each data point to ensure that the range of velocities that was set was not exceeded by the absolute values in the recorded time series.

The ADV recorders were set for continuous sampling at 16 hertz with a velocity range of ±1m/s. Data was filtered by allowing a maximum SNR of 10, a correlation minimum of 70%, a velocity range of ±1m/s and, to remove spikes, by allowing a maximum acceleration of the flow from one measurement to the next of no more than that which could be attributed to gravity (9.8m/s). Secondary current vectors were plotted directly from this data, however, primary velocities were manually contoured owing to the strongly anisotropic distribution of the data which resulted from both the collection method and subsequent data processing, which rendered some data points unusable.

xxx

Appendix 6

METHOD FOR CALCULATING SHEAR STRESS

This appendix describes the Law of the Wall shear stress calculation technique and how it is applied in Chapter 6.

Newton's Law of Viscosity dictates that the direct measure of shear stress in fully turbulent flow is defined by:

$$\tau = \varepsilon \frac{du}{dy}$$

where ε is the eddy viscosity and du/dy is the velocity gradient from the boundary. However, eddy viscosity is not a parameter for which values can be readily acquired, and estimates of this parameter are indirect in nature. The equation presented above is thus a primarily theoretical one (Gordon et al., 2004) used in the subsequent derivation of more applied but indirect shear stress equations. Perhaps the most accurate of these approaches is that which accounts for eddy viscosity and the effect of this parameter on the velocity profile through measurements of turbulence (Kim et al., 2000). In the near bed zone of the flow profile, turbulence is proportional to shear stress (Stapleton and Huntley, 1995; Kim et al., 2000), and the derivation of turbulent kinetic energy (TKE) allows for a transformation of turbulence to shear stress (τ_{TKE}). Data collected in this study using the ADV's was suited to the calculation of τ_{TKE}, however, owing to time constraints, the technique is not employed, but will be the focus of future research.

Shear stress distribution was estimated using velocity measurements and Law of the Wall, and produced the log profile shear stress estimate (τ_{LP}), calculated using:

$$\frac{u}{u_*} = 5.75 \log\left(\frac{30y}{k}\right)$$

where u is the turbulent averaged velocity at distance y from the bed, and u_* is the shear velocity and which indirectly incorporates the eddy-viscosity effect by the slope of the velocity profile. This equation can be rearranged to yield:

$$u_* = \frac{b}{5.75}$$

where b is the gradient of the velocity profile in the fully turbulent boundary layer.

Bed shear is then calculated using the equation:

$$\tau_{LP} = \rho(u_*)^2$$

where ρ is the density of water (kg/m^3) (Gordon et al., 2004).

The velocity profile does not behave logarithmically through the entire water column and the Law of the Wall can only be applied to those velocity readings taken within the fully turbulent sub-layer, which has been approximated to persist to up to 50% of the flow depth; <10% (Bathurst, 1979), 10-20% (Bathurst, 1993), 20% (Bridge and Jarvis, 1976), 50% (Biron et al., 1998). Local conditions dictate the depth to which the semi-logarithmic profile persists in the water column (Biron et al., 1998).

Velocity measurements within the fully turbulent sub layer of the Barrington swamp channel bends were limited, owing primarily to the size of the instruments. In particular, the large ADV devices used in Edwards Creek and Barrington River bends could be deployed typically no lower than 0.1m from the bed (~10% of flow depth), and often closer to 0.2m (~<30% flow depth). In contrast, OTT data collected in Polblue Creek were often as close as 0.05m from the bed (~5% of flow depth). Visual analysis of the profiles produced in this project suggests that for the entry and exit cross-sections in the three bends in Polblue Creek, only the bottom two velocity measurements in each vertical profile were located within the sub-layer. As secondary current strength increased through each of the bends, even the bottom two points in the profile sometimes ceased to conform to the Law of the Wall. Most studies have used two or more velocity values from within the turbulent

sub-layer (Bathurst, 1979; Kim et al., 2000; Tabata and Hickin, 2003) to produce the slope of the profile in this region.

The Law of the Wall technique applied here uses the slope of the regression line from the lowest point beneath 20% of the flow depth to the origin (τ_{LP}). While this technique is not encouraged in the literature, it was considered that values of bed shear stress in bends were reliable, for comparison relative to one another, if not the *absolute* values. This is consistent with the assumption of Bathurst (1979) and the problems he experienced with his shear stress calculation technique. Furthermore, grain shear stresses calculated in Chapter 4 for hydraulic geometry stations near each bend were able to be compared with the τ_{LP} values to check for consistency. The problem of determining boundary shear stresses in the study highlight the problem of such measurements in small rough-boundary channels where miniaturised equipment (e.g. Roy et al., 2004) or acoustic profilers (e.g. McLean and Wolfe, 1999) are required.